Mechanisms Regulating PKA Phosphorylation of the Key Cardiac Proteins Troponin I and Hsp20

by

HELEN VICTORIA EDWARDS

A thesis submitted in fulfilment of the requirements for the degree of Doctor of Philosophy

Institute of Cardiovascular and Medical Sciences

College of Medical, Veterinary and Life Sciences

University of Glasgow

April 2012

Abstract

Reversible modification of protein function by PKA phosphorylation is critical to a variety of processes in the heart, including the modulation of cardiac output in response to stress, and the transduction of cardioprotective signals. As a result, PKA phosphorylation events must be tightly regulated. This regulation is achieved by compartmentalisation of cAMP/PKA signal transduction cascades, which is mediated by phosphodiesterase enzymes (PDEs) and A-kinase anchoring proteins (AKAPs). PDEs provide the only means of hydroysing cAMP in cells, and in recent years, the use of genetically encoded FRET-based cAMP sensors has allowed direct visualisation of discrete cAMP microdomains created by subcellular tethering of PDEs in cardiac cells. The physical compartmentalisation of PKA by AKAPs ensures that only a small subpopulation of PKA is activated by these cAMP microdomains. Macromolecular complexes nucleated by AKAPs bring together cAMP effectors, signal terminating enzymes and other scaffold proteins, to facilitate PKA signaling events. The aim of this thesis was to investigate the signaling elements which participate in these complexes to modulate PKA phosphorylation of the myofilament protein troponin I and the small heat shock protein Hsp20 in the heart. Both of these proteins are phosphorylated by PKA at their N termini in response to β-adrenergic stimulation, resulting in increased cardiac output and enhanced cardioprotection.

PKA phosphorylation of TnI mediates the fight or flight response, by reducing the Ca^{2+} sensitivity of the myofilament and altering the strength of contraction and rate of relaxation of the heart to increase cardiac output. In the first part of this thesis, I investigated the specific PDE isoforms which regulate cAMP/PKA signaling at the myofilament. A novel FRET-based cAMP sensor which is targeted to troponin I at the myofilament demonstrated that PDE4 is the main phosphodiesterase family which modulates cAMP levels in the subcellular compartment around troponin I. Biochemical studies identified a specific association between troponin I and the long phosphodiesterase isoform PDE4D9. The binding site for PDE4D9 on troponin I was mapped using peptide array technology to a region on the flexible C terminus of the

myofilament protein, and the sequence information used to design a cell permeable peptide disruptor of this interaction. Disruption of the troponin I-PDE4D9 complex in cells using this peptide was sufficient to promote PKA phosphorylation of troponin I in the absence of other stimuli. This approach may be of benefit in the treatment of diseases such as heart failure, where PKA phosphorylation of myofilament proteins is known to be reduced. Control of post-translational modifications at the level of the myofilament by specific PDE isoform inhibitors represents a promising therapeutic avenue which has not yet been explored.

In the second part of the thesis I investigated the signaling components which regulate PKA phosphorylation of Hsp20. Hsp20 is known to protect against ischaemic injury and cardiac hypertrophy, and its cardioprotective actions are enhanced by PKA phosphorylation on Ser16. Biochemical studies identified an interaction between Hsp20 and AKAP-Lbc in cardiac cells, and selective knockdown of AKAP-Lbc confirmed that this interaction is required for β-adrenergic-induced PKA phosphorylation of Hsp20 and the anti-apoptotic effects of Hsp20 in cardiac myocytes. FRET-based studies using a cAMP sensor targeted to Hsp20 demonstrated the role of PDE4 isoforms in modulating cAMP levels around Hsp20, and biochemical techniques identified PDE4D isoforms in the macromolecular complex formed by Hsp20 and AKAP-Lbc. The AKAP-Lbc/PKA/Hsp20/PDE4D complex appears to play a key role in cardioprotection via the modulation of Hsp20 Ser16 phosphorylation, and selective targeting of signaling elements that enhance this modification represents a new therapeutic avenue for the prevention and treatment of pathological cardiac remodelling and ischaemic injury.

Acknowledgements

Firstly, I would like to thank my supervisor Dr George Baillie for his advice, support and guidance, and for all of the opportunities he has encouraged me to pursue over the course of my PhD.

Secondly, I would like to thank all of the past and present members of the Gardiner lab, for valuable discussions, advice, ideas and tea breaks over the past few years. In particular, I would like to thank Jon Day for his unfailing enthusiasm, support and surreptitious supply of chocolate bars. I would also like to thank Professor Miles Houslay for his many valuable suggestions for my project.

Three months of my PhD was spent at the University of Washington, Seattle, in the laboratory of Professor John Scott. I sincerely want to thank John and all of the members of the Scott lab for making me feel so welcome, providing me with reagents, and for their advice on experiments and techniques, particularly Donelson Smith, Catherine Pawson and Chris Means. I also want to thank Dr Enno Klussmann and members of his lab at the FMP, Berlin, in particular Philipp Skroblin, for assistance with the ^{32}P RII overlays.

Lastly, I would like to thank my friends and family who have helped me through this process. In particular I would like to mention Kirsty MacKenzie, Jill McKane and Lynn Williamson, and also my parents and my sister Lindsey, who have all tolerated an immense amount of stressing over the past few months!

Table of Contents

MECHANISMS REGULATING PKA PHOSPHORYLATION OF THE KEY CARDIAC PROTEINS TROPONIN I AND HSP20

List of Tables

List of Figures

Abbreviations

Ab	Antibody
AC	Adenylyl cyclase
ACS	Acute coronary syndrome
AKAP	A-kinase anchoring protein
AKAR	A-kinase activity reporter
AMP	Adenosine monophosphate
AR	Adrenergic receptor
ATP	Adenosine triphosphate
bp	Basepairs
BSA	Bovine serum albumin
C	PKA catalytic subunit
cAMP	Cyclic 3’5’-adenosine monophosphate
CaM	Calmodulin
CaN	Calcineurin
CFP	Cyan fluorescent protein
cGMP	Cyclic 3’5’-guanosine monophosphate
CICR	Calcium-induced calcium release
CNBD	Cyclic nucleotide-binding domain
CNG	Cyclic nucleotide-gated channel
COPD	Chronic obstructive pulmonary disease

DAG	Diacylglycerol
DH	Dbl homology domain
Dig	Digoxigenin
DISC	Disrupted in schizophrenia
DMEM	Dulbecco's modified Eagle's medium
DMSO	Dimethylsulfoxide
ECC	Excitation-contraction coupling
ECL	Enhanced chemiluminescence
E.coli	*Escherichia coli*
eGFP	Enhanced green fluorescent protein
EHNA	Erythro-9-(2-hydroxy-3-nonyl)adenine
Epac	Exchange protein directly activated by cAMP
ERK	Extracellular signal regulated kinase
FRET	Förster/fluorescence resonance energy transfer
FSK	Forskolin
GAF	cGMP-specific PDE/*Anabena* adenylyl cyclase/ Fh1a domain
GDP	Guanosine diphosphate
GEF	Guanine nucleotide exchange factor
GFP	Green fluorescent protein
Gi	Inhibitory G protein
GPCR	G protein-coupled receptor
GRK	G protein-coupled receptor kinase

Gs	Stimulatory G protein
GTP	Guanosine triphosphate
HDAC	Histone deacetylase
HEK	Human embryonic kidney
Hsp	Heat shock protein
IBMX	3-isobutyl-1-methylxanthine
IC50	Half maximal inhibitor concentration
IP_3	Inositol triphosphate
Iso	Isoproterenol
I/R	Ischaemia/reperfusion
kM	Michaelis constant (Concentration of substrate leading to half maximal enzyme velocity)
Lbc	Lymphoid blast crisis
LDH	Lactate dehydrogenase
LTCC	L-type calcium channel
mAKAP	Muscle-specific A-kinase anchoring protein
MAPK	Mitogen-activated protein kinase
MEF	Myocyte enhancer factor
mRNA	Messenger RNA
NCX	Na^+/Ca^{2+} exchanger
NRVM	Neonatal rat ventricular cardiac myocytes
PAS	Period circadian protein/Aryl hydrocarbon receptor nuclear translocator/Single minded protein domain

PDE	Phosphodiesterase
PH	Pleckstrin homology domain
PLB	Phospholamban
PKA	cAMP-dependent protein kinase A
PKC	Protein kinase C
PKD	Protein kinase D
PKI	Protein kinase inhibitor
PP	Protein phosphatase
PPi	Pyrophosphate
R	PKA regulatory subunit
RyR	Ryanodine receptor
RyR2	Cardiac ryanodine receptor
SERCA	Sarco(endo)plasmic reticulum Ca^{2+} ATPase
shRNA	Short hairpin RNA
sHsp	Small/low molecular weight heat shock protein
siRNA	Small interfering RNA
SR	Sarcoplasmic reticulum
TG	Transgenic
TM	Tropomyosin
Tn	Troponin complex
TnC	Troponin C
TNF	Tumour necrosis factor

TnI	Troponin I
TnT	Troponin T
TUNEL	Terminal deoxynucleotidyltransferase-mediated dUTP nick-end labeling
UCR	Upstream conserved region
V_{max}	Maximal enzyme velocity
YFP	Yellow fluorescent protein

Publications and Conferences

Publications

Edwards, H. V., Scott, J. D. and Baillie, G. S. (2012) The A-kinase anchoring protein AKAP-Lbc facilitates cardioprotective PKA phosphorylation of Hsp20 on Serine 16. Submitted for publication.

Edwards, H. V., Scott, J. D., Baillie, G. S. (2012) PKA phosphorylation of the small heat shock protein Hsp20 enhances its cardioprotective effects. Biochemical Society Transactions. 40, 210-214

Edwards, H. V., Christian, F., Baillie, G. S. (2011) cAMP: Novel concepts in compartmentalised signalling. Seminars in Cell and Developmental Biology. 23, 181-190

Edwards, H. V., Cameron, R. T., Baillie, G. S. (2011) The emerging role of Hsp20 as a multifunctional protective agent. Cellular Signalling. 23, 1447-1454

Sin, Y. Y., **Edwards, H. V.**, Li, X., Day, J. P., Christian, F., Dunlop, A. J., Adams, D. R., Zaccolo, M., Houslay, M. D., Baillie, G. S. (2011) Disruption of the cyclic AMP phosphodiesterase-4 (PDE4)–HSP20 complex attenuates the β-agonist induced hypertrophic response in cardiac myocytes. Journal of Molecular and Cellular Cardiology. 50, 872-883

Conferences

2011	Presenter - Novel cAMP signaling paradigms: New insights into the development and progression of chronic inflammatory diseases. British Pharmacological Society (London, UK)
2011	Presenter - New Advances in cAMP Signaling. Signaling 2011: A Biochemical Society Centenary Celebration (Edinburgh, UK)
2011	Presenter - cAMP Signaling in Heart Disease. Fondation Leducq meeting (Torino, Italy)

2011 Poster – Peptide Arrays as Tools for Study of Protein Interactions. Protein and Peptide Science Group Conference (London, UK)

2010 Poster - 3rd International Meeting on Anchored cAMP Signaling Pathways; 3rd International AKAP Meeting; FEBS Workshop on Spatiotemporal Dynamics of Signaling (Oslo, Norway)

2009 Presenter - cAMP Signaling in Heart Disease, Fondation Leducq meeting (San Francisco, USA)

2008 Attended - cAMP Signaling in Heart Disease, Fondation Leducq meeting (Paris, France)

1.

Introduction

1.1 Signal transduction and the second messenger concept

Signal transduction is the process by which an extracellular ligand binds to and activates a cell surface receptor, eliciting a specific intracellular response. This concept is now a central tenet in biology. Extracellular ligands may be thought of as the 'first messengers' in signal transduction cascades, and are usually hormones or neurotransmitters which cannot cross the plasma membrane. Instead, their signals are transduced into an alteration in the concentration of intracellular 'second messengers' in order to achieve an appropriate response (Sutherland 1972). The first of these to be discovered, and one of the most studied second messengers, is the cyclic nucleotide 3'5'-adenosine monophosphate, or cAMP (Figure 1-1) (Beavo & Brunton 2002). Other second messengers include cyclic 3'5'-guanosine monophosphate (cGMP), calcium, and the phosphatidylinositol derivatives inositol triphosphate (IP_3) and diacylglycerol (DAG) (Berridge 1984).

cAMP was identified as a second messenger as early as 1958 by Earl Sutherland (Sutherland & Rall 1958). Sutherland was investigating how the hormone adrenaline led to activation of glycogen phosphorylase and subsequent glycogenolysis in dog liver, and observed that a heat stable factor was required to activate the phosphorylase enzyme. Chemical analysis showed that this factor contained 1:1:1 ratios of adenine, ribose and phosphate, and could be enzymatically inactivated to 5'AMP. The discovery of cAMP and

its relation to the mechanisms of hormone action led to Sutherland winning a Nobel Prize in 1971. Indeed, between 1971 and 2000, discoveries about cyclic nucleotides and signal transduction garnered 5 separate Nobel Prizes, indicating the fundamental nature of this field (Beavo & Brunton 2002). cAMP signal transduction cascades have now been implicated in the control of a vast array of intracellular processes, including glucose metabolism, muscle contraction, regulation of gene transcription and cell survival (Delghandi et al 2005, Solaro 2008).

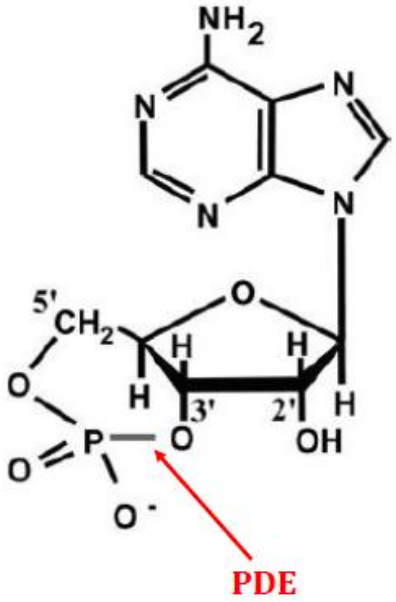

Figure 1-1 Structure of the second messenger cyclic adenosine 3'5'-monophosphate (cAMP). The 3' bond hydrolysed by phosphodiesterase (PDE) enzymes is indicated by a red arrow. Adapted from (Bender & Beavo 2006).

1.2 cAMP generation

1.2.1 G protein-coupled receptors

The first step in cAMP signal transduction is the binding of a ligand to a cell surface receptor. G protein-coupled receptors (GPCRs) represent the largest family of transmembrane receptors; in fact, around 2% of the genes in the mammalian genome are thought to code for GPCRs (Hollmann et al 2005). All GPCRs are composed of 7 α-helices

that span the plasma membrane, connected by 4 intracellular and 3 extracellular loops, and N terminal and C terminal tails which may be subject to post-translational modifications (Ji et al 1998) (Figure 1-2). Ligand specificity is determined by different regions within the receptor transmembrane domains and loops for different receptor subfamilies.

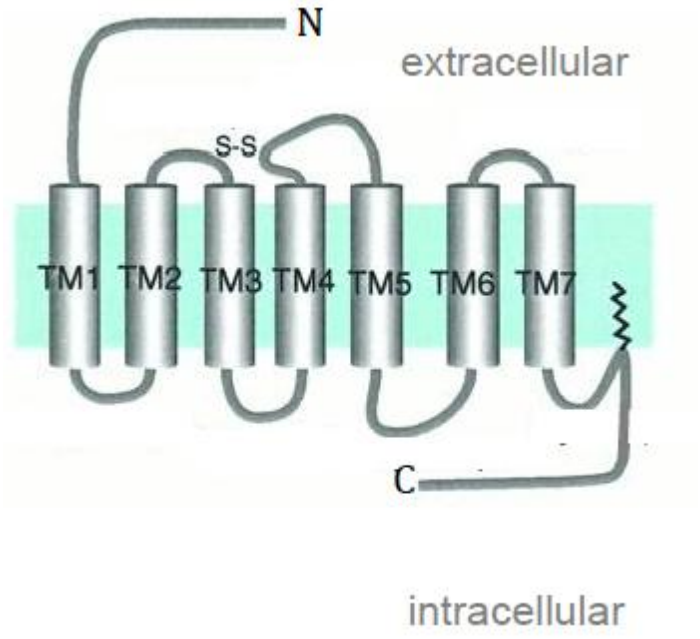

Figure 1-2 Structure of a typical G protein-coupled receptor. Adapted from (Ji et al 1998). Though regulated by many different agonists, GPCRs share a common heptahelical structure. The 7 transmembrane α-helices (TM1-7) are linked by 3 extracellular loops (exoloops) and 4 intracellular loops (endoloops), which are involved in determining ligand specificity (Ji et al 1998).

Despite their structural similarities, ligand binding to GPCRs can bring about very different physiological effects. Two of the best studied GPCRs are the β1- and β2-adrenergic receptors (ARs) in the heart. During conditions of stress, the heart must increase its rate and strength of contraction in order to meet the additional physiological demands of the body. The sympathetic nervous system stimulates cardiac function through the release of the hormonal neurotransmitters adrenaline and noradrenaline, which bind to β1- and β2-ARs on the plasma membrane of cardiac myocytes (Xiang & Kobilka 2003). Despite high receptor homology, ligand binding to different β-AR subtypes leads to distinct intracellular effects. Both β1 and β2-ARs couple to the stimulatory G protein Gs; however,

β2-AR also couple to the inhibitory G protein Gi (Xiao 2000). The dominant effects of β1 stimulation are an increase in heart rate (chronotropy), force of contraction (inotropy) and rate of relaxation (lusitropy), while β2 stimulation has only modest effects on heart rate. Chronic β1 stimulation is associated with a detrimental cardiac phenotype, with increased cardiac myocyte hypertrophy and apoptosis, whereas β2 stimulation promotes cell survival (Zhu et al 2003, Zhu et al 2001) (Figure 1-3). Thus, activation of very similar GPCRs can invoke distinct intracellular signal transduction pathways to mediate specific outcomes.

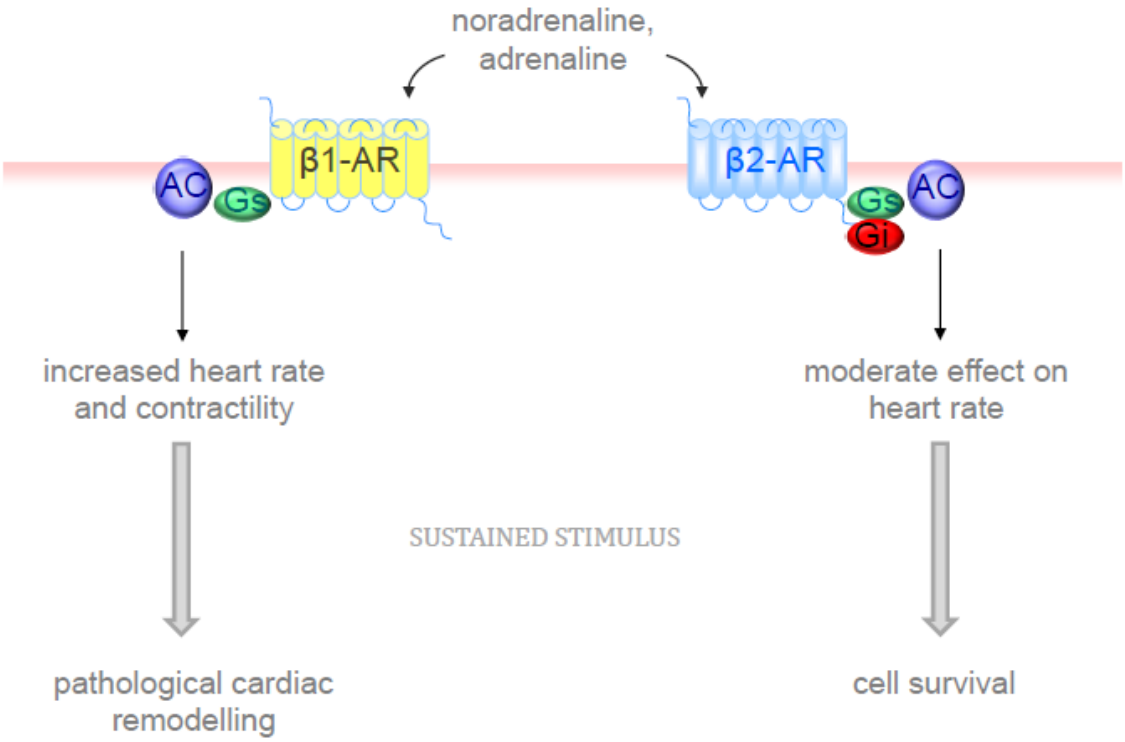

Figure 1-3 Adrenergic stimulation of different β-receptor subtypes mediates distinct intracellular effects.
Chronic stimulation of β1-AR leads to pathological cardiac remodelling, cardiac hypertrophy and apoptosis, whereas chronic β2-AR stimulation promotes cell survival. AR, adrenergic receptor; AC, adenylyl cyclase enzyme; Gs, stimulatory G protein; Gi, inhibitory G protein.

1.2.2 G proteins

G proteins are guanine nucleotide-binding proteins, which associate with the intracellular loops and C terminal tail of GPCRs. G proteins act as molecular switches, cycling between

inactive, GDP-bound and active, GTP-bound states. G proteins are heterotrimeric, consisting of α, β and γ subunits (Hollmann et al 2005). They may be classified into 4 families according to the presence of different α subunits as: Gs, Gi, Gq/11 and G12/13. Ligand binding to a GPCR induces a conformational change in the receptor which leads to coupling to and activation of one or more G proteins, via exchange of GDP for GTP. Activated G proteins dissociate into α-GTP and βγ subunits, which can interact with specific effector proteins. α and βγ subunits may bind to the same effector to mediate opposing or synergistic effects (Table 1-1) (Hollmann et al 2005). The major effectors of G protein subunits are the adenylyl cyclase enzymes described below.

1.2.3 Adenylyl cyclases

Adenylyl cyclases (ACs) are enzymes which catalyse the conversion of adenosine triphosphate (ATP) into cAMP (Figure 1-4). Nine isoforms of ACs have been identified to date, which are summarised in Table 1-1 (Willoughby & Cooper 2007).

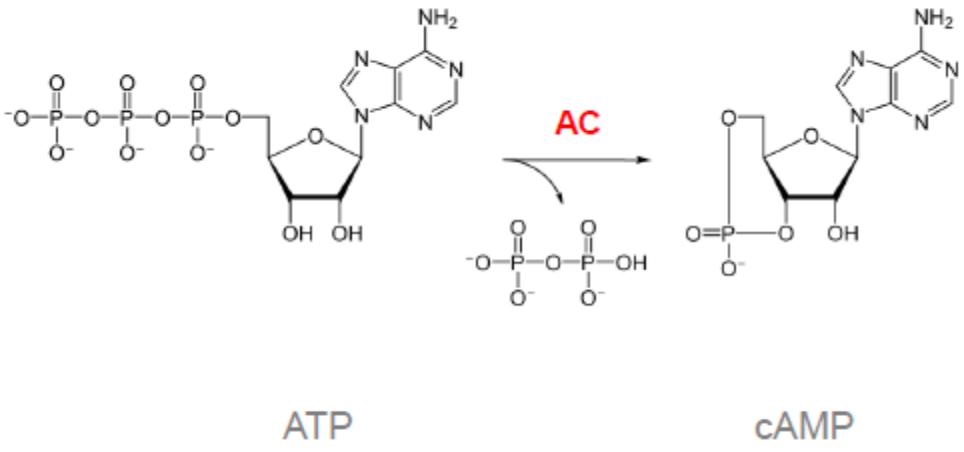

Figure 1-4 Conversion of ATP to cyclic adenosine 3'5'-monophosphate (cAMP) by adenylyl cyclase enzymes.
Adenylyl cyclases catalyse the conversion of ATP to pyrophosphate (PPi) and 3'5'-cAMP, which acts as a second messenger in cells. PDEs catalyse the hydrolytic cleavage of cAMP to 5'AMP, terminating the cAMP signal (Section 1.4, Figure 1-1).

ACs are large proteins with a common secondary structure, consisting of cytoplasmic N and C termini flanking two distinct transmembrane domains, which are joined by a cytoplasmic loop. This loop, together with the C terminus, functions as the ATP binding site and forms the catalytic core of the cyclase (Cooper & Crossthwaite 2006). Despite their structural similarities, ACs share little sequence homology, other than in the catalytic unit, and show different tissue distributions and modes of regulation (summarised in Table 1-1). All ACs are activated to some extent by the stimulatory G protein Gs, while the majority of isoforms are inhibited by Gi. AC activators such as Gs promote a conformational change in the cytosolic domains which form the catalytic unit that facilitates catalysis, while Gi maintains the catalytic unit in an open conformation, preventing formation of the catalytic site and inhibiting ATP binding (Cooper & Crossthwaite 2006, Tesmer et al 1997). ACs may also be regulated by intracellular Ca^{2+} levels, and phosphorylation by PKA and PKC (Table 1-1).

AC isoform	**Major tissue distribution**	**Gαs response**	**Gαi response**	**Gβγ response**	**Other regulatory mechanisms**
AC1	Brain	+	-	-	Ca^{2+}/Calmodulin (CaM)
AC2	Lung, brain	+	No effect	+	PKC
AC3	Pancreas, olfactory epithelium	+	-	No effect	Ca^{2+}/CaM
AC4	Widespread	+	No effect	+	PKC
AC5	Heart	+	-	No effect	PKA, PKC; Ca^{2+}
AC6	Heart, kidney	+	-	No effect	PKA, PKC; Ca^{2+}
AC7	Widespread	+	No effect	No effect	PKC
AC8	Brain, pancreas	+	-	-	PKC; Ca^{2+}
AC9	Widespread	+	-	No effect	PKC; Ca^{2+}

Table 1-1 Summary of expression and regulatory properties of the 9 adenylyl cyclase isoforms. Adapted from (Willoughby & Cooper 2007).

1.3 cAMP effectors

So far, cAMP signal transduction has been described from agonist binding to a GPCR and stimulation of Gαs through to AC production of cAMP. This section will discuss the 3 effectors of cAMP: PKA, Epac and cyclic nucleotide-gated channels (Figure 1-5).

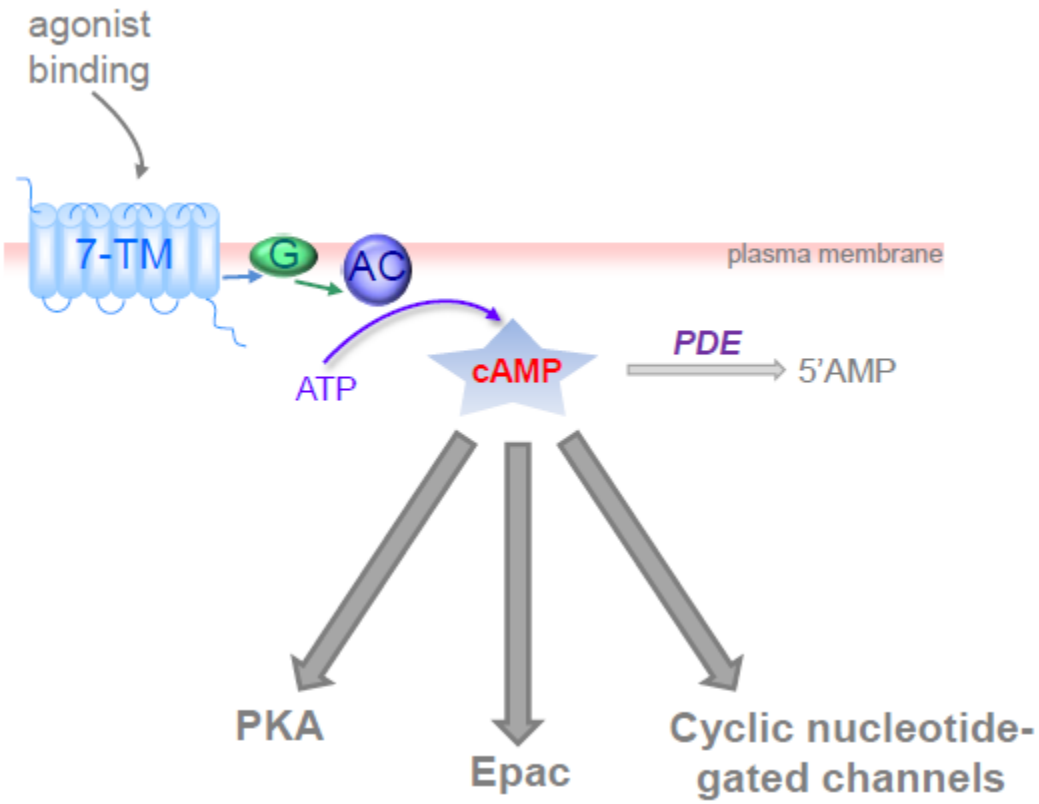

Figure 1-5 An overview of cAMP signaling in cells. cAMP is produced following stimulation of 7 transmembrane domain receptors at the plasma membrane. These receptors couple to G-proteins, which activate adenylyl cyclases leading to the conversion of ATP into cAMP. The effects of cAMP within the cell are mediated by three distinct effector proteins: PKA, Epac and cyclic nucleotide-gated channels. cAMP is degraded by phosphodiesterase enzymes. 7-TM, 7 transmembrane domain receptor; G, G-protein; AC, adenylyl cyclase; PKA, cAMP-dependent protein kinase A; PDE, phosphodiesterase.

1.3.1 PKA

Protein kinase A (PKA) was the first effector of cAMP to be identified. It was originally isolated in the laboratory of Ed Krebs in 1968, and is considered to be the principal cellular receptor for cAMP (Walsh et al 1968). The PKA holoenzyme is a heterotetramer consisting of two regulatory (R) subunits and two catalytic (C) subunits. PKA regulatory subunits are encoded by four genes, which are subdivided into two classes: RI (RIα and RIβ) and RII (RIIα and RIIβ). PKA catalytic subunits are encoded by three genes: Cα, Cβ and Cγ. The subunits possess distinct biochemical and physical properties, and are differentially expressed in different cell types (Tasken & Aandahl 2004). Under resting conditions i.e. conditions of low intracellular cAMP, the regulatory subunits maintain the catalytic subunits in an inactive conformation (Taylor et al 1990). When cAMP levels rise within the cell, two molecules of cAMP bind to each R subunit. This leads to dissociation and activation of the C subunits (Figure 1-6). PKA C subunits phosphorylate their target proteins on serine-threonine residues, which are typically found in a consensus sequence of R-R-X-S/T-X- (Kemp et al 1977).

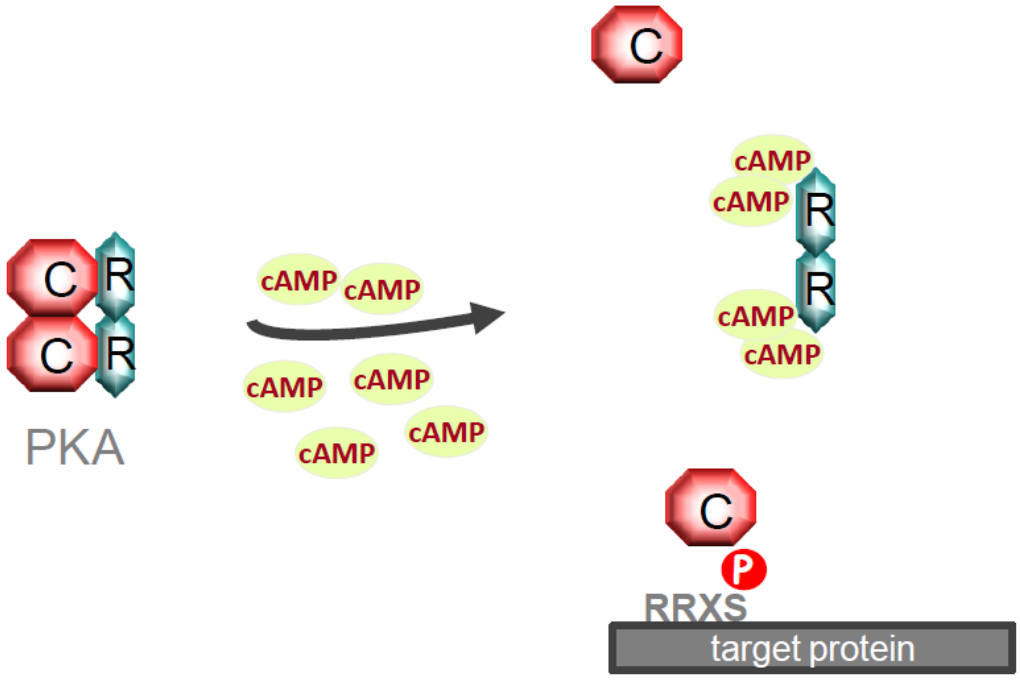

Figure 1-6 Activation of the cAMP-dependent protein kinase (PKA) in response to increased cAMP levels. In resting conditions when cAMP is low, PKA exists as an inactive heterotetramer with an R_2C_2 conformation. The two catalytic subunits are maintained in an inhibited state by the two regulatory subunits. When cAMP levels are elevated, cAMP binds to the R subunits with 2:1 stoichiometry. Active C subunits are released and go on to phosphorylate downstream targets involved in a diverse range of biological processes, such as transcription (Delghandi et al 2005), ion exchange (Marx et al 2002) and muscle contraction (Solaro 2008).

The actions of PKA are opposed by specific protein phosphatases (PPs), which dephosphorylate PKA substrates. PP1 and PP2A are the most abundant of the serine/threonine protein phosphatase families (Virshup & Shenolikar 2009), and are themselves composed of a number of regulatory and catalytic subunits which direct their substrate recognition and specificity (Hubbard & Cohen 1993). PKA is also counterbalanced by the actions of protein kinase inhibitor (PKI), a small naturally occurring polypeptide that exists in the cytoplasm. Three isoforms of PKI have been identified, α, β and γ, which also show cell type-specific expression. PKI binds to free catalytic subunits of PKA and inhibits them in a similar way to PKA regulatory subunits (Taylor et al 2005), and synthetic forms of PKI have been developed as a means of studying the roles of PKA in cellular signaling processes (Murray 2008).

1.3.2 Epac

The exchange proteins activated by cAMP (Epacs) were first discovered in 1998, when de Rooij and co-workers showed that the small GTPase Rap1 could be activated by cAMP independently of PKA (de Rooij et al 1998). Epacs are the most recent effectors of cAMP to be identified. Two isoforms of Epac are known, Epac1 and Epac2, which show differing tissue distributions. Epac1 is abundant in blood vessels, kidney and adipose tissue, whereas Epac2 is highly expressed in the central nervous system and some hormonal tissues (Kawasaki et al 1998, Kilpinen et al 2008). Structurally, the two isoforms are closely related; however, Epac2 has a second cAMP binding domain at its N terminus (de Rooij et al 2000).

Functionally, Epacs act as guanine nucleotide exchange factors (GEFs) for the Rap family of small GTPases. Binding of cAMP to Epac promotes its GEF function, leading to activation of Rap1 and Rap2 via an exchange of GDP for GTP (de Rooij et al 2000). The lack of specific pharmacological inhibitors of Epac initially complicated investigations into the functions of Epac; however, the development of the Epac-selective cAMP analogue 8-pCPT-2'-O-Me-cAMP, also known as 007, has helped identify roles for Epac in a diverse range of biological processes (Enserink et al 2002). These include: effects on synaptic plasticity and memory retrieval (Ouyang et al 2008), potentiation of insulin secretion

(Shibasaki et al 2007), and effects on cardiac contractility via modulation of calcium handling at the sarcoplasmic reticulum (Dodge-Kafka et al 2005) (discussed further in Section 1.6.4.1). Many of these functions are also regulated by PKA, indicating that there is significant crosstalk between PKA and Epac signaling pathways (Bos 2003).

1.3.3 Cyclic nucleotide-gated channels

Cyclic nucleotide-gated channels (CNG) are ion channels, belonging to the superfamily of voltage-gated ion channels, and are activated by cAMP or cGMP binding. Cyclic nucleotides regulate the opening of these channels by binding directly to a conserved cyclic nucleotide-binding domain (CNBD) on the channel (Yu et al 2005). Binding induces a conformational change that serves to open the channel pore. CNG channels are cation channels, and allow the flow of Na^+, K^+ and Ca^{2+} ions across membranes, thus converting cyclic nucleotide signals into changes in membrane potential and intracellular calcium levels. CNG channels were originally identified in retinal photoreceptors and olfactory neurons, and play a vital role in transducing sensory signals (Kaupp & Seifert 2002). CNG channels are also present at high levels in the sino-atrial node and conduction system of the heart, where they are involved in the control of cardiac automaticity (Baruscotti et al 2010).

1.4 cAMP degradation by phosphodiesterases

cAMP is vital to many cellular signal transduction cascades. Cyclic nucleotide phosphodiesterases (PDEs) represent the only means of degrading cAMP within cells, and are therefore crucial regulators of all aspects of cAMP signaling (Conti & Beavo 2007, Houslay 2010). PDEs hydrolyse cAMP and cGMP to 5'AMP and 5'GMP respectively, with varying degrees of specificity. Twenty one genes encoding PDEs have been identified in the human genome, and these have been grouped into 11 PDE families, based on their amino acid sequences, structures, enzyme kinetics, modes of regulation and tissue distributions (Conti & Beavo 2007, Houslay 2010) (Figure 1-8 and Table 1-2). Of the 11 families identified, PDEs 3, 4, 7 and 8 selectively hydrolyse cAMP, while PDEs 5, 6 and 9

are selective for cGMP, and PDEs 1, 2, 10 and 11 hydrolyse both cyclic nucleotides with varying efficiencies (Conti & Beavo 2007). To date, over 50 PDE isoforms are known. These are generated via alternative mRNA splicing and the use of multiple promoter sites (Houslay et al 2007).

1.4.1 The 11 PDE families: structures and specificities

1.4.1.1. Catalytic and regulatory domains

PDEs have a modular structure, consisting of catalytic and regulatory domains. Although they do not share a high sequence identity, the structural information available indicates that the catalytic domain is highly conserved across the 11 families (Xu et al 2000, Zhang et al 2004). The catalytic domain of PDEs consists of 16 α-helices grouped into 3 subdomains, which form a deep binding pocket for either cAMP, cGMP or inhibitors. Many of the amino acid residues which are conserved across all PDEs are found in this active site pocket (Zhang et al 2004). The catalytic domain also co-ordinates one Zn^{2+} ion and one Mg^{2+} ion (Xu et al 2000), which are essential for catalysis. Substrate selectivity is thought to be determined by the position of an invariant glutamine residue which stabilises the purine ring of the cyclic nucleotide in the binding pocket. Depending on the orientation of this residue in the pocket, the enzyme will have specificity for either cAMP, cGMP, or both (Zhang et al 2004). This is referred to as a “glutamine switch mechanism”. Other amino acids conserved across PDE families are also thought to contribute to substrate and inhibitor specificities by altering the shape and size of the binding pocket (Wang et al 2005).

PDEs differ markedly at their N and C termini, and may possess a number of different regulatory domains. These include regions for ligand binding, inhibition of the catalytic domain, kinase phosphorylation sites and domains which mediate oligomerisation (Conti & Beavo 2007). These will be discussed further in the following sections on individual PDE families. The characteristics of the 11 PDE families are summarised in Table 1-2 below, and their domain structure is illustrated in Figure 1-8.

PDE family	Genes	Substrate (cAMP, cGMP)	Regulation	Tissue distribution	Inhibitors
PDE1	A, B, C	Both; cGMP preferentially	Ca^{2+}/CaM; PKA phosphorylation	Heart, vascular smooth muscle, CNS	Vinpocetine
PDE2	A	Both; equal kMs	cGMP via GAF domains	Adrenal, heart, liver, brain	EHNA, BAY 60-7550
PDE3	A, B	cAMP	Inhibited by cGMP. Activated by PKA/Akt phosphorylation	Cardiovascular system, lung, liver, adipose tissue	Cilostamide, Cilostazol, Milrinone
PDE4	A, B, C, D	cAMP	UCR1 and UCR2; phosphorylation by PKA and ERK1/2		Rolipram, Roflumilast
PDE5	A	cGMP	cGMP via GAF domains; PKA and PKG	Lung, heart, smooth muscle, brain, kidney	Sildenafil, Tadalafil, Zaprinast, Dipyridamole
PDE6	A, B, C	cGMP	Rhodopsin, transducin; cGMP via GAFs	Retinal photo-receptors	PDE5 inhibitors
PDE7	A, B	cAMP		Pancreas, brain, heart, immune system	ASB16165
PDE8	A, B	cAMP	PAS domain	Heart, reproductive tissue, bowel, thyroid	Dipyridamole
PDE9	A	cGMP		Brain	Zaprinast, BAY 73-6691
PDE10	A	Both; cAMP preferentially	GAF domains; PKA	Brain	Novel agents (see text), IBMX, Zaprinast
PDE11	A	Both; similar Km and V_{max} values	GAF domains	Skeletal muscle, kidney, liver, prostate, testis	IBMX, Dipyridamole, Tadalafil

Table 1-2 Summary of the characteristics of the 11 PDE families.

1.4.1.2. PDE1

PDE1 enzymes are encoded by 3 genes, A-C, all of which have multiple promoter sequences and splice variants (Zhao et al 1997). PDE1 enzymes have two Ca^{2+}/calmodulin (CaM) binding domains in their N termini (Lynch et al 2006). Binding of 4 Ca^{2+} ions to these domains results in PDE activation, and increased cyclic nucleotide hydrolysis. PDE1 isoforms can hydrolyse both cAMP and cGMP, but have around a 20 fold lower kM for cGMP and therefore preferentially hydrolyse cGMP over cAMP (Francis et al 2001). The N terminus of PDE1 also contains a PKA phosphorylation site, and PKA phosphorylation of PDE1 has been shown to reduce its affinity for Ca^{2+}/CaM (Yan et al 1996).

PDE1 isoforms are particularly highly expressed in the cardiovascular and central nervous systems, where they have been linked with vascular smooth muscle proliferation (Rybalkin et al 1997) and the pathogenesis of Parkinson's disease (Laddha & Bhatnagar 2009). PDE1 activity is inhibited by the synthetic alkaloid vinpocetine (Hagiwara et al 1984).

1.4.1.3. PDE2

Three splice variants of PDE2 are encoded by a single gene, *PDE2A* (Rosman et al 1997). PDE2, PDE5, PDE6, PDE10 and PDE11 enzymes all contain two GAF domains within their N terminus (Ho et al 2000, Lynch et al 2006). GAF domains are cGMP binding domains, and the acronym 'GAF' derives from the first proteins these domains were identified in (c**G**MP-specific PDEs, ***A****nabena* adenylyl cyclases and the *E. coli* transcription factor **F**h1a) (Aravind & Ponting 1997). Binding of cGMP to the GAF domains stimulates the hydrolytic activity of the enzyme. PDE2 enzymes hydrolyse both cAMP and cGMP with roughly equal kMs (Erneux et al 1981). The GAF domains promote cAMP hydrolysis; thus, a small rise in intracellular cGMP will lead to a fall in cAMP levels. However, higher levels of cGMP will then compete out cAMP at the active site of the enzyme, leading to cGMP hydrolysis with inhibition of cAMP hydrolysis (Martinez et al 2002).

PDE2 is mainly expressed in the cytosol of the adrenal gland, heart, liver and brain (Yanaka et al 2003, Yang et al 1994). In the brain, it is thought to regulate hippocampal cGMP signaling and NMDA receptor-linked signaling pathways involved in the

development of memory (Suvarna & O'Donnell 2002). PDE2 is inhibited by erythro-9-(2-hydroxy-3-nonyl)adenine (EHNA) (Podzuweit et al 1995), which binds to both the catalytic and regulatory regions of the PDE (Michie et al 1996), and by BAY 60-7550, an EHNA analogue with greater potency (Boess et al 2004).

1.4.1.4. PDE3

PDE3 enzymes are encoded by 2 genes (Reinhardt et al 1995). PDE3 isoforms show high specificity for cAMP, and, although cGMP can also bind the active site of the enzyme with a similar affinity, it is only weakly hydrolysed (Manganiello et al 1995). cGMP can, therefore, inhibit cAMP hydrolysis by PDE3 (Francis et al 2001). PDE3 isoforms can be phosphorylated and activated by both PKA and Akt (PKB) (Manganiello & Degerman 1999).

PDE3A and PDE3B show quite distinct tissue distributions. PDE3A is highly expressed in the cardiovascular system and lung while PDE3B mRNA is abundant in adipose tissue and hepatocytes (Reinhardt et al 1995). In fact, PDE3B plays a crucial role in regulating the effects of cAMP on insulin signaling in insulin responsive-tissue (Zhao et al 2002). PDE3B is phosphorylated and activated by Akt in response to insulin stimulation of sensitive cells, leading to increased cAMP hydrolysis, and effects on lipolysis, gluconeogenesis and glycogenolysis (Geoffroy et al 2001). The role of PDE3 in the cardiovascular system is discussed further in Section 1.4.3. PDE3 is inhibited by cilostamide, milrinone and cilostazol, which is used clinically in the treatment of intermittent claudication (Strandness et al 2002).

1.4.1.5. PDE4

Members of the PDE4 family are of particular importance in the cardiovascular system (Houslay et al 2007). This family will be discussed in detail in Section 1.4.2 below.

1.4.1.6. PDE5

Three splice variants of the PDE5A gene have been identified, which differ at their N termini (Kotera et al 1999, Rybalkin et al 2003). PDE5A is cGMP-specific, and contains GAF-A and GAF-B domains (McAllister-Lucas et al 1995). Binding of cGMP to the GAF

domains facilitates N terminal phosphorylation of the PDE by PKA and PKG, which activates cGMP hydrolysis (Francis et al 2001, Smith et al 2000). PDE5 is most highly expressed in the lung, heart, cerebellum, kidney and smooth muscle (Giordano et al 2001). cGMP is an important regulator of smooth muscle function (Figure 1-7) (Rybalkin et al 2003), and a number of commercially successful clinical inhibitors of PDE5 have been developed which regulate smooth muscle tone. These include sildenafil (Viagra, Pfizer Pharmaceuticals) and tadalafil (Cialis, ICOS/GlaxoSmithKline) which are both licensed for the treatment of erectile dysfunction (Boolell et al 1996, Padma-Nathan et al 2001). PDE5 inhibitors are also used in the treatment of pulmonary artery hypertension (Singh 2010).

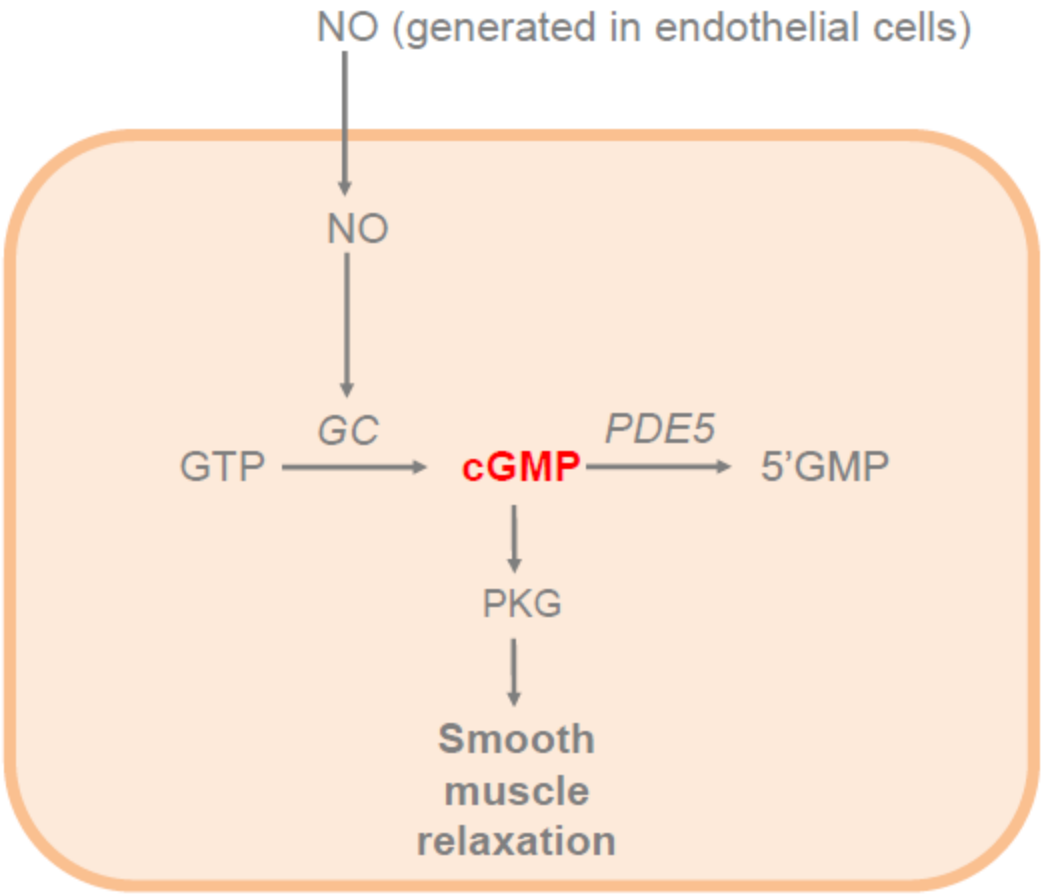

Figure 1-7 Regulation of vascular smooth muscle tone by cGMP and PDE5.
Adapted from (Rybalkin et al 2003). Nitric oxide (NO) is a well known mediator of vasodilation. NO activates guanylyl cyclase (GC) in smooth muscle cells, leading to increased cGMP levels and activation of the cGMP-dependent protein kinase (PKG). PKG phosphorylates several downstream targets, including myosin phosphatase (Surks et al 1999) and smooth muscle calcium channels (Fukao et al 1999). This leads to reduced intracellular Ca^{2+} concentration and sensitivity to Ca^{2+}, and decreased smooth muscle tone (Schlossmann et al 2003). PDE5 hydrolyses cGMP and is found in all types of smooth muscle, where it plays a pivotal role in regulating this pathway (Rybalkin et al 2003). Inhibitors of PDE5 increase cGMP levels and therefore enhance smooth muscle relaxation.

1.4.1.7. PDE6

Three genes (A-C) encode phosphodiesterase 6 isoforms. PDE6 is cGMP-specific, and is highly expressed in the retina, on the internal membrane of photoreceptors (Gillespie & Beavo 1988). These specialised cells contain light sensitive pigments (opsins) which become activated upon exposure to light. Changes in cGMP levels help to transmit this signal to the plasma membrane. In the dark, PDE6 adopts an inactive conformation, with an inhibitory γ subunit occupying the catalytic site (Mou et al 1999). Excitation of the visual pigment rhodopsin by light activates the coupled G protein transducin (Arshavsky et al 2002). Transducin then binds to PDE6, displacing this inhibitory subunit and leading to enhanced cGMP hydrolysis (Mou & Cote 2001). The resulting fall in cGMP levels leads to closure of cGMP-gated ion channels, membrane hyperpolarisation and generation of a membrane potential at photoreceptor synapses (Cote 2004). PDE6 also possesses 2 regulatory GAF domains, and binding of cGMP to these domains increases the affinity of the PDE for the inhibitory subunit (Mou et al 1999). There are no specific inhibitors of PDE6; however, most PDE5 inhibitors also show some inhibition of PDE6 due to their similar catalytic sites. In fact, some retinal effects have been observed with sildenafil (Luu et al 2001), although the clinical relevance of this is unclear.

1.4.1.8. PDE7

The PDE7-11 families are the least well studied phosphodiesterases. PDE7 enzymes are specific for cAMP and are coded for by two genes (Beavo 1995). PDE7B is principally expressed in the pancreas, brain and heart (Hetman et al 2000). PDE7A is expressed at high levels in cells of the immune system, particularly in T lymphocytes, where it is upregulated in response to T-cell activation (Smith et al 2003). Thus, inhibition of PDE7 by compounds such as the novel PDE7A inhibitor ASB16165 may have important anti-inflammatory effects (Kadoshima-Yamaoka et al 2009).

1.4.1.9. PDE8

PDE8A and PDE8B comprise the PDE8 family (Fisher et al 1998, Hayashi et al 1998). Members of this family are highly specific for cAMP (Francis et al 2001), and contain a PAS domain (named after 3 proteins which express this domain: **P**eriod circadian protein, **A**ryl

hydrocarbon receptor nuclear translocator protein and **S**ingle minded protein) (Tei et al 1997). Recent structural studies suggest that this domain may allosterically regulate cAMP binding to the PDE (Wang et al 2008).

PDE8A is highly expressed in the testis, ovary and bowel (Fisher et al 1998), while PDE8B expression appears to be thyroid-specific (Hayashi et al 1998). PDE8 is insensitive to most PDE inhibitors, including the broad spectrum PDE inhibitor isobutyl-methylxanthine (IBMX) (Wang et al 2008). IBMX binds to a common region of the catalytic domain of many PDE families, acting as a non-specific, competitive inhibitor of cyclic nucleotide binding (Huai et al 2004). Structural studies of the catalytic domain of PDE8A1 have identified 2 additional helices in this region, and defined an important role for Tyr748 in the prevention of IBMX binding. Mutation of this residue to phenylalanine increased the sensitivity of the PDE to non-specific PDE inhibitors (Wang et al 2008). PDE8 activity is blocked by the inhibitor of platelet aggregation dipyridamole with an IC50 of 5-9μM (Fisher et al 1998).

Recently, PDE8A has been linked to calcium handling in the heart by a study employing PDE8A knockout mice. PDE8A transcripts and protein were detected in the ventricles of wildtype mice hearts, and altered calcium transients were observed in PDE8A-/- mice compared with wildtype mice, following stimulation with the synthetic β-agonist isoproterenol (Patrucco et al 2010). Thus, PDE8A may play a role in the regulation of cardiac contraction. PDE8B expression has also been found to be upregulated in the hippocampus of Alzheimer's disease brains, therefore both PDE8 subfamilies may represent important therapeutic targets (Perez-Torres et al 2003).

1.4.1.10. PDE9

PDE9 is encoded by a single gene with a large number of splice variants (Guipponi et al 1998). The mRNA of certain PDE9 isoforms is highly expressed in the cortex and hippocampus of the brain (Reyes-Irisarri et al 2007). Interestingly, the locus for PDE9A maps to a region of chromosome 21 which is known to be associated with several genetic disorders, including bipolar affective disorder (Guipponi et al 1998). PDE9A is also

inhibited by the PDE5 inhibitor zaprinast, but not by the non-selective inhibitor IBMX (Soderling et al 1998). Recently, a novel selective inhibitor of PDE9, BAY 73-6691, has been developed which enhanced formation and retention of long term memory in rats (van der Staay et al 2008), indicating the possibility of an important neuropsychiatric role for enzymes of this family.

1.4.1.11. PDE10

Members of the PDE10A family show dual specificity for cAMP and cGMP, with kMs of 0.05 and 3µM respectively. The V_{max} for cAMP is 4.7 times higher and therefore this substrate is preferentially hydrolysed. In common with PDE2, 5, 6 and 11, they contain 2 GAF domains at their N termini, which may have a regulatory function (Soderling et al 1999). The PDE10A2 isoform is PKA phosphorylated on its N terminus at Thr16, and this modification appears to regulate its subcellular distribution between the cytosol and Golgi in rat neurons (Kotera et al 2004).

PDE10A is highly expressed in the brain, particularly the caudate nucleus and putamen, and is also abundant in the thyroid and testis (Fujishige et al 1999). PDE10A knockout mice display decreased behavioural responses to stimuli, and altered striatal dopaminergic signaling consistent with rodent models of schizophrenia (Siuciak et al 2006, Siuciak et al 2008). Novel selective PDE10A inhibitors are currently being developed and are of great interest as potential therapeutic agents for this complex disorder (Hage et al 2009, Malamas et al 2011a, Malamas et al 2011b).

1.4.1.12. PDE11

The single PDE11 gene has 4 splice variants (Fawcett et al 2000). PDE11A has GAF domains at its N terminus, and PDE11A mRNA is seen predominantly in skeletal muscle, kidney, liver, prostate and testis. PDE11 hydrolyses cAMP and cGMP with similar kM and V_{max} values, and is likely to regulate levels of both cyclic nucleotides *in vivo* (Fawcett et al 2000). Structurally, PDE11 shares most similarity with PDE5, and is modestly inhibited by tadalafil (Francis 2005); however, it is also inhibited by IBMX and dipyridamole (Fawcett et al 2000). Studies of PDE11-/- mice have suggested a role in the generation of

spermatozoa. This has raised concerns because of the increasing use of tadalafil (Wayman et al 2005), though evidence linking PDE11A to spermatogenesis in humans is lacking (Francis 2005).

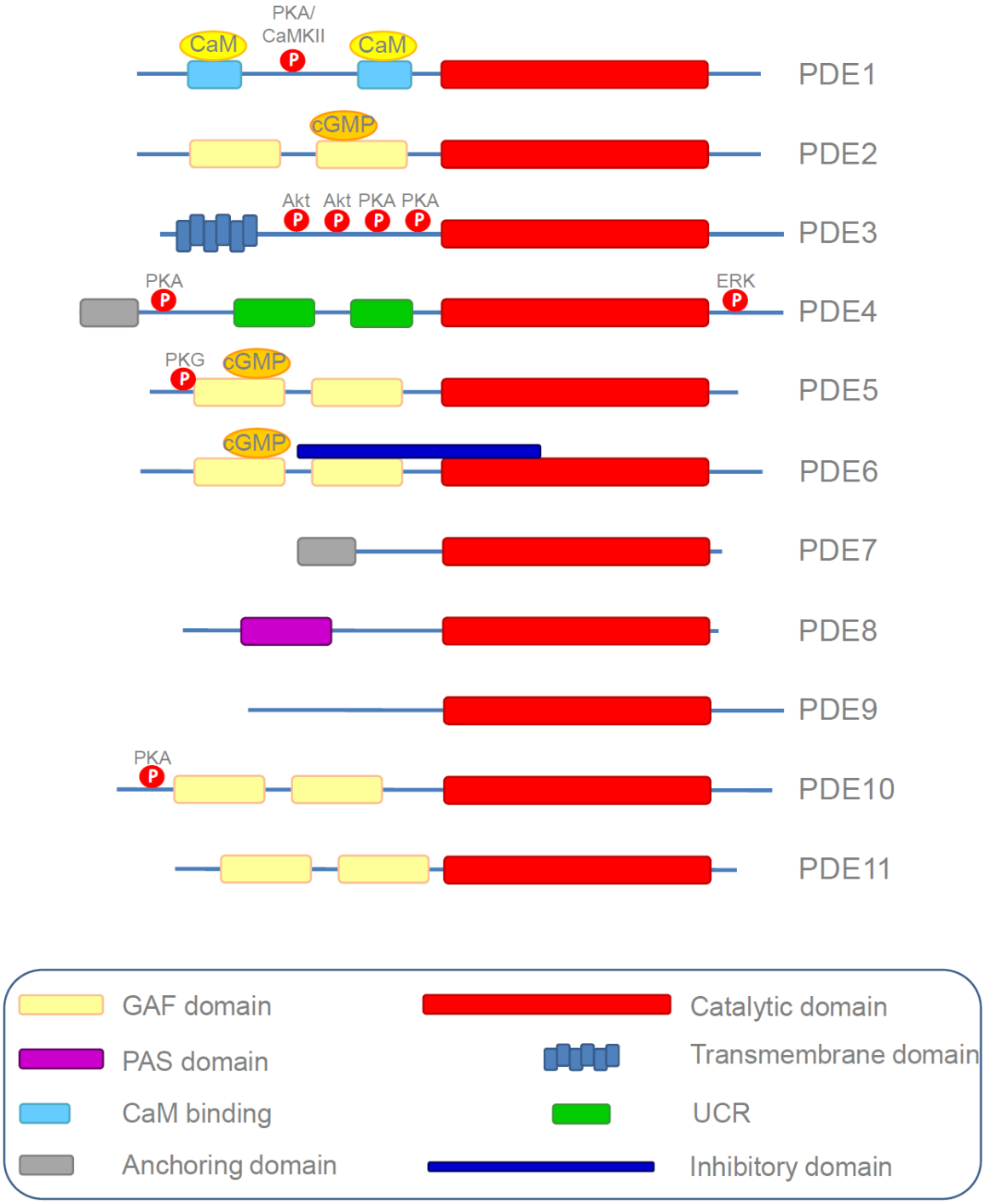

Figure 1-8 Domain structures of PDE families 1-11. Adapted from (Conti & Beavo 2007). The 11 PDE families shown are grouped according to their differing structures, kinetics, tissue distributions and modes of regulation. The domain structures of PDE1-11 and the associated regulatory mechanisms for each family are described in Sections 1.4.1.2. to 1.4.1.12., and summarised in Table 1-2.

1.4.2 PDE4

PDE4 enzymes are cAMP-specific phosphodiesterases. The PDE4 family is encoded by 4 genes: PDE4A, PDE4B, PDE4C and PDE4D. These are located on chromosomes 1, 5 and 19 in humans, and encode over 20 different isoforms, by means of alternate mRNA splicing and the use of multiple promoter sites (Houslay & Adams 2003, Houslay et al 2007). PDE4 isoforms have a modular structure, consisting of an isoform-specific N terminus, regulatory domains termed upstream conserved regions (UCRs), the conserved catalytic domain common to all PDE families, and a subfamily-specific C terminal region (Lynch et al 2007).

1.4.2.1. N terminal region

The N terminal region of PDE4 is unique to each isoform, and plays an important role in protein-protein interactions and intracellular targeting of the enzyme (Houslay 2010). For example, PDE4D5 isoforms are targeted to the signaling scaffold protein β-arrestin at the plasma membrane to modulate β-adrenergic signaling (Bolger et al 2006, Bolger et al 2003).

1.4.2.2. Upstream conserved regions (UCRs)

PDE4 isoforms can be sub-classified based on the presence of two regulatory domains, UCR1 and UCR2 (Houslay & Adams 2003) (Figure 1-9 and Table 1-3). Long forms possess both UCR1 and UCR2, as well as two linker regions (LRs) which join them to the catalytic domain. Short forms lack UCR1 and the first linker region, and super short forms lack UCR1 and LR1, and also have an N terminal truncation of UCR2. Finally, dead short isoforms such as PDE4A7 lack UCR1 and UCR2, and have a truncated catalytic domain which renders them catalytically inactive (Houslay et al 2007). It is thought that UCR1 and UCR2 interact to form a regulatory module that co-ordinates phosphorylation of the PDE by PKA and ERK and regulates the catalytic domain (MacKenzie et al 2000, MacKenzie et al 2002).

PDE4 Class	Truncations	Isoforms
Long	None	4A4/5, 8, 10, 11 4B1, 3, 4 4C1, 2, 3 4D3, 4, 5, 7, 8, 9
Short	Lack UCR1	4B2 4D1, 2
Super short	Lack UCR1, LR1, N terminus of UCR2	4A1 4B5 4D6
Dead short	Lack UCR1 and UCR2; truncated catalytic unit	4A7

Table 1-3 Classification of PDE4 isoforms.

1.4.2.3. Conserved catalytic domain

The catalytic domain of PDE4 is common to all the PDE families, and has already been discussed (Section 1.4.1.1.).

1.4.2.4. Unique C terminal region

The final exon of PDE4 genes encodes a subfamily-specific C terminal region. The significance of this region is not fully understood, but may involve a regulatory function, as recent structural studies of PDE4 isoforms bound to inhibitors have revealed. The sequence differences in this region have been exploited by our laboratory to make the subfamily-specific antisera used in Chapters 4 and 5, and in the design of more specific PDE inhibitors (Burgin et al 2010, Houslay & Adams 2010).

Figure 1-9 Domain structure of PDE4 isoforms. Adapted from (Houslay & Adams 2003). PDE4 isoforms are classified by the presence or absence of two upstream conserved regions (UCR1 and UCR2). Long isoforms have both UCR1 and UCR2. Short isoforms lack UCR1, while super short isoforms lack UCR1 and have an N terminal truncation of UCR2. A fourth form of PDE4, 'dead short', exists, which lacks both UCR1 and UCR2, and is therefore catalytically inactive.

1.4.2.5. Cellular functions of distinct PDE4 subfamilies

Members of the PDE4B subfamily have been linked with schizophrenia. *DISC1* and *DISC2* (**D**isrupted **I**n **Sc**hizophrenia 1 and 2) were identified as novel genes spanning a translocation breakpoint strongly associated with schizophrenia in a large Scottish family (Blackwood et al 2001). The *DISC1* gene encodes a scaffolding protein which can interact with the UCR2 domain of PDE4B (Millar et al 2005). The DISC1-PDE4B interaction is maximal in resting cells, and it appears that upon stimulation of cells leading to a rise in cAMP, DISC1 may activate and release this sequestered PDE4B to regulate local cAMP levels. Consistent with this, mutations in DISC1 which give rise to schizophrenia and depression phenotypes in mice are located within binding sites for PDE4B (Millar et al 2007).

PDE4B also appears to play a role in the immune system. Much of this information has come from studies of PDE4B knockout mice. PDE4B -/- mouse macrophages display defective production of the inflammatory cytokine TNFα (Jin et al 2005), and neutrophils from these mice showed altered expression of surface adhesion molecules and defective chemotaxis (Ariga et al 2004). Thus, there is considerable interest in defining the role of this subfamily in the pathogenesis of chronic inflammatory diseases such as asthma and chronic obstructive pulmonary disease (COPD) (Houslay et al 2007).

The PDE4D subfamily consists of 11 isoforms, PDE4D1-11. Several of these isoforms have only recently been discovered (PDE4D6-11), and so little is known about their respective functions (Chandrasekaran et al 2008, Gretarsdottir et al 2003, Lynex et al 2008, Wang et al 2003). PDE4D knockout mice exhibit behavioural effects consistent with an anti-depressive phenotype, suggesting an important role for this subtype in the pathophysiology and pharmacotherapy of depression (Zhang et al 2002).

PDE4D is also important in the cardiovascular system. PDE4D knockout mice develop progressive age-related cardiomyopathies and are susceptible to exercise-induced cardiac arrhythmias and sudden cardiac death, despite apparently normal global cAMP signaling (Lehnart et al 2005). The mechanisms behind these effects will be discussed in Section 1.6.5.

1.4.2.6. PDE4 inhibition and its clinical implications

As PDE4 is the major cAMP-hydrolysing family in many cells types, it represents a promising therapeutic target. PDE4 subfamilies have been implicated in diseases of the central nervous system, immunological and respiratory systems. The increasing clinical use of PDE5 inhibitors such as sildenafil has spurred attempts to replicate this success with PDE4 inhibitors. Rolipram (4-[3-(Cyclopentyloxy)-4-methoxyphenyl]-2-pyrrolidinone) is the prototypical inhibitor of enzymes of the PDE4 family (Figure 1-10). This compound is directed against the active site of the PDE, binding competitively with cAMP, and therefore inhibits all PDE4 family members with similar efficacy (Spina 2008). Due to this blanket inhibition of PDE4, the development of PDE4 inhibitors for clinical use has unfortunately been hampered by unacceptable dose-related side-effects, in particular

emesis, diarrhoea and headache (Pages et al 2009). Pharmaceutical companies have, therefore, focused considerable efforts on designing compounds and methods of drug delivery with an improved therapeutic range (Pages et al 2009). In the past 12 months, one such PDE4 inhibitor, Roflumilast (DAXAS®, Bristol-Myers-Squibb) (Figure 1-10), has been licensed in the UK for the treatment of severe exacerbations of COPD, a highly prevalent, poorly reversible inflammatory disease of the airways. In Phase III clinical trials, Roflumilast was found to reduce the requirement for steroid and antibiotic treatments, and reduce hospitalisation resulting from exacerbations of COPD (Calverley et al 2009, Fabbri et al 2009).

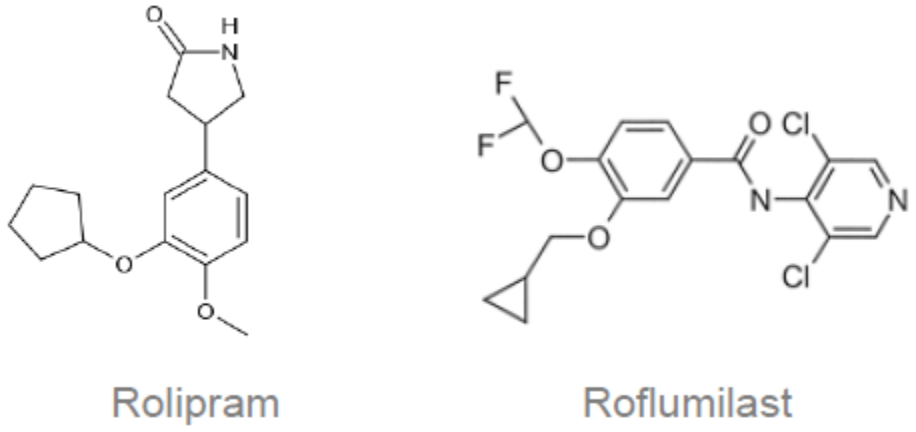

Figure 1-10 Chemical structures of the PDE4 inhibitors Rolipram and Roflumilast. Adapted from (Pages et al 2009).
Rolipram (chemical formula $C_{16}H_{21}N0_3$) is the prototypical inhibitor of PDE4 family members. Roflumilast is a long-acting PDE4 inhibitor which has been developed by the pharmaceutical industry for the treatment of severe exacerbations of chronic obstructive pulmonary disease (COPD) (Calverley et al 2009).

Designing selective inhibitors of PDE4 subfamilies remains challenging, due to the high homology of PDE4 catalytic domains. A recent study, which determined the co-crystal structures of PDE4 bound to a number of inhibitors, revealed a novel mode of inhibitor binding to PDE4, involving UCR2 rather than the active site (Burgin et al 2010). This study may facilitate the design of small molecule PDE4 subtype-specific inhibitors which exhibit less class-related side-effects (Houslay & Adams 2010).

1.4.3 The roles of individual PDE isoforms in the heart

PDE2, PDE3, PDE4 and PDE5 are the main phosphodiesterase families expressed in the heart; however, it has recently been appreciated that members of the PDE1 (Vandeput et al 2007) and PDE8 families (Patrucco et al 2010) also show cardiac expression. PDE3 and PDE4 provide the major cAMP-hydrolysing activity in rat cardiac myocytes, with PDE4 having double the activity of PDE3 (Mongillo et al 2004, Richter et al 2005). Together these 2 families account for around 90% of cAMP hydrolysis (Richter et al 2005), with the PDE4D subfamily contributing around 60% of the cAMP hydrolysing activity of PDE4 (Mongillo et al 2004).

The non-redundant nature of individual PDE4 isoforms is well illustrated in the heart. Several recent studies have highlighted the importance of PDEs in normal cardiac signaling, and specific roles for individual PDE isoforms in key processes such as excitation-contraction coupling are now being defined. For example, the long phosphodiesterase isoform PDE4D3 has been shown to exist in a complex with the ryanodine receptor (RyR2) which mediates calcium release from the SR, and maintain it in a PKA-hypophosphorylated state (Dodge-Kafka et al 2005). This interaction is discussed further in Section 1.6.4.1.

1.4.3.1. PDE4D5 and β-arrestin

Specific PDE isoforms have also been shown to associate with β-adrenergic receptors to mediate distinct effects. β-arrestins are cytosolic proteins which are recruited to activated β2-adrenergic receptors following phosphorylation of the C terminal tail of the receptor by G-protein receptor coupled kinase (GRK) (Kohout & Lefkowitz 2003, Perry & Lefkowitz 2002). This prevents further interaction of the receptors with G-proteins, thereby desensitising the receptor and leading to uncoupling of the response. Our laboratory and others have shown that β-arrestins recruit a subpopulation of PDE4D5 to activated β2-adrenergic receptors to promote receptor desensitisation by hydrolysing the cAMP which has already been produced (Perry et al 2002) (Figure 1-11). Binding sites for β-arrestin on PDE4D5 have now been mapped to its unique N terminal region, and the C terminal of the conserved catalytic domain (Bolger et al 2006, Bolger et al 2003). Thus, PDE4D5 limits the activity of membrane-bound PKA, by reducing local cAMP levels (Perry et al 2002).

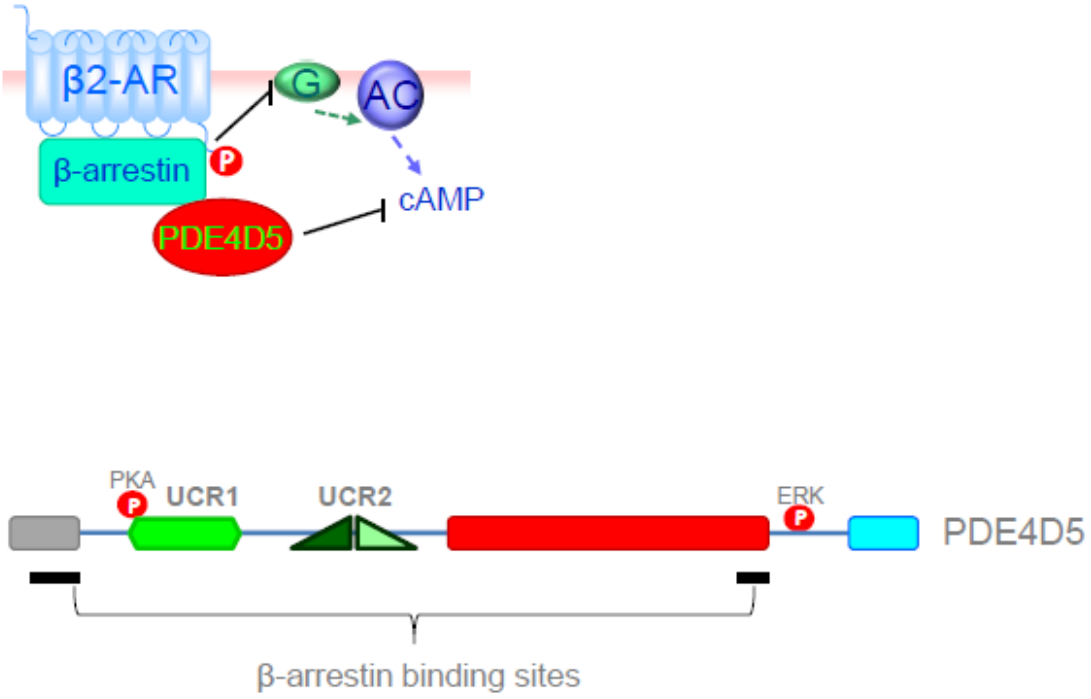

Figure 1-11 Interaction of β-arrestin and PDE4D5.
Upper panel: Schematic representation of β-arrestin binding to the GRK-phosphorylated β2-adrenergic receptor. This interaction sterically inhibits association of the receptor with stimulatory G proteins, and reduces adenylyl cyclase activation and cAMP production. β-arrestin recruits the long PDE4 isoform PDE4D5 to the receptor, leading to hydrolysis of cAMP which has already been produced, and promoting receptor desensitisation. Lower panel: PDE4D5 possesses 2 distinct interaction sites for β-arrestin. The N terminal site overlaps an interaction site for the scaffold protein RACK1, so alterations in RACK1 levels may modulate β-adrenergic signaling (Bolger et al 2006).

1.4.3.2. PDE4D8 and β-adrenergic receptors

The β1 and β2 adrenergic receptors are structurally very similar; however, they play very distinct physiological and pathological roles within the heart (Xiao et al 2004) (described in Section 1.2.1). For almost a decade, it has been known that PDE4D5 is recruited to the β2-adrenergic receptor complex, via its association with β-arrestin (Perry et al 2002), though no PDEs were known to associate with the β1 receptor. Recently, PDE4D8 has been shown to bind directly to the unoccupied β1-adrenergic receptor. Agonist occupancy of the receptor leads to dissociation of the PDE-receptor complex. PDE binding may induce a conformational change in the receptor, or recruit other proteins to the receptor (Richter et al 2008). Thus, β1 and β2-adrenergic receptors may be regulated in distinct manners by PDEs (Figure 1-12).

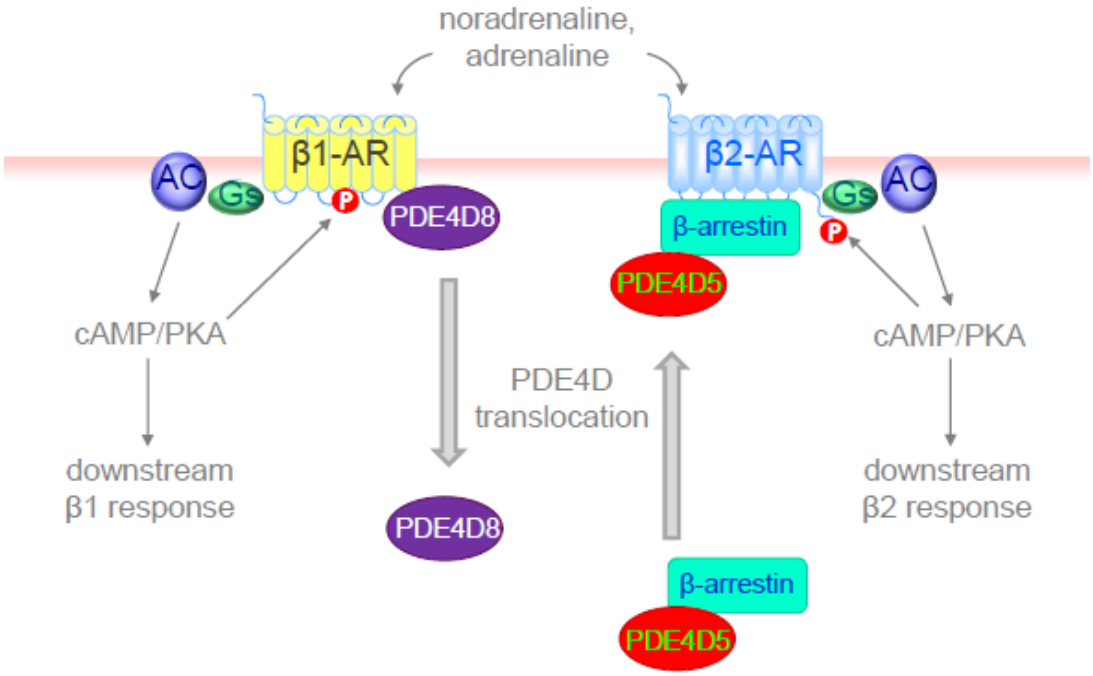

Figure 1-12 Specific interactions of PDE4D isoforms with β-adrenergic receptor subtypes. Adapted from (Richter et al 2008). β1 and β2-adrenergic receptors form complexes with different PDE4D isoforms. The modes of interaction and the effects of agonist binding are distinct for the two receptor subtypes. PDE4D8 is recruited to the unoccupied β1 receptor under basal conditions and associates directly to regulate cAMP levels, whereas PDE4D5 translocates to the occupied β2 receptor and interacts with it via the signaling scaffold protein β-arrestin (Perry et al 2002, Richter et al 2008).

1.5 Excitation-contraction coupling and cAMP signaling in the heart

1.5.1 Cardiac contraction

Cardiac excitation-contraction coupling (ECC) is the process by which electrical excitation of the heart is coupled to contraction and relaxation (Bers 2002). Under normal conditions, the heart acts as its own pacemaker. In the course of one heart beat, a wave of depolarisation initiates in the sino-atrial node and propagates through the atria and atrio-ventricular node into the ventricles (Bers & Despa 2006). During this depolarisation, Ca^{2+} enters the cells via L-type Ca^{2+} channels, generating an inward calcium current (I_{Ca}) (Figure 1-13). L-type Ca^{2+} channels are located mainly at the junction of the cardiac

myocyte plasma membrane (sarcolemma) and the sarcoplasmic reticulum (SR), a specialised intracellular Ca^{2+} store. Increasing I_{Ca} leads to a local increase in Ca^{2+} at the SR, and triggers the release of large quantities of stored Ca^{2+} ions from it via Ca^{2+} release channels known as ryanodine receptors (RyR). This process is referred to as Ca^{2+}-induced Ca^{2+} release (CICR). Free intracellular Ca^{2+} ($[Ca^{2+}]i$) then binds to the myofilaments which comprise the muscle fibres, and triggers contraction (Bers & Despa 2006). This process must be reversed for relaxation to occur. Ca^{2+} is transported back into the SR via the sarco(endo)plasmic reticulum Ca^{2+} ATPase pump (SERCA), and into the extracellular space through the actions of the sarcolemmal Na^{+}/Ca^{2+} exchanger (NCX). $[Ca^{2+}]i$ falls, Ca^{2+} dissociates from the myofilaments, and a single heartbeat is completed, ready for the cycle to begin again (Figure 1-13).

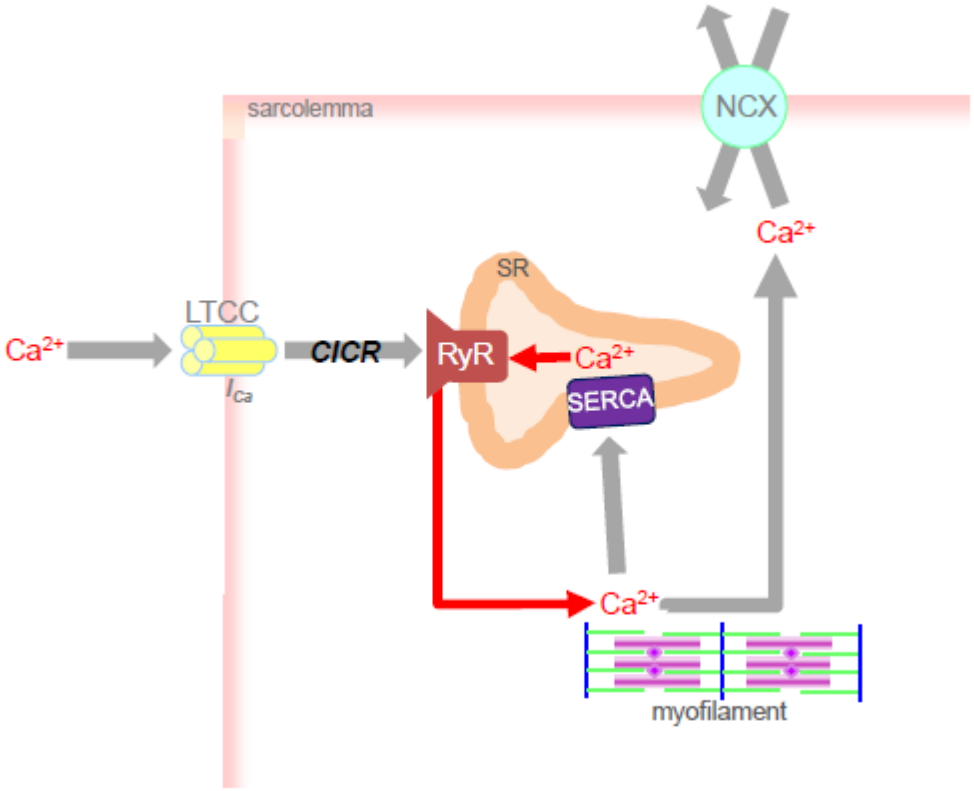

Figure 1-13 Excitation-contraction coupling in the heart. Adapted from (Bers & Despa 2006). Ca^{2+} enters cardiac myocytes via L-type calcium channels, leading to a local rise in $[Ca^{2+}]i$ at the SR. This triggers Ca^{2+}-induced release of Ca^{2+} from SR ryanodine receptor channels. Free Ca^{2+} associates with the myofilaments, leading to contraction of the heart (known as systole) and the propulsion of oxygenated blood around the body. Ca^{2+} is then taken back up into the SR or expelled from the cytosol through Na^{+}/Ca^{2+} exchangers at the sarcolemma, leading to a corresponding fall in $[Ca^{2+}]i$. Ca^{2+} dissociates from the myofilaments, and relaxation (diastole) occurs. The relaxed heart is able to fill with blood, ready for the process to begin again.

Myofilaments are composed of protein-rich bundles of thick and thin filaments. Thick filaments are formed primarily from the protein myosin, while thin filaments are predominantly actin-based. The basic contractile unit of the myofilament is the sarcomere (Figure 1-14). Contraction occurs when the head domain of myosin in the thick filament interacts with actin in the thin filament to form crossbridges, causing the filaments to slide past each other in an ATP-dependent process, and the sarcomeres to shorten (Hernandez et al 2001) (Figure 1-14). A number of proteins are associated with the thick and thin filaments to regulate this process. The best studied of these is the troponin complex associated with the thin filament.

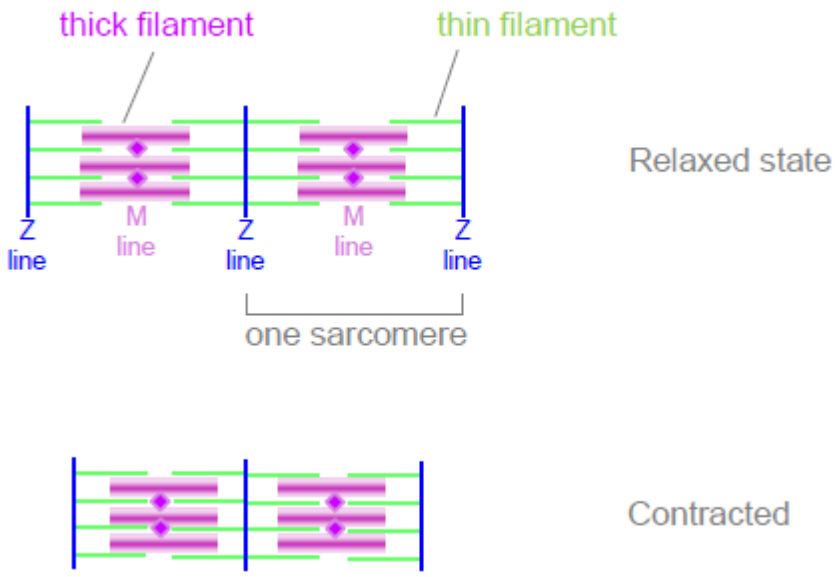

Figure 1-14 Contraction and relaxation of the sarcomere.
The sarcomere is the smallest contractile unit of the myofilament, measuring about 2 µm in length. Up to 100 000 aligned sarcomeres may be present in one myofilament. Sarcomeres are composed of overlapping thick and thin filaments. Thin filaments are formed by actin, and are anchored to the Z lines (Z discs) which form the boundaries of one sarcomeric unit. Thick filaments are composed of myosin, and are cross-linked to the M line in the middle of the sarcomere, and linked to the Z line by the giant protein titin, which maintains the structure of the sarcomere (Engel et al 2004). The M and Z lines are named for their microscopic appearance, and the overlapping nature of the myofilament proteins gives rise to the characteristic striations of these cells. For contraction to occur, nerve impulses must be transmitted to the sarcolemma where they give rise to an action potential. This action potential triggers the influx of Ca^{2+} ions and Ca^{2+} release from the SR described above. Ca^{2+} binds to the myofilament as described below, and leads to conformational changes which allow actin and myosin to interact. The globular head of myosin forms crossbridges with actin, and the filaments slide over each other leading to shortening of the sarcomere. This movement is powered by the intrinsic ATP hydrolytic activity of the myosin head (Engel et al 2004).

1.5.2 The troponin complex and tropomyosin

A number of proteins are associated with actin and myosin in the sarcomere, such as the myosin-associated proteins myosin-binding protein-C and titin, and the actin-associated proteins troponin and tropomyosin (summarised in Table 1-4). These proteins have multiple functions, including maintaining the structural integrity of the myofilament, organising the filaments during development, and modulation of contraction (Engel et al 2004, Solaro 2010), and mutations in them have been linked to the development of various diseases, such as familial hypertrophic cardiomyopathy (Hernandez et al 2001).

In the heart and skeletal muscle, the principal regulators of contraction are the thin filament-associated proteins troponin (Tn) and tropomyosin (TM) (Engel et al 2004). Tropomyosin is a 65kDa coiled coil of 2 α-helices, measuring 41nm by 2nm. In the thin filament, actin monomers are polymerised to form long helical strands. TM lies in a groove on the surface of the actin helices, with each TM molecule spanning 7 actin monomers.

Protein	MW , Structure	Location	Function
Actin	42kDa, globular monomer	Thin filament, as helical polymer	Forms thin filament, interacts with myosin
α-actinin	190kDa dimer	Z line	Integrates Z line, binds and ? links actin and titin
Myosin	520kDa hexamer	Thick filament, as helical polymer	Forms thick filament, ATP-dependent filament sliding
Myosin-binding protein C	250kDa	Binds myosin at 43nm intervals	Myofibrillogenesis in development, stabilises filament, modulates contraction
Titin	3MDa	Extends from Z line to M line	Sarcomeric development and stability
Tropomyosin	65kDa coiled coil dimer	Thin filament, one molecule stretches over 7 molecules of actin	Filament stability and regulation of contraction
Troponin	80kDa complex of 3 subunits	Thin filament; one per tropomyosin	Regulation of contraction

Table 1-4 Structure and function of major sarcomeric proteins. Adapted from (Engel et al 2004).

The 80kDa Tn complex consists of 3 proteins: troponin C (TnC), troponin T (TnT) and troponin I (TnI), which are named according to their first identified functions. Tn**C** is a **C**a^{2+}-binding protein, Tn**T** binds to **t**ropomyosin, and Tn**I** forms the **i**nhibitory subunit of the heterotrimeric complex (Engel et al 2004). The crystal structure of the core Tn complex in Ca^{2+} saturated and unsaturated forms has now been solved, which has provided a wealth of information on how this complex regulates contraction (Takeda et al 2003).

1.5.2.1. Troponin C

TnC is the Ca^{2+}-binding component of Tn, and functions as a Ca^{2+} sensor. TnC is an 18kDa globular protein, with binding sites for TnT, TnI and tropomyosin (Engel et al 2004). TnC exists in a dumbbell shape, with 2 globular heads with helix-loop-helix conformations, linked by a central α-helix. These globular heads contain the Ca^{2+} binding sites. In the Ca^{2+} unbound form, the helices flanking the Ca^{2+} binding sites of TnC are closely aligned, creating a 'closed' conformation. Upon Ca^{2+} saturation, the protein undergoes a conformational change, with these helices rotating to create a more open conformation which exposes TnI binding sites on TnC. TnC and TnI are then able to interact (Takeda et al 2003) (Figure 1-16).

1.5.2.2. Troponin T

TnT provides the main link between the Tn complex and tropomyosin. TnT has a molecular weight of approximately 34kDa, and possesses an extended N terminal region and a globular C terminal head. Interactions with TM occur via the N terminus, while the C terminus of the protein contains binding sites for TnC and TnI. One Tn complex binds to one TM molecule via TnT, thus Tn and TM are both equally spaced along the actin filament. A helical region of TnT interacts with helix 2 of TnI to form a rigid structure know as the IT arm (Figure 1-16), which may be involved in TM positioning on actin (Takeda et al 2003).

1.5.2.3. Troponin I

Cardiac troponin I (TnI) is a key mediator of cardiac contraction and relaxation, and forms the inhibitory component of the troponin complex (Layland et al 2005, Solaro 2010, Solaro et al 2008). TnI is a 210 amino acid protein with a molecular mass of 28kDa. A 32 amino acid N terminal extension is present in cardiac isoforms of TnI, but lacking in skeletal muscle isoforms of the protein (Solaro et al 1976). This N terminal region contains two neighbouring consensus PKA phosphorylation sites, at Ser22 and Ser23. TnI consists of 4 α-helices, and contains sites for actin and TnC binding at its C terminus (Galinska-Rakoczy et al 2008, Takeda et al 2003) (Figure 1-15). Helix 2 participates in the IT arm with TnT (Takeda et al 2003).

Figure 1-15 Schematic representation of the domain structure of cardiac troponin I (cTnI). TnI is a 210 amino acid protein integral to the contraction of cardiac and skeletal muscle. TnI contains binding sites for TnT and TnC (as shown), and exists in a heterotrimeric complex with these proteins to regulate actin-myosin interactions. The C terminus of TnI is able to interact directly with actin (Galinska-Rakoczy et al 2008). The cardiac isoform of TnI, cTnI, possesses a unique 32 amino acid N terminal extension which contains 2 consensus PKA phosphorylation sites. cTnI is, therefore, subject to regulation by β-adrenergic/cAMP/PKA signaling pathways (Solaro et al 1976). The 4 α-helices of TnI are indicated in purple, and amino acids defining each helix are numbered.

At low $[Ca^{2+}]i$, equivalent to a period of cardiac relaxation, TnT and TnI hold TM in a fixed position on actin. This conceals the myosin binding sites on actin, preventing actin-myosin interactions and inhibiting crossbridge formation. During contraction, release of Ca^{2+} from SR stores leads to a transient rise in cytosolic Ca^{2+} levels (Bers 2002). Ca^{2+} binds to TnC, causing a conformational change that exposes binding sites for TnI on TnC (Engel et al 2004, Galinska-Rakoczy et al 2008, Galinska et al 2010, Howarth et al 2007). Binding of TnI helix 3 to the N lobe of TnC in the presence of Ca^{2+} acts as a molecular switch and induces release of the C terminal of TnI from interactions with actin-TM (Takeda et al 2003). This results in a shift in the position of TM on actin, and exposes myosin binding sites. Crossbridge formation can then occur, leading to force generation and contraction (Figure 1-16).

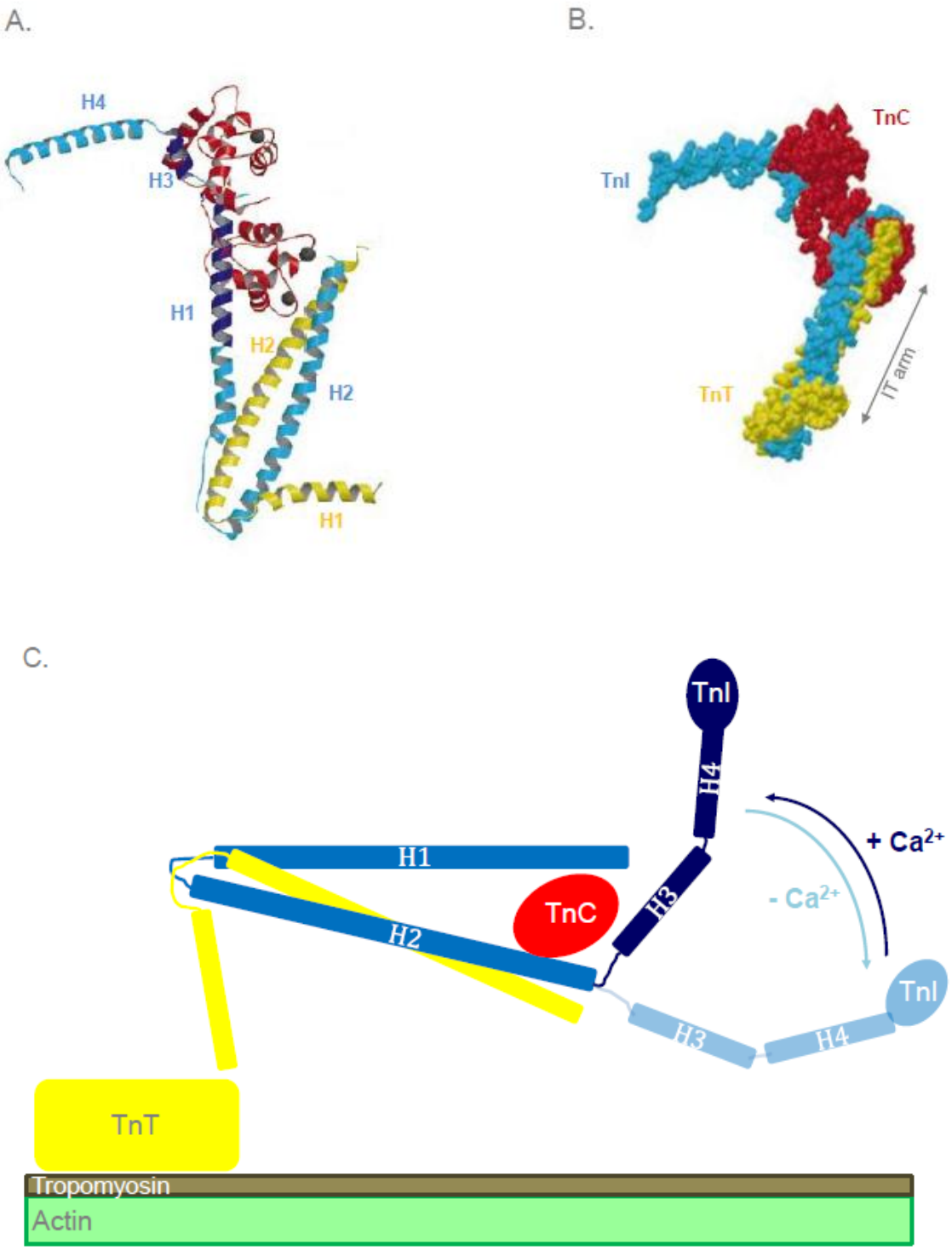

Figure 1-16 Structure of the core troponin complex. Adapted from (Takeda et al 2003). Troponin I is shown in blue, troponin C in red and troponin T in yellow. The three Ca^{2+} ions co-ordinated by TnC are shown as black spheres. A. Predicted secondary structure of the complex. The second α-helices of TnI and TnT form a rigid coiled coil known as the IT arm, which anchors the complex to tropomyosin on the thin filament. Ca^{2+} binding to TnC leads to a conformational change which frees the C terminal of TnI from interactions with actin. This alters the position of TM relative to the thin filament, and promotes actin-myosin interactions (Takeda et al 2003). B. Space-filling model of the complex. C. Movement of the flexible C terminus of TnI in response to Ca^{2+} binding to TnC. Adapted from (Takeda et al 2003). In the absence of Ca^{2+}, TnI remains associated with actin (light blue conformation). When Ca^{2+} binds to TnC, helix 3 of TnI acts as a molecular switch, and the C terminus of TnI moves away from actin (dark blue conformation).

1.5.2.4. Modification of TnI by phosphorylation

Phosphorylation of myofilament proteins represents a major mechanism for the modulation of myofilament calcium sensitivity and contractile properties. A number of cardiac proteins are phosphorylated in response to cAMP signal transduction cascades, including the RyR and LTCC (Bers 2004), leading to enhanced cardiac output. TnI has been extensively studied in this regard, as it contains a number of phosphorylation sites for different kinases which may modify its effects (Solaro 2008). The most important phosphorylation of TnI is mediated by PKA.

PKA Phosphorylation of TnI

Phosphorylation of TnI by PKA is required to allow the heart to respond appropriately to increased physiological demands. Physiological stressors, such as exercise and fear, result in a rise in the levels of the circulating catecholamines adrenaline and noradrenaline. Catecholamines bind to and stimulate β-adrenergic receptors on the surface of cardiac myocytes. This triggers increased intracellular generation of the second messenger cAMP, which activates PKA, leading to the phosphorylation of key downstream targets involved in excitation-contraction coupling. These include the RyR at the SR and myofilament proteins such as TnI. The net result is to increase the rate and efficiency of myocyte contraction, and improve cardiac output (Mudd & Kass 2008) (Figure 1-17).

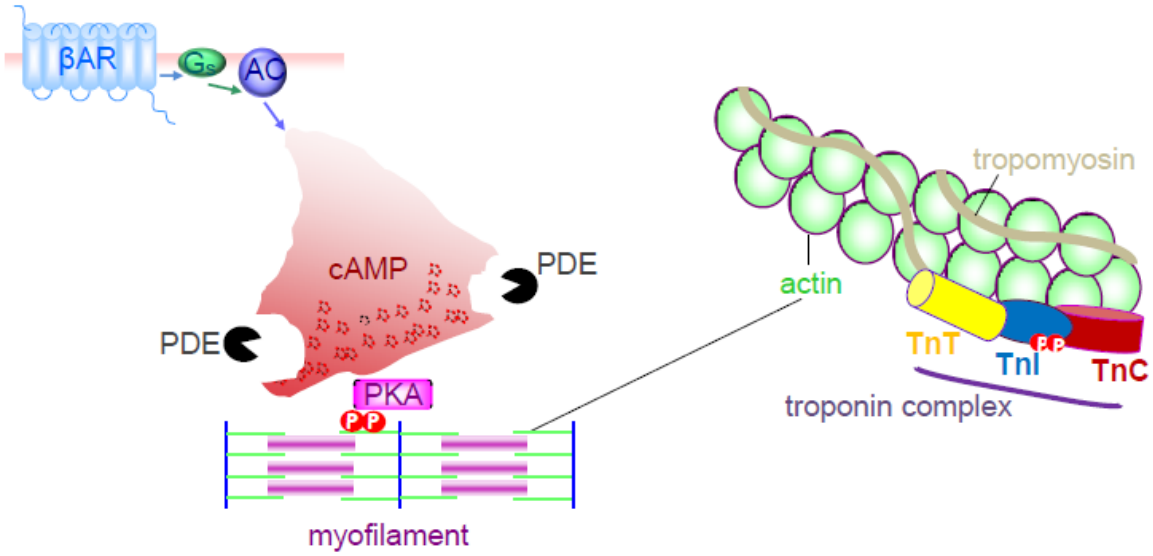

Figure 1-17 Regulation of myofilament contraction by a cAMP/PKA signal transduction cascade. β1-adrenergic stimulation couples the receptor to the stimulatory G protein Gαs. This activates adenylyl cyclase isoforms, leading to the generation of cAMP and activation of PKA. PKA then goes on to phosphorylate key proteins involved in ECC, such as TnI at the cardiac myofilament. PKA phosphorylation of TnI has both positive inotropic and lusitropic effects. The right panel illustrates the location of the Tn complex on the thin filament.

TnI is phosphorylated by PKA at two neighbouring serine residues (Ser 22/Ser23 in mouse, Ser23/Ser24 in humans) on a unique 32 amino acid N terminal region of the protein only present in cardiac isoforms of the protein (Solaro et al 1976). This dual phosphorylation causes a conformational change in TnI which diminishes its interaction with TnC, resulting in a desensitisation of the myofilament to Ca^{2+} which promotes relaxation (Stelzer et al 2007). Cardiac relaxation is also referred to as lusitropy. Earlier relaxation facilitates rapid filling of the heart with blood during diastole, contributing to improved cardiac output.

Transgenic (TG) mouse models expressing TnI PKA phosphorylation site mutants have been invaluable in investigating the functional consequences of this modification *in vivo*. TG mice were generated with cardiac expression of the short skeletal muscle (ss) isoform of TnI. This isoform lacks the unique N terminal extension containing the PKA sites (Figure 1-18). ssTnI transgenic mice demonstrated attenuation of the lusitropic response to β-adrenergic stimulation (F'Entzke et al 1999). Mice with Ser22/Ser23 to Alanine mutations (cTnI-S22A/S23A) showed a similar response, with abolition of the expected reduction in myofilament sensitivity to Ca^{2+} following β-stimulation (Pi et al 2002, Pi et al 2003).

Conversely, animals overexpressing an S22D/S23D mutant version of full length TnI, which mimics constitutive phosphorylation, showed enhanced left ventricular relaxation *in vivo* (Takimoto et al 2004). Thus, PKA phosphorylation of TnI on Ser22/Ser23 in response to β-agonist stimulation contributes to the enhanced rate of myocardial relaxation which is necessary to cope with increased cardiac demand (Biesiadecki et al 2010, Solaro & van der Velden 2010) .

Figure 1-18 Mutations in TnI PKA sites have important functional consequences for relaxation of the heart.
TG mice expressing TnI mutants lacking a PKA-phosphorylatable N terminus demonstrate reduced lusitropy, whereas lusitropy is enhanced in TnI phospho-mimic animals. Efficient lusitropy (relaxation) aids the rapid filling which is required at high heart rates.

PKA phosphorylation of TnI also has positive effects on cardiac contraction (inotropy). The positive inotropic response to β-agonists is blunted in S22A/S23A animals (Layland et al 2005), while S22D/S23D animals display significantly enhanced contractile function at baseline and an increased rate of crossbridge cycling (Takimoto et al 2004). Thus, Ser22/Ser23 phosphorylation of TnI by PKA increases both the force of cardiac contraction and the rate of relaxation.

PKC Phosphorylation

α1-adrenergic signaling cascades activate PKC isoforms. TnI is a potential substrate for PKC at 5 sites: Ser22/Ser23, Ser43/Ser45 and Thr144. The most physiologically relevant of these are Ser43/Ser45 and Thr144 (Layland et al 2005). Cardiac myocytes stimulated with PKC activators show immediate phosphorylation of Thr144, followed by Ser43/Ser45, with Ser22/Ser23 only being phosphorylated following prolonged α-agonist exposure (Westfall et al 2005).

The functional outcome of PKC phosphorylation of Ser22/Ser23 is also now disputed, though early work suggested it may confer similar effects to PKA (Noland et al 1995). In fact, phosphorylation of Ser22/Ser23 by PKC may depend greatly on the status of downstream phosphorylation sites, as studies of TnI-S43A/S45A transgenic mice showed enhanced PKCε phosphorylation of Ser22/Ser23 (Roman et al 2004).

PKC phosphorylation of Thr144 has been proposed to sensitise the myofilaments to calcium (Burkart et al 2003, Solaro 2008). Thr144 is the most easily accessible of the potential PKC sites on TnI, and it is proposed that this modification decreases the sliding velocity of the myofilaments, contributing to a negative inotropic response (Burkart et al 2003).

Ser43/Ser45 phosphorylation also contributes to the negative inotropic response. Phosphorylation at these sites was achieved in reconstituted detergent-skinned fibre bundles by stimulation with α-agonists, or by mutation to glutamine (S43D/S45D) to

mimic constitutive phosphorylation. In both cases, maximum Ca^{2+}-activated muscle tension was reduced, probably by decreasing the rate of crossbridge detachment (Burkart et al 2003, Layland et al 2005). This pathway may contribute to the systolic dysfunction observed in heart failure (Layland et al 2005).

1.6 Control of cellular processes by cAMP compartmentalisation

The concept of intracellular compartmentalisation of cAMP arose almost two decades ago from seminal studies performed in cardiac myocytes. Activation of β-adrenergic receptors and prostaglandin receptors was shown to result in similar increases in cellular cAMP; however, whereas β-adrenergic stimulation coupled to cardiac myocyte contraction and PKA phosphorylation of downstream effectors such as TnI, prostaglandin receptor stimulation did not (Brunton et al 1981, Buxton & Brunton 1983). These differences in response could only be explained if cAMP was compartmentalised within the cell. More recently, the use of genetically encoded cAMP sensors has provided further evidence for this concept, allowing the real time direct visualisation of compartmentalised cAMP gradients within intact cardiac myocytes (Zaccolo et al 2005, Zaccolo & Pozzan 2002).

1.6.1 Measurement of cAMP gradients using FRET

Measurement of cAMP gradients has relied largely on fluorescent microscopic techniques, which utilise the phenomenon of fluorescence resonance energy transfer (also known as Förster resonance energy transfer (Förster 1948), or FRET). Real time spatial and temporal changes in cAMP at a subcellular level can be measured with high resolution, illustrating the complexity of cAMP compartmentalisation in living cells (Di Benedetto et al 2008). FRET describes the process of energy transfer between two fluorophores, a donor and an acceptor, which are often cyan- and yellow- fluorescent proteins (CFP and YFP). Excitation of the donor by a particular wavelength will lead to a characteristic emission by the donor. However, if the donor and acceptor are in close proximity, and their emission and excitation spectra overlap, intermolecular FRET occurs

and the acceptor emission is predominantly detected (Figure 1-19). FRET can be used to measure protein-protein interactions, when the donor and acceptor fluorophores are linked to a pair of interacting proteins, and to monitor conformational changes in a single protein (Nikolaev & Lohse 2006).

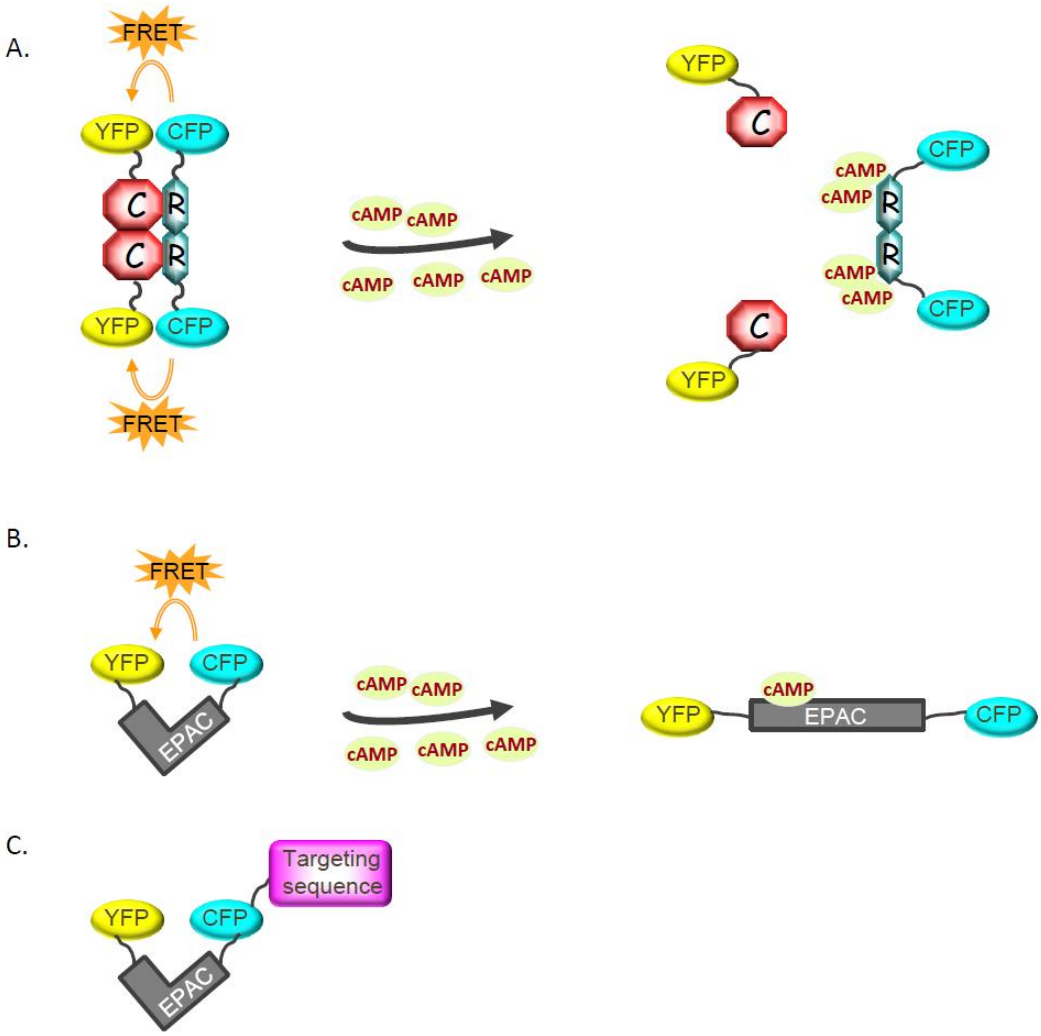

Figure 1-19 Genetic engineering of different FRET sensors to monitor real time changes in cAMP levels in the heart.
A. Sensor based on PKA, with CFP and YFP linked to the R and C subunits of PKA respectively. In basal conditions, cAMP is low and PKA is in its inactive conformation. Excitation of CFP at 440nm will result in FRET, as CFP and YFP are in close proximity, and YFP emission at 545nm. In stimulated cells, cAMP rises. Two molecules of cAMP bind to each PKA-R subunit, leading to dissociation of active catalytic units. CFP and YFP thus diffuse further apart and FRET is reduced, leading to detection of CFP emission at 480nm. Changes in FRET ratio (480/545nm) are directly proportional to R/C subunit dissociation, and therefore to cAMP levels (Zaccolo & Pozzan 2002). B. FRET sensor with CFP and YFP linked to the cAMP-binding domain of Epac1. Binding of cAMP leads to a conformational change in the sensor that moves the fluorophores further apart, abolishing FRET (Nikolaev et al 2004). C. New FRET sensors have now been developed where a targeting sequence is linked to one of the fluorophores to localise the sensor to a particular intracellular region. This enables monitoring of cAMP gradients in different subcellular micro-compartments (Herget et al 2008).

The actions of cAMP are mediated by three types of effector: PKA, cyclic nucleotide-gated channels, and Epac (Bos 2003) (Section 1.3). To date, a variety of FRET sensors based on PKA and Epac have been used to monitor cardiac cAMP dynamics. In fact, the first direct observation that diffusion of cAMP was restricted in the heart was made using a genetically encoded PKA-based cAMP sensor. Zaccolo and Pozzan fused CFP and YFP to the R and C subunits of PKA respectively (Zaccolo & Pozzan 2002). Thus, in conditions of low cAMP, the PKA holoenzyme is intact and FRET can occur. When cAMP rises, it binds to the R subunits, leading to a conformational change that releases active C subunits. The distance between CFP and YFP is increased, and FRET is abolished. Using this technique, β-adrenergic stimulation of neonatal cardiac myocytes was shown to generate multiple discrete microdomains of high cAMP which activated a subset of PKA within the cells (Figure 1-20C). Treatment with the non-specific PDE inhibitor IBMX destroyed these gradients, indicating that PDEs limit the diffusion of cAMP and help to shape cAMP gradients within cells (Figure 1-20D) (Zaccolo & Pozzan 2002).

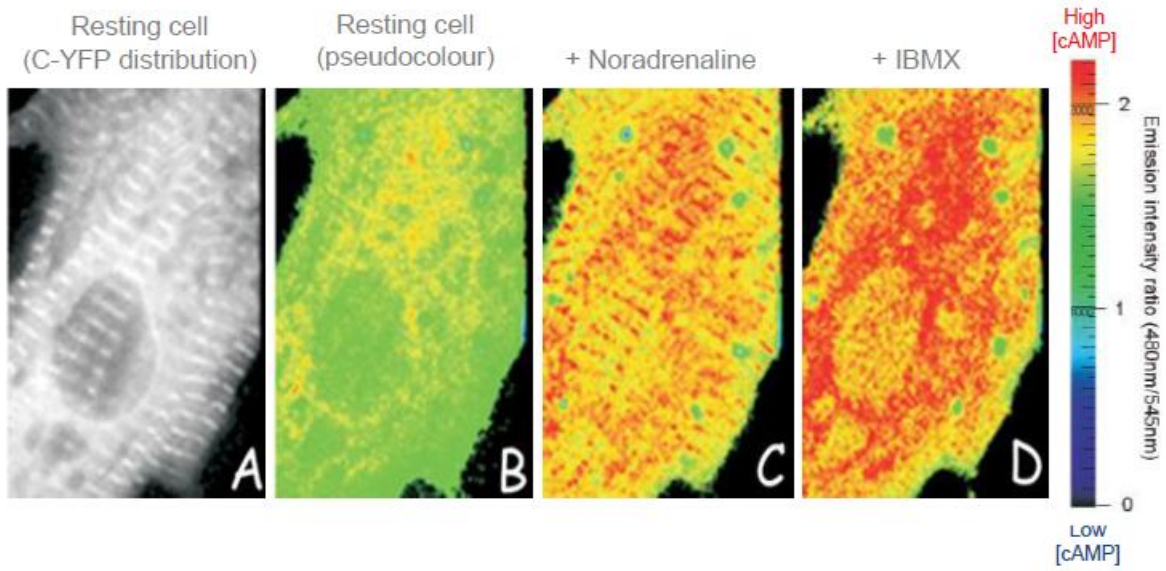

Figure 1-20 Discrete microdomains of cAMP in cardiac myocytes measured by FRET. Adapted from (Zaccolo & Pozzan 2002).
Localised increases in cAMP are illustrated in neonatal cardiac myocytes co-transfected with PKA C-YFP and PKA R-CFP. A. Distribution of C-YFP. B–D. FRET ratios (480/545nm) of the same cell as pseudocolour images. B. Resting cell with relatively uniform distribution of basal cAMP. C. Cell stimulated with 10µM noradrenaline to activate the β-adrenergic signaling pathway. Changes in FRET ratio, which are proportional to cAMP concentration, are seen to occur within discrete subcellular regions, corresponding to cellular striations. D. Same cell treated with 100µM IBMX to non-specifically inhibit phosphodiesterase activity. The compartmentalisation of cAMP generated in response to noradrenaline stimulus is destroyed, indicating that PDE activity limits free diffusion of cAMP, and is necessary to maintain cAMP compartmentalisation.

Several refinements of FRET techniques have been suggested, including the use of genetically engineered mice, which express a FRET sensor as a transgene. Such transgenic sensor animals would express the sensor uniformly across a particular tissue, introducing the possibility of measuring cAMP levels in intact organs or even in whole animals. This approach has already been successfully used to monitor neuronal cAMP levels in transgenic fruit flies with tissue-specific expression of a PKA-based sensor (Lissandron et al 2007, Lissandron & Zaccolo 2006). FRET sensors fused to individual PDE isoforms have also been developed which have, for the first time, allowed measurement of changes in cyclic nucleotide concentration around particular PDEs (Herget et al 2008).

One major drawback of using FRET has been the conversion of measured FRET ratios into absolute cAMP concentrations. Recently, Böerner *et al* addressed this issue using a protocol which allows more precise measurement of cAMP concentrations and kinetics. By calibrating FRET sensors *in vivo*, first by inhibiting adenylyl cyclase activity so that cAMP drops below the threshold detectable by the sensor, then by fully stimulating the sensor with a cell permeable cAMP analogue, actual cAMP levels can now be accurately estimated during a FRET experiment (Boerner et al 2011).

The use of FRET-based techniques has addressed the need for monitoring real time spatial and temporal changes in cAMP. Methods based on activation of all three effectors of cAMP (PKA, Epac and cyclic nucleotide-gated channels) have been developed, and combining these with new approaches, such as sensors linked to PDEs, and transgenic sensor animals, is likely to provide a wealth of information on compartmentalised cAMP signaling at distinct intracellular locations.

1.6.2 PDEs shape cAMP gradients

cAMP is freely diffusible, and could potentially flood the interior of the cell, leading to inappropriate phosphorylation and activation of downstream PKA targets (Houslay et al 2007). This situation is avoided by the opposing action of cyclic nucleotide phosphodiesterases (PDEs). Members of the PDE superfamily provide the only means of

hydrolysing cAMP within the cell, and intracellular targeting of PDEs enables the creation of sub-cellular compartments with high levels of cAMP relative to the surrounding environment (Baillie 2009). Thus, PDEs have the capacity to influence activation of PKA, and the phosphorylation status of PKA target proteins.

1.6.3 Physical compartmentalisation of PKA by AKAPs

The idea of physical compartmentalisation as a mechanism to confer specificity upon the cAMP signaling pathway was first suggested in 1977, when Corbin and co-workers determined that PKA existed in cells as soluble and particulate fractions. Stimulation of the cells with prostaglandin E1 activated the soluble fraction, whereas stimulation with the synthetic β-agonist isoproterenol activated both fractions (Corbin et al 1977). It is now accepted that particulate PKA is in fact PKA bound to scaffold proteins known as A-kinase anchoring proteins (AKAPs) (Kapiloff & Chandrasekhar 2011). AKAPs are a functionally related group of scaffold proteins that organise cellular signaling pathways by physically tethering PKA and other signaling enzymes to specific locations within the cell. The first AKAP was identified in brain tissue, when PKA type II was found to associate with the microtubule-associated scaffold protein MAP2 (Theurkauf & Vallee 1982). Since then, various techniques have been developed to identify AKAPs, often using PKA-RII as a probe. Lohmann and co-workers used radio-labelled RII subunits to probe nitrocellulose membranes, and were able to identify a number of RII binding proteins in bovine brain and heart (Lohmann et al 1984). This “RII overlay” technique has now been adapted and used to characterise many other AKAPs, and, to date, more than fifty AKAPs have been discovered (Kapiloff & Chandrasekhar 2011, Welch et al 2010).

Due to slight differences in their electrophoretic properties between species, and alternative splicing patterns, a complex nomenclature for AKAPs has evolved. For example, the *AKAP5* gene gives rise to three products: AKAP79 (human), AKAP150 (mouse) and AKAP75 (bovine). As well as their diverse nomenclature, the subcellular localisations and associations of AKAPs are also diverse (Table 1-5):

AKAP name(s)	Gene	Associations	Localisation
AKAP-Lbc	*AKAP13*	PKD, PKCη, Rho, 14-3-3	Cytoplasm, actin cytoskeleton
AKAP18 (α, β, γ, δ isoforms) AKAP15	*AKAP7*	Aquaporin-2, PDE4D; SERCA2 and phospholamban (δ)	Plasma membrane (α, β), cytosolic and nuclear (γ, δ), sarcoplasmic reticulum (δ)
AKAP79 AKAP150 AKAP75	*AKAP5*	β1-adrenergic receptor, PP2B, NMDA receptor	Plasma membrane, post-synaptic densities
mAKAP AKAP100	*AKAP6*	PDE4D3, Epac, ryanodine receptor, ERK5, AC5	Nuclear envelope, sarcoplasmic reticulum
Gravin (α, β, γ) AKAP250	*AKAP12*	PKC, cyclin D, β2-adrenergic receptor	Myristoylated membrane, cytoskeleton
Yotiao AKAP350 AKAP450	*AKAP9*	PP1, PP2A, KCNQ1 potassium channel, NMDA receptor	Centrosome, Golgi, plasma membrane
MAP2		Tubulin, F-actin	Microtubules
AKAP220	*AKAP11*	PP1, GSK3β	Vesicles

Table 1-5 Subcellular localisation of a number of important AKAPs. Adapted from (Welch et al 2010).

The defining characteristic of an AKAP is its ability to anchor PKA holoenzyme. AKAPs possess an amphipathic helix of 14-18 amino acids, which creates a hydrophilic region of high binding affinity on the surface of the AKAP (Carr et al 1991). This region associates tightly with a groove in the dimerisation/docking (D/D) domain at the N terminal of the R subunit (Newlon et al 1999, Scott et al 1990). Most AKAPs exhibit high affinity for PKA RII subunits; however, a number of AKAPs have now been identified which can also interact with RI subunits, although typically with 10-100 fold lower affinity. These are referred to as dual specificity AKAPs, and include ezrin and AKAP220 (Herberg et al 2000). Recently, RI-specific AKAPs have also been discovered. At the mitochondria, sphingosine kinase interacting protein (SKIP) binds RI with a nanomolar dissociation constant, similar to the affinity of interaction observed with RII-specific AKAPs (Means et al 2011).

1.6.4 Cardiac AKAPs and modulation of excitation-contraction coupling

As an important second messenger that regulates multiple pathways within the cardiac myocyte, cAMP signals must be tightly controlled and integrated with those from other second messengers such as calcium. The formation of macromolecular signaling complexes, referred to as "signalosomes", or signaling nodes, by AKAPs allows co-ordination of cAMP and other upstream signals with downstream effectors, by incorporating components of different signaling pathways and signal terminating enzymes. Many AKAPs have been characterised in the heart (Figure 1-21), and several of these are known to play a role in excitation-contraction coupling via modulation of calcium handling. For example, AKAP18 isoforms target PKA to SERCA2 (Lygren et al 2007), AKAP79/150 directs PKA phosphorylation of the cardiac LTCC (Gao et al 1997), and mAKAP targets PKA to ryanodine receptors at the SR (Marx et al 2000). The macromolecular complexes that regulate the cardiac RyR, SERCA and voltage-gated potassium channel will be described in more detail below.

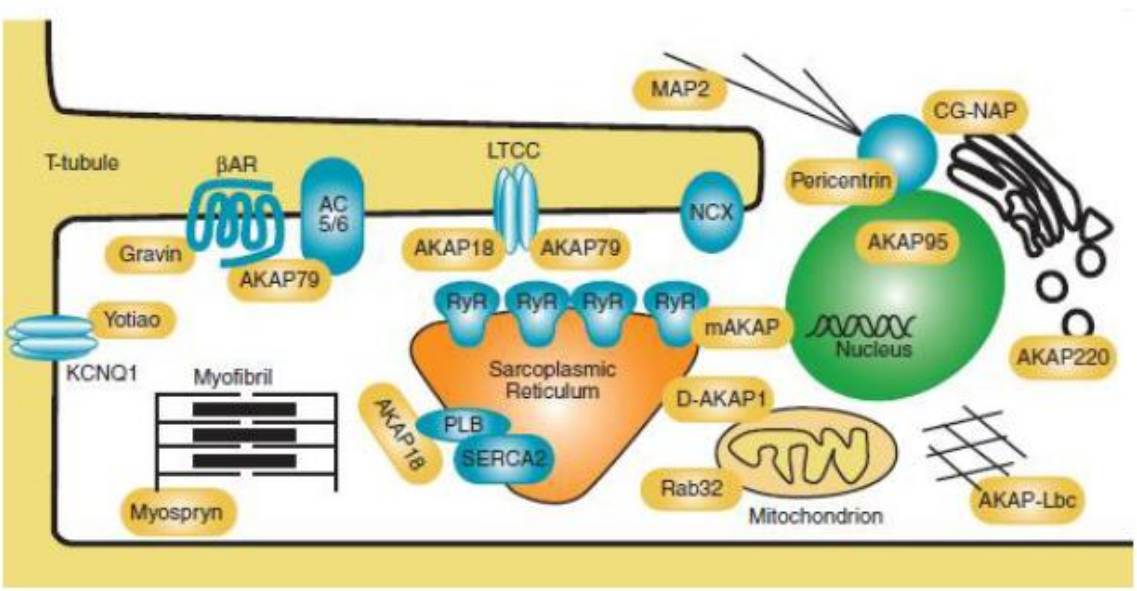

Figure 1-21 Co-ordination of signaling events in the heart is achieved by localised scaffolding of PKA by AKAPs. Adapted from (Welch et al 2010).
Multiple roles for AKAPs have been identified in cardiac myocytes, including excitation-contraction coupling and hypertrophic remodelling, which are described in more detail below. AKAPs have been shown to associate with and regulate the function of a number of key cardiac proteins, including the RyR (mAKAP), LTCC (AKAP18/AKAP79), β-adrenergic receptor (AKAP79/gravin), voltage-gated potassium channel sununit KCNQ1 (yotiao), SERCA2 and phospholamban (AKAP18) (see Table 1-5).

1.6.4.1. mAKAP and the ryanodine receptor

The macromolecular complex formed by the muscle-specific A-kinase anchoring protein (mAKAP) and the ryanodine receptor (RyR) has been well characterised, and will be used as an example of how cAMP/PKA signals can be finely regulated and integrated with other signaling pathways in the heart.

mAKAP is a 250kDa anchoring protein which directs PKA to the nuclear membrane and sarcoplasmic reticulum (SR) in cardiac myocytes (Kapiloff et al 1999, Marx et al 2000, Ruehr et al 2003). The cardiac isoform of the ryanodine receptor (RyR2) is a calcium release channel located predominantly at the SR of cardiac myocytes. A small amount of RyR2 is also located at the nuclear envelope. During EC coupling, calcium influx through L-type calcium channels at the sarcolemma triggers the release of larger quantities of calcium ions from SR stores, via RyR2. This leads to activation of the myofilaments and cardiac contraction (Bers 2004). mAKAP anchors PKA to RyR2, positioning it in close proximity to a known PKA phosphorylation site, Serine 2808, on RyR2. PKA phosphorylation of this residue has been proposed to enhance the open probability of the channel (Marx et al 2000). Anchoring of PKA via mAKAP would allow the phosphorylation status of the channel, and therefore its open probability, to be regulated locally, thus linking compartmentalised cAMP signaling with calcium signals (Ruehr et al 2003). However, it should be noted that controversy exists as to the relevance of Ser 2808 phosphorylation by PKA in modulating channel function (Bers 2012, Xiao et al 2005). A recent study employing transgenic mice, in which this RyR2 phosphorylation site was mutated to alanine, found no discernible difference in either cardiac contractility or calcium handling after induced myocardial infarction between transgenic and wildtype mice (Zhang et al 2012). A number of phosphorylation sites have been identified on RyR2, which may function to regulate channel opening, including a second PKA site at Ser 2030, and CaMKII phosphorylation of the nearby Ser2814 site; however, the relative importance of these sites is also controversial (Ai et al 2005, Huke & Bers 2008, Xiao et al 2005).

Recently, the N terminus of mAKAP has been shown to selectively bind AC5 in the heart (Cooper & Crossthwaite 2006, Kapiloff et al 2009). AC5 and AC6 are the most abundant cyclase isoforms in cardiac myocytes (Hanoune & Defer 2001); however, mAKAP-

associated AC activity is totally absent in AC5 knockout hearts, indicating a specific association between the two (Cooper & Crossthwaite 2006). mAKAP association can regulate activity of AC5 via a negative feedback loop. cAMP synthesis by AC5 activates mAKAP-bound PKA, which then phosphorylates AC5, inhibiting further cAMP production (Figure 1-22). The participation of adenylyl cyclases in AKAP macromolecular complexes together with cAMP effectors and downstream targets illustrates how a localised pool of cAMP generated by an AC can lead to specific physiological effects (Dessauer 2009).

Signal-terminating enzymes (PDEs and protein phosphatases (PPs)) which counteract the effects of second messengers are increasingly being shown to participate in macromolecular signaling complexes. mAKAP is known to directly associate with PDE4D3 (Dodge et al 2001). Tethering of PDE4D3 in close proximity to PKA allows it to regulate the activity of mAKAP-bound PKA, via hydrolysis of local cAMP. PP2B, also known as calcineurin, has also been shown to associate with mAKAP, along with PP2A (Dodge-Kafka et al 2010, Pare et al 2005).

cAMP is considered to act principally through the effector PKA to mediate many of its intracellular effects. However, it is now widely accepted that it may also mediate its effects via the activation of other proteins, such as Epacs (de Rooij et al 1998). Epac1 co-purifies with mAKAP in rat heart extract (Dodge-Kafka et al 2005). Interestingly, this interaction is indirect, and is in fact mediated via PDE4D3. cAMP has long been known to regulate growth factor signalling, and PDE4D3 is phosphorylated on Ser579 by ERK, leading to reduced activity of the PDE (Baillie et al 2000, Hoffmann et al 1999). Dodge-Kafka and co-workers predicted that the mAKAP complex might also include a MAP kinase to counterbalance actions of the anchored PDE. Cellular binding studies showed that PDE4D3 functions as a scaffolding protein for both ERK5 and Epac1 in the mAKAP complex (Dodge-Kafka et al 2005). Activation of Epac1 by cAMP leads to the induction of a Rap1 signaling pathway, which inhibits mAKAP-associated ERK5 (Figure 1-22) (Dodge-Kafka et al 2005).

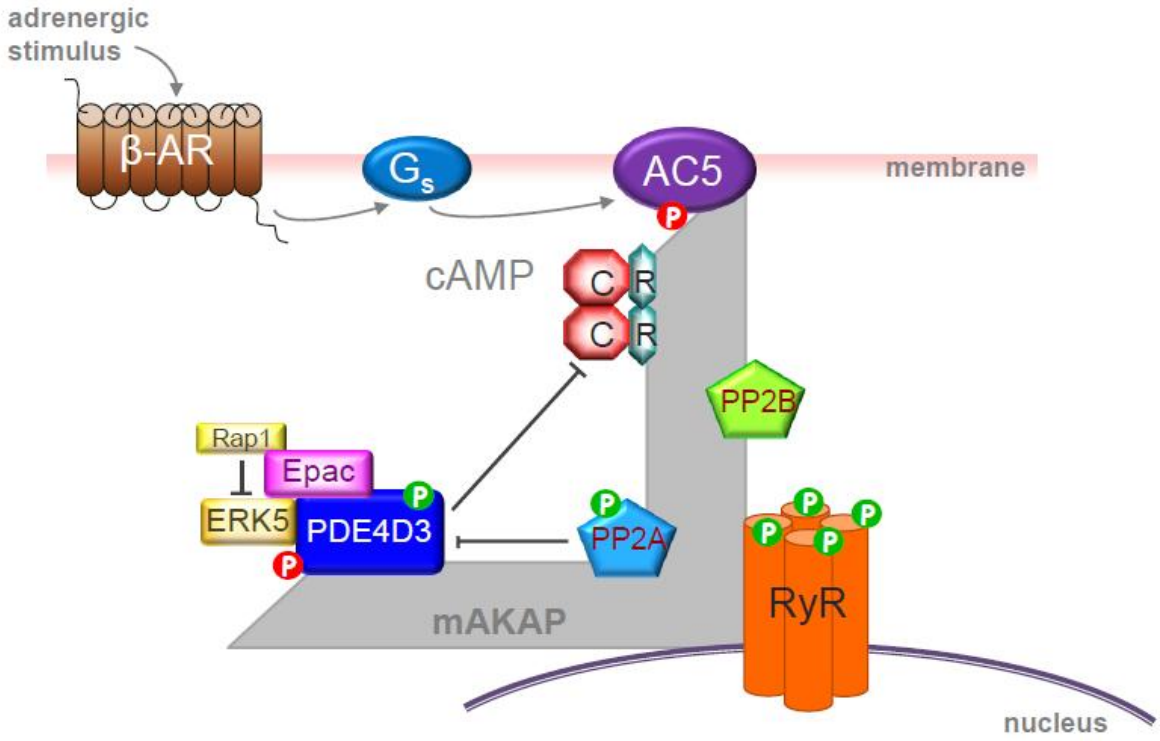

Figure 1-22 The mAKAP/RyR2 macromolecular signaling complex regulates cAMP compartmentalisation at multiple levels in the heart.
mAKAP directly scaffolds PKA, AC5, the cardiac ryanodine receptor, PDE4D3, and protein phosphatases PP2A and PP2B. Epac1 and ERK5 also participate in the mAKAP/RyR complex via their association with PDE4D3. Following generation of cAMP, PKA (shown here in its R_2C_2 form) is activated and can phosphorylate AC5, RyR, PDE4D3 and PP2A. This leads to inhibition of the cyclase, and enhanced PDE4D3 activity, contributing to a reduction in cAMP levels. However, phosphorylation of PP2A within the complex counteracts this negative feedback loop by promoting dephosphorylation of the anchored PDE. Phosphorylation of PDE4D3 by ERK5 also reduces activity of the PDE; however, this effect is opposed by the actions of an Epac1-Rap1-mediated pathway. PKA phosphorylation of RyR has been proposed to increase the open probability of the channel. Thus, cAMP, calcium and growth factor signals are integrated by the same macromolecular signaling complex in the heart. A green P indicates an activating phosphorylation and a red P indicates a deactivating phosphorylation.

1.6.4.2. Yotiao and the voltage-gated potassium channel

Several other AKAPs have been identified in the heart that compartmentalise PKA in proximity to a variety of effectors of EC coupling, such as ion channels and the contractile machinery (Scott & Santana 2010). Yotiao (AKAP9) associates with the KCNQ1 subunit of the voltage-gated cardiac potassium channel I_{KS}. Scaffolding by Yotiao brings PKA into the vicinity of KCNQ1, where it phosphorylates it on Serine 27 in response to β-adrenergic stimulation. This allows regulation of cardiac action potential duration by increasing the slow outward potassium ion current (Chen & Kass 2011, Marx et al 2002). Mutations in Yotiao which disrupt its binding to I_{KS} have been linked with long QT syndrome, a

propensity to ventricular tachyarrhythmias, syncope and sudden cardiac death (Chen et al 2007). The Yotiao/potassium channel complex has now been shown to contain the signal terminating enzymes PP1 and PDE4D3 (Marx et al 2002, Terrenoire et al 2009). Thus, scaffolding of various signaling elements by Yotiao allows the creation of a compartmentalised signaling environment that finely regulates I_{KS} function.

1.6.4.3. AKAP15/18 isoforms and phospholamban

The AKAP18δ isoform facilitates PKA phosphorylation of the SERCA2-associated regulatory protein phospholamban (PLB) (Lygren et al 2007). SERCA2 controls calcium reuptake into the SR, which is a rate-limiting step for relaxation and adequate filling of the heart during diastole (Szentesi et al 2004). Phospholamban negatively regulates SERCA2 by binding to it and reducing its ATPase activity, effectively inhibiting its Ca^{2+} pumping action (MacLennan & Kranias 2003). PKA phosphorylation of phospholamban on Serine 16 leads to dissociation of the protein from SERCA2, and relieves this inhibitory effect. Thus, β-adrenergic stimulation enhances cardiac relaxation, allowing for more rapid filling and enhanced cardiac output (Lygren et al 2007).

By scaffolding PKA, PDEs and protein phosphatases within the same complex, very fine regulation of local cAMP levels can be achieved via the actions of multiple feedback loops and the integration of multiple signaling pathways. New binding partners which participate in these complexes are constantly being discovered, which is helping us to understand how cAMP signals are compartmentalised within cardiac myocytes.

1.6.5 Abnormal cAMP signaling is associated with cardiac pathophysiology

Extraordinarily tight regulation of cAMP can be attained by cardiac myocytes, with cAMP signals being integrated with those from calcium and MAP kinases, and disruption of any of these signaling elements may lead to cardiac disease.

AC5 activity in the heart has been associated with pathological remodelling. AC5 knockout mice are resistant to cardiac stress, show protection against cardiac hypertrophy, apoptosis, and fibrosis, and have an increased median lifespan of around 30% (Yan et al 2007). Disruption of endogenous AC-mAKAP complexes by overexpressing the mAKAP AC-binding domain increased cellular cAMP and led to a hypertrophic phenotype in cardiac myocytes (Kapiloff et al 2009). Inhibition of AC binding to the AKAP would prevent its phosphorylation by PKA, and decrease its proximity to mAKAP-anchored PDE4D3, thus favouring cAMP production. Therefore, regulation of AC5 activity through its association with the mAKAP macromolecular complex appears to be important in hypertrophic signaling.

Levels of PDE4D3 associated with the ryanodine receptor complex have also been linked with the development of cardiac disease. PDE4D knockout mice are associated with development of progressive cardiomyopathy and cardiac arrhythmias (Lehnart et al 2005). PDE4D3 levels were found to be decreased in the RyR2 complex of failing human hearts, and it has been proposed that this leads to hyperphosphorylation of the channel by PKA, and a 'leaky channel' phenotype associated with cardiac dysfunction and increased risk of arrhythmias (Lehnart et al 2005). However, it should be noted again that some studies have disputed these findings (discussed further in Section 1.6.4.1.). Thus mAKAP-associated defects could result in hypertrophy, while RyR-associated hyperphosphorylation is associated with heart failure and arrhythmias in some studies.

Interfering with the tight control of cAMP signaling co-ordinated by macromolecular complexes can lead to severe pathological outcomes, and further studies are clearly required to determine the physiological effects of RyR hyperphosphorylation by PKA.

1.6.6 AKAP-Lbc

The scaffold protein AKAP-Lbc (AKAP13) is expressed at high levels in the heart, where it plays a number of important roles. AKAP-Lbc is a product of the Lbc (Lymphoid blast crisis) oncogene. This gene was first discovered in 1994 when DNA from a chronic myeloid

leukaemia acute phase sample was found to be tumorigenic in nude mice (Toksoz & Williams 1994). It is now known that the oncogenic product of the Lbc gene is in fact a truncated form of AKAP-Lbc lacking regulatory domains (Sterpetti et al 1999). Full length AKAP-Lbc has a molecular weight of 320kDa, and contains an N terminal EF hand motif followed by dbl oncogene homology (DH) and pleckstrin homology (PH) domains (Figure 1-23). The DH domain is associated with guanine nucleotide exchange activity for small GTPases such as Rho, and so AKAP-Lbc functions as a guanine nucleotide exchange factor (GEF) for Rho. In addition to PKA, AKAP-Lbc also scaffolds isoforms of PKC and PKD (Carnegie et al 2004). AKAP-Lbc has, therefore, been implicated in the control of a myriad of cellular processes, including transcriptional regulation, cell cycle progression and cytoskeletal reorganisation (Cerione & Zheng 1996, Welch et al 2010). The PKA anchoring domain of AKAP-Lbc contains the Ht31 peptide sequence, which has been extensively used to characterise PKA-AKAP interactions (Carr et al 1992). Synthetic peptides based on this sequence, which represents the region required for PKA-RII binding, are used in assays to block interactions of suspected AKAPs with RII, and downstream effects on the phosphorylation of PKA target proteins are observed.

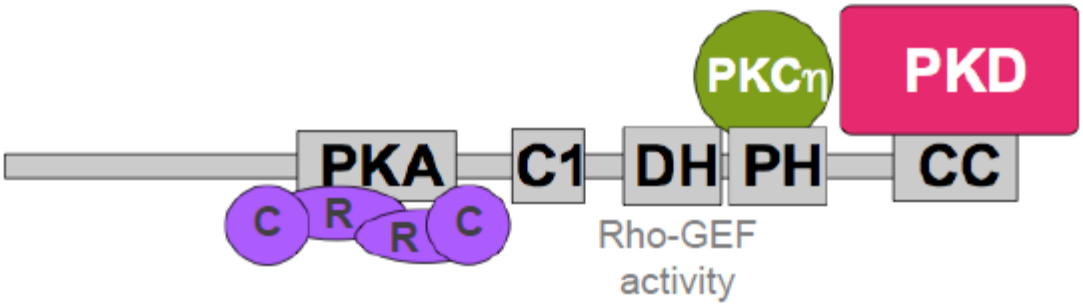

Figure 1-23 Domain structure and kinase anchoring sites of AKAP-Lbc.
AKAP-Lbc contains tandem DH and PH domains. The DH domain has intrinsic Rho-GEF activity for the small GTPase Rho. Activation of Rho GTPase is associated with cell cycle progression, gene transcription and cytoskeletal organisation (Cerione & Zheng 1996). The PH domain anchors PKCη isoforms, and PKD is anchored at the C terminus of the protein. The C1 domain is homologous to the N terminal of PKC, and binds diacylglycerol (Azzi et al 1992). PKA RII is anchored by an N terminal region of AKAP-Lbc containing the Ht31 peptide sequence (Asp^{493}-Leu-Ile-Glu-Glu-Ala-Ala-Ser-Arg-Ile-Val-Asp-Ala-Val-Ile-Glu-Gln-Val-Lys-Ala-Ala-Tyr) (Carr et al 1992).

1.6.6.1. AKAP-Lbc and cardiac hypertrophy

As a scaffold protein with intrinsic Rho-GEF activity that anchors multiple protein kinases, it is unsurprising that AKAP-Lbc has important cardiac effects. AKAP-Lbc is abundant in the heart, where it shows predominantly cytosolic localisation (Carnegie et al 2008). AKAP-Lbc has been found to assemble an activation complex for anchored PKD in cardiac myocytes. PKCη isoforms which are recruited to the anchoring protein phosphorylate Serine 744 and Serine 748 within the catalytic domain of PKD, leading to PKD activation. PKA then directs phosphorylation of Serine 2737 at the C terminus of PKD to facilitate release of the activated kinase from the scaffold protein into the cytoplasm (Carnegie et al 2004).

AKAP-Lbc has been implicated in the development of cardiac hypertrophy. Cardiac expression of AKAP-Lbc is increased in response to hypertrophic stimuli such as phenylephrine, which activates α1-adrenoceptors (Appert-Collin et al 2007, Carnegie et al 2008). As AKAP-Lbc functions to assemble an activation complex for anchored PKD, increased expression of the scaffold protein augments PKD signaling pathways. PKD-mediated phosphorylation of class II histone deacetylases (HDACs) occurs in the nucleus. This promotes nuclear export of HDACs, and results in derepression of the transcription factor myocyte enhancer factor 2 (MEF2). MEF2 in turn promotes transcription of hypertrophic genes involved in cardiac contraction and cellular metabolism (Figure 1-24). This genetic reprogramming of the cardiomyocyte leads to its reversion to a developmental phenotype, and is known as the fetal gene response (Carnegie et al 2008, Heineke & Molkentin 2006).

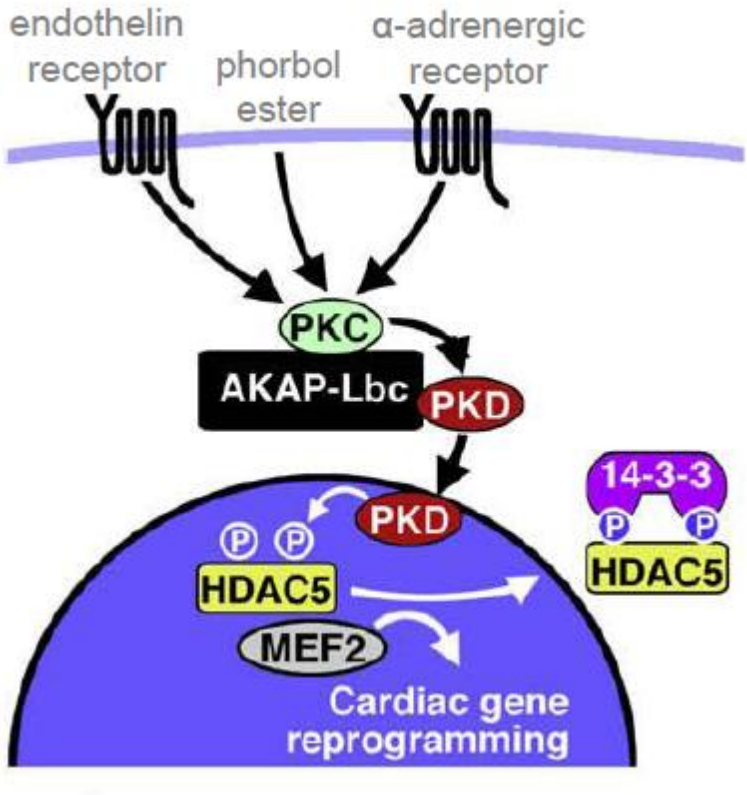

Figure 1-24 AKAP-Lbc regulates cardiac hypertrophy via a PKD-HDAC5-MEF2-dependent signaling pathway. Adapted from (Carnegie et al 2008).
Hypertrophic stimuli such as phenylephrine, which activates α1-adrenoceptors, endothelin, and phorbol esters, lead to increased expression of AKAP-Lbc. This augments activation of PKD, leading to serine phosphorylation and nuclear export of the class II histone deacetylase HDAC5, derepression of MEF2 transcription factor in the nucleus and initiation of a fetal gene response. Fetal cardiac genes which are expressed include β-myosin heavy chain (β-MHC) and atrial natriuretic factor (ANF) which can affect cardiac energy consumption and cardiac output (Patrizio et al 2008).

The importance of AKAP-Lbc in normal cardiac development is illustrated further by a recent study using knockout mice. Cardiomyocytes from AKAP-Lbc null mice exhibited deficient sarcomere formation, developing hearts appeared thin-walled with reduced trabeculation, and cardiac development arrested at embryonic day 10, suggesting a role for AKAP-Lbc in cardiomyocyte differentiation. The condition was lethal around embryonic day 13. Knockout mice were found to have reduced expression of MEF2, whereas overexpression of AKAP-Lbc in H9C2 cells augmented MEF2 activity (Mayers et al 2010).

The small GTPase Rho is a long established mediator of cardiac hypertrophy via the α1-adrenergic signaling pathway (Sah et al 1996). In cardiomyocytes, RhoA promotes the activation of protein kinase N and various stress-activated protein kinases which control the transcription of hypertrophic genes (Appert-Collin et al 2007). The RhoGEF activity of AKAP-Lbc is crucial for α1-adrenergic activation of Rho. Suppression of AKAP-Lbc expression with either short hairpin RNA (shRNA) or small interfering RNA (siRNA) to specifically knockdown AKAP-Lbc expression in neonatal rat ventricular cardiac myocytes significantly reduced phenylephrine-induced cardiac hypertrophy (Appert-Collin et al 2007, Carnegie et al 2008). When AKAP-Lbc expression was rescued with a mutant version lacking Rho-GEF activity, the agonist-induced hypertrophic phenotype was restored. However, this effect was blocked when cells were rescued with a truncated form of AKAP-Lbc that does not bind PKD1, indicating that scaffolding of PKD by AKAP-Lbc is a key factor in mediating this hypertrophic response (Carnegie et al 2008).

1.6.6.2. AKAP-Lbc and cancer signaling

Aberrant phosphorylation events by protein kinases are known to play a significant role in the development of cancers, therefore protein kinase signaling is tightly regulated within cells (Smith et al 2011). It has recently been shown that AKAP-Lbc associates with another scaffold protein, Kinase Suppressor of Ras-1 (KSR-1), to form the core of a signaling network (Smith et al 2010). KSR-1 scaffolds kinase members of the ERK/MAPK family. Thus, cAMP signals can be integrated with those of the Ras/Raf/MEK/ERK signaling pathway, which couples growth factor signaling to cell proliferation (Kolch 2005). PKA anchored to AKAP-Lbc phosphorylates KSR-1 on Ser838, and this phosphorylation event appears to be necessary for maximum stimulation of the ERK pathway, as mutation of Ser838 to Alanine impaired growth factor-stimulated ERK activation in HEK293 cells (Smith et al 2010). AKAP-Lbc also anchors Raf, therefore AKAP-Lbc can enhance ERK signaling by anchoring Raf in the vicinity of MEK, and by promoting PKA phosphorylation of Ser 838 on KSR-1 (Smith et al 2010).

1.7 Heat shock proteins in the heart

Heat shock proteins (Hsps) are a diverse group of molecular chaperones that are upregulated in response to cellular stress. Originally described in *Drosophila melanogaster* as a group of proteins whose expression was increased at elevated temperatures (Tissieres et al 1974), Hsps have been extensively characterised, and a variety of cellular triggers for their induction have now been identified, such as ischaemia/reperfusion (I/R) injury (Qian et al 2009), oxidative stress (Morimoto 1993) and glucose deprivation (Sciandra & Subjeck 1983). The chaperone activities of Hsps include the prevention of protein misfolding, refolding of denatured proteins, and their targeting for proteolytic degradation (Willis & Patterson 2010). Many heat shock proteins are now known to play essential protective roles in the cardiovascular system.

Heat shock proteins may be broadly classified according to their molecular weights as either high molecular weight or low molecular weight/small heat shock proteins (sHsps).

1.7.1 High molecular weight Hsps

Two of the most studied high molecular weight heat shock protein families are Hsp90 and Hsp70. Hsp90 is the most abundant chaperone in the cytosol, and is induced by cellular stress (Pearl & Prodromou 2006). Hsp90 plays a pivotal role in signal transduction, as it is essential for maintaining the conformation of many protein kinases and cell receptors within signaling networks (Zhao et al 2005). Hsp70 family members are also abundant in the cytosol, and can also be induced by stress (Young et al 2004). Like Hsp90, Hsp70 functions to promote protein folding and inhibit protein aggregation (Young 2010).

1.7.2 Small/low molecular weight Hsps

The sHsps, which include Hsp20, are less frequently induced by heat stress, and several family members, such as Hsp27 and alphaB-crystallin, are known to be abundant in cardiac and skeletal muscle, where they increase in response to stress to protect against muscle ischaemia (Fan & Kranias 2010, Willis & Patterson 2010). sHsps are a diverse group of proteins with different subcellular localisations and tissue distributions (Fan et al 2005a). To date, 10 sHsp isoforms have been identified (Table 1-6), and these are formally classified as HspB1-B10 (Kappe et al 2003). sHsps range in size from 12 to 43 kDa, and are characterised by a stretch of amino acids in their C termini known as an alpha-crystallin domain, which facilitates their chaperone activities (Kappe et al 2003).

HUGO name	Alternative name	Heat induction	Localisation
HspB1	Hsp27	+	Ubiquitous
HspB2	MKBP	-	Cardiac
HspB3	HspL27	-	Cardiac
HspB4	CRYAA	-	Eye
HspB5	CRYAB	+	Ubiquitous
HspB6	Hsp20	-	Ubiquitous
HspB7	cvHsp	?	Cardiac
HspB8	Hsp22	+	Ubiquitous
HspB9	None	?	Testis
HspB10	ODF1	?	Testis

Table 1-6 An overview of small heat shock proteins.

1.7.3 Hsp20

1.7.3.1 Structure of Hsp20

Hsp20, also known as HspB6, is expressed at high levels in cardiac, skeletal and vascular smooth muscle, where it represents up to 1% of total protein (Dreiza et al 2010, Fan et al 2005a). In addition to the alpha-crystallin domain common to sHsps, Hsp20 also possesses an N terminal domain which is involved in inhibiting platelet aggregation, and a region similar to the inhibitory region of troponin I, which is thought to be involved in actin binding (Figure 1-25) (Fan & Kranias 2010). Hsp20 has long been a focus of interest in the field of cardiovascular research, as it is the only sHsp to contain a cAMP/cGMP-dependent protein kinase (PKA/PKG) consensus phosphorylation sequence, R^{13}-R-A-**S**^{16}- within its N terminus (Beall et al 1999, Fan et al 2005a). Thus, Hsp20 may be regulated by the β-adrenergic/cAMP/PKA signaling pathway, which is known to be chronically activated in heart failure.

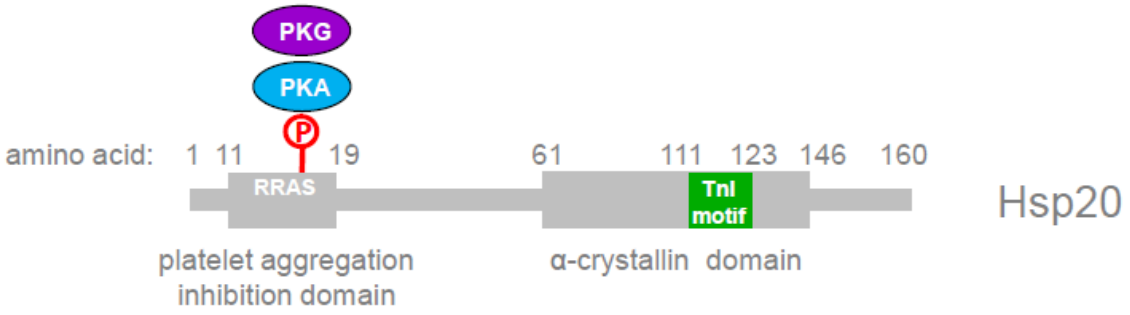

Figure 1-25 The domain structure of Hsp20.
Hsp20 is a 160 amino acid protein. A 9 amino acid motif (W^{11}LRRASAPL^{19}) at its N terminus has been shown to inhibit platelet aggregation (Fan & Kranias 2010). This region encompasses a PKA/PKG consensus phosphorylation sequence, RRAS^{16}, which allows the function of the protein to be regulated by cAMP levels via the β-adrenergic signaling pathway. The C terminal alpha-crystallin domain is common to all sHsps, and aids in their chaperone activities (Qian et al 2009). In Hsp20, this domain also encompasses a region similar to the inhibitory region of troponin I (GFVAREFHRRYRL), shown here in green, which may facilitate its interaction with actin (Fan & Kranias 2010). PKG phosphorylation of Hsp20, in response to nitric oxide stimulation of guanylyl cyclases, and generation of cyclic GMP, has been shown to modulate smooth muscle relaxation, (Beall et al 1999, Flynn et al 2003, Rembold et al 2000).

1.7.3.2. Cardioprotective actions of Hsp20

Heart failure, resulting from ischaemic heart disease and cardiomyopathy, presents an increasing medical and financial burden. Strategies which selectively modulate components of the β-adrenergic signaling pathway have long been of interest in the search for more effective treatments for heart failure (Mudd & Kass 2008). Hsp20 has been well studied in the cardiovascular system, due to the unique ability of this chaperone to be phosphorylated by PKA. Hsp20 is phosphorylated by PKA in response to β-adrenergic stimulation in ischaemic mice hearts (Qian et al 2009). Levels of PKA-phosphorylated Hsp20 are also increased in failing human hearts compared with donor hearts (Qian et al 2009). It is now established that Hsp20 has a range of cardioprotective functions, which are described below, and it is of considerable interest as a potential therapeutic target in cardiac disease.

Ischaemia/reperfusion injury

One of the commonest causes of heart failure is myocardial ischaemia, with subsequent progression to infarction. Ischaemia, resulting from restriction of coronary blood flow, leads to a characteristic sequence of pathological changes, which manifest clinically as ventricular dysfunction and cardiac failure (Buja 2005). Even transient ischaemia can lead to myocardial necrosis and apoptosis. Coronary reperfusion is the major therapeutic strategy employed to reduce morbidity and mortality following myocardial ischaemia to prevent progression to infarction, though it is now recognized that reperfusion itself may have deleterious effects. Improved tissue oxygenation after reperfusion allows resumption of ATP generation, but damage to the electron transport chain leads to the generation of oxidative stress by the mitochondria, in the form of reactive oxygen species (ROS), which result in myocardial necrosis and apoptosis (Buja 2005, Murphy & Steenburgen 2008). This phenomenon is known as ischaemia/reperfusion (I/R) injury.

It is now established that Hsp20 plays a major role in protecting against I/R injury in the heart. Major evidence in support of this role has come from the use of transgenic (TG) mouse models. TG mouse lines with cardiac-specific overexpression of Hsp20 display a 6-fold reduction in infarct size and improved functional recovery of contractile performance

during the reperfusion period compared with wildtype hearts (Fan et al 2005b) (Figure 1-26). When subjected to *in vivo* ischaemia/reperfusion, via coronary artery ligation, TG hearts also showed a significantly lower infarct region-to-risk ratio and total LDH levels released from TG hearts were half that of wildtype, indicating reduced necrotic damage (Fan et al 2005b). Many of the cardioprotective effects of Hsp20 are known to depend on PKA phosphorylation of Ser16 at the N-terminal of Hsp20 (Fan et al 2004a). Levels of phospho-Ser16 Hsp20 were significantly increased in TG hearts following I/R (Fan et al 2005b). Moreover, in an Hsp20 mouse model overexpressing phospho-null Hsp20 (Ser16 substituted for Alanine), TG hearts demonstrated complete reversal of the cardioprotective phenotype observed with overexpression of wildtype Hsp20. The phospho-null animals exhibited reduced recovery of contractile function post-I/R, and increased necrotic and apoptotic damage (Qian et al 2009). The differences in response observed between animals expressing wildtype or phospho-null Hsp20 may be due to differential activation of autophagy pathways. Autophagy is a physiological catabolic pathway by which the cell degrades and recycles damaged organelles and is upregulated under conditions of myocardial stress including ischaemia/reperfusion and cardiac failure (Gustaffson & Gottlieb 2009). Autophagy was activated in wildtype hearts, but inhibited in S16A hearts post-I/R. Pretreatment of S16A hearts with an activator of autophagy (rapamycin, which inhibits mTOR) improved their functional recovery (Qian et al 2009). These results suggest that the increased susceptibility of TG hearts overexpressing the phospho-null Hsp20 may therefore be linked to an inability to activate autophagy. The role of Hsp20 in ischaemia has been further cemented by the observation that Hsp20 expression levels may be altered by micro-RNA in ischaemic hearts. Micro-RNAs are small non-coding RNAs, which regulate gene expression at the post-transcriptional level, via RNA destruction or the formation of silencing complexes. Hsp20 expression is regulated by the micro-RNA miR-320, which targets the 3'UTR of Hsp20, acting as a negative regulator of translation. miR-320 is upregulated in ischaemic hearts (Ren et al 2009), thus raising the possibility that manipulation of miR-320 levels may provide a therapeutic strategy for limiting I/R injury.

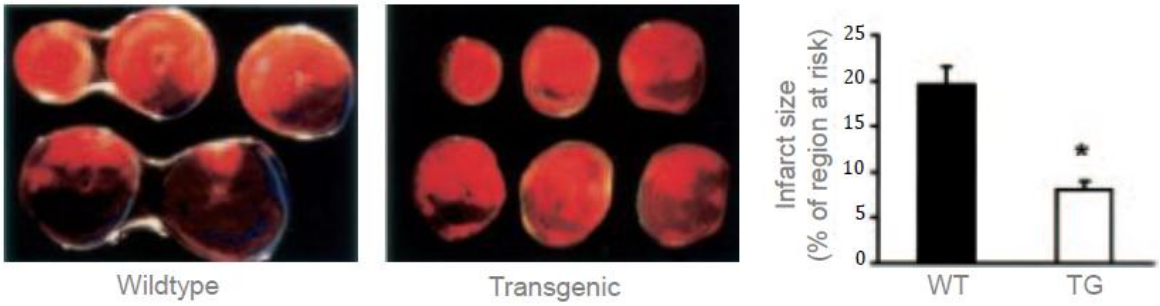

Figure 1-26 Overexpression of Hsp20 protects against ischaemia/reperfusion injury in the heart. Adapted from (Fan et al 2005b).
Transgenic (TG) overexpression of Hsp20 significantly reduced *in vivo* infarct size after 30 minutes of myocardial ischaemia compared with wildtype (WT) animals. Ischaemia was produced via occlusion of the left anterior descending coronary artery (LAD). Infarcted tissue appears black. Hearts from 6 animals are represented for each group.

Anti-apoptotic effects

Apoptosis (programmed cell death) can occur under both physiological and pathological conditions, including I/R. Apoptosis is characterised biochemically by the activation of a cascade of cysteine proteases (caspases) and damage to the mitochondria with subsequent release of cytochrome c, and morphologically by double stranded DNA fragmentation and cell shrinkage (Buja 2005). Apoptosis can be triggered in cardiomyocytes following chronic β-adrenergic stimulation and it has recently been shown that Hsp20 can counter this effect by physically interacting with key pro-apoptotic signaling proteins (Fan et al 2005b). Overexpression of wildtype Hsp20 protects cultured rat cardiac myocytes from β-agonist-induced apoptosis, as determined by a reduction in the number of pyknotic nuclei, TUNEL (terminal deoxynucleotidyltransferase-mediated dUTP nick-end labeling) assay, reduction in caspase-3 activity and DNA laddering (Fan et al 2004a). Moreover, a phospho-mimic mutant of Hsp20 (Ser16 to Asp substitution) expressed in isolated adult cardiac myocytes conferred full protection from apoptosis whereas the phospho-null mutant (Ser16 to Ala) did not. These results highlight the importance of Ser16 phosphorylation in switching Hsp20 to a more cardioprotective state. Consistent with the importance of Ser16 phosphorylation in cardioprotection, a single nucleotide polymorphism (C59T) has recently been identified in Hsp20 that results

in a Proline to Leucine substitution at position 20, just downstream of the PKA consensus phosphorylation site. This P20L variant of Hsp20 is associated with reduced Ser16 phosphorylation, and attenuation of anti-apoptotic effects (Nicolaou et al 2008). The anti-apoptotic effects of Hsp20 are thought to be mediated by its interaction with the pro-apoptotic protein Bax (Fan et al 2005b). This association prevents Bax translocation from the cytosol to the mitochondria during I/R, where it could damage mitochondrial integrity by releasing cytochrome c, with subsequent activation of caspase-3. Consistent with Hsp20 physically preventing translocation of Bax, caspase-3 activity was repressed following I/R injury in TG hearts overexpressing Hsp20. Post-I/R infarct size was also greatly reduced in TG hearts, as was apoptotic cell death, as measured by DNA fragmentation (Fan et al 2005b). Other Hsps, such as the mitochondrial protein Hsp60 and α-crystallins, have also been shown to form complexes with Bax (Kirchhoff et al 2002, Mao et al 2004). Thus, Hsps may critically regulate the Bax-caspase pathway to protect against I/R-induced cardiomyocyte apoptosis.

Cardiac hypertrophy

Cardiac hypertrophy may be a physiological response, induced by exercise, or a pathological response, usually to pressure/volume overload from hypertension or valvular heart disease (Willis & Patterson 2010). In both cases, there is an increase in cardiomyocyte size. In physiological hypertrophy, for example, in the case of elite athletes, this leads to an improvement in cardiac function, however pathological hypertrophy eventually leads to cardiac failure, via mechanisms that are still not completely understood. Expression levels of a number of cardiac chaperones, including the sHsps Hsp20 and Hsp22, and the high molecular weight Hsp70 family, have been shown to increase in response to hypertrophic stimuli such as aortic constriction and chronic β-adrenergic stimulation. Hsp20 expression is increased in response to hypertrophic stimuli, such as chronic β-adrenergic stimulation (Fan et al 2004b, Qian et al 2009). TG mice with cardiac-specific overexpression of Hsp20 and subject to chronic β-adrenergic stimulation with the synthetic agonist isoproterenol, are protected from the increases in heart weight/body weight ratio and cardiomyocyte size that are the hallmarks of cardiac hypertrophy (Fan et al 2006). In addition, TG hearts show reduced induction of the fetal gene response that accompanies hypertrophy. These effects have

been linked to suppression of ASK-1 (apoptosis signal-regulating kinase 1) signaling, with reduced activation of the downstream JNK(c-Jun N terminal kinase)/p38 signaling pathway (Fan et al 2006).

The importance of phosphorylation of Hsp20 at Serine 16 in protection against cardiac hypertrophy has recently been highlighted by a study from our laboratory, investigating a unique role for cAMP-specific phosphodiesterases (PDEs). Members of the PDE4 family were shown to form a complex with Hsp20, which maintains it in a dephosphorylated state until chronic β-adrenergic stimulation and a consequent sustained rise in cAMP saturates the PDE, allowing phosphorylation of Hsp20 (Sin et al 2011). Using peptide array technology and in vitro binding assays, the docking site for Hsp20 on PDE4 was mapped to the conserved catalytic region of the PDE. This sequence information was then used to design a cell-permeable disruptor peptide which specifically inhibited the interaction between Hsp20 and PDE4. Treatment of neonatal rat cardiomyocytes with this peptide disruptor led to highly phosphorylated endogenous Hsp20, and attenuation of β-agonist-induced hypertrophy, as determined by a reduction in cardiomyocyte size and measurement of fetal gene expression (Sin et al 2011). This study provides further direct evidence that alteration of the phosphorylation status of Hsp20, and not just the expression level of the protein, is required for its full cardioprotective effects.

Myofilament effects

Under basal conditions, Hsp20 is found predominantly in the cytoplasm (Fan et al 2004a); however, under ischaemic stress, Hsp20 translocates to the myofilaments in adult rat heart and skeletal muscle (Golenhofen et al 2004). Similarly, following isoproterenol stimulation of isolated adult rat cardiomyocytes, Hsp20 has been observed to redistribute to the myofilaments, where it co-localises with actin (Fan et al 2004a). Myofilament regulatory and cytoskeletal proteins are lost or degraded in hearts subjected to I/R, and this is an important part of the pathogenesis of ischaemic injury to the myocardium (Van Eyk et al 1998). Transgenic hearts overexpressing Hsp20 displayed less damage to the myofilaments post-I/R, suggesting that Hsp20 functions to maintain muscle integrity during I/R (Fan et al 2005b). Thus, following ischaemic stress, Hsp20 may translocate to

the myofilaments to protect them from further damage. Hsp20 is widely recognised as an actin binding protein (Brophy et al 1999a, Brophy et al 1999b) and it may act to stabilise the cytoskeleton under conditions of stress (Dreiza et al 2005, Fan et al 2004a) or sequester damaged intracellular proteins to the cytoskeleton (Verschuure et al 2002). This protection of the cytoskeleton is also linked to the phosphorylation status of Hsp20, as the interaction between Hsp20 with actin is augmented following phosphorylation of the heat shock protein (Brophy et al 1999b, Fan et al 2005b, Fan et al 2004b).

Vascular smooth muscle effects

As well as being highly expressed in the heart, Hsp20 is also constitutively expressed in vascular, airway, uterine smooth muscle and skeletal muscle (Dreiza et al). Activation of cyclic nucleotide signaling pathways leads to the vasorelaxation of most types of smooth muscle. An 11 amino acid region of Hsp20's highly conserved α-crystallin domain shares significant sequence homology with part of the inhibitory region of the thin filament protein TnI (Rembold 2007). TnI interacts closely with actin and associated thin filament proteins to regulate crossbridge formation and force generation in response to fluctuations in intracellular calcium levels (Engel et al 2004). Hsp20 has also been shown to interact directly with the actin cytoskeleton (Tessier et al 2003) and this interaction is increased by Ser16 phosphorylation (Rembold et al 2000) Thus, like TnI, phosphorylated Hsp20 may interact with actin to modulate smooth muscle relaxation. Phospho-Hsp20 has been linked with the relaxation of saphenous vein (McLemore et al 2005, Tessier et al 2004), relaxation of cultured vascular smooth muscle cells (Brophy et al 2002), and vasorelaxation of porcine coronary artery (Tessier et al 2004).

Platelet aggregation

Platelets become tethered to the extracellular matrix at sites of vascular injury via glycoprotein receptor complexes expressed on their surfaces to stop excessive haemorrhage after vascular trauma (Davi & Patrono 2007). The local release of inflammatory mediators, such as thromboxane-A_2, serves to amplify this response, leading to the formation of a platelet plug. Fibrinogen and von Willebrand factor form

inter-platelet bridges, further stabilising the growing thrombus to achieve haemostasis (Davi & Patrono 2007). During atherosclerotic plaque rupture, the platelet response, with subsequent formation of arterial thrombus, and luminal occlusion, may lead to the development of acute coronary syndrome (ACS) (Choi & Mintz 2010), a spectrum of unstable coronary artery diseases ranging from unstable angina to myocardial infarction. Anti-platelet agents form a major part of the treatment of ACS, and are well recognised as reducing cardiovascular morbidity and mortality (Sakhuja et al 2010). Hsp20 possesses potent anti-platelet activity and has been shown to inhibit thrombin-induced platelet aggregation in a dose-dependent manner, and to specifically bind human platelets, with a kD of 310nM (Niwa et al 2000). Recombinant Hsp20 linked to the TAT protein transduction domain also inhibited collagen-induced platelet aggregation in human citrated whole blood in a dose-dependent manner (McLemore et al 2004). Furthermore, levels of Hsp20 were found to be markedly lower in an *in vivo* hamster model of carotid artery endothelial injury, suggesting that it may be secreted from the vascular wall immediately after endothelial injury, to act as a regulator of platelet function in the circulation (Kozawa et al 2002). The mechanism behind the anti-platelet activity of Hsp20 is not fully understood but is partially due to inhibition of thrombin-induced calcium influx in platelets (Niwa et al 2000) and reduced phosphoinositide hydrolysis by phospholipase C (Kozawa et al 2002). Other sHsps may have effects on platelet aggregation, as synthetic peptides isolated from both Hsp20 and alphaB-crystallin have potent anti-platelet effects *in vitro* (Matsuno et al 2003). Thus, modulation of local levels of sHsps such as Hsp20 may provide a new therapeutic strategy in acute coronary syndromes.

2.

Thesis Aims

cAMP signaling to PKA is tightly regulated in space and time, both by the physical compartmentalisation of PKA by AKAPs, and by the creation of localised cAMP gradients by phosphodiesterase enzymes. PKA phosphorylation of cardiac proteins is critical to many essential cardiac processes, such as excitation-contraction coupling and cardioprotection. Two such proteins are the myofilament protein troponin I (TnI), and the cytosolic small heat shock protein Hsp20.

cAMP-dependent PKA phosphorylation of TnI on Ser22/Ser23 enhances the efficiency of cardiac contraction in response to physiological stress. To date, little is known about the PDEs and AKAPs which regulate cAMP/PKA signaling at the myofilament. The aims of this study were:

- to discover which PDE isoforms regulate cAMP levels at the myofilament, and thereby influence PKA activation, and phosphorylation of TnI
- to identify AKAPs which may scaffold PKA at the myofilament to facilitate this phosphorylation event

Hsp20 protects against a number of pathological cardiac processes, including cardiac hypertrophy and apoptosis. Following β-adrenergic stimulation, Hsp20 is phosphorylated on Ser16 by PKA, and its cardioprotective abilities are enhanced by this phosphorylation event. Selective targeting of signaling elements that can enhance this modification could

represent a new therapeutic avenue for the prevention and treatment of myocardial remodelling and ischaemic injury. Recent work from our laboratory implicates members of the PDE4 family in regulating local cAMP levels around Hsp20 via a direct interaction between Hsp20 and the catalytic domain of the PDE (Sin et al 2011); however, no AKAP has been identified to scaffold the pool of PKA that phosphorylates Hsp20.

- The final aim of this thesis was to identify this AKAP.

3.

Materials and Methods

3.1 Materials

All materials and chemicals were from Sigma-Aldrich (Gillingham, Dorset, UK), unless otherwise stated.

3.2 General Molecular Biology Procedures

3.2.1 Transformation of Chemically Competent Cells

Chemically competent TOP10 cells (Invitrogen) were stored at -80°C and thawed on ice for 10 minutes immediately prior to use. 10ng of plasmid DNA was added per 50µl aliquot of competent cells on ice, and mixed gently. Tubes were incubated for 15 minutes on ice, heat shocked for 30 seconds at 42°C, and returned to ice for a further 2 minutes. 450µl of pre-warmed SOC media (Invitrogen) was added to the cells, and tubes incubated at 37°C for 1 hour in a shaking incubator. Agar plates were prepared by autoclaving LB broth (1% (w/v) tryptone, 0.5% (w/v) yeast extract, 170mM NaCl), cooling the mixture to handling temperature, then adding the appropriate antibiotic for the plasmid antibiotic resistance gene, before pouring into 90mm Petri dishes to set. 50-200µl of the transformation mix was spread onto pre-warmed agar plates and plates incubated upside down overnight at 37°C. Colony growth indicated successful transformation of cells. Unused agar plates were stored sealed at 4°C for up to one month.

3.2.2 Preparation of Plasmid DNA

Single colonies were picked from agar plates using a sterile pipette tip, and grown overnight in 5ml of LB containing the appropriate antibiotic at 37°C in an orbital shaker set at 220rpm. 0.8ml of culture was removed for preparation of glycerol stocks (Section 3.2.3). The remaining culture was saved for plasmid isolation using a QIAprep Spin Miniprep Kit (Qiagen), following the manufacturer's protocol for plasmid purification with a microcentrifuge. Alternatively, the remaining culture was used to inoculate 250ml of LB plus antibiotic in a 1L flask, and incubated overnight at 37°C with shaking. The Qiagen Plasmid Maxi Kit was then used to isolate larger amounts of plasmid DNA. Purified plasmid DNA was eluted in sterile dH_20 and stored at -20°C.

3.2.3 Storage of Plasmid DNA

0.8ml of overnight culture was added to 0.2ml of autoclaved glycerol in a cryovial. This plasmid stock was then snap frozen on dry ice and stored at -80°C. In general, plasmids were transformed into DH5α chemically competent cells (Invitrogen), which are suitable for long term storage. When plasmid DNA was required from glycerol stocks, the stock was scraped with a pipette tip to collect cells, and the tip placed in 5ml of sterile LB containing the appropriate antibiotic for plasmid selection. This was then grown overnight at 37°C with shaking and either mini-prepped or used to inoculate a larger culture for a maxi-prep (Section 3.2.2).

3.2.4 Agarose Gel Electrophoresis

Agarose gel electrophoresis was employed to separate DNA molecules by size, by moving negatively charged DNA through an agarose matrix via the application of an electrical charge. The Bio-Rad Sub-Cell GT electrophoresis system was used. A 1% agarose solution was prepared by dissolving agarose in 1x TAE buffer (40mM Tris-Cl, 20mM glacial acetic acid, 1mM EDTA) by heating in a microwave oven. The solution was cooled to handling temperature, and 1:10 000 SYBR Safe DNA gel stain (Invitrogen) added. The solution was then poured into a gel mould and allowed to set. DNA samples were prepared for loading using a 1:6 dilution of 6x DNA loading buffer (0.25% (w/v) bromophenol blue, 0.25% (w/v) xylene cyanol FF and 40% (w/v) sucrose). 10µl of GeneRuler 100 bp or 1kb ladder

(Thermo Scientific) was added to the first lane to enable identification of the size of individual DNA fragments. DNA samples were then loaded and subjected to gel electrophoresis in a tank submerged in 1x TAE buffer at 100V for approximately 1 hour. DNA molecules were visualised under ultraviolet transillumination.

3.2.5 Quantification of DNA concentration

A NanoDrop 2000 micro-volume spectrophotometer (Thermo Scientific) was used to accurately quantify DNA concentration. Absorbance was measured at 260nm, and purity estimated using the 260nm:280nm absorbance ratio.

3.2.6 DNA Sequencing

DNA sequencing was performed by the University of Dundee Sequencing Service, http://www.dnaseq.co.uk/ or the University of Washington Biochemistry DNA Sequencing Facility, http://dnaseq.bchem.washington.edu/bdsf/. DNA samples were supplied as per the web instructions, and sequencing carried out using either standard or custom primers. Analysis of DNA sequencing was performed using Geneious software, version 5.5.

3.2.7 Generation of Hsp20-V5-His Plasmid

To produce Hsp20 with a V5 epitope tag, pcDNA3.1-Hsp20-V5-His-TOPO (referred to in the text as Hsp20-V5) was generated by amplifying the open reading frame (ORF) of Hsp20 from pcDNA6.2-Hsp20, using the following primers:

Forward: GCACAAGCTTATGGAGATCCCTGTGCCTGTGC

Reverse: GCACAAGCTTGGCTGCGGCTGGCGGTGG

pcDNA6.2-Hsp20 was kindly provided by Dr Jon Day.

The reaction mixture for PCR was as shown below (final volume 50µl). Enzyme and PCR buffer were from Thermo Scientific:

DNA template 0.2µl (approx. 100ng)

Forward and Reverse primers (10mM stocks) 1.5µl of each

dNTPs (10mM stock) 2µl

10x PCR buffer 5µl

Sterile dH_20 38.8µl

Phusion II enzyme 1µl

The following PCR conditions were used:

95°C for 2 minutes

95°C for 30 seconds

70°C for 60 seconds for 25 cycles

72°C for 60 seconds

4°C hold

The PCR product was subjected to electrophoresis on a 1% agarose gel (Section 3.2.4). When viewed under ultraviolet transillumination, a product of around 500bp was identified in the PCR lane, corresponding to the 483bp Hsp20 ORF. This band was cut out and gel purified using a Qiagen Gel Purification Kit, according to the manufacturer's instructions. The purified product was then quantified and TOPO cloned into the pcDNA3.1-V5-His-TOPO vector (Invitrogen) by incubating 5ng of purified PCR product with 1µl of salt solution (Invitrogen) and 1µl of TOPO vector in a total volume of 5µl with sterile dH_20 at room temperature for 15 minutes. 3µl of this reaction mixture was then transformed into chemically competent TOP10 cells (Section 3.2.1).

3.3 Mammalian Cell Culture

All cell culture was performed in a class II tissue culture hood using an aseptic technique. All reagents were filter-sterilised or autoclaved prior to use.

3.3.1 HEK293 cells

3.3.1.1. Cell maintenance

The HEK293 cell line is derived from transformed human embryonic kidney cells. HEK293 cells were cultured in Dulbecco's modified Eagle's medium (DMEM) supplemented with 10% fetal bovine serum (FBS), 1% penicillin (10 000 U/ml)/streptomycin (10mg/ml) and 2mM L-glutamine. Cells were maintained in an atmosphere of 37°C and 5% CO_2, and passaged at 70-90% confluence. To passage, the growth media was removed and 2ml of 1x trypsin-EDTA added per 10cm^2 of growth area. Cells were incubated at 37°C until they were seen to detach when viewed under a light microscope. 8ml of growth media was then added to inactivate trypsin. Cells were collected by centrifugation at 150g for 3 minutes, and the cell pellet resuspended in 5-10ml fresh growth medium to remove the trypsin, then 1ml of suspended cells and 9ml of complete growth medium was added per 10cm dish. Cells were then re-incubated at 37°C and 5% CO_2 until required. Media was changed every 48 hours.

3.3.1.2. Transient transfection of plasmid DNA

Cells were transfected using TransIT-LT1 transfection reagent (Mirus Bio, Madison, USA). Cells were passaged 24 hours before transfection to ensure 40-60% confluence on the day of transfection, and maintained as described above (Section 3.3.1.1.). For transfection of one 10cm dish, 3µg of plasmid DNA was used. 12µl of Mirus transfection reagent was added to 1.5ml of Opti-MEM (Invitrogen), and the solution pipetted briefly to mix, then incubated at room temperature for 5 minutes. 3µg of plasmid DNA was then added, the solution pipetted once more to mix, and incubated at room temperature for a further 15 minutes. Meanwhile, the cell media was replaced with 9ml of complete growth medium. The transfection solution was then added drop-wise to the dish and swirled to mix. Cells were incubated at 37°C and 5% CO_2 for 24-48 hours to allow plasmid expression, prior to performing experiments.

3.3.1.3. Preparation of whole cell lysates

Cells were treated as described in the text, the culture medium aspirated and adherent cells rinsed twice in ice cold PBS. Cells were harvested in ice cold 3T3 lysis buffer (25mM

HEPES, 50mM NaCl, 2.5mM EDTA, 50mM NaF, 30mM Na pyrophosphate, 10% glycerol, 1% Triton X-100, pH 7.5) containing 1x complete EDTA-free protease inhibitor cocktail (Roche, Burgess Hill, UK). 500µl of lysis buffer was used for one 10cm dish. Cells were incubated with lysis buffer on ice for 5 minutes, then collected using a plastic cell scraper and transferred to pre-chilled Eppendorf tubes. Lysates were centrifuged at 4°C and 600g for 10 minutes to pellet insoluble material. The supernatant containing cellular proteins was retained and subjected to protein assay, or snap frozen and stored at -80°C prior to use.

3.3.2 Neonatal Rat Ventricular Cardiac Myocytes

3.3.2.1. Isolation of Neonatal Rat Cardiac Myocytes

Neonatal rat ventricular cardiac myocytes (NRVM) are a commonly used cell model to study cardiac biochemistry and cell signaling processes, as they are not terminally differentiated and can therefore be cultured in vitro. NRVM were isolated from 1-5 day old Sprague-Dawley rats, in accordance with local animal handling protocols. Hearts were immediately placed in ice cold ADS buffer (120mM NaCl, 20mM HEPES, 1mM NaH_2PO_4, 5mM glucose, 5.4mM KCl, 0.8mM $MgSO_4$, pH 7.4), and dissected on ice to remove non-ventricular tissue. Ventricles were minced into $1mm^3$ pieces and subjected to 4-5 rounds of enzymatic digestion at 37°C for 20 minutes, in 0.06% (w/v) pancreatin and 0.03% (w/v) type II collagenase (Worthington Biochemical Corporation, Lakewood, NJ) in sterile ADS buffer. Digestions were stopped by the addition of FBS. Cells were pelleted at 260g for 5 minutes, then gently resuspended in plating medium comprising a 4:1 ratio of DMEM/Medium 199 (M199) supplemented with 10% horse serum, 5% FBS, 1% penicillin-streptomycin and 2mM L-glutamine. Cells were pre-plated for 2 hours at 37°C and 5% CO_2 in sterile tissue culture flasks to allow preferential attachment of cardiac fibroblasts. Non-adherent cardiomyocytes were then removed, pelleted as before, and resuspended in fresh plating medium ready for cell counting. Cardiac myocytes were seeded as described in Section 3.3.2.2. and incubated at 37°C and 5% CO_2. After 24 hours, the media was replaced with maintenance medium comprising DMEM/M199 (4:1) supplemented with 5% horse serum, 1% penicillin-streptomycin and 2mM L-glutamine. The cardiac myocyte population isolated by this method was approximately 95% pure, as confirmed by α-actinin staining (Figure 3-1).

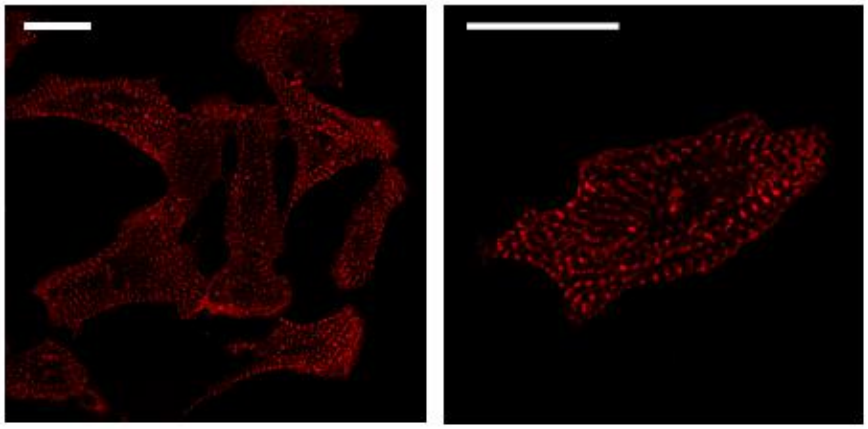

Figure 3-1 Immunofluorescence staining of enzyme-purified cardiac cells indicates a high population of cardiac myocytes.
α-actinin is a component of the contractile machinery of cardiac myocytes, therefore allows differentiation between myocytes and cardiac fibroblasts which could contaminate the culture. Left panel: > 95% pure cardiac myocyte population. Right panel: close-up of a single cardiac myocyte demonstrating characteristic α-actinin staining pattern. Scale bars represent 20µM.

3.3.2.2. Cell seeding

For immunocytochemistry and FRET experiments, sterile glass coverslips were coated with 1µg/cm^2 mouse laminin (BD Biosciences, Oxford, UK), rinsed with sterile dH_20, air-dried and stored in 6 well plates at 4°C. Prior to use, plates were warmed at 37°C. 700 000 cells were added per well in a final volume of 3ml media. For all other experiments, NRVM were grown in sterile tissue culture dishes or plates coated with 1% (w/v) bovine gelatin.

3.3.2.3. Transient transfection of plasmid DNA

NRVM were transiently transfected in 6 well plates with plasmid DNA using TransFectin lipid reagent (Bio-Rad). 3µg of plasmid DNA was used per well. DNA was added to 250µl of M199 medium. 9µl of TransFectin reagent was added to a further 250µl of M199. Tubes were incubated separately for 5 minutes at room temperature before combining and incubating for a further 20 minutes at room temperature. Meanwhile, the cell growth medium was replaced with 2.5ml of fresh maintenance medium per well. The transfection solution was then added drop-wise, and plates incubated at 37°C and 5% CO_2 overnight. Media was replaced with 3ml of fresh maintenance media after 24 hours, and

cells were used for experiments 24-48 hours after transfection, to allow expression of plasmid DNA.

3.3.2.4. Preparation of NRVM cellular lysates

Cells were treated as described in the text and Table 3-1, the culture medium aspirated and adherent cells rinsed twice in ice cold PBS. Cells were harvested in ice cold RIPA lysis buffer (50mM Tris, 150mM NaCl, 5mM EDTA, 50mM NaF, 12mM Na deoxycholate, 1% NP40, 0.1% SDS, pH7.4) containing 1x complete EDTA-free protease inhibitor cocktail (Roche). 150µl of lysis buffer was used per well of a 6 well plate. Cells were incubated with lysis buffer on ice for 5 minutes, then collected using a plastic cell scraper and transferred to pre-chilled Eppendorf tubes. Lysates were passed twice through a 26 gauge needle, and centrifuged at 4°C and 600g for 10 minutes to pellet insoluble material. The supernatant containing cellular proteins was retained and subjected to protein assay, or snap frozen and stored at -80°C prior to use.

Compound	Mode of action	Final concentration
EHNA	PDE2 inhibitor	10µM
Cilostamide	PDE3 inhibitor	10µM
Rolipram	PDE4 inhibitor	10µM
Zaprinast	PDE5 inhibitor	10µM
Dipyridamole	PDE8 inhibitor	100µM
IBMX	Non-specific PDE inhibitor	100µM
Forskolin	Adenylyl cyclase activator	50µM
Isoproterenol	Synthetic β-adrenoceptor agonist	1nM-1µM (see text for details)

Table 3-1 Agonist and inhibitor treatments of NRVM

3.3.3 Human Cardiac Myocytes

Human cardiac myocytes (HCM) (ScienCell Research Laboratories, Carlsbad, CA) are isolated from human ventricles. Cells were preserved at -80°C, and thawed at 37°C immediately prior to use. HCM were cultured in Human Cardiac Myocyte medium supplemented with 5% FBS, 1% penicillin-streptomycin and 1% Cardiac Myocyte Growth Supplement (all from ScienCell), and maintained in an atmosphere of 37°C and 5% CO_2. Cells were plated onto 10cm tissue culture dishes which had been pre-coated with 3µg/cm^2 of poly-L-lysine, rinsed twice with sterile dH_20, and air-dried. HCM cannot be passaged often as they terminally differentiate in culture, and the cardiac fibroblast population takes over the culture, so they are only used up to passage 6. To passage HCM, 2ml of 1x trypsin-EDTA solution was added per 10cm dish, once the cells had reached greater than 90% confluence, and cells incubated for a short time at room temperature, until they were seen to round up under a light microscope. 8ml of complete growth medium was then added to neutralise the trypsin, and cells centrifuged at 160g for 3 minutes, before gently resuspending in 10ml complete growth medium. HCM were then counted and plated out at a density of 5000 cells/cm^2, as per the manufacturer's instructions.

3.4 General Biochemical Techniques

3.4.1 Protein Assay

The concentration of protein in cell lysates, and of purified recombinant proteins, was determined using the Bradford method (Bradford 1976). Protein assays were performed in clear 96 well plates. All samples were prepared in a final volume of 50µl sterile dH_20, and were tested in triplicate. A standard curve of known BSA concentrations between 0 and 5 µg was prepared. Each protein sample of unknown concentration was then diluted 1:50 – 1:200 in sterile dH_20. Bradford reagent (Bio-Rad) was diluted 1:5 in sterile dH_20, and 200µl of diluted reagent added per well. Samples and standards were analysed with a 595nm filter on an Anthos 2010 plate reader using ADAP software. Protein concentrations were calculated using a curve derived from the BSA standard values, and adjusted for sample dilution.

3.4.2 SDS-PAGE

Sodium dodecylsulphate polyacrylamide gel electrophoresis (SDS-PAGE) was used to separate proteins by molecular weight. Proteins were separated using the Invitrogen NuPage Novex gel system. Protein samples were denatured and reduced for gel electrophoresis by diluting in 5x Laemmli protein sample buffer (Bio-Rad) and boiling for 5 minutes, then 1-100µg of protein per well was loaded directly onto 4-12% Bis-Tris NuPage gels. Gels were immersed in NuPage MES (for <50kDa proteins) or MOPS (for >50kDa proteins) running buffer. 3µl of Bio-Rad Precision Plus Dual Colour Protein Standard was added to the first well of each gel. This is a pre-stained standard protein ladder used to aid analysis of the molecular weight of the protein samples. Protein samples were subjected to gel electrophoresis at 180V for approximately 1.5 hours, or until protein separation was achieved.

3.4.3. Western Immunoblotting

Proteins separated by SDS-PAGE were transferred to nitrocellulose membranes using the Invitrogen XCell II Blot Module and 1x NuPage transfer buffer containing 20% methanol (v/v), as per the manufacturer's instructions. Proteins were transferred either at 30V for 1.5 hours, or 12V for 16 hours. Efficacy of transfer was assessed by visualisation of the pre-stained molecular weight marker on the nitrocellulose membrane. Membranes were then incubated for 1 hour at room temperature with constant agitation in 5% (w/v) milk solution consisting of Marvel milk powder in 1x TBST (20mM Tris-Cl pH 7.6, 150mM NaCl, 0.1% Tween 20) to block non-specific antibody binding sites. Primary antibody against the protein of interest was added to fresh 1% milk solution at the appropriate dilution (see Table 3-2 for details of primary antibodies used), and incubated with the membrane overnight at 4°C with constant agitation. The membrane was then washed 3 times for 5 minutes in 1x TBST, and incubated in fresh 1% milk solution with the appropriate HRP-conjugated secondary antibody at a dilution of 1:5000 for 1 hour at room temperature, with constant agitation (see Table 3-3 for details of secondary antibodies used). The membrane was washed 3 times for 5 minutes in TBST, and subjected to analysis using the enhanced chemi-luminescence (ECL) method (Amersham BioSciences, Little Chalfont, UK) to detect antibody complexes bound to proteins of interest. Membranes were rinsed with ECL solution for 1 minute and then exposed to light-sensitive autoradiography film, which

was developed on a Kodak X-Omat Model 2000 processor. Images were quantified using Image J (NIH, Bethesda, MD) and statistical significance determined as described in Section 3.8.

Primary Antibody	Type; clone number	Specificity/Immunogen	Dilution	Supplier	Application
α-actinin	Mouse monoclonal; EA-53	Purified rabbit skeletal muscle α-actinin	1:2000	Abcam	IF
Cardiac troponin I	Mouse monoclonal; 284 (19C7)	Epitope between amino acids 41-49 of cTnI	1:1000-1:5000	Abcam	WB, IP, IF
Phospho-Ser22/Ser23 cardiac troponin I	Rabbit polyclonal	Synthetic phosphopeptide derived from mouse TnI around phosphorylation site (RRSSA)	1:5000	Abcam	WB
Hsp20	Rabbit polyclonal	Native Hsp20 purified from human skeletal muscle	1:1000	Upstate (Millipore)	WB
Phospho-Ser16 Hsp20	Rabbit polyclonal	Synthetic phosphopeptide derived from human Hsp20 around S16 phospho site (RASAP)	1:1000	Abcam	WB
HspB6	Mouse monoclonal; HSP20-11	Full length recombinant Hsp20	1:500-1:2000	Abnova	IF
AKAP-Lbc (V096)	Rabbit polyclonal	Purified human his-AKAP-Lbc, amino acids 789-1186	1:500-1:2000	Professor John Scott, Seattle, WA	WB, IP, IF
Pan-PDE4D	Sheep serum	Conserved C terminal region of PDE4D isoforms in all species	1:1000-1:5000	In-house	WB, IP, IF
PDE4D9	Rabbit polyclonal	Isoform-specific N terminal sequence	1:1000	Millipore	WB, IP, IF
Pan-PDE4A	Rabbit serum	Conserved C terminal region of rat PDE4A isoforms	1:2000	In-house	WB, IP
Pan-PDE4B	Sheep serum	Conserved C terminal region of PDE4B isoforms in all species	1:5000	In-house	WB, IP
GST	Mouse monoclonal; B-14	Full length protein	1:1000	Santa Cruz	WB
Rack1	Mouse monoclonal; B-3	Amino acids 131-317 of human RACK1	1:1000	Santa Cruz	WB
V5	Mouse monoclonal; R960-25	V5 epitope tag	1:5000	Invitrogen	WB, IP
FLAG-M2	Mouse monoclonal; M2	FLAG epitope tag	1:1000	Sigma	WB, IP
GFP	Mouse	Full length GFP (Aequorea	1:1000	Santa Cruz	WB, IP

	monoclonal; B-2	victoria)			
Digoxigenin-HRP	Mouse monoclonal; HRP.21H8	Reacts with free and bound digoxigenin	1:4000	Abcam	WB
PKA RI	Mouse monoclonal; 18/PKA[RI]	Mouse PKA RI, amino acids 225-381	1:1000	BD Biosciences	WB
PKA RII	Mouse monoclonal; 40/PKA, 47/PKA	Mouse PKA RIIα, amino acids 1-404; human PKA RIIβ, amino acids 1-418	1:1000	BD Biosciences	WB
PKA C subunits	Mouse monoclonal; 5B	Human PKA C, amino acids 18-347	1:1000	BD Biosciences	WB

WB, Western immunoblotting; IP, immunoprecipitation; IF, immunofluorescence

Table 3-2 Primary antibodies

Secondary Antibody	Type	Specificity/Immunogen	Dilution	Supplier; Cat no	Application
FLAG-HRP	Mouse monoclonal; M2	FLAG peptide	1:5000	Sigma	WB
V5-HRP	Mouse monoclonal; R961-25	V5 epitope tag	1:5000	Invitrogen	WB
Anti-mouse-HRP	Sheep	IgG	1:5000	GE Healthcare	WB
Anti-rabbit-HRP	Goat	IgG	1:5000	Sigma	WB
Anti-goat-HRP	Rabbit	IgG	1:5000	Sigma	WB
Donkey anti-sheep 488/594	Donkey	IgG heavy and light (H+L) chains from sheep	1:2000	Molecular Probes	IF
Donkey anti-rabbit 488/594	Donkey	IgG H+L from rabbit	1:2000	Molecular Probes	IF
Donkey anti-mouse 488/594	Donkey	IgG H+L from mouse	1:2000	Molecular Probes	IF

Table 3-3 Secondary antibodies

3.4.4 Coomassie Staining

Coomassie staining was used to visualise some proteins following SDS-PAGE. Pre-cast NuPage gels were removed from the plastic cassettes and rinsed in sterile dH_20. Gels were then incubated in 50ml of Coomassie stain (1.25g Coomassie Brilliant Blue R250, 444ml methanol, 56ml acetic acid in a final volume of 1L dH_20) at room temperature for 2 hours with gentle agitation. Coomassie stain was then replaced with destain (444ml methanol, 56ml acetic acid in a final volume of 1L dH_20) and agitated at room temperature for 6-12 hours, changing the destain every 4-6 hours, until all residual Coomassie stain was removed. Coomassie stain remained bound to all of the proteins present in the gel, allowing the identification of overexpressed proteins by comparison to the molecular weight markers.

3.4.5 siRNA knockdown of AKAP-Lbc

AKAP-Lbc knockdown was achieved using a small interfering RNA (siRNA) oligonucleotide against the AKAP-Lbc gene (*AKAP13*). Silencer select validated siRNA (sequence: GCAUAUUGCUUGUAACUCA) and control siRNA were obtained from Ambion (Austin, TX). Cells were passaged into 6 well plates and transfected at 40% confluence. For one well, 4µl of DharmaFECT I (Dharmacon - Thermo Scientific) transfection reagent was incubated in 200µl of Opti-MEM for 5 minutes at room temperature. 10µl of 20µM siRNA (0.2nmoles) was then added using barrier tips, and the tube mixed and incubated at room temperature for a further 20 minutes. 200µl was added per well, the growth medium changed after 24 hours, and cells harvested at 72 hours. Efficiency of knockdown was determined by Western immunoblotting.

3.5 Protein-Protein Interactions

3.5.1 Co-immunoprecipitation (Co-IP)

All steps were performed at 4°C. Following cell lysis and determination of protein concentration, samples were equilibrated to 1µg/µl in lysis buffer. 20µl of protein A/G beads (Santa Cruz Biotechnology, CA, USA) were added per 1ml of lysate in an Eppendorf tube, and tubes incubated with end-over-end rotation for 30 minutes to pre-clear the

lysate of any proteins which might non-specifically bind to the beads. Beads were pelleted at 16 000g for 1 minute and the pre-cleared supernatant removed to a fresh tube. 100µl of supernatant was removed and boiled for 5 minutes in an equal volume of 2x protein sample buffer, and stored at -20°C. This represented the IP "input". The remaining supernatant was divided between 2 tubes (450µl per tube), and 20µl of resuspended protein A/G beads added to each tube. 1-4µg of antibody to the protein of interest (or its epitope tag, if using transfected cells) was added to one tube (the "IP") and an equal amount of isotype-matched non-specific IgG (Cell Signaling Technology, Danvers, MA) added to the second tube as a control. Tubes were incubated overnight with rotation, then beads were pelleted at 6000g for 30 seconds and the supernatant carefully discarded. Beads were washed with 1ml of either HSE buffer (20mM HEPES, 150mM NaCl, 5mM EDTA) or 3T3 lysis buffer 3 times as above, then finally resuspended in an equal volume of 2x protein sample buffer and boiled for 5 minutes. All samples (input, control, IP) were separated by SDS-PAGE, and then transferred to nitrocellulose and immunoblotted, as described in Section 3.4.3.

3.5.2 Expression and Purification of GST Fusion Proteins

3.5.2.1. GST-PDE4D9

pGEX-6P1-PDE4D9 was kindly provided by Dr Allan Dunlop. This plasmid was transformed into BL21-CodonPlus competent cells (Stratagene, La Jolla, CA) as described in Section 3.2.1, and grown overnight at 15°C in 10ml of LB broth containing the appropriate antibiotic with orbital shaking at 220rpm. This starter culture was then used to inoculate a 500ml LB culture containing antibiotic, which was grown at 15°C with shaking for 2-3 hours. 1ml of this culture was removed at regular intervals, and the optical density at 600nm (OD600) measured against 1ml of sterile LB using a spectrophotometer. Once OD600 reached 0.6-1, bacteria could be assumed to be in a log phase, where they are growing exponentially. Expression of the fusion protein was then induced by adding 1mM isopropyl β-D-1-thiogalactoside (IPTG), and the culture grown for a further 3 hours and pelleted at 4400g for 10 minutes at 4°C. The pellet was resuspended in 10ml of ice cold GST lysis buffer (50mM Tris-Cl pH8.0, 100mM NaCl) and frozen overnight at -20°C. Upon thawing, 1mM DTT, 1mg/ml lysozyme and 1x protease inhibitor cocktail (Roche) were

added, and the suspension sonicated 4 times for 30 seconds on ice to encourage further cell lysis, with 1 minute between each sonication. Cell debris was pelleted at 12 000g for 30 minutes, and the supernatant removed to a fresh tube. 500µl of pre-washed glutathione beads (GE Healthcare, Little Chalfont, UK) in a 50% slurry with GST lysis buffer were added, and tubes incubated for 2 hours with end-over end rotation at 4°C. Beads were then collected in a gravity flow column and washed 3 times with 10ml of GST lysis buffer. Following the final wash, the column was capped and 0.5-1ml of GST elution buffer (50mM Tris-Cl pH8.0, 10mM reduced glutathione) incubated with the beads for 5 minutes. The cap was then removed and the eluent collected. This elution step was performed 3 times in total. Eluent was dialysed overnight in 2L of GST dialysis buffer (50mM Tris-Cl pH8.0, 100mM NaCl, 5% (v/v) glycerol) to remove glutathione. Samples were removed at each stage, boiled in 5x protein sample buffer, and analysed by SDS-PAGE and Coomassie staining as described in Sections 3.4.3 and 3.4.4, to determine protein expression.

3.5.2.2. GST-AKAP-Lbc fragments and GST pulldown assay

pGEX-4T1-AKAP-Lbc fragments 1-6 plasmids were kindly provided by Donelson Smith. Plasmids were transformed into BL21(DE3)pLysS cells (Stratagene), as described in Section 3.2.1, and grown overnight at 15-37°C in LB media with appropriate antibiotic. These starter cultures were then used to inoculate larger cultures, as in Section 3.5.2.1., and grown at 15-37°C with shaking for 2-3 hours unti OD600 reached 0.6-1. Fusion protein expression was then induced and the culture grown for a further 3 hours and pelleted as described in Section 3.5.2.1. Proteins were purified as in Section 3.5.2.1. 500µl of pre-washed glutathione beads in 50% slurry with GST lysis buffer were added to supernatants containing purified proteins, and tubes were incubated for 2 hours with end-over end rotation at 4°C. Beads were then washed 3 times with 15ml of GST binding buffer (25mM Tris pH7.4, 150mM NaCl, 1mM EDTA), with 0.5% Triton-X100 added for the final wash. Finally, beads were suspended in 500µl of GST binding buffer and used for GST pulldown assays. For pulldown assays, 500µl of HEK293 lysate containing overexpressed Hsp20-V5 was added per tube, tubes incubated at 4°C for 2 hours with gentle agitation, then washed 4 times in chilled HSE buffer containing 0.1% NP-40 at 200g for 5 minutes. Beads were then boiled in 4x protein sample buffer, and lysates separated by gel electrophoresis.

3.5.3 Solid phase peptide array

Peptide arrays are generated by direct synthesis of peptides onto Whatman cellulose membranes. Arrays of overlapping 25mer peptides, sequentially shifted by 5 amino acids, are generated, as shown in Figure 3-2. These arrays cover the entire sequence of the protein of interest, and are able to bind purified fusion proteins, providing information on protein-protein interactions, and the sites critical for these interactions (Bolger et al 2006, Frank 2002). Peptide arrays were synthesised in-house, using an AutoSpot-Robot ASS 222 (Intavis Bioanalyical Instruments, Köhn, Germany). Arrays were stored dry at 4°C prior to use. To investigate possible protein-protein interactions, peptide arrays were first activated by rinsing for 1 minute in 100% ethanol, then washed in 1x TBST for 10 minutes. Non-specific binding was blocked by incubating with 5% milk solution for 2 hours at room temperature with gentle agitation. The array was then incubated with 10µg/ml of the purified protein of interest in 1% milk solution at 4°C overnight. After 16 hours, the array was washed 3 times for 10 minutes in TBST and incubated with primary antibody to the purified protein of interest at the appropriate dilution for 2 hours at room temperature. After a further 3 washes in TBST, the appropriate HRP-conjugated secondary antibody was added for 1 hour at room temperature. Finally, the array was washed 3 times in TBST, and exposed to ECL and film (as in Section 3.4.3).

Peptide arrays were stripped in stripping buffer (20mM dithiothreitol, 70mM SDS, 60mM Tris-Cl pH6.8) by heating to 70°C for 30 minutes, then rinsed twice in TBST for 10 minutes. Arrays were air dried and stored sealed in plastic at 4°C. Arrays were reused a maximum of 2 times, and were re-probed with primary and secondary antibody to check stripping efficiency prior to use.

For each peptide array experiment with a GST-tagged fusion protein, the array was first incubated with GST alone as a control to identify sites which might bind the GST tag rather than the protein of interest. Where potential binding sites were identified on film as spots, the 25mer amino acid sequence corresponding to the spot was identified and an “Alanine Scan” of the region generated by producing a peptide array consisting of the wildtype spot, and then each residue sequentially mutated to alanine. If the original residue was alanine, it was mutated to aspartate instead. The resulting alanine scan was

then probed with the protein of interest as above. If mutation of a residue to alanine abolished binding of the fusion protein of interest, this provided evidence for it being involved in the interaction between the two proteins.

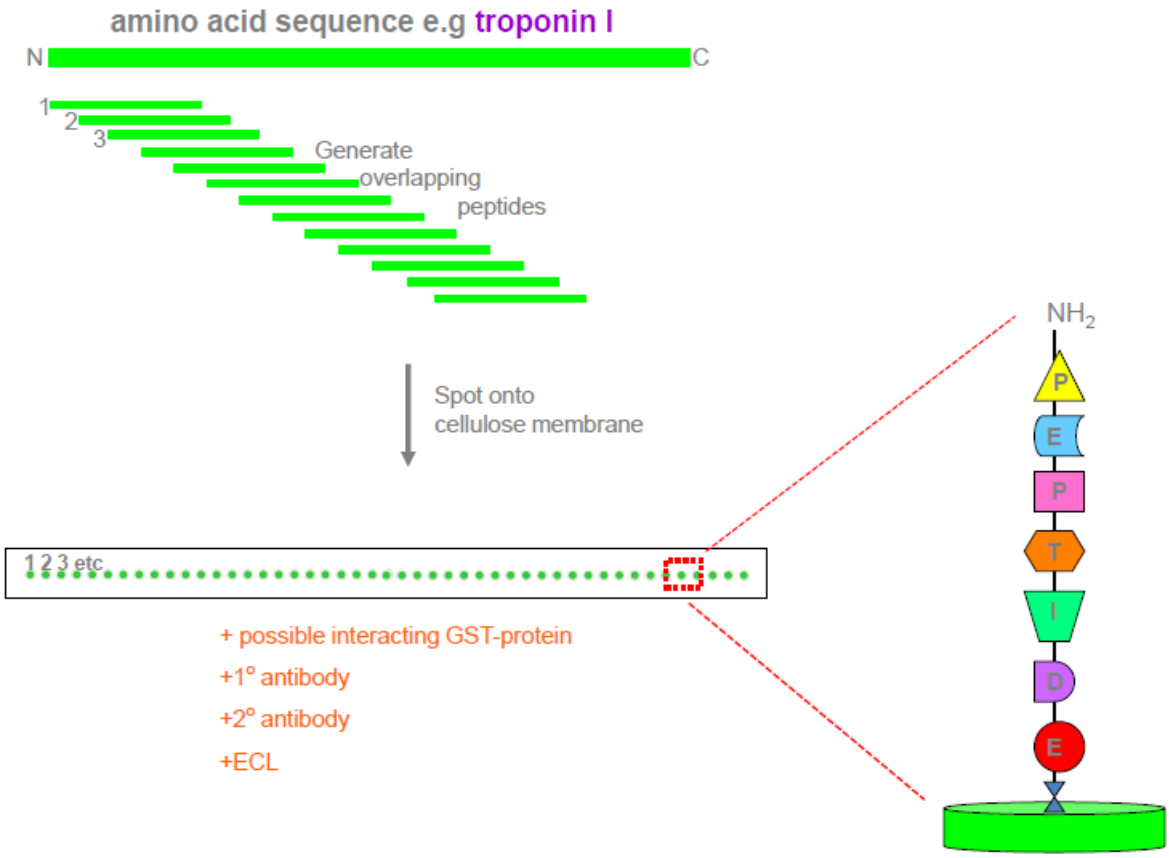

Figure 3-2 Schematic representation of a peptide array approach. Adapted from Dr George Baillie.
A series of overlapping peptides are generated from the amino acid sequence of the protein of interest. Individual amino acids are then precisely spotted onto a cellulose membrane to generate each of these overlapping peptides (1,2, 3, etc). The array is then incubated with a purified protein that is thought to interact with the protein of interest. Primary antibody against the potential interacting protein is then added, followed by HRP-linked secondary antibody, and immunoblots are developed using the ECL method described in Section 3.4.3. Dark spots on the film indicate potential interaction sites on the protein of interest.

3.6 Microscopy

3.6.1 Fluorescence Resonance Energy Transfer

Fluorescence resonance energy transfer (also known as Förster resonance energy transfer or FRET) describes the process of energy transfer between two fluorophores, a donor and an acceptor, which are often CFP and YFP. Excitation of the donor by a particular wavelength leads to a characteristic emission by the donor. However, if the donor and acceptor are in close proximity, and their emission and excitation spectra overlap, intermolecular FRET occurs, and the acceptor emission is predominantly detected (Figure 1-19).

3.6.1.1. FRET Sensors

FRET sensors can be linked to other proteins. The FRET sensors employed in this study were based on the Epac1-camps sensor (Nikolaev et al 2004), which consists of the cAMP-binding domain of Epac1 sandwiched between CFP and YFP (Figure 3-3). Binding of cAMP to Epac results in a conformational change which increases the distance between the two fluorophores, reducing the FRET signal.

Figure 3-3 Schematic of Epac1-camps FRET sensor. Adapted from (Nikolaev et al 2004). Residues E157 to E316 of Epac1, which encompass the cAMP binding domain of the protein, are cloned between YFP and CFP fluorophores to produce the intact sensor.

Generation of Hsp20:Epac1-camps FRET sensor

TnI:Epac1-camps and Hsp20:Epac1-camps targeted FRET sensors were generated by Dr Jon Day. The Hsp20 open reading frame, excluding the stop codon, was amplified from

the Ultimate ORF clone IOH57317 (Invitrogen) using the following primers to incorporate *Hin*dIII restriction sites at both 5' and 3' ends:

Forward primer: 5'-GCACAAGCTTATGGAGATCCCTGTGCCTGTGC-3'
Reverse primer: 5'-GCACAAGCTTGGCTGCGGCTGGCGGTGG-3'

The resulting fragment was cloned, in frame, into the *Hin*dIII site 5' to the Epac1-based sensor. Clones were screened for correct orientation of insert and correct clones were sequenced.

Generation of TnI:Epac1-camps FRET sensor

TnI:Epac1-camps was cloned as above. Primer sequences are detailed below:

Forward primer: 5'-GCACAAGCTTACCATGGCGGATGGGAGCAGCGATGC-3'
Reverse primer: 5'-GCACAAGCTTGCTCTCAAACTTTTTCTTGCG -3'

3.6.1.2. FRET Imaging

Neonatal rat ventricular cardiac myocytes were isolated and seeded onto glass coverslips at a density of 700 000 cells per coverslip, as described in Sections 3.3.2.1. and 3.3.2.2. Targeted FRET sensors were transiently transfected 24 hours after seeding, as described in Section 3.3.2.3. The Epac1-camps sensor was used as a control for all experiments. Cells were imaged 24-48 hours following transfection. Measurements were obtained from cells buffered in a pH7.4 solution of 125mM NaCl, 5mM KCl, 20mM HEPES, 1mM Na_3PO_4, 1mM $MgSO_4$, 1mM $CaCl_2$ and 5.5mM glucose, at room temperature. Cells were stimulated in real time with 1nM isoproterenol, 10µM rolipram, 10µM cilostamide, 50µM forskolin and 100µM IBMX, and imaged on an Olympus IX71 inverted microscope with a 100x oil immersion objective (Zeiss). The microscope was equipped with a beam splitter optical device (Photometrics) which splits emitted light into two beams using a dichroic filter. Wavelengths shorter than 505nm, including 480nm CFP emissions, are directed to a CFP emission filter, and wavelengths longer than 505nm, including 545nm YFP emission, are directed to a YFP emission filter. Therefore, both YFP and CFP images can be collected.

3.6.1.3. Data Acquisition

Images were acquired using MetaFluor software (Molecular Devices). First, one transfected cell was focused upon under the 100x objective. Only beating cells were imaged, to ensure no fibroblasts were included, as these can be difficult to distinguish from cardiac myocytes morphologically. Only one cell can be imaged per coverslip, so typically an n of 6-10 coverslips was used for one experimental condition. The exposure time, during which the sample was illuminated by excitation at 440nm and CFP and YFP signals acquired, was set at 200ms. Data was acquired every 10 seconds from a user-defined region of interest (ROI) within the cell. These conditions resulted in minimal photo-bleaching of samples, and allowed selection of specific cell areas from which data could be acquired. A background ROI was also selected, to allow subtraction of background noise for CFP and YFP data. FRET changes were measured following background subtraction by dividing the intensity of emissions at 480nm and 545nm, following excitation at 440nm, to give a FRET ratio. Data are expressed as dR/R_0, where R = FRET ratio at time t (sec), R_0 = FRET ratio at time zero, and $dR = R - R_0$. Graphs are presented as means +/- SEM.

3.6.2. Immunocytochemical staining of cardiac myocytes

Cells were fixed on glass coverslips in ice cold paraformaldehyde and methanol solution for 5 minutes (0.6:9.4 ratio of 16% paraformaldehyde to 100% methanol), then washed twice for 5 minutes in PBS with gentle agitation. Coverslips were protected from light at all times from this point. Cells were permeabilised for 20 minutes at room temperature with PBST (0.1% Triton-X100 in PBS), then washed for 5 minutes in PBS alone. Non-specific antibody binding sites were blocked by incubating with blocking buffer (0.2% fish gelatin (w/v), 0.3% BSA (w/v) in PBS) for either 30 minutes at room temperature, or overnight at 4°C, then coverslips were washed twice in PBS for 5 minutes. One or two primary antibodies were diluted to the desired concentrations in blocking buffer, 100µl of the solution applied to parafilm, and coverslips laid face down onto the antibody for 2 hours at room temperature. For each coverslip treated with primary antibody, an IgG control was also prepared, using equal amounts of the appropriate normal IgGs. Coverslips were then washed three times for 10 minutes in PBS, and incubated with 1:500 dilution of appropriate fluorescently labelled secondary antibodies in a final volume of

500µl per coverslip (Table 3-2). This step took place for either 1 hour at room temperature, or overnight at 4°C. Following secondary antibody incubation, coverslips were washed once in PBS and mounted onto glass slides using ProLong Gold antifade reagent with DAPI (4',6-diamidino-2-phenylindole) nuclear stain (Molecular Probes) and air dried. Coverslips were stored at 4°C and protected from light.

3.6.3 Confocal Microscopy

Cells were imaged using a 63x Zeiss oil immersion objective on a Zeiss Pascal LSM510 laser-scanning confocal microscope (Carl Zeiss, Germany). An argon laser was used to excite 488nm fluorescently labelled secondary antibodies. Helium/neon lasers were used to excite 568nm fluorescently labelled secondary antibodies. Zeiss Pascal software was used to collate image files.

3.7 Cell-based assays

3.7.1 Phosphodiesterase activity assay

PDE activity was measured in a two step radioactive assay of cAMP hydrolysis, which has previously been described (Marchmont & Houslay 1980). In the first step, samples are incubated with 8-[3H]-labelled cAMP substrate, and PDEs in the sample hydrolyse this to [3H]-5'-AMP. In the second step, addition of snake venom hydrolyses the 5'AMP to [3H]-adenosine, and incubation with an anion exchange resin binds any negatively charged, unhydrolysed cAMP, separating it from the adenosine. The amount of [3H]-adenosine is then calculated by scintillation counting, to determine the rate of cAMP hydrolysis.

All steps were performed at 4°C unless indicated. Samples were measured in triplicate. cAMP substrate solution for the assay consisted of 2µl of 1mM cAMP and 3µl of 8-[3H]-cAMP per ml of PDE assay buffer (20mM Tris-Cl pH 7.4, 10mM $MgCl_2$). Cellular lysates were freshly prepared in KHEM buffer (50mM KCl, 50mM HEPES pH7.2, 10mM EGTA, 1.9mM $MgCl_2$). A volume of lysate containing the required amount of protein was diluted in PDE assay buffer to 50µl final volume (this amount was previously determined in a pilot assay using increasing amounts of protein). If the effect of a PDE inhibitor was to be

assessed, 10mM stock solutions of inhibitors in DMSO were diluted 1:100 in KHEM, and 10µl of diluted inhibitor solution or KHEM plus the equivalent amount of DMSO alone was added to 40µl of protein sample. 50µl of KHEM buffer was used as a blank control. 50µl of cAMP substrate solution was added per tube to give a total reaction volume of 100µl, tubes were mixed gently and incubated at 30°C for 10 minutes to allow cAMP hydrolysis to occur. Samples were then boiled for 2 minutes to inactivate PDEs and terminate the reaction.

Tubes were cooled on ice for 15 minutes and 25µl of 1mg/ml snake venom from Ophiophagus Hannah added per tube. Tubes were mixed gently and incubated at 30°C for 10 minutes to allow conversion of AMP to adenosine. 400µl of Dowex anion exchange resin:H_20:100% ethanol (1:1:1 ratio) was added per tube, tubes were vortexed and incubated on ice for 15 minutes to allow binding of negatively charged unhydrolysed cAMP to the resin. Tubes were then re-vortexed, and centrifuged for 3 minutes at 16000g to pellet the Dowex. 150µl of supernatant was removed from each tube and added to a fresh 1.5ml tube containing 1ml of Opti Flow SAFE 1 scintillant. 50µl of cAMP substrate solution was also added to 1ml of scintillant, to assess total counts per minute for the assay. All tubes were then vortexed thoroughly, and the amount of 8-[3H]-adenosine in the supernatant (which is proportional to cAMP hydrolysis) determined by counting on a Wallac 1409 Liquid Scintillation Counter. Radioactive waste was handled and disposed of according to local protocols.

The specific PDE activity of each sample was corrected for background using the blank reaction and calculated in pmol cAMP hydrolysed/min/mg protein as follows:

PDE activity = 2.61 x [(average counts of 3 repeats – average of blanks)/average total] x 10^{-11} x 10^{12} x (1000/µg protein)

Where 2.61 corrects for the use of 150µl of supernatant from the Dowex stage (the total volume of the supernatant is 391.5µl),

x 10^{-11} corrects the value for the 10 mins over which hydrolysis occurs and corrects to moles of cAMP used, and x 10^{12} corrects to pmoles,

x (1000/µg protein) corrects for protein concentration.

3.7.2 Caspase-3 apoptosis assay

The Caspase-Glo 3/7 assay (Promega) was used to determine caspase-3 activity in cellular lysates. This is a luminescence assay, where luminescence is produced by caspase cleavage of the provided substrate, and is proportional to caspase-3 activity. All experiments were performed in triplicate. Relative luminescence was measured on a Mithras LB940 plate reader using 96 well white-walled tissue culture plates (Corning), and data collected using MikroWin 2000 software. Caspase-Glo reagent was added to untreated cells in media as a negative control. Purified caspase-3 enzyme (BIOMOL) was used as a positive control. Luminescence was measured for media and Caspase-Glo reagent alone (without cells) to obtain a blank value, and this was subtracted from other measurements.

3.8 Statistical analysis

In this thesis, all experiments were performed an n of 3 times, unless otherwise specified in the figure legend. Statistical significance was calculated using either an unpaired two tailed *t*-test in Microsoft Excel or by one way analysis of variance (ANOVA) using Graph Pad Prism software, as stated in the figure legend. A P value > 0.05 was considered not significant (ns), $P < 0.05$ was considered significant (*), $P < 0.01$ was considered very significant (**), and $P < 0.001$ was considered extremely significant (**).

4.

The phosphodiesterase isoform PDE4D9 regulates PKA phosphorylation of cardiac troponin I

4.1 Introduction

Cyclic 3’5’ adenosine monophosphate (cAMP) is a ubiquitous second messenger. Signal transduction cascades involving cAMP regulate a vast array of intracellular processes, including gene transcription (Delghandi et al 2005), neurotransmission (O'Donnell & Zhang 2004), cardiac contractility (Stelzer et al 2007), growth and differentiation (Smith et al 2010), and aspects of the immune response (Smith et al 2003). Intracellular levels of cAMP depend on the balance between cAMP synthesis by adenylyl cyclase (AC) isoforms (Willoughby & Cooper 2007) and cAMP hydrolysis by phosphodiesterase (PDE) enzymes (Baillie 2009). Members of the PDE1 (Rybalkin et al 1997) , PDE2 (Stangherlin et al 2011), PDE3 (Reinhardt et al 1995), PDE4 (Houslay et al 2007), PDE5 (Giordano et al 2001) and PDE8 (Patrucco et al 2010) families are all expressed in the cardiovascular system to some extent; however, PDE3 and PDE4 are thought to mediate the majority of cAMP hydrolysis in the heart (Houslay et al 2007, Mongillo et al 2004).

Over three decades ago, seminal studies in cardiac myocytes introduced the theory that cAMP is compartmentalised within cells (Brunton et al 1981, Buxton & Brunton 1983). Since then, a wealth of evidence has accumulated to support the concept of compartmentalised cAMP signaling (Baillie & Houslay 2005, Fischmeister et al 2006,

Lissandron & Zaccolo 2006, Zaccolo & Pozzan 2002). Once cAMP is generated by AC5 and AC6 isoforms at the plasma membrane of cardiac myocytes, it diffuses rapidly, and could potentially flood the cytosol (Hanoune & Defer 2001, Houslay et al 2007). Only three cAMP effectors have been identified, including the cyclic AMP-dependent protein kinase, PKA (Walsh et al 1968). PKA is found in macromolecular complexes, which may localise to the plasma membrane, the internal membranes of organelles, the nucleus, or remain soluble in the cytosol (Di Benedetto et al 2008, Kapiloff et al 1999, Perry et al 2002). PKA has the potential to phosphorylate a huge number of intracellular targets on the basis of its activation by one common second messenger signal from cAMP, and so very tight regulation of this process is necessary to maintain specificity within the cAMP/PKA signal transduction cascade. In other words, cAMP must specifically target a small group of downstream effectors, whilst inappropriate activation of others is prevented. It is now accepted that such a high degree of specificity is achieved by the compartmentalisation of cAMP effectors and the formation of subcellular cAMP gradients (Houslay 2010).

Phosphodiesterases represent the only means of degrading cAMP within the cell, and are integral to the compartmentalisation of cAMP (Conti & Beavo 2007). Targeting of PDE hydrolytic activity to specific subcellular locations allows the simultaneous creation of multiple localised concentration gradients of cAMP. These cAMP microdomains can then activate specific subcellular pools of cAMP effector proteins (Baillie 2009). In this way, very fine spatial and temporal control of cAMP signaling can be achieved.

PDEs are now known to be targeted to several of the complexes involved in cardiac β-adrenergic signaling and excitation-contraction coupling (ECC). The long PDE4 isoform, PDE4D3, associates with the cardiac ryanodine receptor and PKA at the sarcoplasmic reticulum and nuclear envelope, where it participates in a negative feedback loop. Under basal conditions, tonic activity of the PDE maintains local cAMP levels below the threshold for PKA activation. Following β-adrenergic stimulation, a rise in cAMP both activates PKA and increases PDE activity (Dodge et al 2001) via PKA-mediated phosphorylation of PDE4D3 on Ser54 (Sette & Conti 1996). This favours cAMP hydrolysis and subsequent inactivation of PKA. Another PDE4 long isoform, PDE4D5, has been demonstrated to bind to the signaling scaffold protein β-arrestin via its unique N terminus

(Bolger et al 2006, Perry et al 2002). Recruitment of a β-arrestin-PDE4D5 complex to the agonist-occupied β2-adrenergic receptor leads to desensitisation of the receptor by β-arrestin, lowering cAMP production by ACs. PDE4D5 then serves to hydrolyse cAMP which has already been produced in the sub-plasma membrane compartment, further downregulating the activity of local PKA (Baillie 2009).

PKA phosphorylation events play a key role in enhancing cardiac contractility. The heart responds to physiological stress by altering its rate of contraction (chronotropy), force of contraction (inotropy) and rate of relaxation (lusitropy), resulting in an increased cardiac output to combat the precipitating stress (Triposkiadis et al 2009). This response is triggered by elevated levels of circulating catecholamines, such as adrenaline, which bind to β1-adrenergic receptors, leading to cAMP generation and PKA phosphorylation of cardiac myofilament proteins and proteins regulating excitation-contraction coupling. Phosphorylation of the cardiac myofilament protein troponin I (TnI) has been demonstrated to alter both the calcium sensitivity of the myofilament (Stelzer et al 2007) and its contractile properties (Takimoto et al 2004). PKA phosphorylates TnI on two neighbouring Serine residues within a unique N terminal region which is absent in skeletal muscle isoforms of the protein (Solaro et al 1976). PKA phosphorylation of TnI has been linked with an enhanced rate of relaxation and force of contraction in transgenic mouse hearts (Takimoto et al 2004). PKA phosphorylation events are tightly controlled due to the generation of localised cAMP gradients by PDEs. Although particular PDE isoforms have been linked with regulating the PKA phosphorylation of certain cardiac proteins involved in ECC, such as the ryanodine receptor (Dodge et al 2001) and the voltage-gated potassium channel (Terrenoire et al 2009), to date, nothing is known about PDEs that may regulate cAMP signaling and PKA phosphorylation of TnI at the myofilament. PDE activity in the vicinity of TnI would favour cAMP hydrolysis and inactivation of PKA. The actions of myofilament-associated PDEs would, therefore, influence cardiac contractility, and such enzymes would represent a novel therapeutic target in the treatment of diseases such as heart failure, where β1-adrenergic signaling pathways are known to be chronically downregulated (Triposkiadis et al 2009).

4.1.1 Experimental aims

It has never been shown that specific PDEs regulate cAMP levels around TnI at the cardiac myofilament. The aim of the experimental work detailed in this chapter was to discover whether PDE isoforms hydrolyse cAMP around TnI, and thereby regulate the PKA phosphorylation status of TnI. The role of an AKAP in facilitating PKA phosphorylation of TnI was also investigated.

4.1.2 Experimental procedure

1) A FRET-based cAMP sensor which localised to TnI at the myofilament was developed. Expression and localisation of this sensor was tested in neonatal rat ventricular cardiac myocytes (NRVM).

2) Cells expressing the TnI-linked cAMP sensor were treated with different PDE family inhibitors, and changes in myofilament cAMP dynamics were measured by FRET.

3) Neonatal rat ventricular cardiac myocytes (NRVM) were treated with different PDE family inhibitors, and the effects on PKA phosphorylation of TnI were determined by immunoblotting.

4) Specific association of TnI with different PDE subfamilies and individual isoforms was investigated by co-immunoprecipitation and colocalisation studies.

5) The interaction sites for PDEs on TnI were mapped by peptide array.

6) The presence of an AKAP to mediate PKA phosphorylation of TnI was investigated using Ht31 peptide and RII overlay techniques

4.2 Results

4.2.1 Expression and localisation of a TnI-linked cAMP FRET sensor

Fluorescence resonance energy transfer (FRET) describes the process of energy transfer between two fluorophores, often cyan- and yellow- fluorescent proteins (CFP and YFP), which occurs when the fluorophores are in close proximity (Section 1.6.1). Epac1-camps is a genetically encoded cAMP sensor consisting of YFP and CFP fluorophores linked to the cAMP binding domain of Epac1 (Nikolaev et al 2004). When cAMP levels are low, excitation of CFP at 440nm will result in FRET and the detection of YFP emission at 545nm, as the two fluorophores are close together. When cAMP levels rise, cAMP binds to the Epac1 component, leading to a conformational change in the sensor. The two fluorophores move further apart, FRET is reduced, and CFP emission at 480nm is detected instead (Figure 4-1A). Changes in FRET ratio (480/545nm) are directly proportional to cAMP levels in the cell (Zaccolo & Pozzan 2002). Epac1-camps is commonly used to study cAMP dynamics within intact cells. This sensor was selected for FRET experiments due to its high sensitivity, equal expression of YFP and CFP moieties, and its ability to measure changes in cAMP with high temporal resolution (Nikolaev et al 2004). Recently, novel Epac-based FRET sensors have been generated by linking them to other proteins, allowing their targeting to specific subcellular compartments (Herget et al 2008, Sin et al 2011). Thus, high spatial resolution of cAMP dynamics can also be achieved using these sensors.

In order to measure cAMP dynamics at the myofilament, a novel fusion protein was generated by fusing Epac1-camps to the C terminus of TnI. This sensor was kindly provided by Dr Jon Day at the University of Glasgow. The novel sensor was designated TnI:Epac1-camps (Figure 4-1B).

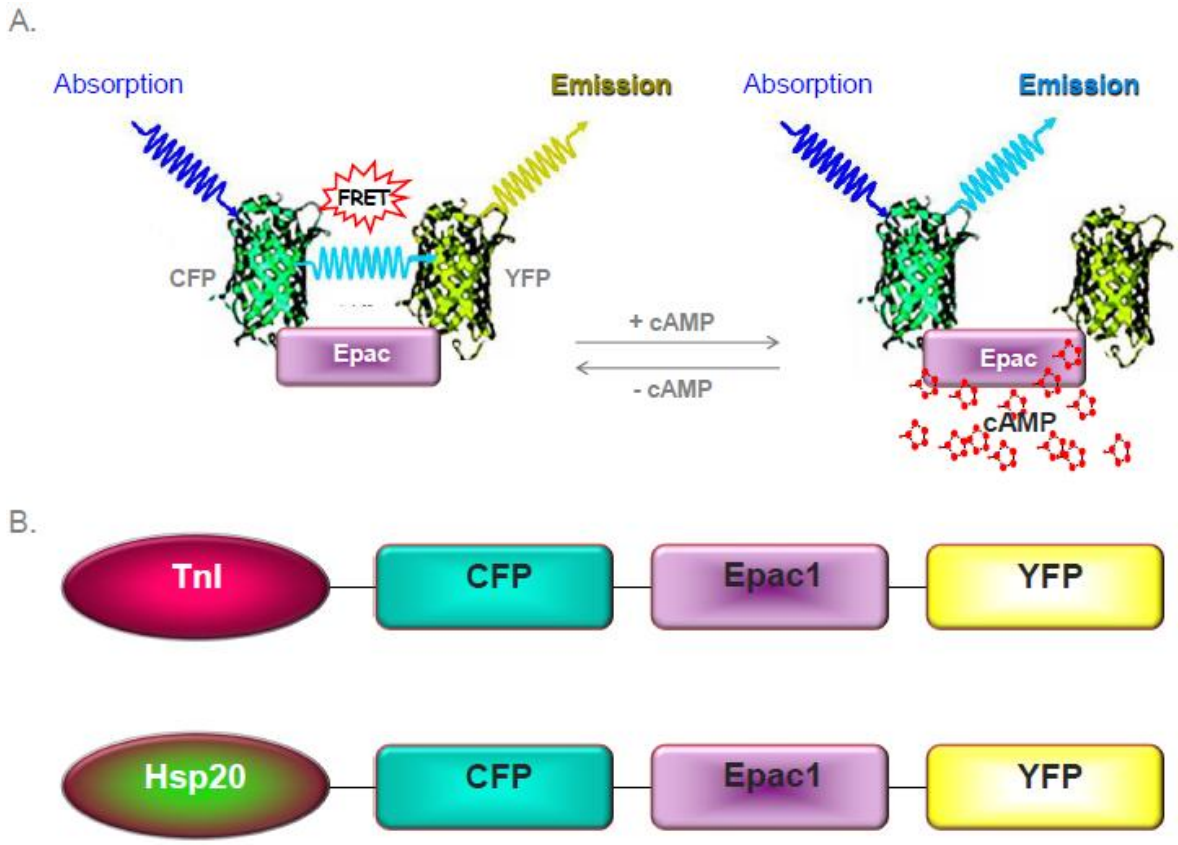

Figure 4-1 FRET measured by the Epac1-camps sensor.
A. In this sensor, the GFP variants cyan fluorescent protein (CFP) and yellow fluorescent protein (YFP) are linked by residues E157-E316 of the cAMP binding domain of Epac1 (Nikolaev et al 2004). In the absence of cAMP, the 2 fluorophores are in close proximity and FRET can occur. When cAMP levels rise, cAMP binds to the sensor leading to a conformational change in the Epac1 domain, the fluorophores are moved apart, and FRET is abolished. B. Schematic representation of the TnI:Epac1-camps sensor. TnI was cloned 5' of this sensor to generate a novel fusion protein which localised to the myofilament.

Epac1-camps and TnI:Epac1-camps were transfected into cultured neonatal rat ventricular cardiac myocytes (NRVM). NRVM are terminally differentiated cells, and are a widely used model to study cardiac physiology and pathophysiology due to their ability to beat spontaneously, respond to pharmacological stimuli and undergo gene transfer (Maass & Buvoli 2007). All experiments in this thesis were performed in this cell type, unless otherwise stated. Expression and appropriate localisation of the two sensors was determined by fluorescence microscopy of YFP (Figure 4-2). Epac1-camps showed uniform distribution throughout the cytosol. This sensor contains only part of the cAMP binding domain of full length Epac1, and therefore lacks any localisation sequences.

Epac1-camps was used as a control for generalised cytosolic cAMP signaling during all subsequent FRET experiments. TnI-Epac1-camps localised with a striated pattern in NRVM. Myofilaments are composed of repeating contractile units known as sarcomeres, which comprise overlapping thin and thick protein filaments, giving them a characteristic striated appearance under the microscope. TnI forms part of the heterotrimeric Tn complex which is evenly spaced along the thin filament, with 1 Tn complex per 7 monomers of actin (Engel et al 2004). Thus the appearance of TnI:Epac1-camps under YFP fluorescence is consistent with it localising to TnI at the myofilaments (Figure 4-2A). The localisation pattern of TnI was confirmed in NRVM which had been fixed and immunocytochemically stained with a TnI-specific antibody (Figure 4-2B).

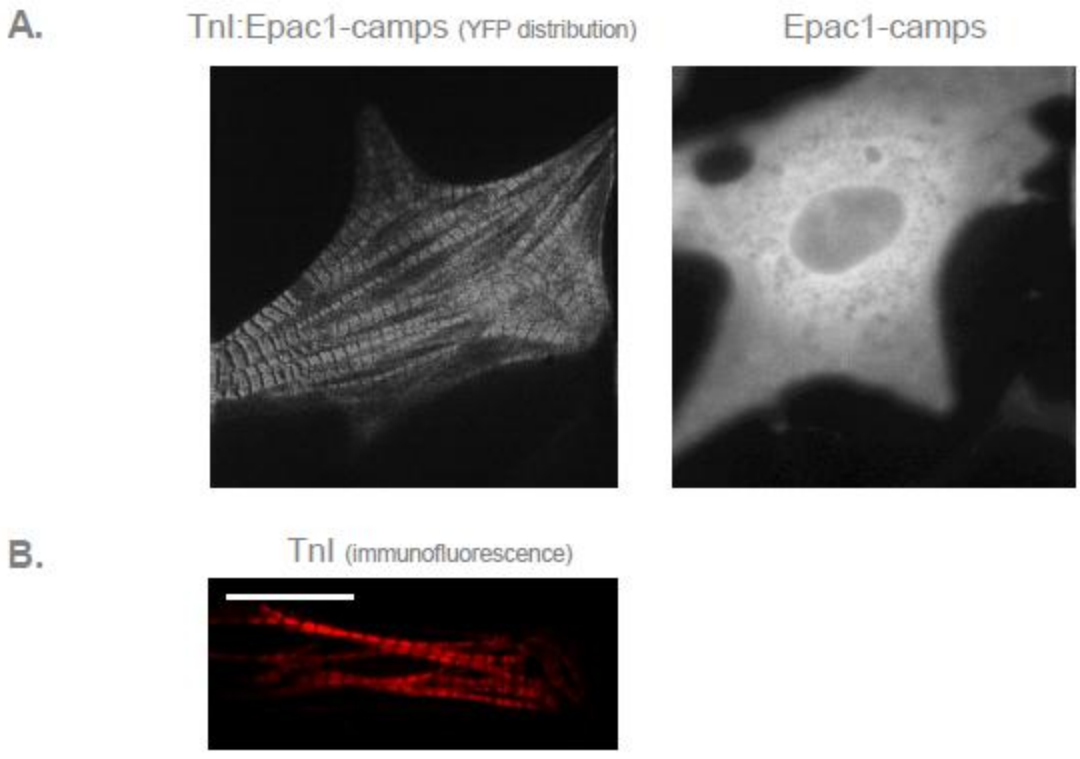

Figure 4-2 Localisation of Epac1-camps and TnI:Epac1-camps FRET sensors in NRVM. A. TnI:Epac1-camps localises to the myofilament, leading to a characteristic striated distribution pattern. Epac1-camps shows cytoplasmic distribution, as it lacks any localisation sequences. Images were obtained from live cells using a laser confocal microscope at 100x magnification. B. Immunocytochemical analysis and fluorescence microscopy of a fixed NRVM stained with anti-TnI antibodies, showing identical distribution to the TnI FRET sensor. Scale bar represents 20µM.

4.2.2 Characterisation of the properties of TnI:Epac1-camps

In order to test the efficiency of both FRET sensors in measuring cAMP levels within their respective subcellular compartments, the maximal activation of each sensor was determined. This characterisation was particularly important for the novel TnI:Epac1-camps sensor, to ensure that fusion of TnI to the CFP fluorophore did not interfere with the ability of the sensor to detect changes in cAMP levels. NRVM were transfected with either the TnI-targeted sensor or Epac1-camps. A large quantity of intracellular cAMP was then generated by real time stimulus of transfected cells with forskolin (FSK) and isobutyl-methylxanthine (IBMX). FSK is an adenylyl cyclase activator and stimulates cAMP production by cardiac ACs, whereas IBMX is a non-specific PDE inhibitor that blocks cAMP degradation. Both sensors were able to rapidly detect the change in cAMP levels. The magnitude of response was similar for both FRET sensors (22.3% ± 2.0% for TnI:Epac1-camps and 20% ± 1.7% for Epac1-camps) (Figure 4-3A),and there was no statistically significant difference between these two values, indicating that the presence of the TnI moiety does not significantly impair the ability of Epac1-camps to measure changes in cAMP levels.

Changes in intracellular [cAMP] can be estimated from changes in FRET. FRET can be expressed as the ratio (R) of CFP emission intensity over YFP emission intensity following excitation of the cell at 440nm ($R = CFP_{480}/YFP_{545}$). Changes in this FRET ratio were expressed as the increase in CFP/YFP ratio over the CFP/YFP ratio at time zero (R0), as described in the Materials and Methods (Section 3.6.1.3) and (Mongillo et al 2004). As [cAMP] rises in the vicinity of the FRET sensor, the two fluorophores move further apart, and FRET is diminished, resulting in predominantly CFP emission. The CFP/YFP ratio therefore increases in proportion to the rise in [cAMP]i (Mongillo et al 2004, Zaccolo & Pozzan 2002).

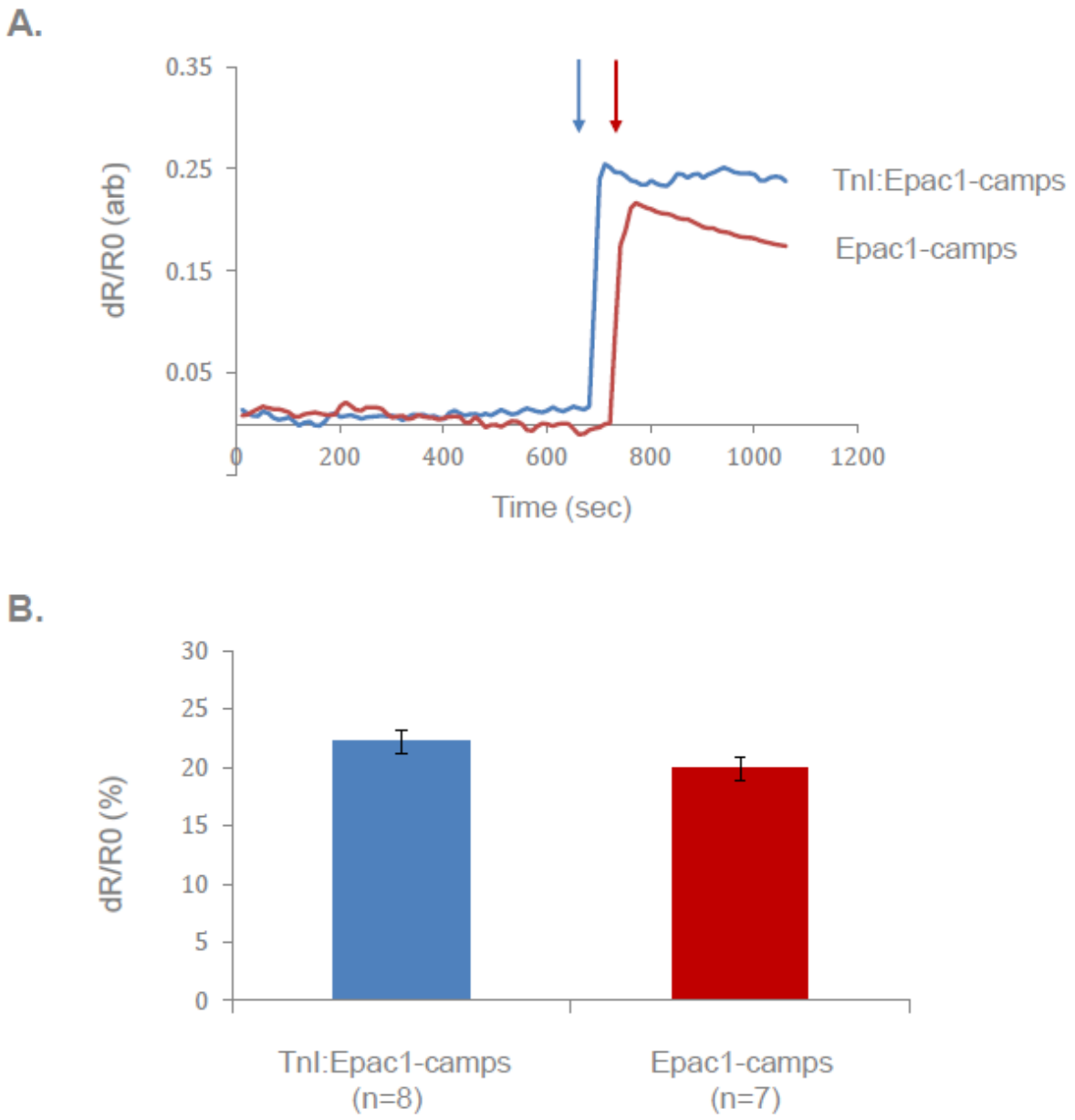

Figure 4-3 Maximal activation of Epac1-camps and TnI:Epac1-camps in response to saturating intracellular concentrations of cAMP.
NRVM transfected with the different FRET sensors were stimulated with 50µM FSK and 100µM IBMX, and the changes in FRET ratio calculated as described in the text. A. Representative traces of change in FRET ratio over time for the 2 sensors. Arrows indicate the time at which the FSK/IBMX stimulus was applied for each sensor. B. Graph of the percentage change in FRET ratio for both sensors. No significant difference in the maximal FRET ratio was observed between the two sensors. Error bars indicate standard error of the mean (SEM), and n numbers for each experiment are shown in brackets. Each n number indicates a single measurement from an individual cell.

4.2.3 PDE4 regulates cAMP levels around TnI

4.2.3.1. PDE4 provides the greatest cAMP hydrolytic activity in NRVM

PDE 1, 2, 3, 4, 5 and 8 are known to be expressed in the heart to different extents; however their individual contributions to cAMP hydrolysis in NRVM have not all been assessed. As a first step to determining which PDE isoforms regulate cAMP around TnI at the myofilament, the individual contributions of each of the PDE families to cAMP hydrolysis in unstimulated NRVM lysates were measured (Figure 4-4). A variety of inhibitors of the different PDE families are available (Table 1-2). Lysates were treated with PDE family inhibitors, as described in the figure legend, and the amount of cAMP hydrolysis calculated by phosphodiesterase activity assay (Section 3.7.1) (Marchmont & Houslay 1980). As expected, treatment with the non-selective PDE inhibitor IBMX resulted in a dramatic decrease in cAMP hydrolysing activity. IBMX inhibits all PDE families, with the exception of PDE8 (Wang et al 2008). Rolipram, which inhibits all members of the PDE4 family, had a similar effect to IBMX , indicating that PDE4 is responsible for the majority of cAMP hydrolysing activity in this cell type. This is in agreement with previous data from Mongillo and co-workers, who looked at the relative contributions of PDE3 and PDE4 to cAMP hydrolysis in this cell type (Mongillo et al 2004). Inhibition of PDE5 with zaprinast, and PDE8 with dipyridamole also significantly reduced cAMP hydrolysis in these cells. Dipyridamole inhibits PDE8 with an IC50 of 4.5μM, and PDE5 with an IC50 of 0.9μM (Soderling et al 1998), and it may be that some off-target effects on other PDE families were observed with these inhibitors.

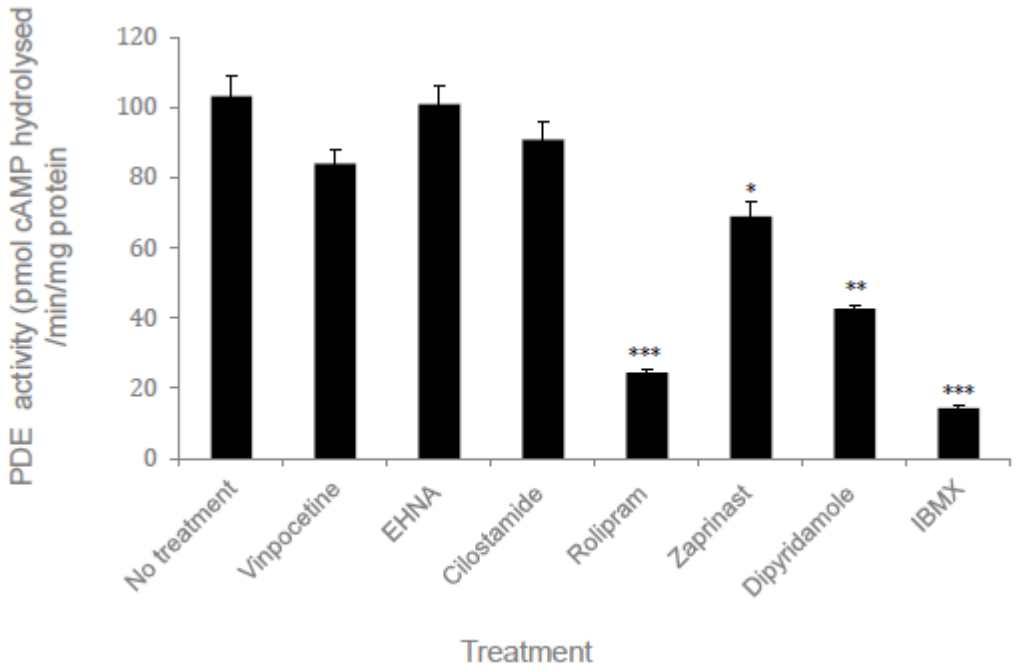

Figure 4-4 cAMP hydrolysing activities of different PDE families in NRVM.
NRVM lysates were treated with 10µM concentrations of different PDE family inhibitors (100µM IBMX), and cAMP hydrolytic activity assessed by the method of Marchmont and Houslay, described in Section 3.7.1. PDE activity was calculated in pmol cAMP hydrolysed/min/mg of protein. Inhibition of PDE1 (vinpocentine), PDE2 (EHNA) and PDE3 (cilostamide) had no significant effect on cAMP hydrolysis in NRVM, whereas PDE5 (zaprinast) and PDE8 (dipyridamole) inhibition both led to significant reductions in cAMP hydrolysed when compared with untreated lysates (*P<0.05 and **P<0.01 respectively). PDE4 inhibition with rolipram was associated with the greatest reduction in cAMP hydrolysis (*P<0.001), comparable to that of the non-specific PDE inhibitor IBMX. Therefore, PDE4 appears to be the most important family regulating cAMP hydrolysis in NRVM. Each data point represents an n of 3 separate experiments, and statistical significance was calculated using an unpaired two tailed *t*-test.**

4.2.3.2. A FRET sensor targeted to TnI reveals that PDE4 modulates the pool of cAMP around TnI

Next, I wanted to determine the PDE(s) responsible for cAMP hydrolysis at the myofilament. The use of targeted FRET sensors has enabled the real time monitoring of cAMP levels within specific subcellular compartments. TnI:Epac1-camps is a novel genetically encoded cAMP sensor which measures cAMP levels around TnI. Given that the majority of cAMP hydrolytic activity in NRVM is contributed by PDE4, it seemed reasonable to assume that members of the PDE4 family might play a major role in regulating cAMP levels around TnI. TnI:Epac1-camps and Epac1-camps were transfected

into cells, and changes in FRET (and therefore [cAMP]) were measured following inhibition of PDE4 (Figure 4-5). The effect of PDE3 inhibition on FRET was also investigated, as PDE3 and PDE4 are thought to be the predominant families expressed in cardiac myocytes (Houslay et al 2007). As in Figure 4-3, non-selective inhibition of PDEs with IBMX generated large changes in the FRET ratio, and the observed effects were similar for both sensors. In addition, both sensors responded similarly to cAMP generated via stimulation of β-adrenergic signaling pathways with the synthetic β-agonist isoproterenol (Iso). Treatment with the PDE4 inhibitor rolipram led to an increase in FRET measured by both sensors; however significantly greater FRET was measured by TnI:Epac1-camps (5.1% ± 1.1% compared with 2.9% ± 0.1% for Epac1-camps, $P<0.05$). Treatment with the PDE3 inhibitor cilostamide also led to a measurable increase in FRET for both sensors, but this time, Epac1-camps detected a greater FRET response (4.2% ± 0.8% compared with 1.7% ± 0.9% for TnI:Epac1-camps, $P<0.05$). Thus, it appears that the two sensors are measuring changes in cAMP levels in two distinct subcellular compartments, the cytosol and the cAMP microdomain around TnI at the myofilament. Inhibition of PDE4 led to a larger rise in cAMP at the myofilament than inhibition of PDE3, indicating that PDE4 regulate cAMP levels around TnI, and may, therefore, regulate PKA activation of TnI.

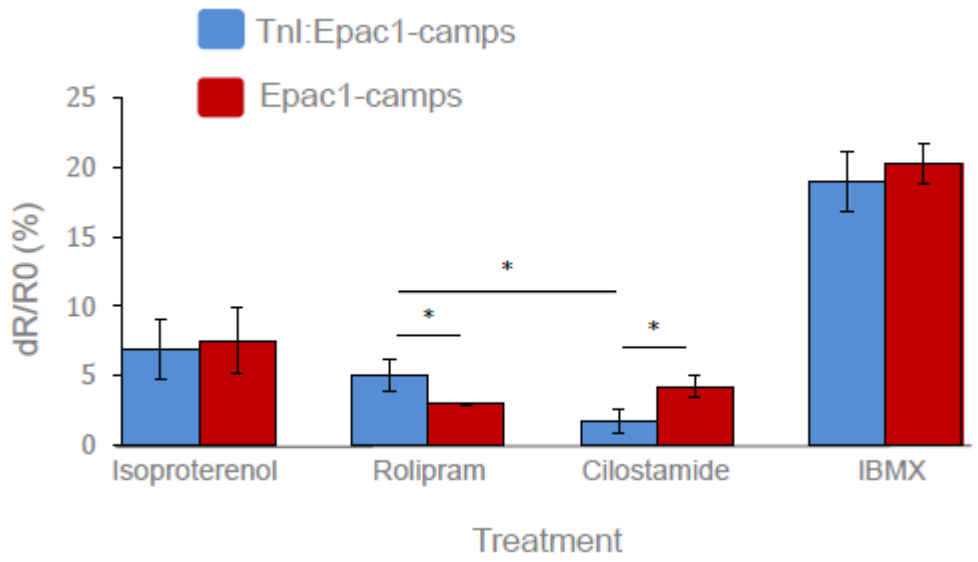

Figure 4-5 Changes in FRET ratio in different intracellular compartments in response to PDE family inhibition.
Cells were treated with either 1nM isoproterenol (as 10nM was found to be saturating), 10µM cilostamide or 10µM rolipram, followed by 100µM IBMX to saturate the sensors. The change in FRET ratio measured by TnI:Epac1-camps was significantly greater in the presence of rolipram than cilostamide (P<0.05), indicating that PDE4 plays the predominant role in regulating cAMP levels around TnI at the myofilament (n=7-10 for each experimental condition). No significant difference was observed between response of the two sensors to Iso (TnI:Epac1-camps, 6.9% ± 2.1%; Epac1-camps, 7.5% ± 2.4%) or IBMX (TnI:Epac1-camps, 19.0% ± 2.1%; Epac1-camps, 20.3% ± 1.4%). * P<0.05. Statistical significance was calculated using one way analysis of variance (ANOVA).

The kinetics of the TnI:Epac1-camps sensor were also studied. FRET responses to Iso and IBMX measured by this sensor were very rapid, being detected almost immediately after application of the stimulus (Figure 4-6, grey arrows). Stimulation of the cells with rolipram resulted in a similar magnitude of change in FRET ratio as for Iso, but the effect was much slower. This could be explained by the fact that Iso acts on β-AR at the cell surface to generate intracellular cAMP, whereas rolipram must cross the plasma membrane to bring about its effects, and acts on basal cAMP levels.

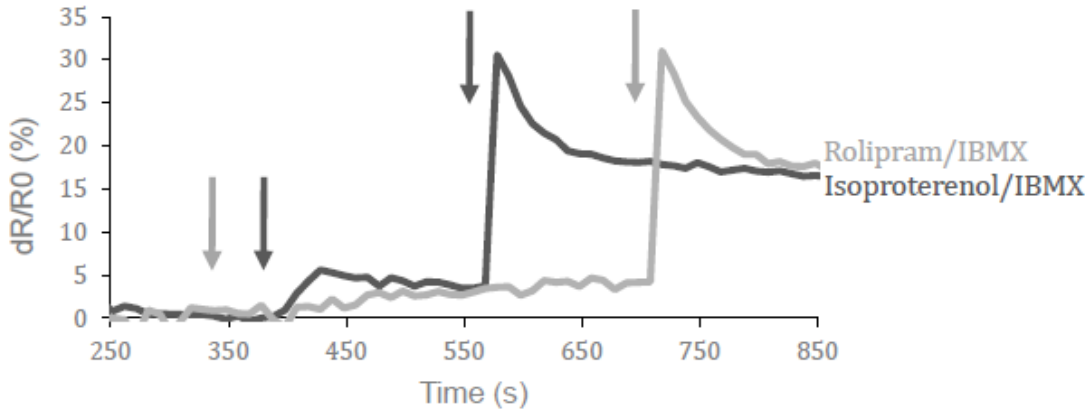

Figure 4-6 Representative traces of changes in FRET ratio measured by TnI:Epac1-camps in response to stimulation with rolipram or isoproterenol.
Application of each stimulus is indicated by an arrow. Rolipram stimulus was applied first, and followed by IBMX stimulus once the response had plateaued. The magnitude of response was similar for isoproterenol (1nM; dark grey trace) and rolipram (10µM; light grey trace); however, the response to rolipram was much slower to develop. Rolipram has to cross the plasma membrane to mediate its effects on basal cAMP levels, whereas isoproterenol acts directly on β1-adrenergic receptors on the cell surface to mediate generation of the second messenger, and therefore leads to more rapid changes in FRET ratio. The response of both sensors to a saturating concentration of IBMX (100µM) was similar. n = 7-10 for each experimental condition.

4.2.3.3. PDE4 regulates PKA phosphorylation of TnI at the myofilament

The experiments detailed so far using the novel targeted FRET sensor, TnI:Epac1-camps, demonstrate that PDE4 family members provide the majority of the cAMP hydrolysing activity around TnI. I next wanted to determine whether this modulation of cAMP levels translated into effects on the PKA phosphorylation status of TnI. To this end, NRVM were treated with inhibitors of the main PDE families expressed in cardiac myocytes, and the effects on PKA phosphorylation of TnI at Ser22/Ser23 determined by Western immunoblotting (Figure 4-7). Phosphorylation levels of TnI in untreated cells were used as a negative control, and Iso treatment (which is known to activate β-adrenergic signaling pathways, resulting in PKA phosphorylation of myofilament proteins such as TnI) acted as a positive control. Inhibition of PDE4 with rolipram resulted in a significant increase in PKA phosphorylation of TnI at Ser22/Ser23 ($P<0.01$), consistent with a role for this enzyme family in modulating cAMP levels around TnI. Dipyridamole treatment also led to significant increases in TnI phosphorylation ($P<0.05$). PDE8A has recently been shown to modulate ECC in cardiac myocytes. Experiments performed in PDE8A-/- mice indicate that

PDE8A is involved in modulating Ca^{2+} transients at the L-type calcium channels and SR in response to β-adrenergic stimulation (Patrucco et al 2010). Thus, it is conceivable that PDE8A may also be involved in Ca^{2+} responses at the myofilament. However, at the concentration used, dipyridamole is known to inhibit other PDE families in addition to PDE8, in particular the cGMP-selective PDEs PDE5, PDE6 and PDE11, and so it is likely that the observed increases in TnI phosphorylation represent off-target inhibitor effects.

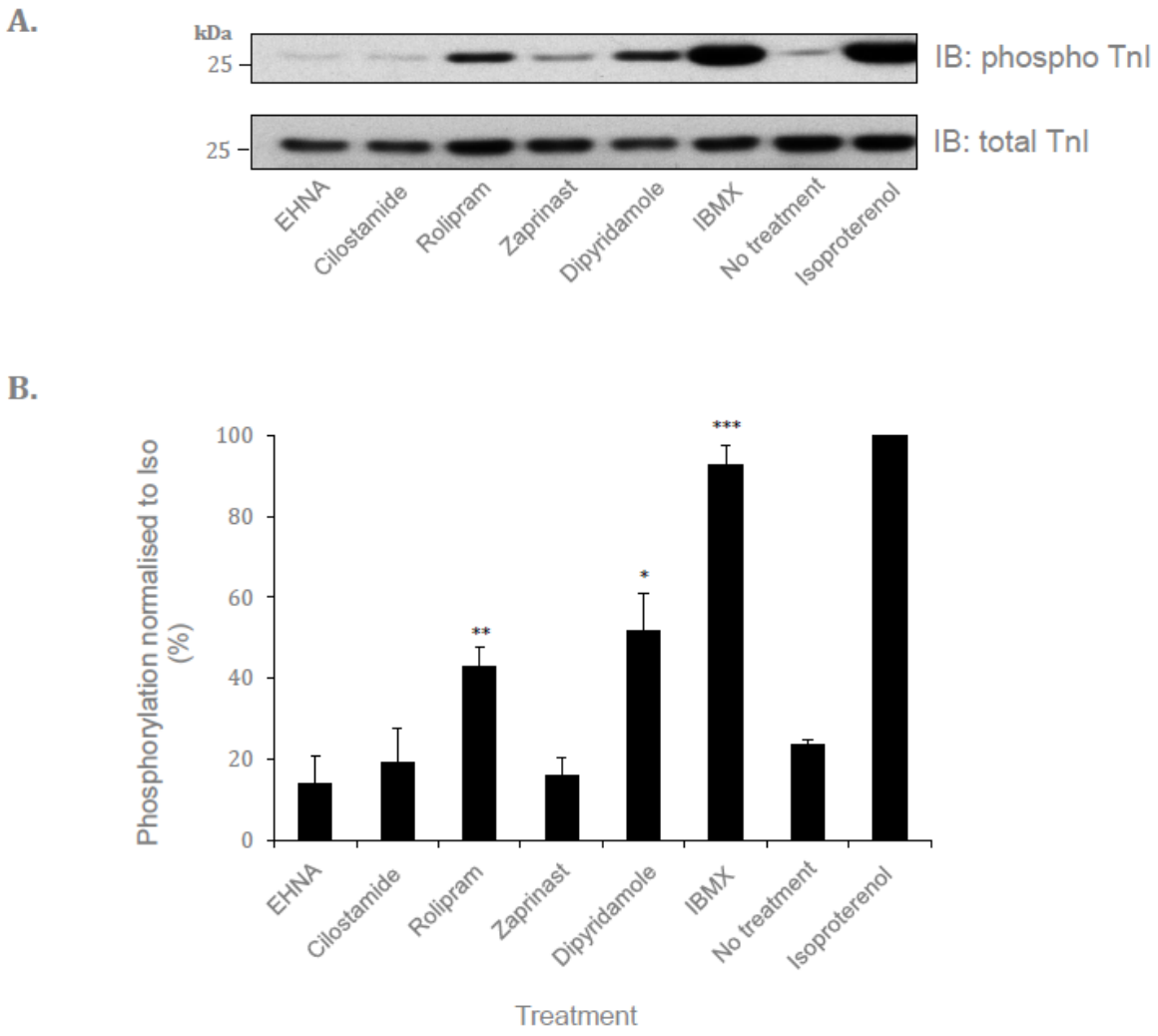

Figure 4-7 Effect of PDE family inhibitors on PKA phosphorylation of TnI at Ser22/Ser23. NRVM were treated with different PDE inhibitors (10μM: EHNA, cilostamide, rolipram, zaprinast, dipyridamole; 100μM IBMX) or isoproterenol (10μM, to saturate the response), for 10 minutes. A. Cells were harvested, and the amounts of PKA-phosphorylated TnI and total TnI determined by Western immunoblotting. A representative immunoblot is shown. B. Quantification of data shown in part A by densitometry. Inhibition of PDE4 with rolipram significantly increased PKA phosphorylation of TnI at Ser22/Ser23 over basal levels (P<0.01), indicating that this PDE family regulates the pool of cAMP around TnI. Data shown represents the mean ± SEM of 3 separate experiments. * P<0.05; ** P<0.01; *** P<0.001.

The effects of PDE4 inhibition on TnI phosphorylation were investigated further over a rolipram time course (Figure 4-8). NRVM were pre-treated with rolipram and then stimulated with a submaximal concentration of Iso over time, or treated with Iso alone. Iso stimulation led to a very rapid and sustained phosphorylation of TnI at Ser22/Ser23, consistent with the role of TnI phosphorylation in enhancing cardiac output in response to β-AR signaling (Stelzer et al 2007, Takimoto et al 2004). Pre-treatment with rolipram increased the percentage of PKA-phosphorylated TnI at all the time points shown, indicating that generation of cAMP in response to Iso is augmented by local inhibition of PDE4-mediated cAMP hydrolysis.

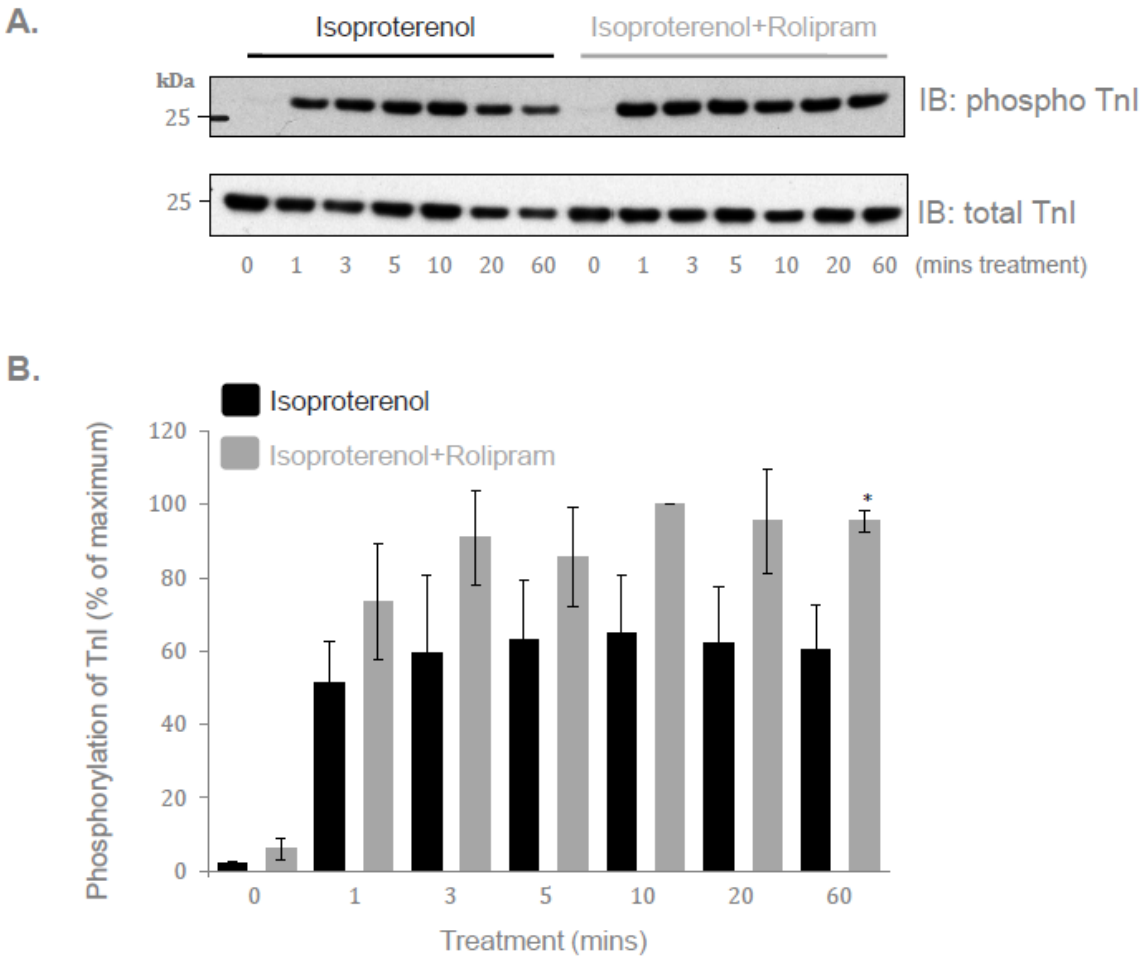

Figure 4-8 Time course of NRVM treatment with isoproterenol and rolipram.
NRVM were treated with either Iso alone, or pre-treated with the PDE4 inhibitor rolipram for 10 minutes, then stimulated with 10nM Iso for 1, 3, 5, 10, 20 or 60 minutes. A. Representative Western immunoblot of Iso and Iso + Rolipram time courses. Addition of PDE4 inhibitor increased PKA phosphorylation of TnI at Ser22/Ser23 over that observed with Iso alone. B. Quantification of data in part A. Data represents the average from an n of 3 experiments normalised to the maximum level of phosphorylation observed. * P<0.05.

4.2.4 TnI associates with members of the phosphodiesterase 4D subfamily

The above experiments indicate that members of the PDE4 family regulate cAMP levels around TnI. The PDE4 family is large, consisting of 4 subfamilies: 4A, 4B, 4C and 4D, and over 20 different isoforms (Houslay et al 2007). Only the PDE4A, 4B and 4D subfamilies are expressed in the heart (Fischmeister et al 2006). Rolipram acts as a competitive inhibitor of cAMP at the common catalytic site of PDE4, and therefore cannot provide specific information on the activity of particular isoform(s) (Spina 2008). It has previously been shown that in NRVM the majority of PDE4 cAMP hydrolytic activity is provided by the PDE4D subfamily, with a small contribution from PDE4B, and virtually no contribution from PDE4A or PDE4C (Mongillo et al 2004). It therefore seemed reasonable to investigate whether members of the PDE4D subfamily could regulate the myofilament pool of cAMP via an association with TnI. Consistent with this hypothesis, PDE4D co-immunoprecipitated with TnI in NRVM lysates (Figure 4-9). Immunoprecipitation was performed using either anti-TnI antibody or normal IgG as a control, and an immunoblot was then probed with an antibody raised against the subfamily-specific C terminal region of PDE4D.

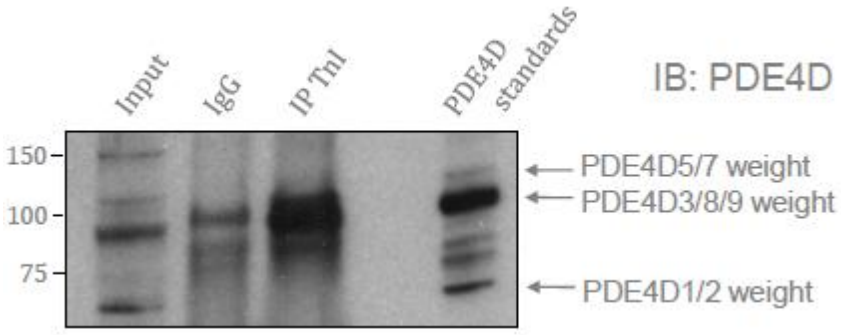

Figure 4-9 Co-immunoprecipitation of PDE4D isoforms with TnI.
An immunoblot of a TnI immunoprecipitation (IP) was performed using an in house Pan PDE4D antibody. The reciprocal IP could not be performed, due to the similarities in molecular weight of TnI and IgG light chains.

The association between TnI and PDE4D was investigated further by immunofluorescence. Adult rat ventricular cardiac myocytes (ARVM) were fixed and immunostained with antibodies against cardiac TnI and Pan PDE4D. Adult cardiac myocytes were selected as they have fully developed sarcomeres, with prominent striations which are easy to visualise under the microscope. As expected, TnI (red) showed a striated distribution, consistent with the regular spacing of the Tn complex along the thin filaments. PDE4D (green) also showed a degree of striation, although some PDE4D was also evident in the cytosol, in keeping with the variety of cellular roles that have been ascribed to members of this subfamily (Dodge et al 2001, Lehnart et al 2005). TnI and PDE4D could be seen to colocalise (yellow spots) at the sarcomeres, with a Pearson colocalisation coefficient of 0.748. The Pearson coefficient (r) quantifies the correlation between pixel intensity of the two channels measured. r values range between -1 and +1. A value of -1 indicates that when one channel signal increases, the other decreases accordingly (perfect negative correlation), and a value of +1 indicates that both channel signals increase in a similar ratio (perfect correlation) (Adler & Parmryd 2010). Therefore, a Pearson co-efficient of 0.748 indicates that TnI and PDE4D are highly likely to colocalise within the cell.

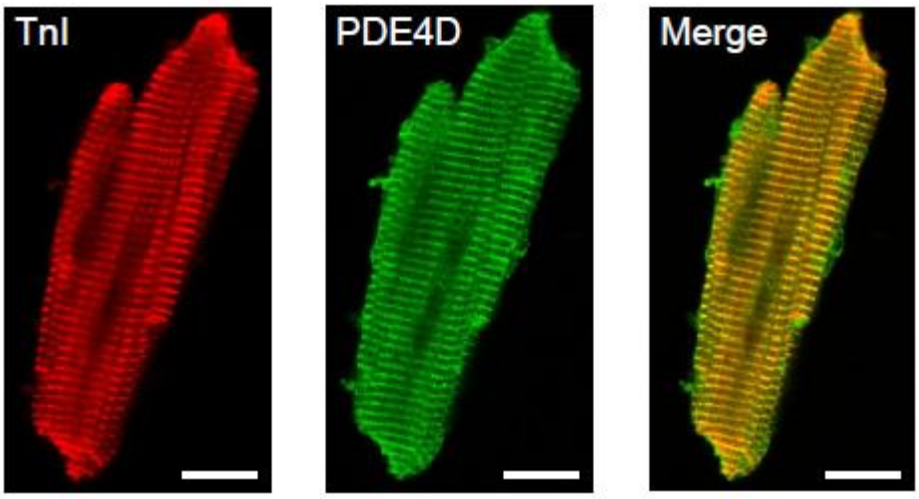

Figure 4-10 Colocalisation of PDE4D and TnI in the cardiac myofilament.
Colocalisation (yellow regions) of TnI (red) and PDE4D (green) was determined by fixation of rat ventricular cardiac myocytes in methanol/paraformaldehyde as described in Section 3.6.2, and staining for immunofluorescence with anti-cardiac troponin I and anti-pan PDE4D antibodies. Images were obtained at 63x magnification on a Zeiss Pascal Confocal microscope, and collected using Zeiss Pascal software. A Pearson colocalisation coefficient (r) was calculated using Image J software. For these images, r = 0.748, indicating a high degree of colocalisation. Scale bars represent 20µM.

4.2.5 PDE4D9 associates with the myofilament protein TnI

The importance of PDE4D in the cardiovascular system has previously been illustrated by studies involving PDE4D knockout mice. These mice develop progressive age-related cardiomyopathies and are susceptible to exercise-induced cardiac arrhythmias and sudden cardiac death, despite apparently normal global cAMP signaling (Lehnart et al 2005). Furthermore, a number of studies have demonstrated that specific PDE4D isoforms associate with key ion channels, receptors and SR proteins to regulate cAMP/PKA signaling in the heart (De Arcangelis et al 2009, Dodge et al 2001, Perry et al 2002, Terrenoire et al 2009). Members of the PDE4D subfamily have been shown here to co-immunoprecipitate with TnI from cellular lysates, and to colocalise with TnI at the cardiac myofilament. PDE4D consists of 11 isoforms, PDE4D1-11, and mRNA transcripts for 4D1, 4D2, 4D3, 4D5, 4D7, 4D8 and 4D9 isoforms have previously been detected in heart tissue (Richter et al 2005).

4.2.5.1. PDE4D1, 4D5 and 4D9 mRNA transcripts are highly expressed in NRVM

Quantitative PCR (qPCR) was performed to determine the relative mRNA expression levels of the different PDE4D isoforms in NRVM (Figure 4-11). This work was kindly performed by David Henderson at the University of Glasgow. 6 isoforms were expressed at significant levels, with PDE4D9 showing the highest expression. PDE4D7 transcripts were expressed at very low levels, consistent with previous data (Richter et al 2005). PDE4 isoforms are classified as long, short and super short, based on the presence or absence of various regulatory domains (Section 1.4.2.2.). Both long (4D3, 5, 7, 8 and 9) and short (4D1) transcripts were identified in NRVM. No function has yet been ascribed to the short forms, although a number of roles have been ascribed to long forms (described in Section 1.4.3).

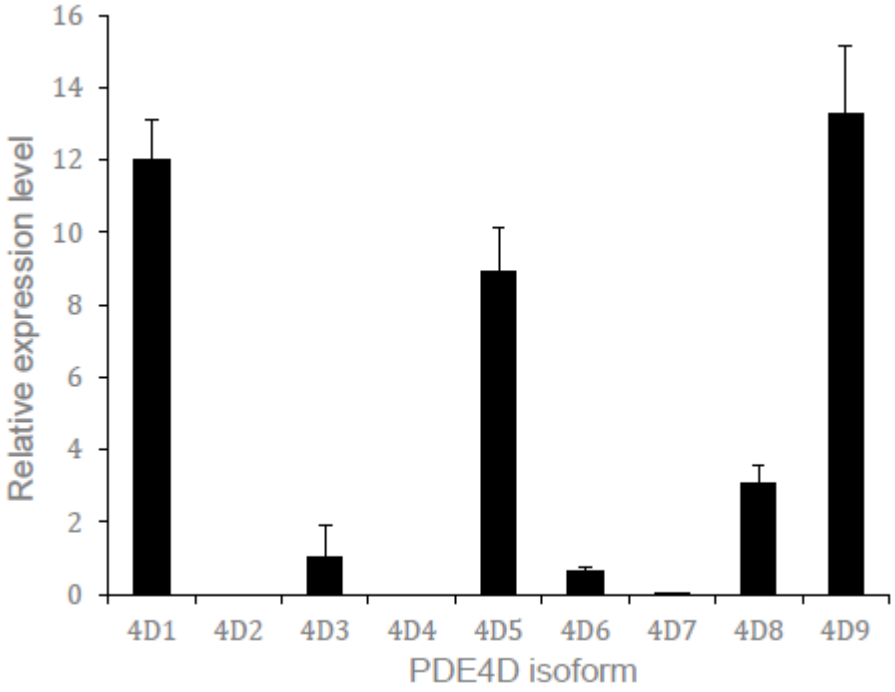

Figure 4-11 Relative mRNA expression levels of PDE4D isoforms in NRVM.
Expression levels were determined by quantitative PCR . The PDE4D10 and PDE4D11 isoforms were identified after this experiment was performed (Chandrasekaran et al 2008, Lynex et al 2008), and so are not included here. Data represents an n of 3 experiments on different cardiomyocyte preparations.

4.2.5.2. PDE4D9 associates with TnI in NRVM

During the course of my PhD, a number of PDE4D isoform-specific antibodies were developed by members of our laboratory. Much of the PDE4 amino acid sequence is common to all isoforms; however, each isoform possesses a unique N terminal sequence of variable length, which is involved in subcellular targeting and protein-protein interactions (Houslay 2010). The presence of this variable region also allows the isoforms to be differentiated by polyacrylamide gel electrophoresis on the basis of their molecular weights. PDE4D3, 4D8 and 4D9 are around 95kDa, while PDE4D5 and 4D7 appear slightly higher on gels, at around 105kDa. Based on their unique regions, N terminal-specific antibodies were successfully developed against PDE4D3, 4D5, 4D7 and 4D9 isoforms, which are all thought to be expressed in NRVM. TnI was immunoprecipitated from NRVM lysates, and isoform-specific antibodies used for immunoblotting (Figure 4-12). vsv-tagged versions of different PDE4D isoforms were expressed and used as protein standards. All four isoform-specific antibodies were able to detect these standards at the

appropriate molecular weights. Small amounts of PDE4D3 and 4D5 proteins were detectable in the lysates, but no PDE4D7 protein was identified. 4D7 mRNA levels were very low, and mRNA levels do not necessarily correlate with protein expression, therefore this protein may either not be expressed in NRVM, or the expression level may be below the threshold for detection by this antibody. A significant amount of PDE4D9 was present, consistent with qPCR data. The PDE4D9 isoform co-immunoprecipitated with TnI (Figure 4-12D).

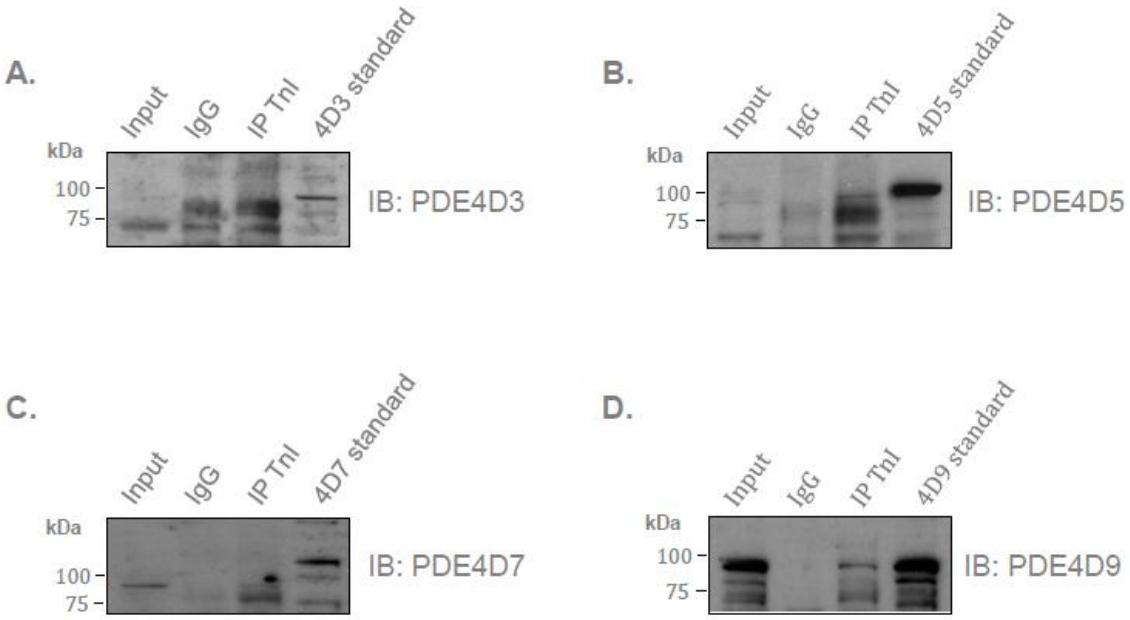

Figure 4-12 Co-immunoprecipitation of PDE4D9 with TnI.
Immunoblots (IB) of TnI immunoprecipitations were performed using isoform-specific PDE4D antibodies. A. IB of PDE4D3. B. IB of PDE4D5.C. IB of PDE4D7. D. IB of PDE4D9. PDE4D9 co-immunoprecipitated with TnI, whereas the other isoforms tested did not. The appropriate vsv-tagged human PDE4D isoforms were used as standard markers.

This association was confirmed using immunofluorescence techniques. Adult rat ventricular cardiac myocytes (ARVM) were fixed and immunostained with antibodies against cardiac TnI and PDE4D9. TnI (red) again showed a striated distribution. PDE4D9 (green) also showed a striated pattern; however, staining for this enzyme was also positive in the cytosol and at the plasma membrane, where it has previously been shown to associate with the β-adrenergic receptor (De Arcangelis et al 2009, Richter et al 2008).

The Pearson colocalisation coefficient was 0.565 for TnI and PDE4D9, consistent with their colocalisation at the myofilament.

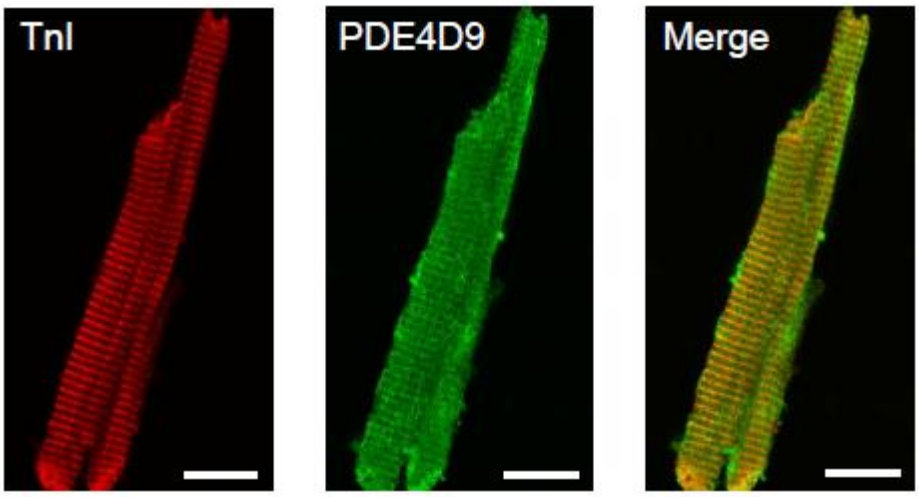

Figure 4-13 Colocalisation of PDE4D9 and TnI.
Colocalisation (yellow regions) of TnI (red) and PDE4D9 (green) was determined by fixation of rat ventricular cardiac myocytes and staining for immunofluorescence with anti-cardiac troponin I and anti-N terminal-specific PDE4D9 antibodies. The Pearson colocalisation coefficient (r) was calculated using Image J software to be 0.565 for these images, indicating a significant degree of colocalisation. Scale bars represent 20µM.

4.2.5.3. PDE4D9 interacts with the flexible C terminus of TnI

PDE4D9 has been shown to associate with TnI in NRVM. In order to determine the specific residues involved in this interaction, a peptide array approach was employed. Peptide arrays consist of short peptides immobilised on cellulose membranes. The peptide sequences overlap so that they cover the entire sequence of the protein of interest (Section 3.5.3). Cellulose peptide arrays are able to bind purified fusion proteins, and can therefore provide information on protein-protein interactions, and the residues critical for these interactions (Frank 2002). Peptide arrays have previously been used successfully to locate binding sites for the signaling scaffold protein β-arrestin and the cardioprotective chaperone Hsp20 on PDE4D5 (Bolger et al 2003, Sin et al 2011). A TnI peptide array was generated and probed with purified GST-PDE4D9 fusion protein. Binding sites for PDE4D9 on TnI were identified as black spots (Figure 4-14A, upper panel), following immunoblotting for GST. Purified GST alone was used as a control to

determine any regions of the array which bound non-specifically to the GST component of the fusion protein. The 25mer amino acid sequences of the TnI peptide array are listed in Figure 4-14B. Binding of GST-PDE4D9 was observed on TnI peptide spots corresponding to the C terminal region of the protein. The strongest signal was obtained for spot 33, therefore this region of TnI is likely to mediate interaction with the PDE. The peptide sequence corresponding to spot 33 (G^{161}TRAKESLDLRAHLKQVKKEDIEKE^{185}) was used to generate a second peptide array, known as an 'alanine scan', in which each residue was sequentially mutated to alanine. This was then probed with GST-PDE4D9 and GST as above. Alanine scans can provide information on particular amino acid residues that are critical for binding. If mutation of a residue to alanine abolishes binding of the fusion protein, it is likely to be required for the interaction between the two proteins (Bolger et al 2003). Mutation of two neighbouring lysine residues, K178 and K179, abolished binding of GST-PDE4D9 to TnI (Figure 4-14A, lower panel), indicating that these residues are likely to be crucial for the interaction.

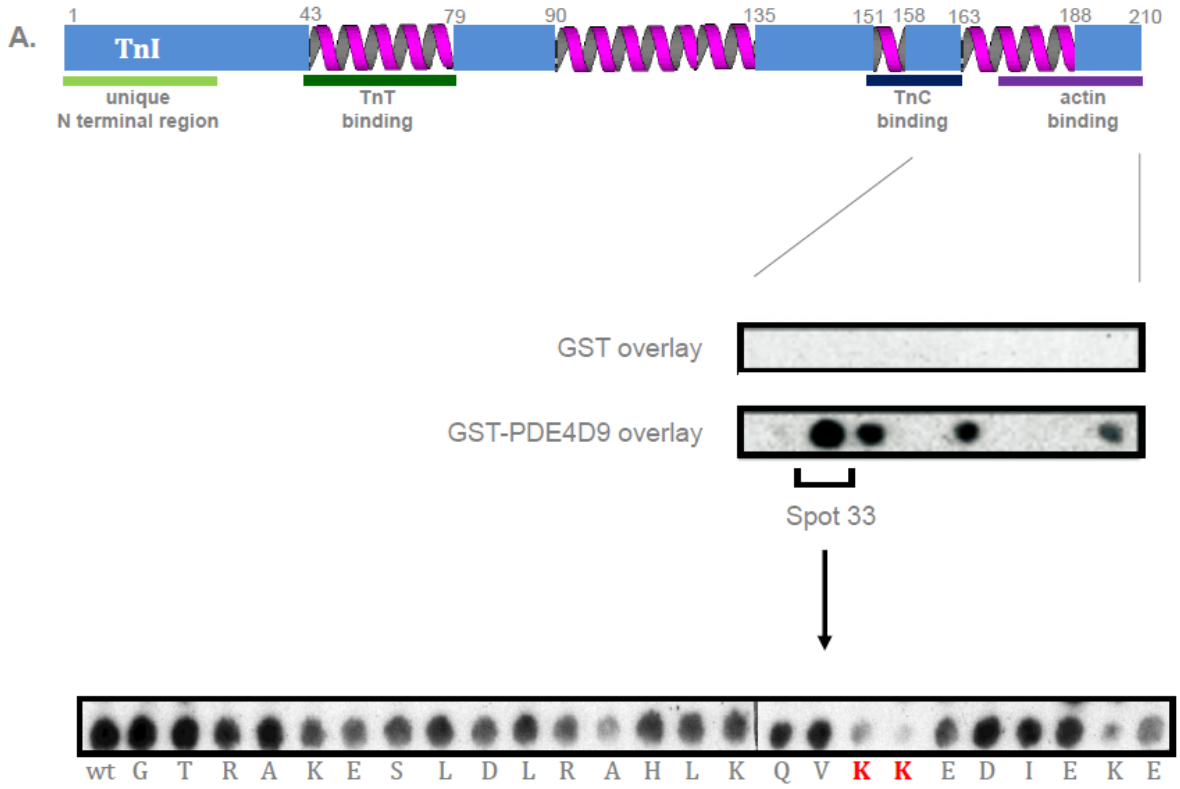

B.

TnI spot	amino acid sequence	TnI spot	amino acid sequence
1	M-A-D-E-S-S-D-A-A-G-E-P-Q-P-A-P-A-P-V-R-R-R-S-S-A	21	L-H-A-R-V-D-K-V-D-E-E-R-Y-D-V-E-A-K-V-T-K-N-I-T-E
2	S-D-A-A-G-E-P-Q-P-A-P-A-P-V-R-R-R-S-S-A-N-Y-R-A-Y	22	D-K-V-D-E-E-R-Y-D-V-E-A-K-V-T-K-N-I-T-E-I-A-D-L-T
3	E-P-Q-P-A-P-A-P-V-R-R-R-S-S-A-N-Y-R-A-Y-A-T-E-P-H	23	E-R-Y-D-V-E-A-K-V-T-K-N-I-T-E-I-A-D-L-T-Q-K-I-Y-D
4	P-A-P-V-R-R-R-S-S-A-N-Y-R-A-Y-A-T-E-P-H-A-K-K-K-S	24	E-A-K-V-T-K-N-I-T-E-I-A-D-L-T-Q-K-I-Y-D-L-R-G-K-F
5	R-R-S-S-A-N-Y-R-A-Y-A-T-E-P-H-A-K-K-K-S-K-I-S-A-S	25	K-N-I-T-E-I-A-D-L-T-Q-K-I-Y-D-L-R-G-K-F-K-R-P-T-L
6	N-Y-R-A-Y-A-T-E-P-H-A-K-K-K-S-K-I-S-A-S-R-K-L-Q-L	26	I-A-D-L-T-Q-K-I-Y-D-L-R-G-K-F-K-R-P-T-L-R-R-V-R-I
7	A-T-E-P-H-A-K-K-K-S-K-I-S-A-S-R-K-L-Q-L-K-T-L-M-L	27	Q-K-I-Y-D-L-R-G-K-F-K-R-P-T-L-R-R-V-R-I-S-A-D-A-M
8	A-K-K-K-S-K-I-S-A-S-R-K-L-Q-L-K-T-L-M-L-Q-I-A-K-Q	28	L-R-G-K-F-K-R-P-T-L-R-R-V-R-I-S-A-D-A-M-M-Q-A-L-L
9	K-I-S-A-S-R-K-L-Q-L-K-T-L-M-L-Q-I-A-K-Q-E-M-E-R-E	29	K-R-P-T-L-R-R-V-R-I-S-A-D-A-M-M-Q-A-L-L-G-T-R-A-K
10	R-K-L-Q-L-K-T-L-M-L-Q-I-A-K-Q-E-M-E-R-E-A-E-E-R-R	30	R-R-V-R-I-S-A-D-A-M-M-Q-A-L-L-G-T-R-A-K-E-S-L-D-L
11	K-T-L-M-L-Q-I-A-K-Q-E-M-E-R-E-A-E-E-R-R-G-E-K-G-R	31	S-A-D-A-M-M-Q-A-L-L-G-T-R-A-K-E-S-L-D-L-R-A-H-L-K
12	Q-I-A-K-Q-E-M-E-R-E-A-E-E-R-R-G-E-K-G-R-V-L-S-T-R	32	M-Q-A-L-L-G-T-R-A-K-E-S-L-D-L-R-A-H-L-K-Q-V-K-K-E
13	E-M-E-R-E-A-E-E-R-R-G-E-K-G-R-V-L-S-T-R-C-Q-P-L-V	33	G-T-R-A-K-E-S-L-D-L-R-A-H-L-K-Q-V-K-K-E-D-I-E-K-E
14	A-E-E-R-R-G-E-K-G-R-V-L-S-T-R-C-Q-P-L-V-L-D-G-L-G	34	E-S-L-D-L-R-A-H-L-K-Q-V-K-K-E-D-I-E-K-E-N-R-E-V-G
15	G-E-K-G-R-V-L-S-T-R-C-Q-P-L-V-L-D-G-L-G-F-E-E-L-Q	35	R-A-H-L-K-Q-V-K-K-E-D-I-E-K-E-N-R-E-V-G-D-W-R-K-N
16	V-L-S-T-R-C-Q-P-L-V-L-D-G-L-G-F-E-E-L-Q-D-L-C-R-Q	36	Q-V-K-K-E-D-I-E-K-E-N-R-E-V-G-D-W-R-K-N-I-D-A-L-S
17	C-Q-P-L-V-L-D-G-L-G-F-E-E-L-Q-D-L-C-R-Q-L-H-A-R-V	37	D-I-E-K-E-N-R-E-V-G-D-W-R-K-N-I-D-A-L-S-G-M-E-G-R
18	L-D-G-L-G-F-E-E-L-Q-D-L-C-R-Q-L-H-A-R-V-D-K-V-D-E	38	N-R-E-V-G-D-W-R-K-N-I-D-A-L-S-G-M-E-G-R-K-K-K-F-E
19	F-E-E-L-Q-D-L-C-R-Q-L-H-A-R-V-D-K-V-D-E-E-R-Y-D-V	39	D-W-R-K-N-I-D-A-L-S-G-M-E-G-R-K-K-K-F-E-G
20	D-L-C-R-Q-L-H-A-R-V-D-K-V-D-E-E-R-Y-D-V-E-A-K-V-T		

Figure 4-14 PDE4D9 binds to the C terminal region of TnI.
The interaction site for PDE4D9 on TnI was mapped to the C terminal of the myofilament protein using peptide array technology. A. Peptide array of the full length sequence of rat cardiac TnI. Strongest binding of the PDE fusion protein to the array occurred at spot 33. Alanine scanning of this sequence identified two key lysine residues, K178 and K179, as important in mediating this interaction. B. List of 25mer amino acid sequences corresponding to numbered spots on the TnI peptide array. The amino acid sequence corresponding to spot 33 is highlighted in red.

K178 and K179 map to a region of TnI at the C terminal of the protein (Figure 4-15). The crystal structure of the core troponin complex has now been solved. Unfortunately, due to problems with crystallisation the N and C termini of TnI were not included in the crystallised complex; however, their relative positions have been predicted from the structural information that was obtained (Takeda et al 2003). K178/K179 reside within helix 4 of TnI, a flexible region which is known to be involved in mediating actin-tropomyosin interactions in response to fluctuations in intracellular calcium levels (Galinska et al 2010, Takeda et al 2003). The folding of the TnI protein is such that this region is likely to be near the N terminal region of the protein where the PKA sites are located. Thus, the presence of PDE activity here could conceivably modulate local cAMP levels, influencing PKA activation and the phosphorylation status of TnI.

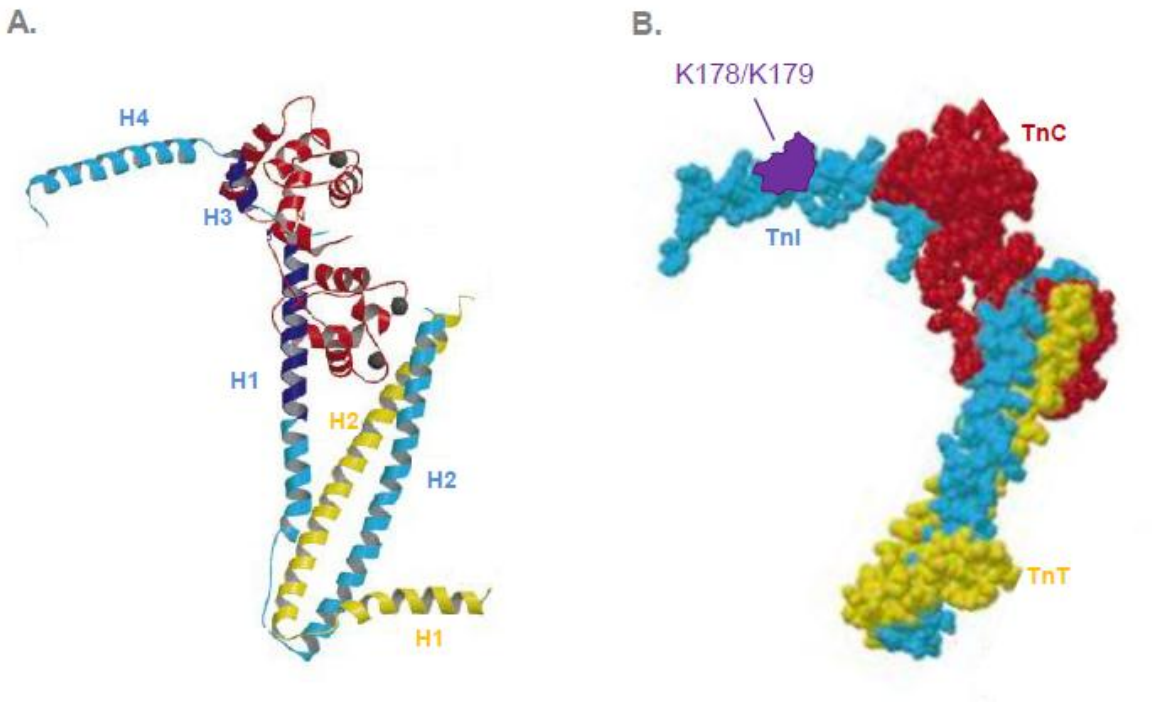

Figure 4-15 Model of TnI structure demonstrating the position of K178/K179. Adapted from (Takeda et al 2003).
The crystal structure of residues 31-163 of TnI has been solved. A. Ribbon structure of the core troponin complex. TnI is shown in blue, TnT in yellow, and TnC in red. K178/K179 are located on helix 4 of TnI, a flexible region at the C terminal of the protein. which mediates interactions with actin-tropomyosin on the thin filament during cardiac contraction B. Space-filling diagram of the Tn complex. The approximate positions of K178 and K179 are indicated in purple, and are close to the start of helix 1 (residue 43), therefore are likely to be located in proximity to Ser22/Ser23.

4.2.6 PDE4D9 regulates PKA phosphorylation of TnI

4.2.6.1. Peptide disruption of the TnI-PDE4D9 complex enhances PKA phosphorylation of TnI

It has been established that PDE4D9 interacts with TnI, and that this interaction is likely to be mediated by two neighbouring lysine residues at the C terminus of the myofilament protein. Next, I wanted to determine whether this PDE could influence cAMP levels around TnI, and thereby affect the phosphorylation status of TnI. Cell permeable peptides have previously been used to disrupt intracellular signaling complexes, leading to altered functional outcomes. For example, the MAPK kinase MEK1 interacts directly with β-arrestin, promoting arrestin phosphorylation by ERK. A 25mer cell permeable β-arrestin peptide encompassing the MEK1 binding site blocked this association in HEK293 cells and reduced arrestin phosphorylation by ERK, favouring agonist-stimulated receptor internalisation (Meng et al 2009). More recently, specific peptide disruption of a complex formed between Hsp20 and PDE4D5 was shown to increase cardioprotective PKA phosphorylation of Hsp20, and confer protection against cardiac hypertrophy in cultured cardiac myocytes (Sin et al 2011). Thus, peptide disruptors are of considerable therapeutic interest, and constitute ideal biological tools for disrupting the localisation of a single pool of PDE, in this case PDE4D9.

I used the TnI sequence information obtained from the peptide array experiments to design a specific peptide disruptor of the TnI-PDE4D9 interaction. A scrambled version of this peptide with identical molecular weight and charge was also designed to act as a control. Both peptides were stearylated, in order to make them cell permeable. Treatment of NRVM with increasing concentrations of the 4D9 disruptor peptide was associated with up to a 5 fold increase in TnI phosphorylation at Ser22/Ser23 over baseline ($P<0.001$), and was comparable with the effect produced by Iso treatment, whereas treatment with equimolar amounts of scrambled control peptide had no effect (Figure 4-16). This effect on TnI phosphorylation was observed under basal conditions i.e. in the absence of any other stimulus, implying that basal levels of cAMP are sufficient to induce PKA activation and TnI phosphorylation without the presence of PDEs.

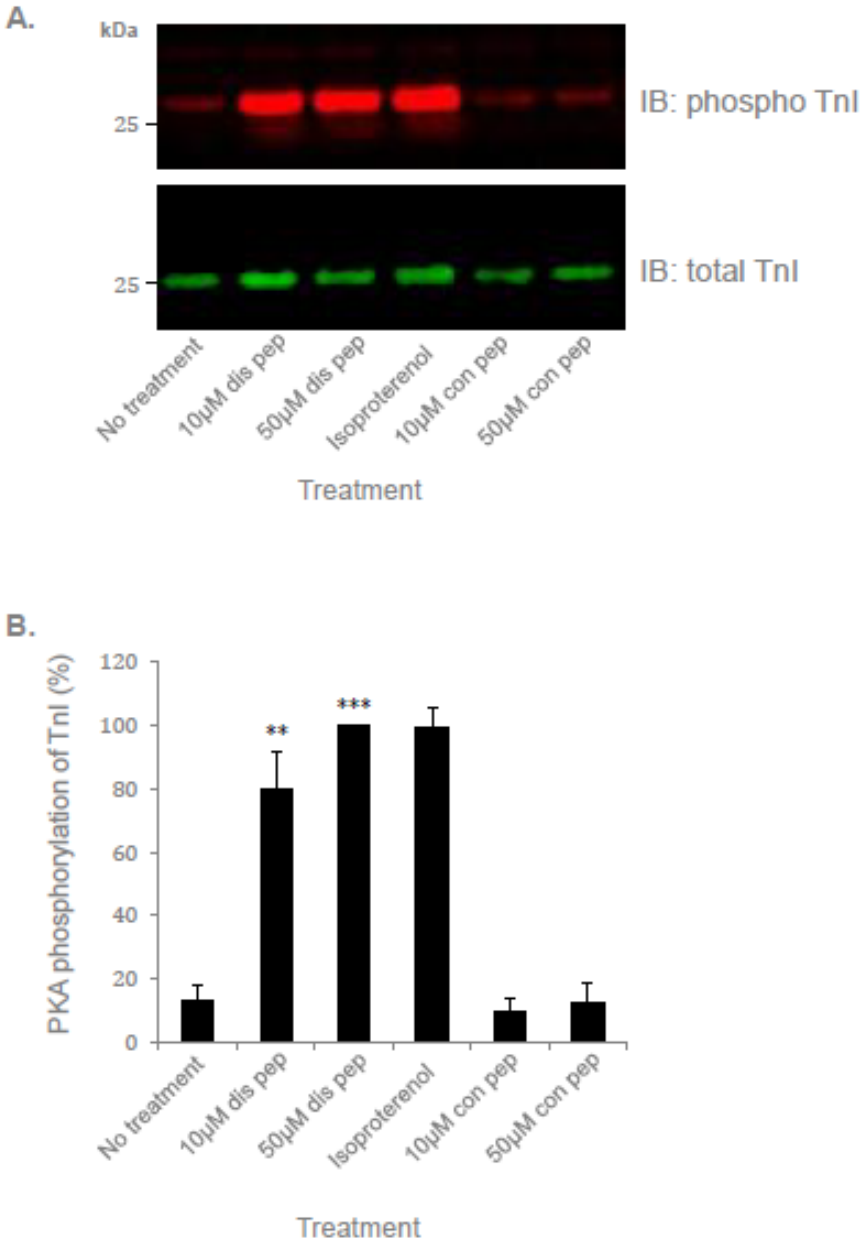

Figure 4-16 Peptide disruption of the TnI-PDE4D9 complex enhances phosphorylation of TnI at Ser22/Ser23.
NRVM were treated with 10μM and 50μM disruptor and control peptides (GenScript) for 3 hours at 37°C and 5% CO_2. The TnI phosphorylation at Ser22/Ser23 was compared to untreated cells, or cells treated with 10μM Iso for 10 minutes to maximise TnI phosphorylation. A. Representative immunoblot of phospho and total TnI levels, with fluorescently labelled secondary antibodies (Molecular Probes). Images were scanned using an Odyssey imager (Licor Biosciences). B. Quantification of data in upper panel, from an n of 3 experiments. Disruptor peptide sequence: St-GTRAKESLDLRAHLKQVKKEDIEKE; control peptide sequence: St-KTELKAERGIKSDVAKERELHDLGK. ** P<0.01; *** P<0.001.

The above data is consistent with a model whereby under basal conditions, PDE4D9 maintains myofilament PKA in an inactive state by hydrolysing local cAMP, leading to low levels of phosphorylated TnI. When local cAMP levels rise, either following β-adrenergic stimulation, or due to disruption of the TnI-PDE complex, PDE activity is saturated. PKA is activated and phosphorylates TnI on Ser22/Ser23, leading to positive contractile effects and enhanced cardiac output(Figure 4-17).

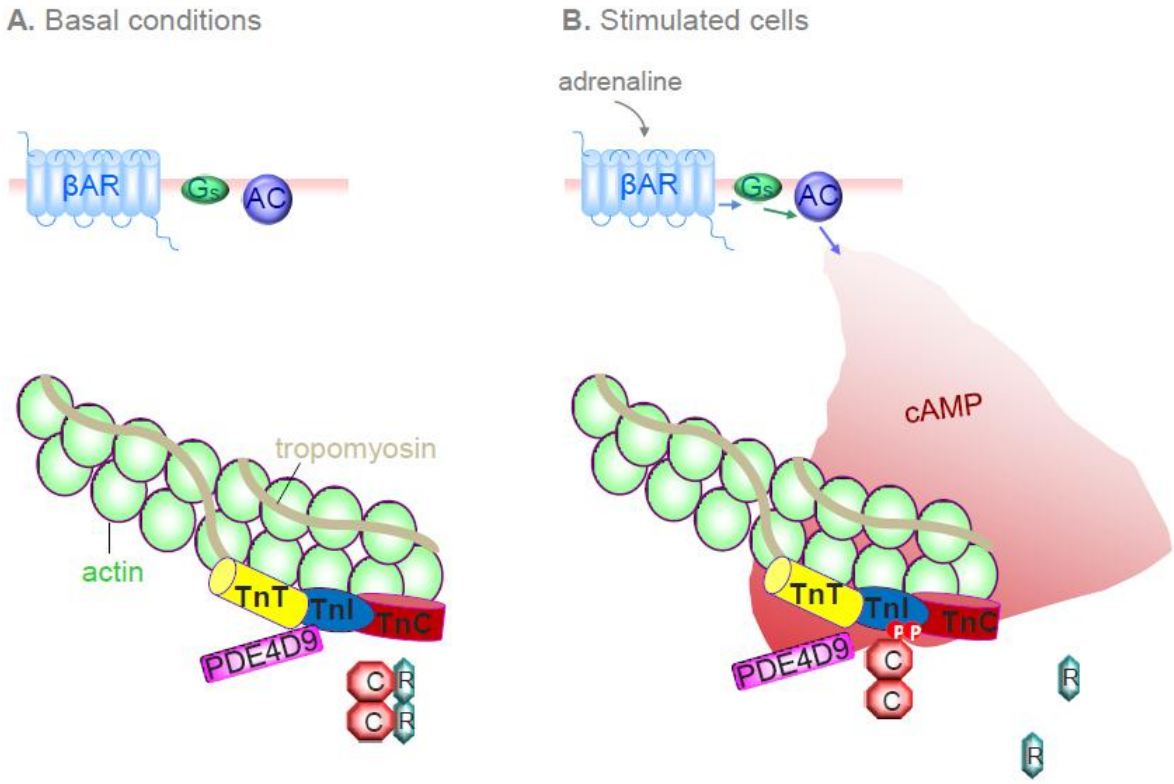

Figure 4-17 Schematic representation of the role of PDE4D9 in regulating PKA phosphorylation of TnI.
A. Under resting conditions, PDE4D9 is associated with the C terminus of TnI at the cardiac myofilament, and hydrolyses local cAMP, maintaining PKA in an inactive (R_2C_2) conformation. TnI remains hypophosphorylated at Ser22/Ser23. B. In response to physiological stress, the β1-adrenergic signaling pathway is activated. cAMP levels rise in the myofilament compartment, saturating the hydrolytic abilities of PDE4D9, and activating the local PKA complement leading to the dissociation of the catalytic (C) and regulatory (R) subunits. TnI is phosphorylated by PKA at its N terminus. This reduces the Ca^{2+} sensitivity of the myofilament and increases the force of contraction and rate of relaxation, resulting in increased cardiac output. Peptide disruption of the TnI-PDE4D9 interaction appears to have a similar effect on TnI phosphorylation. PDE4D9 is displaced from TnI, and basal cAMP levels are sufficient to activate PKA, leading to Ser22/Ser23 phosphorylation.

4.2.7 Investigation into the regulation of PKA phosphorylation of TnI by AKAPs

It has previously been shown that phosphorylation of TnI at Ser22/Ser23 is directed by AKAPs, though no AKAP has been specifically proposed for this role (Fink et al 2001). The above experiments provide convincing evidence for the role of PDE4D9 in modulating cAMP levels around TnI to control PKA activation and Ser22/Ser23 phosphorylation. AKAPs scaffold discrete pools of PKA in the vicinity of their subcellular targets; however, little is known about the AKAPs which regulate PKA phosphorylation of myofilament proteins. To determine whether an AKAP mediated PKA phosphorylation of TnI, I utilised the Ht31 and RII overlay techniques, which are commonly used to detect AKAPs.

PKA is localised to specific subcellular regions through the interaction of its regulatory subunits with AKAPs. The binding surface for PKA on AKAPs is a stretch of between 14 and 18 amino acids which are organised into an amphipathic helix to create a high affinity RII binding surface (Welch et al 2010). The first AKAP in which the amphipathic helix was identified was the human thyroid AKAP Ht31 (Carr et al 1991). Since then, synthetic peptide derivatives of this Ht31 sequence have been developed which can be used to selectively disrupt AKAP-PKA interactions, as they will compete with endogenous AKAPs for RII binding (Carr et al 1992, Fink et al 2001).

Neonatal rat ventricular cardiac myocytes (NRVM) were treated with cell-permeable Ht31 peptide, or a control peptide, Ht31P, which is unable to bind PKA RII. Treatment with the AKAP-disrupting Ht31 peptide had no effect on the phosphorylation of TnI at various time points of Iso stimulation (Figure 4-18). This may have been due to the experimental conditions employed. Cells were pre-treated with 10μM stearylated Ht31 peptides for 2 hours prior to isoproterenol stimulation, and it may be that the peptides did not cross the plasma membrane in sufficient quantities to disrupt AKAP-PKA interactions.

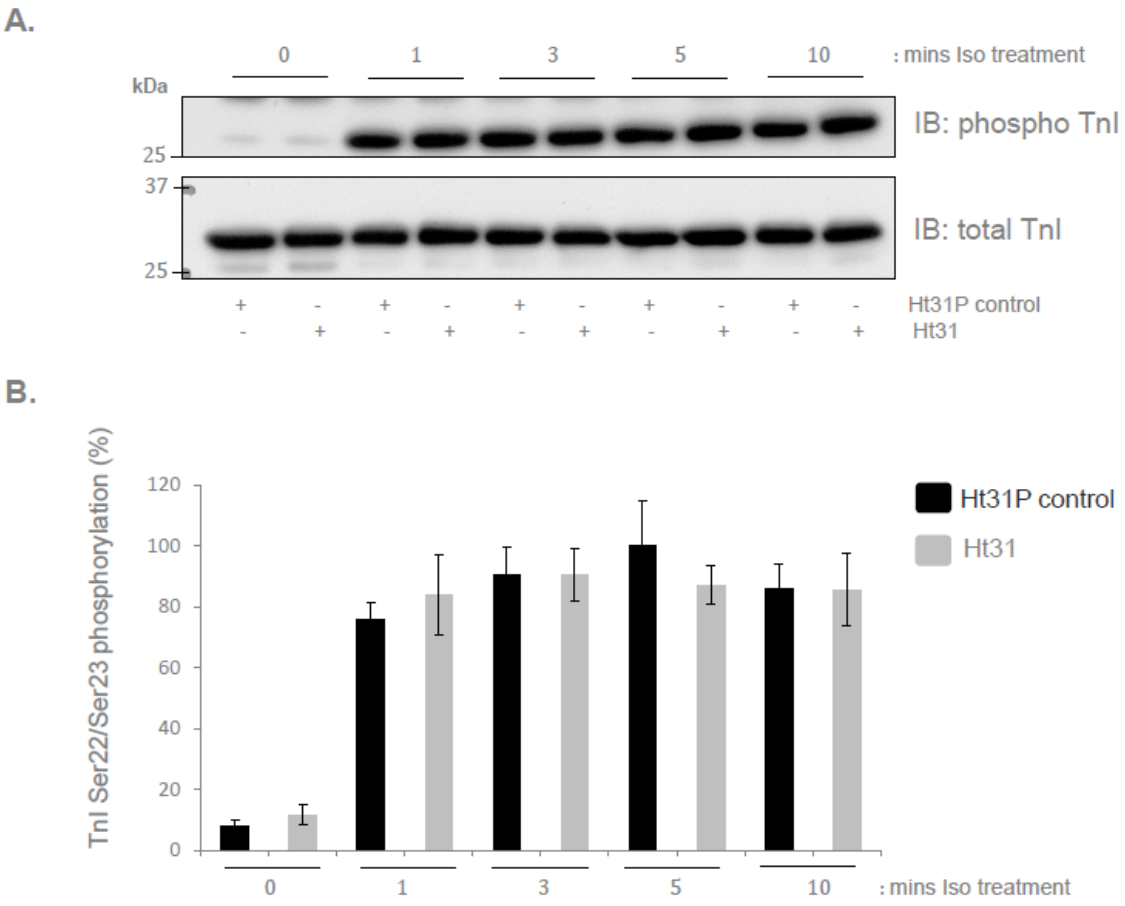

Figure 4-18 Treatment with cell permeable AKAP-competing Ht31 peptide did not disrupt AKAP-PKA interactions in NRVM.
A. Representative immunoblot of TnI phosphorylation in cells that had been pre-treated with 10µM Ht31 peptide or 10µM control peptide (Ht31P) for 2 hours, and stimulated with 10nM isoproterenol for the indicated times. B. Quantification of data in part A, for an n of 3 experiments. No significant difference in PKA phosphorylation of TnI was observed in response to Ht31 treatment.

The defining characteristic of AKAPs is their ability to anchor PKA regulatory subunits. AKAPs retain their ability to bind RII following transfer to nitrocellulose membranes. Proteins can therefore be electrophoretically separated and transferred by conventional means, and the membrane probed with labelled RII subunits to locate any AKAPs present, in a modification of the Western blotting procedure. This method is known as an RII overlay, and has been used to identify numerous AKAPs (Carr & Scott 1992).

To identify any RII binding proteins specifically associating with TnI, an immunoprecipitation (IP) of TnI was performed in NRVM, and subjected to RII overlay with ^{32}P-labelled RII subunits, followed by autoradiography (Figure 4-19A). The same

experiment was repeated on a PDE4D9 immunoprecipitation, in case the AKAP interaction was mediated by the phosphodiesterase (Figure 4-19B). A number of RII binding proteins were detected in the cardiac myocyte lysate (inputs), as would be expected, but no AKAP was detected in the immune complex with either TnI or PDE4D9. This may have been due to the IP conditions, or inadequate transfer of proteins onto the overlay membranes. Many AKAPs are very large proteins, and might therefore be difficult to separate and transfer by conventional methods (Table 1-5).

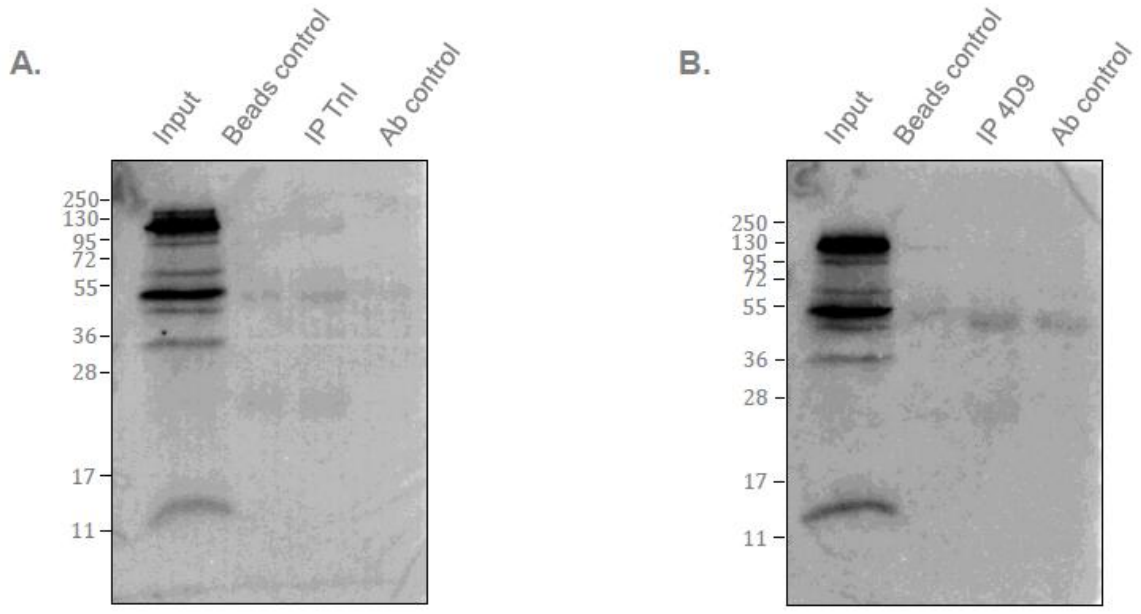

Figure 4-19 RII overlay techniques are unable to identify an AKAP for TnI.
A. Immunoprecipitation of TnI was performed in NRVM and overlayed with radiolabelled RII subunits. Controls consisted of cellular lysate incubated with either beads alone or antibody alone. No RII binding proteins could be detected in association with the immune complex. B. PDE4D9 immunoprecipitations were treated as in part A. No RII binding proteins could be seen to associate with PDE4D9. ^{32}P RII overlays were performed at the Leibniz-Institut für Molekulare Pharmakologie, Berlin, under the supervision of Philipp Skroblin and Dr Enno Klussmann.

Published data indicates that the PKA phosphorylation of TnI is mediated by an AKAP, and RII has been shown to localise to the myofilament with a similar distribution to TnI (Fink et al 2001). To exclude the possibility that TnI itself could act as an AKAP, and anchor PKA, TnI peptide arrays were overlayed with purified PKA R subunits. No binding over background was observed for either RI (Figure 4-20A) or RII subunits (Figure 4-20B). An RII

overlay was performed also on a TnI peptide array. As the ^{32}P RII overlay is relatively insensitive, and failed to detect any RII binding to TnI in a previous experiment, a modification of this technique was employed. It has been reported that a 5-10 fold increase in sensitivity of the overlay technique can be achieved using alternate RII labelling techniques (Carr & Scott 1992). To this end, PKA RII was labelled with the small molecule digoxigenin, which is highly immunogenic, and digoxigenin-RII applied to the TnI peptide array (Figure 4-20C). A peptide encompassing the RII binding domain of AKAP79 was used as an internal control (CONT). No RII binding to TnI could be visualised using this technique. Thus, a variety of techniques failed to identify an AKAP for TnI, and appear to exclude the possibility that TnI can act as an AKAP itself. Thus, based on this data, no AKAP could be identified for TnI at the myofilament.

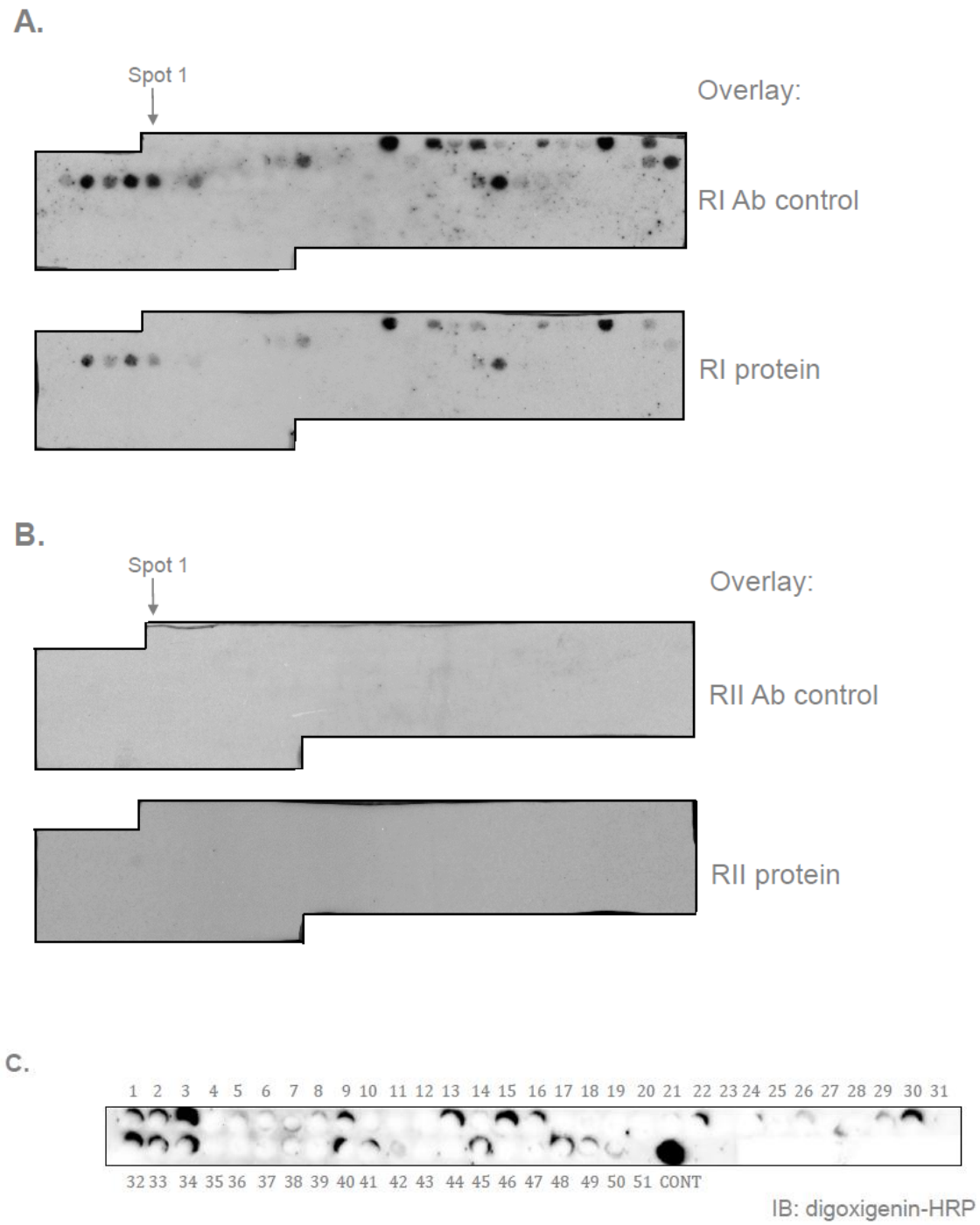

Figure 4-20 PKA R subunits do not bind TnI peptide arrays.
A. A full length TnI peptide array was probed with 10µg/ml purified PKA RI subunits, and immunoblotted with anti-RI antibodies. Primary and secondary antibodies alone were used as a control to detect non-specific antibody binding to the array. B. As in part A, except purified RII subunits were used. No binding above background could be detected for either RI or RII. Purified PKA R subunits were a kind gift from Dr Frank Christian, University of Glasgow. C. Digoxigenin-RII overlay of a TnI peptide array. The RII binding domain of AKAP79 was used as an internal control (CONT). The array was incubated with digoxigenin-labelled RII, and immunoblotted with anti-digoxigenin-HRP antibodies. No RII binding to TnI could be detected using this more sensitive method. Digoxigenin-RII was a kind gift from Dr Dave Canton, University of Washington, Seattle. Dig-RII overlays were performed in the laboratory of Professor John Scott, Department of Pharmacology, University of Washington, Seattle, supervised by Dr Chris Means.

4.3 Discussion

The myofilament protein TnI forms the inhibitory subunit of the heterotrimeric troponin complex which regulates cardiac contraction (Engel et al 2004). Under basal conditions, the flexible C terminus of TnI interacts with actin-tropomyosin to maintain tropomyosin in a position which covers myosin binding sites on actin, preventing crossbridge formation and inhibiting contraction. Ca^{2+} binding to TnC in the Tn complex leads to a conformational change in this protein which favours its interaction with TnI. This results in the release of tropomyosin by TnI, exposure of myosin binding sites on actin, and cardiac contraction (Galinska-Rakoczy et al 2008, Takeda et al 2003). This 28kDa protein is therefore an essential modulator of cardiac contraction.

TnI mediates the myofilament response to stress. PKA phosphorylation of TnI at Ser22/Ser23 in response to β-adrenergic stimulation is associated with a desensitisation of the myofilament to Ca^{2+}, promoting earlier, more efficient relaxation (Stelzer et al 2007), increased crossbridge cycling rate, and enhanced contractility (Takimoto et al 2004). Initially, this response is beneficial, but if the stimulus is prolonged, it may be associated with heart failure. Heart failure is a clinical syndrome characterised by a decline in the pumping ability of the heart. Altered β-adrenergic signaling is a key feature of heart failure (Triposkiadis et al 2009). Prolonged β-adrenergic receptor activation downregulates β-AR and leads to their uncoupling from Gs (Bristow et al 1982). Thus, β-blockers such as atenolol and metoprolol which oppose this process are one of the mainstays of treatment for heart failure. Reduced PKA phosphorylation of myofilament proteins is also seen in heart failure. Levels of PKA-phosphorylated TnI were found to be up to 50% lower in end-stage failure human hearts compared with healthy donor tissue (Van der Velden et al 2002, Zakhary et al 1999). Factors which promote this N terminal modification of TnI could therefore prove to be a useful adjunct in the treatment of heart failure, by ‘switching on’ the initial stress response at the myofilament.

Phosphodiesterases provide the only route for cAMP degradation within cells. Targeting of PDEs to specific subcellular locations leads to the creation of microdomains of cAMP (Baillie 2009). PDE4 activity has been shown to be targeted to the ryanodine receptor and

the voltage-gated potassium channel in the heart, where local alterations in cAMP levels influence the activation of PKA and thereby the phosphorylation status of these key mediators of excitation-contraction coupling (Dodge et al 2001, Terrenoire et al 2009). PDE4 is of particular importance in the heart. PDE4 has been shown to provide the major cardiac cAMP hydrolysing activity (Mongillo et al 2004) (Figure 4-4), and FRET studies using a cAMP sensor targeted to TnI reveal for the first time that PDE4 activity modulates the pool of cAMP around TnI, and that PDE4 activity is higher in this compartment than in the cytosol (Figure 4-5).

Multiple isoforms of PDE4 exist, which differ at their N termini. The non-redundant nature of these isoforms in the heart has previously been illustrated (Bolger et al 2003, De Arcangelis et al 2009, Richter et al 2008). Cells are now thought to be equipped with an array of PDE isoforms, which are targeted to discrete subcellular compartments via their unique N termini, where they regulate distinct signal transduction pathways, and mediate specific physiological outcomes (Baillie 2009, Houslay 2010, Richter et al 2005). A novel association between PDE4D9 and TnI has been demonstrated in this chapter (Figures 4-12 to 4-14). Until recently, little was known about the physiological functions of this 95kDa isoform. PDE4D9 is widely expressed, with mRNA transcripts being detectable in the brain, spleen, lung, heart and kidney tissue of rats (Richter et al 2005), which would be consistent with a ubiquitous functional role for this isoform. PDE4D9 mRNA has also been isolated from osteoblasts, where it is postulated to play a role in bone formation (Nomura-Furuwatari et al 2008). Recently, PDE4D9 has been shown to associate with the β2-adrenergic receptor under basal conditions. Agonist stimulation induced dissociation of PDE4D9 and recruitment of PDE4D5, and knockdown of PDE4D9 expression with shRNA was associated with an enhanced basal contraction rate (De Arcangelis et al 2009). PDE4D9 was also shown to bind to the β1-AR, although to a lesser extent than PDE4D8 (Richter et al 2008). De Archangelis and co-workers propose that PDE4D9 regulates basal cAMP levels at the β2-AR, while PDE4D5 regulates β-AR signaling after agonist binding, likely via its interaction with β-arrestin (De Arcangelis et al 2009). No functional role has been proposed for PDE4D9 which is released from β-ARs following ligand binding, and it would be interesting to employ localisation studies to determine whether this pool of the PDE is recruited to the myofilament to regulate TnI phosphorylation.

Peptide array studies mapped the binding site for PDE4D9 to the C terminal region of TnI (Figure 4-14). The crystal structure of the C terminus of TnI has not been resolved, due to its flexibility. Indeed, this region responds to changes in Ca^{2+} levels by altering its association with actin-tropomyosin on the thin filament (Takeda et al 2003). This movement could conceivably influence the proximity of the PDE and anchored PKA, favouring cAMP hydrolysis and inhibition of the kinase at specific times in the cardiac cycle. The PDE4D9-TnI interaction was found to be mediated by two neighbouring lysine residues (K178/K179), and could be disrupted using a cell permeable peptide, resulting in robust phosphorylation of TnI at Ser22/Ser23 in the absence of other stimuli (Figure 4-16). Cell permeable peptide disruptors have previously been shown by us to confer protection against cardiac hypertrophy in cultured NRVM, as determined by measurements of cell size, and expression of genes consistent with a hypertrophic response (Sin et al 2011). A number of strategies have been employed to attenuate PDE4 activity in cells to date, such as the development of knockout mice (Lehnart et al 2005), and RNA interference techniques (De Arcangelis et al 2009, Lynch et al 2007). These strategies affect the expression of either whole subfamilies of PDE4, or the whole of one isoform, and therefore cannot give specific information on the role of a single pool of PDE within a macromolecular complex. Peptide disruption of a specific PDE complex represents a superior strategy for determining the localised actions of PDEs. This method is particularly useful for isoforms such as PDE4D9, which appear to have multiple roles within the cell. The novel TnI-PDE4D9 disruptor peptide increased basal levels of phosphorylated TnI, and might therefore be expected to promote cardiac contraction. Further experiments are needed to show that the effects observed on TnI phosphorylation are in fact due to peptide-induced dissociation of the TnI-PDE4D9 complex, including attenuation of the co-immunoprecipitation and co-localisation of the two proteins. The peptide's actions should also be confirmed in an ELISA assay using purified proteins. Clearly, the physiological effects of this peptide in cardiac cells also need to be investigated. TnI Ser22/Ser23 phosphorylation is necessary for the lusitropic response to β-agonists, and so the rate of relaxation of cardiac myocytes in the presence and absence of peptide should be determined. It would also be interesting to investigate whether any other feedback mechanisms of control exist within this complex. mAKAP-associated PDE4D3 is phosphorylated by PKA following activation of the kinase, and this serves to enhance activity of the PDE, promoting cAMP hydrolysis. This process is

reversed by mAKAP-associated PP2A (Dodge-Kafka et al 2010). A similar mechanism of control may exist for the pool of PDE4D9 which is associated with TnI.

Interestingly, the two lysine residues which mediate PDE binding to TnI form part of a predicted sumoylation site. SUMO (small ubiquitin-related modifier) is a reversible post-translational modification of lysine residues which has been linked to an extremely diverse range of protein outcomes, including protein stability and cell trafficking (Geiss-Friedlander & Melchior 2007). Recently, it was shown that SERCA2 is sumoylated at K480 and K585, and that this modification is essential to maintain the stability and activity of the Ca^{2+} pump (Kho et al 2011). Furthermore, the levels of SUMO1 and sumoylation of SERCA2 were found to be reduced in failing hearts (Kho et al 2011). The $VK^{178}K^{179}E$ sequence on TnI is strongly predicted to be a sumoylation site using commercially available software (SUMOsp 2.0), and it would be fascinating to confirm this as a genuine SUMO site using *in vitro* sumoylation assays. If TnI is sumoylated at this site, this modification could potentially influence the physiological response to β-agonist stimulation by altering the stability of the myofilament protein, or perhaps induce a conformational change that alters PDE binding.

The final experiments in this chapter aimed to identify an AKAP for the TnI-PDE4D9 complex. Ht31 peptide experiments failed to show the presence of an AKAP in mediating the cAMP-dependent PKA phosphorylation of TnI. This directly contraindicates previous work from 2001 which found that the presence of Ht31 in cells significantly reduced PKA phosphorylation of TnI (Fink et al 2001). Fink and co-workers performed their experiments in adult rat ventricular myocytes infected with adenoviral-Ht31 constructs. These vectors may have been preferentially taken up into cells, in contrast with the stearylated peptide used in my experiments. Stearylation of peptides is a commonly used technique to improve their membrane permeability (Futaki et al 2001), but it is probable that at the concentration used, Ht31 did not reach the myofilament in significant quantities to interfere with AKAP-PKA interactions.

Prior to commencing this study, very little was known about AKAP scaffolding of PKA at the myofilament, though immunocytochemical staining of cardiac myocytes had

demonstrated a striated distribution for RII, consistent with myofilament anchoring of PKA (Fink et al 2001). Two proteins associated with the myofilament, myospryn and synemin, have since been shown to possess RII binding domains. Myospryn is a large costameric protein which functions to couple sarcomeres to the sarcolemma (Sarparanta 2008), and has been shown to localise with RIIα at the peripheral Z disc (Reynolds et al 2007). Synemin performs a similar function, and was found to co-immunoprecipitate with RII in adult rat cardiac myocytes (Russell et al 2006). However, neither of these putative AKAPs have been shown to directly affect the phosphorylation of myofilament proteins such as TnI. Within the last 12 months, one study has identified cardiac troponin T as a novel dual specificity sarcomeric AKAP (Sumandea et al 2010). A yeast two hybrid screen of human heart cDNA libraries identified TnT as an RII interacting protein, and truncation analysis mapped the RII interaction site to residues 212-224 on TnT. As TnT and TnI exist in the same heterotrimeric complex within cells, it might be expected that a TnI immunoprecipitation would co-immunoprecipitate TnT and any associated PKA, and therefore give a positive RII overlay result. This could be verified by immunoblotting of TnI IPs for TnT, and if required, altering the IP conditions to ensure that this co-immunoprecipitation is occurring, before repeating the overlays. Sumandea and co-workers utilised a combination of co-expression of epitope-tagged TnT and PKA R subunits in HEK293 cells, GST pulldown assays and peptide arrays to demonstrate an interaction between PKA and TnT, and it would be interesting to determine whether this interaction is also observed endogenously in the heart, and whether disruption of the interaction affects the phosphorylation of TnI, and the physiological outcomes associated with this modification.

TnT has been proposed to be a dual specificity AKAP, capable of binding both PKA RI and RII subunits. Most AKAPs are RII-selective, exhibiting high affinity for the N terminal region of PKA RII; however, several dual specificity AKAPs have now been identified, including ezrin and AKAP220 (Welch et al 2010). Dual specificity AKAPs are also able to interact with RI, but typically with lower affinity than RII, due to structural differences in the N terminal region of RI (Herberg et al 2000). RI binding to dual specificity AKAPs can be enhanced by the presence of an additional amino acid sequence in proximity to the amphipathic helix, termed an RI-specific region, or RISR (Welch et al 2010). Such a

sequence was identified in TnT (Sumandea et al 2010). If TnT in fact anchored predominantly PKA RI in cardiac myocytes, and TnI was phosphorylated by this pool of PKA RI, this would explain the failure of PKA RII-based overlays to detect AKAPs associated with TnI. Soluble Epac1-based cAMP FRET sensors fused to the AKAP-anchoring domains of RI and RII have recently been used to study the relative localisations of RI and RII within cardiac myocytes (Di Benedetto et al 2008). RI-epac showed a tight striated distribution overlaying with the sarcomeric Z and M lines, whereas RII-epac corresponded more strongly with the M line. Prior to these experiments, RI was thought to have a primarily cytoplasmic distribution within cells (Brunton et al 1981). Thus, PKA RI is found in the same distribution as TnI, and could potentially mediate phosphorylation of the myofilament protein. However, β-adrenergic stimulation, which leads to PKA phosphorylation of TnI, has been shown to generate a pool of cAMP that selectively activates PKA RII over RI (Zaccolo & Pozzan 2002), which would infer that TnI is in fact phosphorylated by PKA RII. It would be interesting to specifically determine the colocalisation of TnI with both PKA RI and RII in cardiac myocytes, and whether selective disruption of AKAP-PKA RI interactions with RI-selective peptides influences the phosphorylation of TnI in any way.

In summary, the data presented in this chapter indicate that PKA phosphorylation of TnI at Ser22/Ser23 is mediated by an anchored pool of PDE4 isoforms. PDE4D9 has been shown for the first time to bind directly to the flexible C terminus of TnI to regulate its PKA phosphorylation, and dissociation of this interaction using a novel peptide disruptor is sufficient to induce phosphorylation of TnI in the absence of other stimuli. Future experiments must investigate the physiological effects of this disruptor peptide in intact cells, as modulation of the TnI-PDE4D9 interaction may prove to be a novel therapeutic avenue for heart failure.

5.

AKAP-Lbc Scaffolding of PKA Facilitates Cardioprotective Phosphorylation of Hsp20

5.1 Introduction

Reversible modification of protein function by PKA phosphorylation is critical for a vast array of intracellular events. The concept of compartmentalised cAMP signals activating discrete subcellular pools of PKA is now well accepted (Beavo & Brunton 2002). In addition to the generation of local cAMP gradients by PDEs, PKA is physically compartmentalised within the cell by AKAPs, thus limiting its availability to only a small subset of target proteins. AKAPs are a functionally related group of proteins characterised by their ability to anchor PKA (Smith & Scott 2006). AKAPs were originally envisaged as proteins with two motifs, one for PKA anchoring and one for subcellular targeting of the AKAP-PKA complex (Dodge & Scott 2000); however, the discovery that they could also anchor protein phosphatases highlighted another important property of AKAPs, their ability to scaffold other key signaling enzymes (Fraser & Scott 1999). It is now appreciated that AKAPs form the core of macromolecular signaling complexes, or 'signalosomes'. Within these complexes, kinases and phosphatases are held in close proximity to effectors and substrates, facilitating the rapid and efficient transmission of intracellular second messenger signals (Welch et al 2010). Thus, AKAPs enable both the spatial and temporal regulation of compartmentalised cAMP/PKA signaling.

A number of macromolecular signaling complexes have been identified in the heart that function to regulate excitation-contraction coupling. One of the best characterised is the mAKAP-ryanodine receptor complex located at the sarcoplasmic reticulum and nuclear membrane of cardiac myocytes (described in Section 1.6.4.1). mAKAP positions PKA close to a consensus phosphorylation site on the RyR calcium release channel, and PKA phosphorylation at this site enhances the open probability of the channel (Marx et al 2000). mAKAP also tethers adenylyl cyclase 5, PDE4D3 and the protein phosphatases PP2A and PP2B in addition to PKA and the RyR, and the anchored PDE4D3 recruits Epac1 and ERK5 to the complex. Therefore, cAMP and Ca^{2+} second messenger signals may be integrated with growth factor signals and specifically disseminated by one signaling network, which is subject to very intricate internal controls (Dodge-Kafka et al 2005). AKAP-nucleated signalosomes have now been described that regulate the voltage-gated potassium channel (Terrenoire et al 2009), the SERCA2 Ca^{2+} ATPase (Lygren et al 2007) the L-type calcium channel (Gao et al 1997, Leroy et al 2011) and the β-adrenergic receptor (Wang et al 2006) in the heart.

PKA phosphorylation events are integral to many essential cardiac processes, from the modulation of contraction dynamics described in Chapter 4, to cell survival and cardioprotection (Fan et al 2004a, Fan et al 2003). Myocardial ischaemia, resulting from impairment of coronary blood supply, is a major cause of morbidity and mortality in the Western world (Murphy & Steenburgen 2008). Ischaemia leads to apoptosis and necrosis (myocardial infarction) which manifests clinically as ventricular dysfunction and cardiac failure. Strategies which restore coronary perfusion and prevent progression to infarction reduce morbidity and mortality (Mudd & Kass 2008), and there is currently much interest in understanding the mechanisms by which the heart protects itself from ischaemic injury, in order to identify new therapeutic avenues.

A variety of kinases are activated during myocardial ischaemia, including PKA and PKC (Heusch et al 2008). It is increasingly recognised that one of the major mediators of cardioprotective signaling is the small heat shock protein Hsp20. Hsp20 is phosphorylated by PKA (and PKG) on Serine 16 at its N terminus, and this modification enhances its cardioprotective actions (Beall et al 1999, Fan et al 2005a). Both Hsp20 expression levels

and its phosphorylation on Ser16 are increased in ischaemic myocardium. Phospho-mimics of Hsp20 (Ser16 to Asp mutants) confer improved protection from β-agonist-induced apoptosis in the heart, whereas phospho-null mutants (Ser16 to Ala) provide no protection (Fan et al 2004b). Furthermore, naturally occurring mutants of Hsp20 at position 20 (P20L substitution) are associated with markedly reduced Hsp20 phosphorylation at Ser16, and this lack of phosphorylation correlates with abrogation of Hsp20's cardioprotective effects (Nicolaou et al 2008).

Although the extracellular stimuli which invoke PKA phosphorylation at Hsp20-Ser16 have been well studied, the signaling events which regulate this modification were poorly understood until recently. Work from our laboratory has now identified a specific interaction between Hsp20 and PDE4 isoforms (Sin et al 2011). Inhibition of PDE4 is sufficient to induce Hsp20-Ser16 phosphorylation in resting cells, and to augment its phosphorylation in β-agonist-stimulated cells. Peptide array technology identified a binding site for Hsp20 on the conserved catalytic domain of PDE4, and this information was used to design a cell permeable peptide which inhibited the interaction of Hsp20 and PDE4. This peptide disruptor was shown to induce PKA phosphorylation of Hsp20 in unstimulated cells, and to protect against β-agonist-induced hypertrophy in neonatal cardiac myocytes, and could therefore represent a promising new therapeutic tool (Sin et al 2011). Hsp20 was also recently shown to interact with the protein phosphatase PP1 at the sarcoplasmic reticulum to modulate Ca^{2+} handling (Qian et al 2011), and could therefore participate in one of the macromolecular signaling complexes described above. However, to date, no AKAP has been identified to scaffold the pool of PKA that phosphorylates Hsp20.

5.1.1 Experimental aims

Hsp20 associates with PDE4 and PP1, and is known to be phosphorylated by PKA at its N terminus. Preliminary studies using the AKAP-competing peptide Ht31 blunted PKA phosphorylation of Hsp20 in neonatal rat ventricular cardiac myocytes, indicating the

association of Hsp20 and an AKAP in a multi-protein complex. The aim of the experimental work detailed in this chapter was to identify this AKAP, and to determine whether disruption of the Hsp20-AKAP interaction significantly impacted upon Hsp20's cardioprotective functions.

5.1.2 Experimental procedure

1) The presence of an AKAP to mediate PKA phosphorylation of Hsp20 was confirmed using Ht31 peptide and RII overlay.

2) Association of Hsp20 with a cytosolic AKAP was demonstrated by co-immunoprecipitation and co-localisation studies.

3) Specific siRNA-mediated knockdown of AKAP expression and transfection of AKAP binding mutants were used to determine changes in the PKA phosphorylation status of Hsp20 and the effects on apoptosis.

4) GST-tagged AKAP fragments were used in a pulldown assay to map the binding site for Hsp20 on the AKAP.

5) The presence of PDE4 in an AKAP-Hsp20 complex was confirmed by co-immunoprecipitations and PDE activity assays.

5.2 Results

5.2.1 An AKAP mediates Ser16 phosphorylation of Hsp20

The small heat shock protein Hsp20 can be phosphorylated by PKA at Ser16 on its N terminus. To confirm that an AKAP mediated the scaffolding of the pool of PKA that phosphorylates Hsp20, an Ht31 peptide assay was used. Neonatal rat ventricular cardiac myocytes (NRVM) were treated with cell-permeable AKAP-disrupting Ht31 peptide (as in

Section 4.2.7) or a control peptide, Ht31P, which is unable to bind PKA RII. Cells were then stimulated with the β-agonist isoproterenol (Iso) to activate PKA, and levels of phospho-Ser16 Hsp20 were assessed (Figure 5-1). In the absence of Iso, Hsp20 remained basally phosphorylated, and there was no significant difference in the phosphorylation of Hsp20 in cells treated with Ht31, Ht31P, or no peptide. Following Iso stimulation, Hsp20 was rapidly phosphorylated at Ser16 by PKA in cells without peptide and in cells treated with the control Ht31P peptide, which is unable to disrupt AKAP-PKA interactions. However, in cells treated with the AKAP-competing peptide Ht31, Hsp20 showed significantly less PKA phosphorylation ($P<0.01$), strongly indicating that AKAP-mediated PKA anchoring is necessary for this phosphorylation event to occur (Figure 5-1).

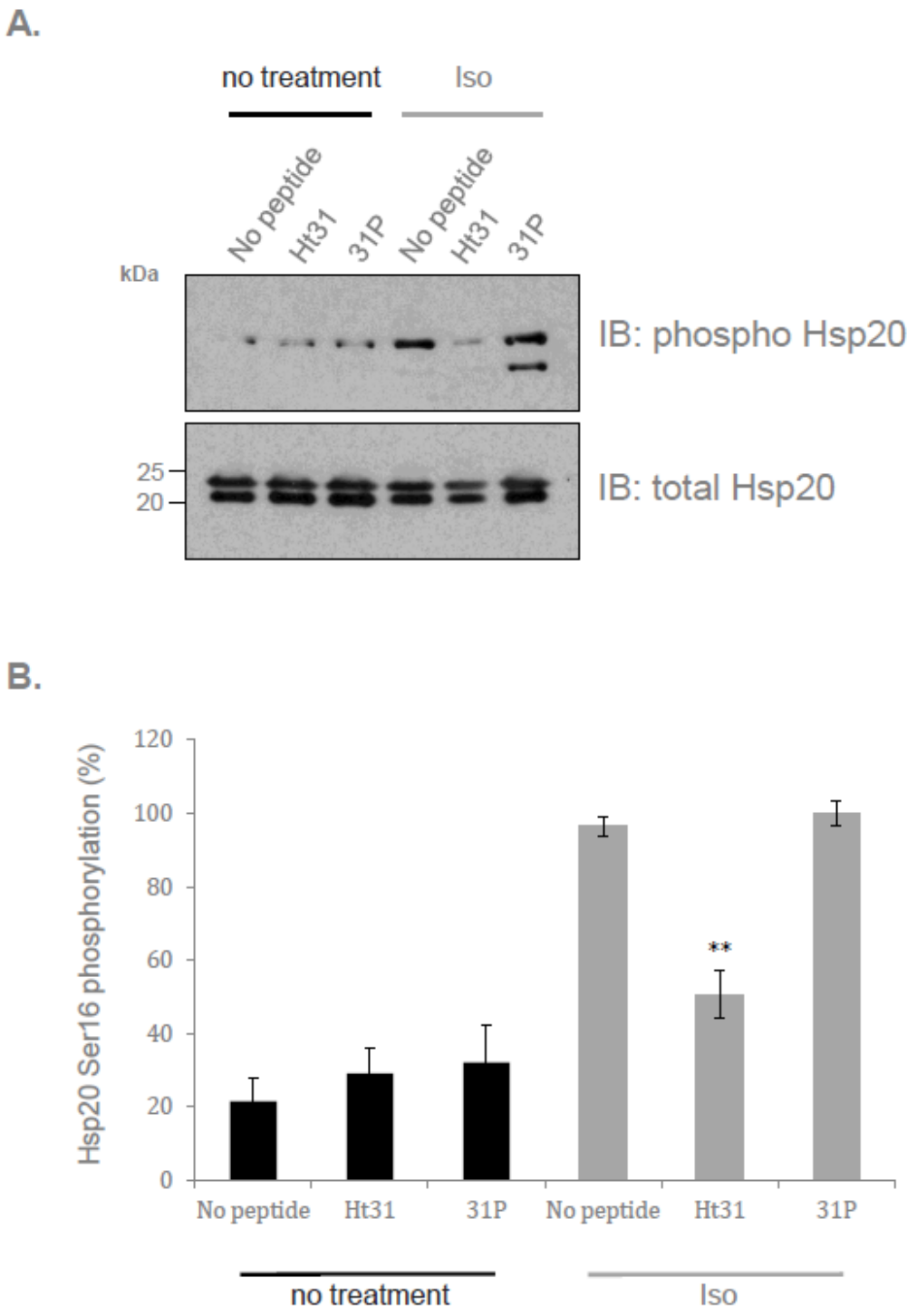

Figure 5-1 Effect of Ht31 treatment on PKA phosphorylation of Hsp20 at Ser16.
NRVM were treated for 30 minutes with 50µM of Ht31 or Ht31P peptides (Promega), or remained untreated (no peptide). Peptides were stearated to increase their membrane permeability. Cells were then stimulated with 1nM isoproterenol (Iso) for 5 minutes to activate PKA, and levels of phosphorylated Ser16 Hsp20 and total Hsp20 determined by Western immunoblotting of cellular lysates and compared to unstimulated cells (no treatment). A. Representative immunoblot of phospho-Ser 16 and total Hsp20 levels. B. Quantification of data in part A. Ht31 treatment significantly reduced PKA phosphorylation of Hsp20 compared with Ht31P treatment or no treatment in Iso-stimulated cells (P<0.01). An n of 3 experiments were performed, and data normalised to the maximum level of phosphorylation. The graph represents means ± SEM. ** P<0.01.

5.2.2 RII overlay identifies a ~300kDa AKAP associated with Hsp20

To identify AKAPs specifically associating with Hsp20, an immunoprecipitation (IP) of Hsp20 was performed in NRVM, and subjected to RII overlay (as in Section 4.2.7) with ^{32}P-labelled RII subunits, followed by autoradiography (Figure 5-2A). Numerous RII binding proteins were detected in the cardiac myocyte lysate as expected ('input' lane); however, no AKAP could be shown to co-immunoprecipitate with Hsp20 by this method.

The failure of the ^{32}P RII overlay could be due to either the immunoprecipitation conditions, or the sensitivity of the technique. Immunoprecipitation using an epitope tag can enhance the amount of precipitated protein. Hsp20 was therefore cloned into the pcDNA3.1/V5-His TOPO vector (Invitrogen) to add a V5 epitope tag, and the Hsp20 IP performed using anti-V5 antibody in lysate from HEK293 cells transfected with this plasmid. The overlay was repeated on an Hsp20-V5 IP using RII labelled with the small, highly immunogenic molecule, digoxigenin, in order to increase the sensitivity of the overlay (Figure 5-2B) (see Section 4.2.7). This time, a very faint band corresponding to an RII-binding protein could be detected which co-immunoprecipitated with Hsp20. This protein was large, with a molecular weight of approximately 300kDa. A corresponding band can be identified in the input lanes of the ^{32}P and digoxigenin overlays; however it is much fainter in the ^{32}P overlay, consistent with the lower sensitivity of this technique.

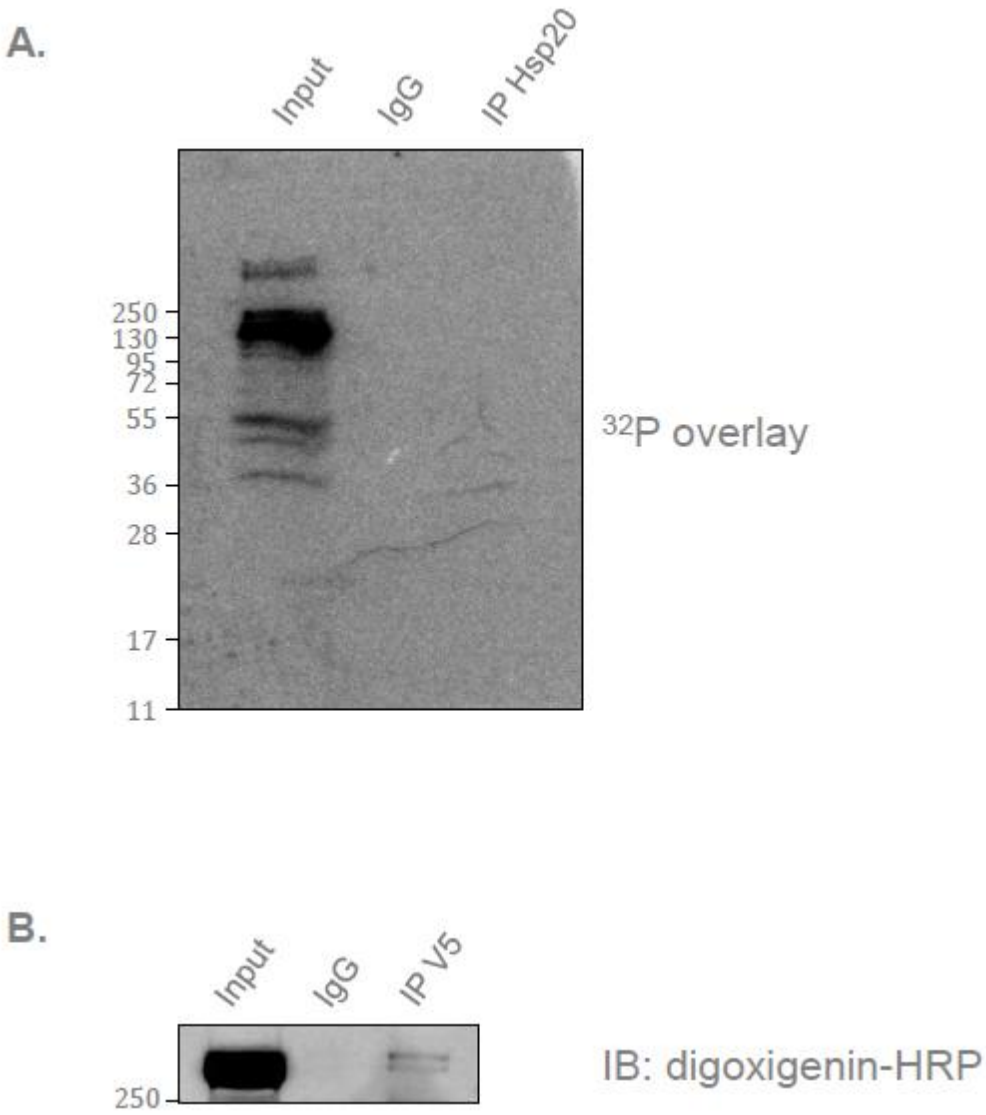

Figure 5-2 RII overlays of an Hsp20 immunoprecipitation.
A. Autoradiograph of a ^{32}P RII overlay of an Hsp20 endogenous immunoprecipitation from NRVM. A number of RII binding proteins can be identified in the cellular lysate (input lane), but no AKAP can be identified co-immunoprecipitating with Hsp20. B. Digoxigenin (Dig)-RII overlay of a V5 IP. Hsp20-V5 was transfected into HEK293 cells, and immunoprecipitated using the V5 epitope tag. A 300kDa AKAP can be identified in the Hsp20-V5 immune complex.

5.2.3 Hsp20 interacts with the cytosolic AKAP Lbc

A number of AKAPs have been identified in the heart (Table 1-5), including AKAP79/150, gravin (Wang et al 2006), AKAP15/18 (Lygren et al 2007), mAKAP (Dodge et al 2001) and AKAP-Lbc (Carnegie et al 2008). AKAP-Lbc is the 320kDa product of the *AKAP13* gene, and on the basis of molecular weight, appeared most likely of these cardiac AKAPs to

represent the Hsp20-associated AKAP identified by the digoxigenin-RII overlay above. To test this hypothesis, HEK293 cells were co-transfected with Hsp20-V5 and Flag-AKAP-Lbc constructs, and co-immunoprecipitation studies were performed (Figure 5-3A and B). Hsp20-V5 was clearly detected in Flag immunoprecipitations of AKAP-Lbc (Figure 5-3A, upper panel). The reciprocal immunoprecipitation was then performed; however, only a small amount of Flag-AKAP-Lbc co-immunoprecipitated with Hsp20-V5 despite various conditions being tested (Figure 5-3B, upper panel). This may be due to stoichiometric reasons, or due to the difficulties of immunoprecipitating a complex containing such a large protein.

In order to provide more physiological evidence for the Hsp20-AKAP-Lbc association, the experiment was repeated in NRVM. Endogenous Hsp20 was detected in AKAP-Lbc immunoprecipitations using an anti-AKAP-Lbc antibody (Figure 5-3C); however, the reciprocal IP was unsuccessful.

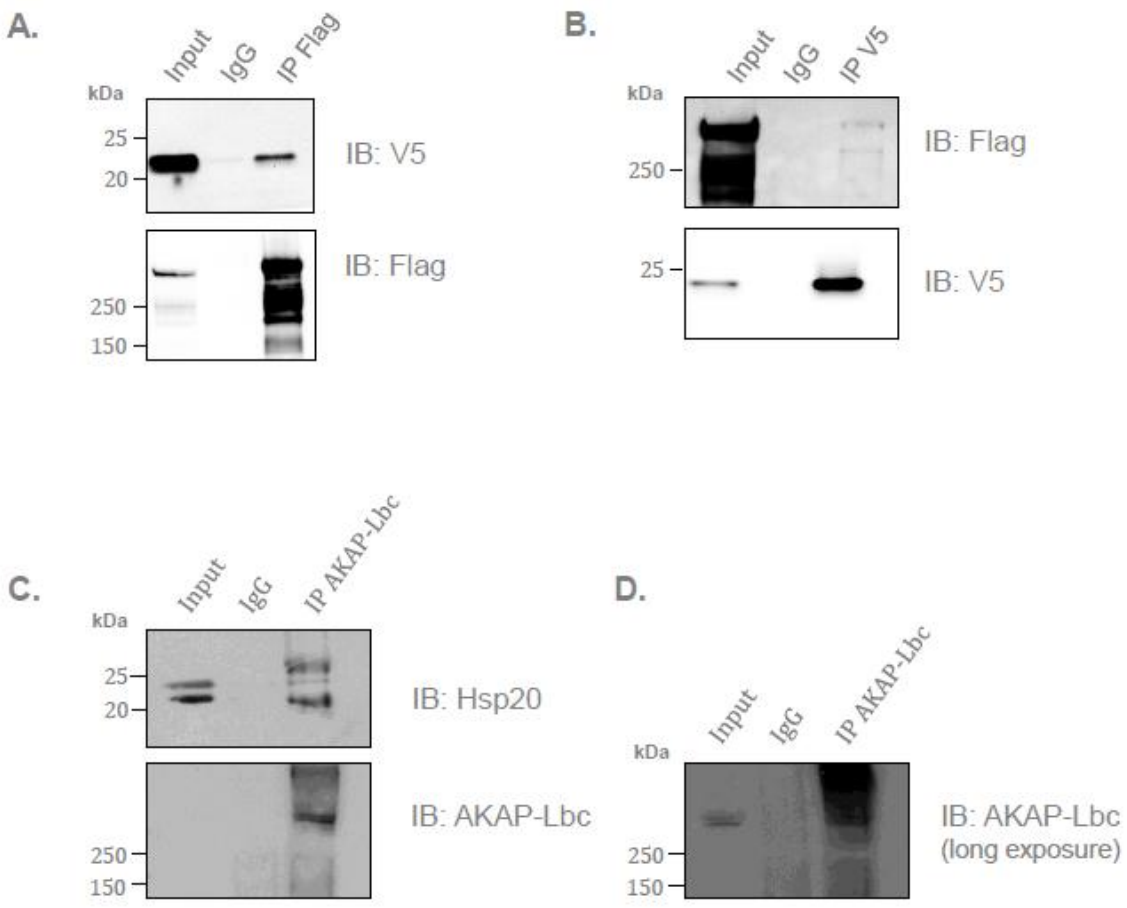

Figure 5-3 Immunoprecipitation studies of Hsp20 and AKAP-Lbc in transfected and untransfected cell lines.

A. Lysates from HEK293 cells co-transfected with Hsp20-V5 and Flag-AKAP-Lbc were immunoprecipitated using anti-Flag antibody or normal IgG as a control, separated by gel electrophoresis and immunoblotted with anti-V5 antibody to detect co-immunoprecipitation of Hsp20-V5. Prior to blotting, nitrocellulose membranes were cut at 100kDa and the upper half of the membrane immunoblotted with anti-Flag antibody to check the efficacy of the IP (lower panel). B. Lysates from the same cells were immunoprecipitated with anti-V5 antibody and immunoblotted with anti-Flag and anti-V5 antibodies as indicated. The pEGFP-N1-Flag-AKAP-Lbc plasmid and anti-AKAP-Lbc antibody (V096) were kind gifts from Dr Donelson Smith, University of Washington, Seattle. C. Endogenous AKAP-Lbc was immunoprecipitated from NRVM lysate using V096 antibody which is raised against the N terminus of AKAP-Lbc (Table 3-1). Cellular lysates were immunoblotted for total Hsp20 and AKAP-Lbc. Hsp20 could be identified in the AKAP-Lbc immune complex. D. Prolonged exposure of AKAP-Lbc IP from part C, enabling visualisation of native AKAP-Lbc in cellular lysates.

Immunofluorescence microscopy was then used to visualise the distribution of these two proteins in cells. AKAP-Lbc has previously been shown to localise to the cytosol and peri-nuclear region of NRVM (Carnegie et al 2008). NRVM were fixed and immunostained for Hsp20 and AKAP-Lbc as indicated. Analysis of these images confirmed that the distribution of Hsp20 and AKAP-Lbc overlapped in these cells with a Pearson co-efficient of 0.710, consistent with a high degree of colocalisation.

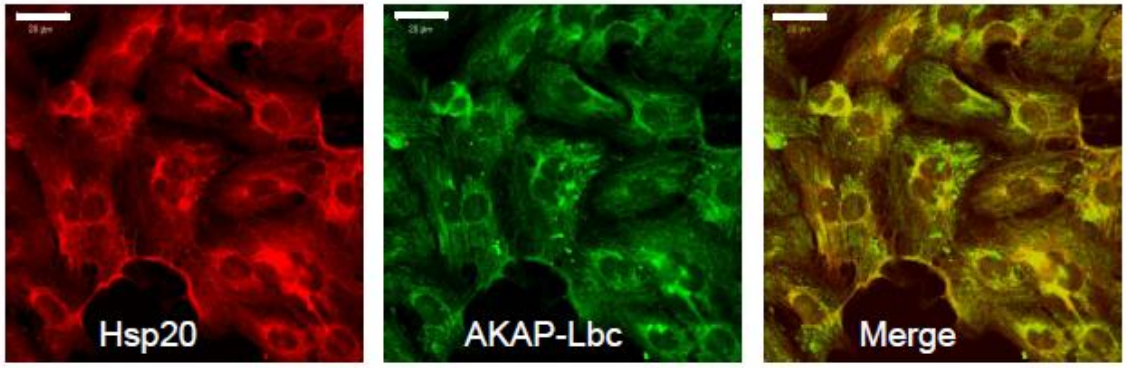

Figure 5-4 Colocalisation of Hsp20 and AKAP-Lbc in neonatal rat cardiac myocytes. Colocalisation (yellow regions) of Hsp20 (red) and AKAP-Lbc (green) was determined by fixation of rat ventricular cardiac myocytes in methanol/paraformaldehyde as described in Section 3.6.2, and staining for immunofluorescence with anti-HspB6 (Hsp20) and anti-V096 (AKAP-Lbc) antibodies. Images were obtained at 63x magnification on a Zeiss Pascal Confocal microscope, and collected using Zeiss Pascal software. A Pearson colocalisation coefficient (r) was calculated using Image J software. For these images, r = 0.710, indicating a high degree of colocalisation. Scale bars represent 20µM.

5.2.4 AKAP-Lbc is required for PKA phosphorylation of Hsp20

5.2.4.1. Selective knockdown of AKAP-Lbc abolishes β-agonist-induced increases in PKA phosphorylation of Hsp20

The above experiments provide evidence for the existence of Hsp20 and AKAP-Lbc together in a complex within cells. In order to establish that AKAP-Lbc is responsible for scaffolding a pool of PKA that is able to phosphorylate Hsp20 within this complex, I examined the effects of AKAP-Lbc gene silencing on β-agonist-induced PKA phosphorylation of Hsp20. Small interfering RNA (siRNA) against AKAP-Lbc was used to

selectively knockdown AKAP-Lbc expression, and phosphorylation of Hsp20 at Ser16 in the presence and absence of Iso was determined by Western immunoblotting (Figure 5-5). Scrambled siRNA was used as a control. AKAP-Lbc siRNA knockdown experiments were performed in human cardiac myocytes (HCM), which are isolated from human ventricles. The HCM cell line was chosen as significant knockdown of AKAP-Lbc expression could be achieved by this RNA interference technique. The efficiency of AKAP-Lbc knockdown was confirmed by immunoblotting.

AKAP-Lbc siRNA-mediated knockdown resulted in a very marked reduction in the expression of AKAP-Lbc protein, whereas treatment with scrambled control siRNA had no effect on protein levels (Figure 5-5A, lower panel). In unstimulated cells, levels of PKA-phosphorylated Hsp20 were low, as expected, and no significant difference was observed between levels of phosphorylated Hsp20 in control siRNA and AKAP-Lbc siRNA-treated cells (Figure 5-5A, upper panel; Figure 5-5B). Following β-adrenergic stimulation and activation of PKA, selective knockdown of AKAP-Lbc completely abolished the expected increase in PKA phosphorylation of Hsp20, whereas control siRNA treatment had no effect ($P<0.05$). Thus, AKAP-Lbc scaffolding of PKA is required for β-agonist-induced Ser16 phosphorylation of Hsp20.

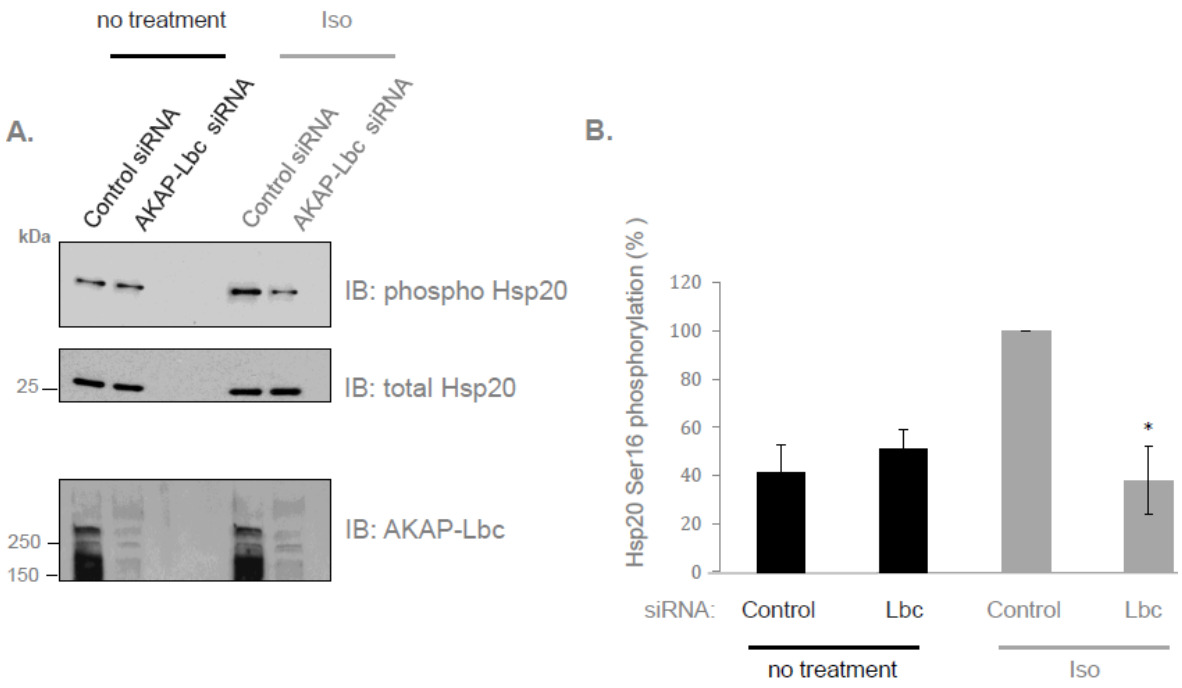

Figure 5-5 AKAP-Lbc gene silencing attenuates the PKA phosphorylation of Hsp20 observed in response to β-agonists.
HCM cells were transfected with siRNA against AKAP-Lbc or scrambled control siRNA. Indicated cells were stimulated with 1nM Iso for 5 minutes immediately prior to harvesting. Lysates were separated by gel electrophoresis and immunoblotted with anti-phospho-Ser16 or total Hsp20 antibodies. A. Upper panel: Representative immunoblots of phospho-Ser16 and total Hsp20 levels. B. Lower panel: AKAP-Lbc immunoblot of the same samples using V096 antibody, indicating efficient knockdown of AKAP-Lbc protein expression. B. Quantification of data from part A. Means ± SEM are shown for an n of 3 experiments. Data are normalised to the maximum level of phosphorylation observed. Hsp20-Ser16 phosphorylation was significantly lower in Iso-stimulated cells treated with AKAP-Lbc siRNA when compared with control siRNA treatment (*P<0.05).

5.2.4.2. PKA anchoring mutants of AKAP-Lbc disrupt cAMP-dependent Hsp20 phosphorylation

The role of AKAP-Lbc in anchoring a pool of PKA that mediates phosphorylation of Hsp20 was further confirmed in NRVM using an AKAP-Lbc mutant, AKAP-Lbc ΔPKA. AKAP-Lbc ΔPKA contains two proline mutations in its RII binding domain (Ala1251Pro and Ile 1260Pro) that disrupt the secondary structure, rendering it unable to anchor PKA (Diviani et al 2001, Smith et al 2010). NRVM were transfected with either AKAP-Lbc ΔPKA or vehicle only (mock transfected), and levels of phosphorylated Hsp20 in the presence and absence of Iso stimulation were determined by Western immunoblotting (Figure 5-6). As expected, robust cAMP-dependent phosphorylation of Hsp20 at Ser16 was observed in

Iso-stimulated cells transfected with vehicle alone. Levels of Hsp20 Ser16 phosphorylation were significantly reduced in both Iso-stimulated and unstimulated cells transfected with AKAP-Lbc ΔPKA when compared to mock transfections (P<0.05 and P<0.01 respectively). This is consistent with the anchoring mutant exerting a dominant negative effect, in other words, ”competing out” wildtype AKAP-Lbc for the interaction with Hsp20. Thus, AKAP-Lbc anchors PKA to facilitate Hsp20 phosphorylation on Ser16.

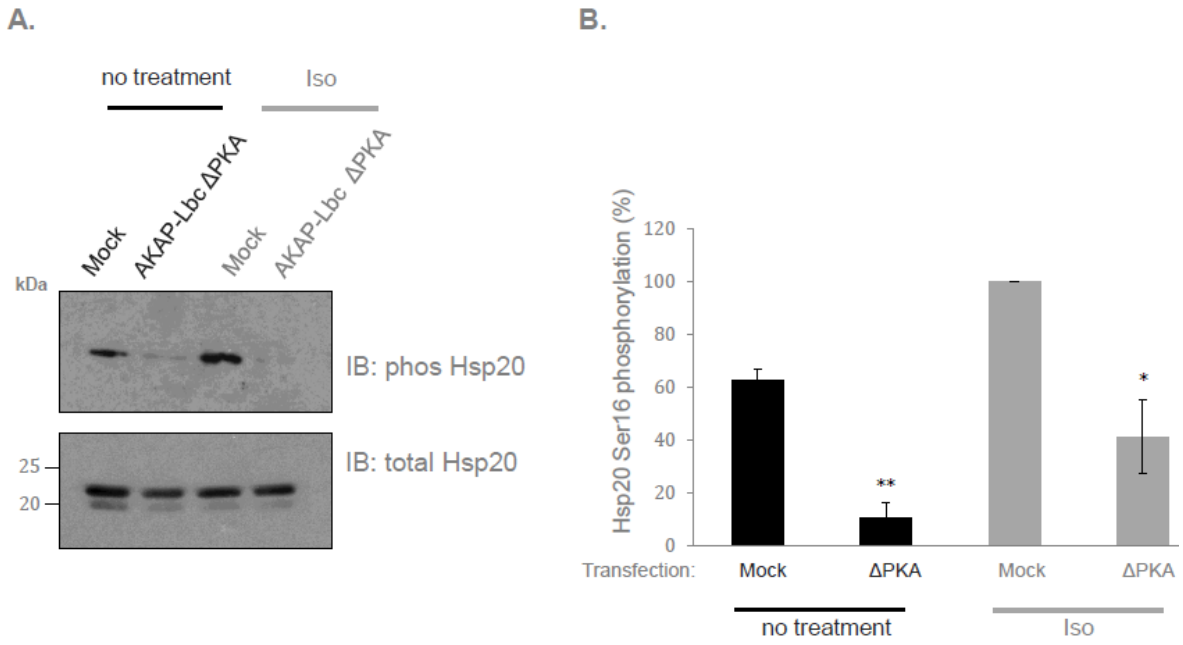

Figure 5-6 A PKA anchoring mutant of AKAP-Lbc attenuates Hsp20 Ser16 phosphorylation. A. NRVM were mock transfected or transfected with AKAP Lbc ΔPKA, a PKA anchoring-defective mutant, and then stimulated with 1nM Iso for 5 minutes or left unstimulated (no treatment). Hsp20 phosphorylation was determined by Western immunoblotting. The pEGFP-N1-AKAP-Lbc ΔPKA plasmid was kindly provided by Donelson Smith. A. Representative immunoblot of phospho-Ser16 and total Hsp20 levels. B. Quantification of data in part A. Data was from an n of 4 experiments, and is presented as means ± SEM. In both Iso-treated and unstimulated cells, transfection with the ΔPKA mutant led to a significant reduction in PKA phosphorylation of Hsp20 (*P<0.05 and **P<0.01 respectively).

5.2.5 AKAP-Lbc scaffolding of PKA is required for the anti-apoptotic cardioprotective function of Hsp20

The cardioprotective abilities of Hsp20 are known to be enhanced following PKA phosphorylation of the heat shock protein on Ser16 (Beall et al 1999, Fan et al 2004a). Overexpression of Hsp20 mutants where Ser16 has been mutated to Asp to mimic

constitutive phosphorylation (S16D) has previously been shown to protect against apoptosis induced by chronic β-adrenergic stimulation, resulting in a 25% reduction in caspase-3 activity (Fan et al 2004a). However, cells transfected with phospho-null mutants (Hsp20-S16A) exhibit no protection from apoptosis. In order to determine whether disruption of the Hsp20-AKAP-Lbc interaction significantly impacted upon Hsp20's cardioprotective functions, cells were transfected with the AKAP-Lbc ΔPKA anchoring defective mutant and the effects on apoptosis measured using a commercially available luminescence assay of caspase-3 activity (Section 3.7.2). Cells were chronically stimulated with Iso to induce apoptosis. Cells transfected with the ΔPKA mutant exhibited a doubling of caspase-3 activity, which is proportional to apoptosis (Figure 5-7). In order to show that this effect was due to a reduction in Hsp20 phosphorylation, cells were then co-transfected with either Hsp20-S16D or Hsp20-S16A mutants. S16D co-transfection was associated with a reduction in caspase-3 activity, whereas transfection of the S16A phospho-null mutant had no effect. Thus, Hsp20-S16D can partially rescue the apoptotic phenotype induced by AKAP-Lbc ΔPKA.

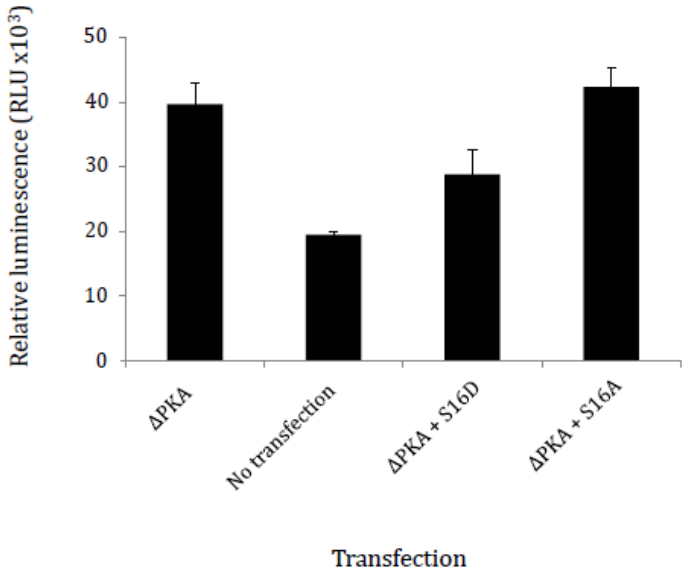

Figure 5-7 Apoptosis is increased in NRVM transfected with PKA anchoring mutants of AKAP-Lbc.
NRVM were transfected with AKAP-Lbc ΔPKA alone, or in conjunction with Hsp20-S16D and Hsp20-S16A. Cells were stimulated with 10μM isoproterenol for 24 hours prior to the assay to induce apoptosis. Untransfected cells were used as a control. Caspase-3 activity was measured in a luminescence assay (described in Section 3.7.2). Hsp20-S16D conferred partial protection against β-agonist-induced apoptosis, as determined by a reduction in caspase-3 activity, whereas S16A mutants had no effect. Data represents the mean ± SEM of an n of 3 experiments.

5.2.6 Hsp20 interacts with a central region of AKAP-Lbc

The above data indicate a physical association between Hsp20 and AKAP-Lbc, and that AKAP-Lbc mediates the cAMP-dependent PKA phosphorylation of Hsp20 at Ser16. AKAP-Lbc is a large 320kDa multi-domain protein which directly interacts with a number of key signaling enzymes, including PKA (Diviani et al 2001), PKCη and PKD (Carnegie et al 2004), B-RAF, and the signaling scaffold protein KSR-1 (Smith et al 2010). In order to gain insight into where Hsp20 binds on the AKAP, I utilised GST fusion proteins encompassing specific regions of AKAP-Lbc in a GST pulldown assay. These fusion proteins have previously been used by others to map the binding sites for PKA, PKC and PKD on AKAP-Lbc (Carnegie et al 2004).

GST-AKAP-Lbc fragments in pGEX-4T1 were expressed in BL21(DE3)pLysS cells and purified as described in Section 3.5.2.2. Six N terminally tagged fusion proteins were generated, covering the full length of AKAP-Lbc (Figure 5-8A). Each of these purified GST-AKAP-Lbc fragments was then used in a pulldown assay, by incubating them with HEK293 lysate containing overexpressed Hsp20-V5. Incubations of the same lysate with GST and with glutathione beads in the absence of fusion protein were also performed as negative controls. Expression of the AKAP-Lbc fragments was confirmed by gel electrophoresis of protein samples and Coomassie staining (Figure 5-8B, lower panel). Fragments 2-5 showed reasonable expression; however fragments 1 and 6 were only poorly expressed, despite varying the conditions used for protein expression and purification, and some degradation of all fusion proteins was evident.

Immunoblotting of GST pulldown supernatants with an antibody against the V5 epitope tag of Hsp20 demonstrated that fragment 4 of AKAP-Lbc interacted with Hsp20-V5 (Figure 5-8B, upper panel). This 534 amino acid region, encompassing amino acids 1388-1922, is adjacent to the PKA anchoring domain of AKAP-Lbc (located within fragment 3), and binding of the heat shock protein here could be envisaged to favour its Ser16 phosphorylation.

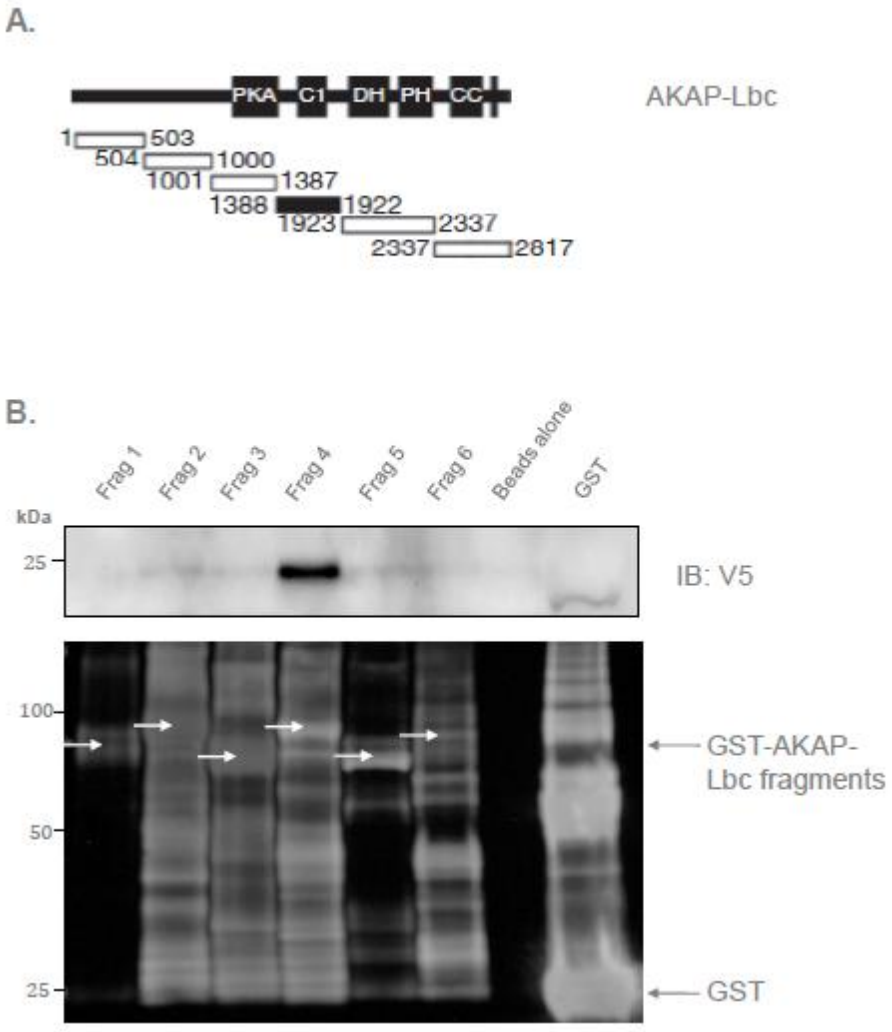

Figure 5-8 The interaction site for Hsp20 on AKAP-Lbc can be mapped to a central region of the AKAP using GST-AKAP-Lbc fusion proteins.
pGEX-4T1 plasmids encoding GST fusion proteins encompassing specific regions of AKAP-Lbc were a kind gift from Donelson Smith. Fusion proteins were expressed in BL21(DE3)pLysS cells and purified as detailed in Section 3.5.2.2. Fusion proteins (Frags 1-6) or purified GST protein were attached to glutathione beads (Section 3.5.2.2), and incubated with lysate from HEK293 cells overexpressing Hsp20-V5. Lysate was also incubated with glutathione beads ('beads alone') and purified GST alone as negative controls. Beads were washed to remove unbound proteins, boiled in protein sample buffer, and samples separated by gel electrophoresis and analysed by immunoblotting. A. Schematic representation of AKAP-Lbc fragments used for GST fusion proteins. The shaded area represents an Hsp20 binding fragment identified in part B. Adapted from (Smith et al 2010). B. Upper panel: Representative immunoblot of Hsp20-V5 pulldown by GST-AKAP-Lbc fragment 4. Lower panel: Coomassie stain of GST-AKAP-Lbc fusion proteins and GST, separated by gel electrophoresis. Colours are inverted to enhance visualisation of the protein fragments.

The above mapping study illustrates a direct interaction of Hsp20 with the central portion of AKAP-Lbc, between residues 1388 and 1922. AKAP-Lbc contains several protein interaction modules, including C terminal Dbl homology and pleckstrin homology

domains, and a cysteine-rich region homologous to the C1 domain of PKC, which is also located within fragment 4 (residues 1792-1830) (Diviani et al 2001). This mapping study must be interpreted with caution, as fragments 1 and 6 of AKAP-Lbc could only be expressed at very low levels, and therefore any binding of Hsp20 to these regions might not have been detected. In order to provide further evidence for a specific interaction between Hsp20 and the central region of AKAP-Lbc, I made use of equivalent N terminal Myc-tagged AKAP-Lbc fragments (Figure 5-9A). HEK293 cells were transfected with Hsp20-V5, and then co-transfected with vectors encoding Myc-AKAP-Lbc fragments 1-6. Lysates were then immunoprecipitated with anti-V5 antibodies or control IgG, separated by gel electrophoresis, and nitrocellulose membranes subjected to immunoblot analysis with anti-myc antibodies (Figure 5-9B, upper panels). Samples were also immunoblotted with anti-V5 antibodies to determine the efficacy of the immunoprecipitations (Figure 5-9B, lower panels). Fragments 1 and 5 were expressed at lower levels, despite increasing the amount of transfected DNA in these cells. Myc-AKAP-Lbc fragment 4 was found to co-immunoprecipitate with Hsp20-V5. This is consistent with the data from the GST pulldown assay described above; thus, it appears that an Hsp20 binding site is present within fragment 4 of AKAP-Lbc.

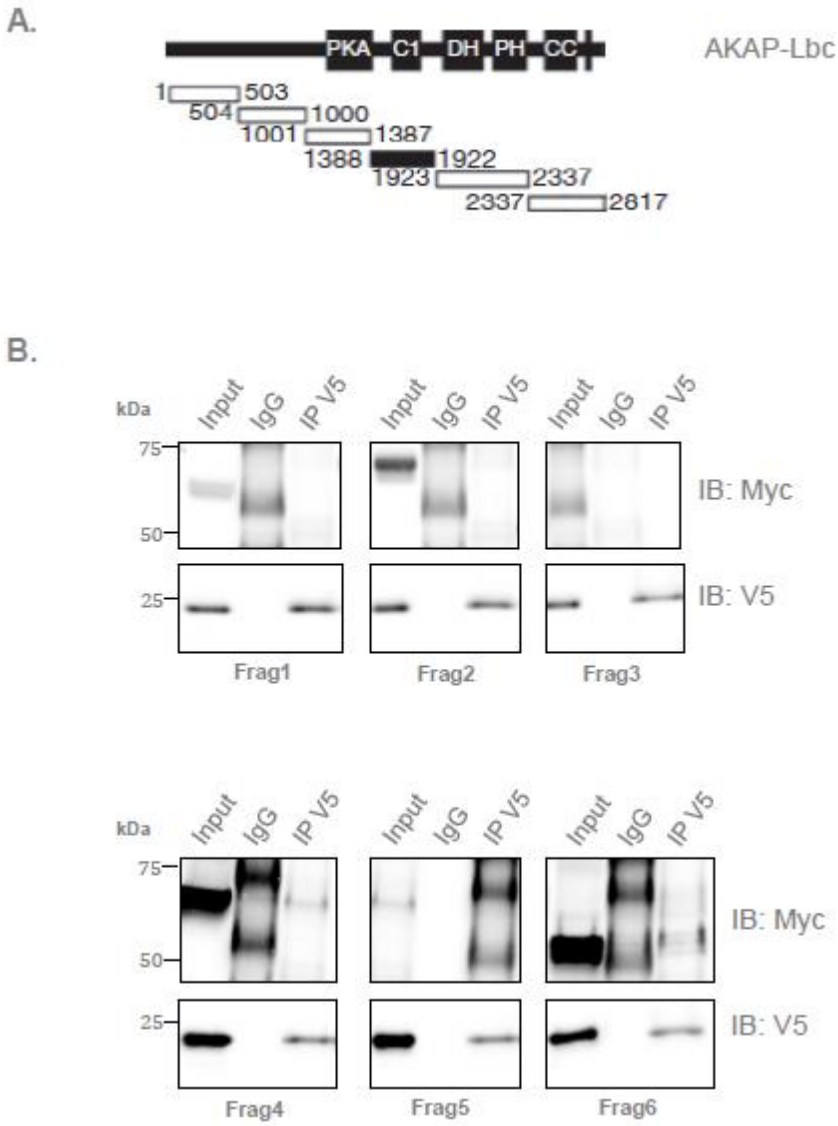

Figure 5-9 Hsp20-V5 and Myc-AKAP-Lbc fragment 4 co-immunoprecipitate in HEK293 cells. Myc-AKAP-Lbc fragments in pDEST12-myc were provided by Donelson Smith. Each fragment was co-transfected into HEK293 cells with Hsp20-V5, and anti-V5 immunoprecipitation performed. A. Schematic representation of Myc-Lbc fragments used in this experiment. AKAP fragments are identical to those used in the GST pulldown experiment above, but possess a Myc tag instead of GST. The shaded area represents an Hsp20 binding fragment. Adapted from (Smith et al 2010). B. V5 immunoprecipitations of transfected HEK293 cell lysates. Samples were separated by gel electrophoresis, transferred to nitrocellulose and membranes divided at the 37kDa molecular weight marker. The top half of each membrane was immunoblotted with anti-myc antibodies to determine which myc-AKAP-Lbc fragments formed an immunocomplex with Hsp20-V5 (upper panels). The bottom half of each membrane was probed with anti-V5 antibody, to assess the efficacy of the IP (lower panels).

5.2.7 The AKAP-Lbc-Hsp20 macromolecular complex includes PDE4D

5.2.7.1. Expression and localisation of an Hsp20-linked cAMP FRET sensor

It is increasingly appreciated that the presence of phosphodiesterase enzymes in macromolecular complexes, along with AKAPs and other proteins, allows for the precise regulation of cAMP/PKA signal transduction cascades (Houslay 2010). The experimental work detailed so far in this chapter provides evidence for the specific association of AKAP-Lbc with the small heat shock protein Hsp20, to mediate its cAMP-dependent PKA phosphorylation on Ser16. Recently, a study from our laboratory has demonstrated a novel interaction between Hsp20 and specific PDE4 isoforms (Sin et al 2011). In this publication, I employed a novel FRET sensor targeted to Hsp20, akin to the targeted TnI:Epac1-camps sensor described in Section 4.2.1, to investigate which PDEs modulate the pool of cAMP around Hsp20 (Figure 5-10A). This sensor was designated Hsp20:Epac1-camps.

Epac1-camps and Hsp20:Epac1-camps were transfected into cultured NRVM to monitor their expression levels and subcellular distribution patterns (Figure 5-10B). Hsp20:Epac1-camps showed a cytosolic and peri-nuclear distribution under YFP fluorescence, similar to the localisation pattern observed in NRVM which had been fixed and stained for immunofluorescence with anti-Hsp20 antibodies (Figure 5-10C, Figure 5-4).

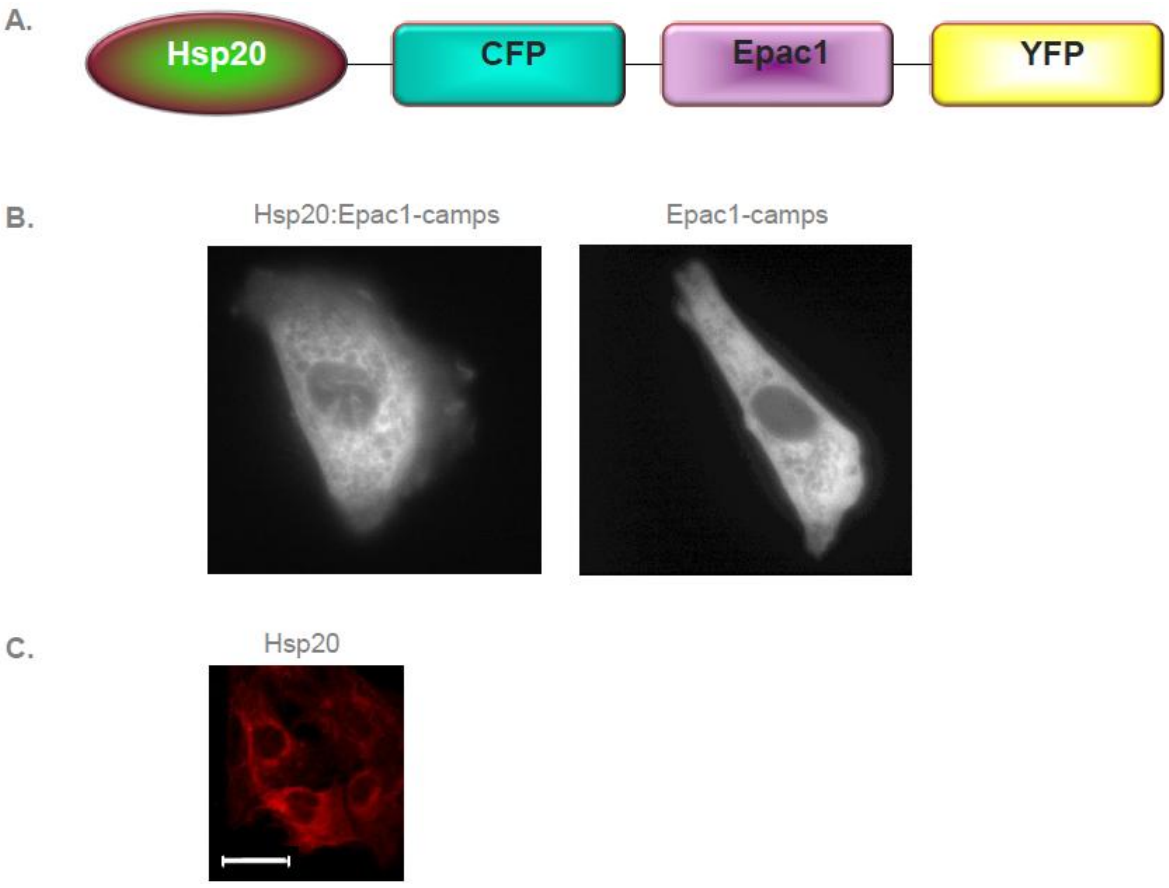

Figure 5-10 Localisation of Epac1-camps and Hsp20:Epac1-camps FRET sensors in NRVM. A. Schematic representation of the Hsp20:Epac1-camps sensor. Hsp20 was cloned 5' of Epac1-camps sensor to generate a novel fusion protein (Section 3.6.1.1.). Cloning was performed by Dr Jon Day. B. YFP fluorescence images of Hsp20:Epac1-camps and Epac1-camps sensors in transfected NRVM. Hsp20:Epac1-camps localises to the cytosol and peri-nuclear region of NRVM, while Epac1-camps shows purely cytoplasmic distribution, as it lacks any localisation sequences. Images were obtained from live cells using a laser confocal microscope at 100x magnification. These images are published in (Sin et al 2011). C. Immunocytochemical analysis and fluorescence microscopy of fixed NRVM stained with anti-HspB6 antibody against Hsp20, showing a similar distribution pattern to the Hsp20 FRET sensor.

5.2.7.2. A targeted FRET sensor reveals that PDE4 modulates the pool of cAMP around Hsp20

In Chapter 4 of this thesis, I demonstrated that the majority of cAMP hydrolytic activity in NRVM is provided by members of the PDE4 family, and that members of this family associate with cardiac troponin I to regulate its PKA phosphorylation. I therefore hypothesised that PDE4 family members might also regulate cAMP levels around Hsp20. To test this hypothesis, NRVM transfected with Hsp20:Epac1-camps were treated with the PDE4 inhibitor rolipram, and the FRET ratio (which is proportional to fluctuations in

cAMP levels) was measured (Figure 5-11). Epac1-camps was used as a control for all FRET experiments. The magnitude of response to β-adrenergic stimulation with Iso was similar for both Epac1-camps and the Hsp20-targeted sensor (12.9% ± 1.5% and 9.0% ± 1.7% change in FRET ratio respectively). Saturating levels of cAMP generated by non-selective inhibition of PDEs with IBMX also provoked a similar response from both sensors (Epac1-camps, 26.4% ± 2.6%; Hsp20:Epac1-camps, 27.2% ± 2.4%) (Figure 5-11A and 5-11C).

A change in FRET ratio of 4.6% ± 1.0% was measured by Epac1-camps in response to rolipram (Figure 5-11B and 5-11C). This is similar to the response measured in the previous chapter (Figure 4-5), indicating consistent behaviour of the control sensor across different experiments. The Hsp20:Epac1-camps sensor measured a much larger change in FRET ratio (11.1% ± 1.8%) than Epac1-camps ($P<0.01$). As the expression level of both sensors is similar (Figure 5-10B), this indicates that PDE4 isoforms are likely to regulate cAMP levels in the subcellular compartments occupied by Hsp20.

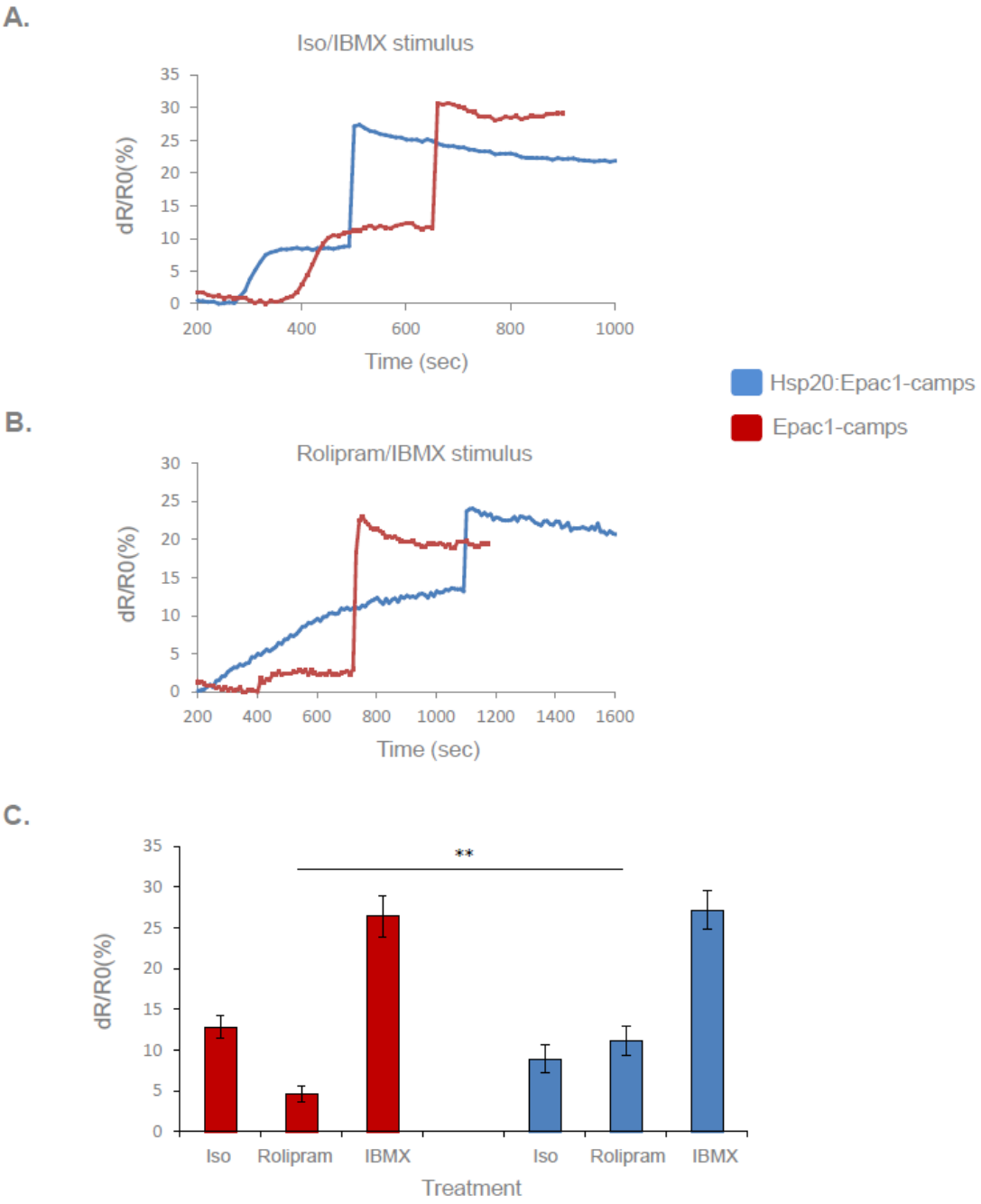

Figure 5-11 Measurement of cAMP levels in the vicinity of Hsp20 using a targeted FRET sensor. NRVM were transfected with either Hsp20:Epac1-camps or the control sensor Epac1-camps, stimulated with 1nM Iso, 10µM rolipram and 100µM IBMX as indicated, and FRET ratios measured. This figure is modified from data published in (Sin et al 2011). A. Representative traces of changes in FRET ratio measured by Hsp20:Epac1-camps (blue) and Epac1-camps (red) in response to real time stimulation with Iso. IBMX stimulation was applied once the response to Iso had plateaued. The magnitude of response to Iso and to IBMX stimuli was similar for both sensors. B. Representative traces of changes in FRET ratio measured by these sensors in response to real time stimulus of NRVM with rolipram, followed by IBMX. A much larger change in FRET ratio was detected by Hsp20:Epac1-camps with rolipram stimulus, consistent with a greater increase in local cAMP levels following PDE4 inhibition. C. Graph of the percentage change in FRET ratio for both sensors. Hsp20:Epac1-camps detected a significantly greater change in FRET ratio (11.1% ± 1.8%) than Epac1-camps (4.6% ± 1.0%) in response to rolipram stimulus (P<0.01). Changes in FRET ratio over time are presented as dR/R0 (%), as described in Section 3.6.1.2. An n of 6-10 cells were used for each experimental condition.**

5.2.7.3. PDE4D isoforms regulate PKA phosphorylation of Hsp20

Following on from this observation, the phosphorylation of Hsp20 was shown to be modulated by PDE4 in HEKβ2 cells (Sin et al 2011), which are a cell line stably overexpressing the Flag- and GFP-tagged β2-adrenergic receptor (Houslay & Baillie 2006). **This work was performed by Dr Xiang Li and Dr George Baillie**. Concomitant rolipram-induced inhibition of PDE4 coupled with Iso stimulation led to a greater increase in Ser16 phosphorylation of Hsp20 over time than was seen following stimulation with Iso alone, indicating a crucial role for PDE4 in regulating this phosphorylation event (Figure 5-12A). PDE4D isoforms were also shown to co-immunoprecipitate with Hsp20 in this cell line (Figure 5-12B). Peptide array technology was then used to map the binding site for Hsp20 to a region within the conserved catalytic unit of PDE4 (Figure 5-12C).

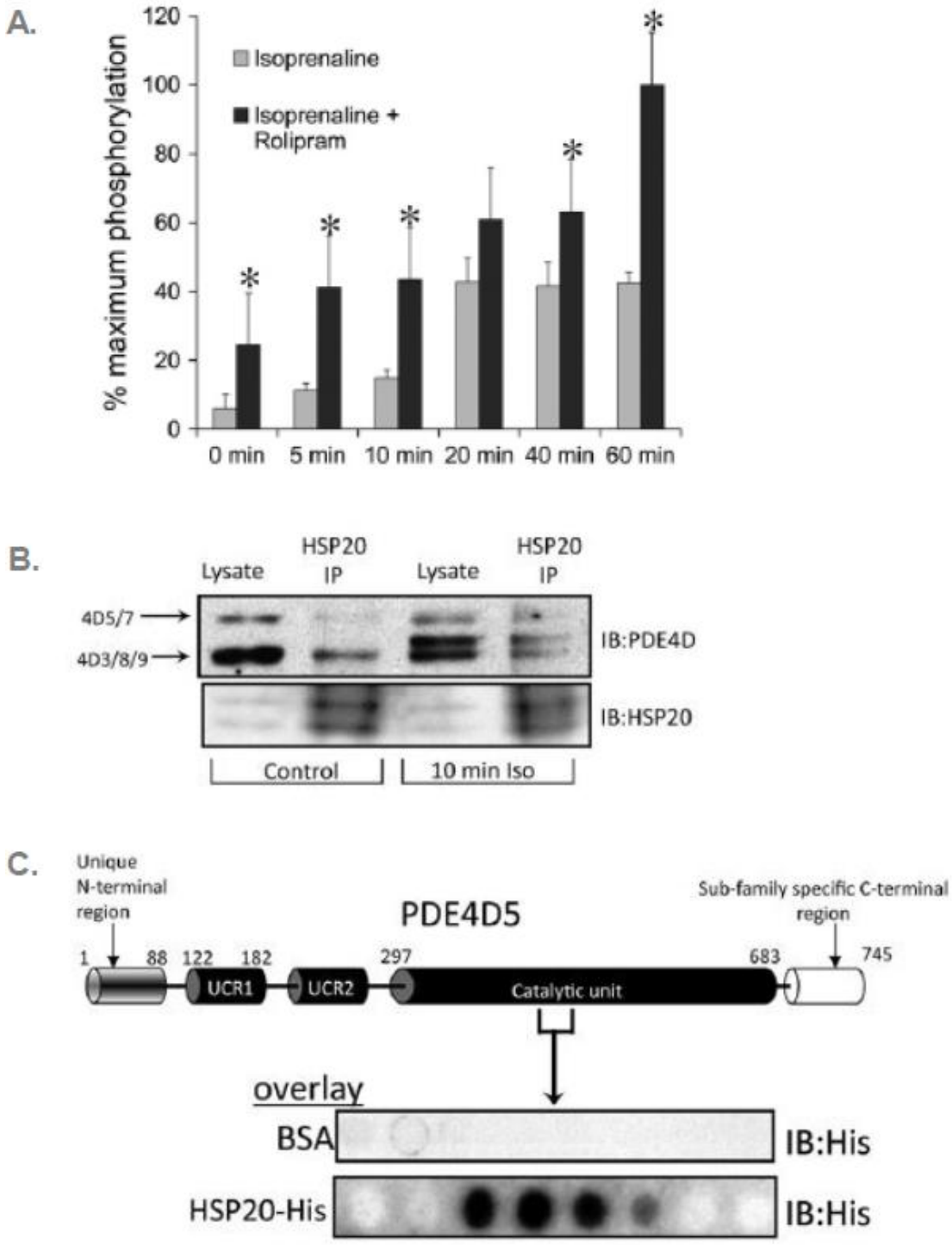

Figure 5-12 PDE4D associates with Hsp20 to regulate its PKA phosphorylation via a region within the conserved catalytic domain of the PDE.
This figure is adapted from (Sin et al 2011), a paper on which I am a co-author. *The work detailed in this figure was performed by Dr Xiang Li and Dr George Baillie.* A. HEKβ2 cells were treated with 1μM isoproterenol (isoprenaline) following pretreatment with 10μM rolipram, for the times shown. Lysates were immunoblotted for phospho-Ser16 and total Hsp20. Quantification of the data from an n of 3 experiments is presented. B. Hsp20 was immunoprecipitated from HEKβ2 lysates, using specific anti-sera, and lysates immunoblotted with anti-PDE4D antibodies. C. A PDE4D5 peptide array was overlayed with His-tagged Hsp20, or BSA as a control. Hsp20 was shown to bind to a sequence within the conserved catalytic unit of PDE4.

5.2.7.4. PDE4D isoforms and Hsp20 are present in a macromolecular complex with AKAP-Lbc

The data presented so far indicate that Hsp20 associates with AKAP-Lbc and PDE4D isoforms. Although multiple protein kinases and other important signaling proteins have been shown to associate with AKAP-Lbc (Carnegie et al 2004, Diviani et al 2001, Smith et al 2010), as yet, no phosphodiesterase has been shown to participate in any AKAP-Lbc-nucleated complex. Based on the experiments detailed above, I hypothesised that Hsp20 and PDE4D should be found in a complex together with AKAP-Lbc. I therefore performed an immunoprecipitation of endogenous AKAP-Lbc from NRVM lysate using anti-AKAP-Lbc antibody (V096). A control immunoprecipitation with normal IgG was also performed. Both Hsp20 and PDE4D isoforms were identified as co-immunoprecipitants with AKAP-Lbc, along with PKA R and C subunits (Figure 5-13A). PDE isoforms with a molecular weight corresponding to PDE4D3/8/9 and PDE4D5/7 were identified in the immune complex. However, it is not possible to say from these experiments whether their interaction with the AKAP is direct, or is mediated by Hsp20.

AKAP-Lbc immunoprecipitation complexes were then screened for PDE activity (Figure 5-13B). The majority of PDE activity associated with AKAP-Lbc was from PDE4, consistent with the data above. However, there also appeared to be a smaller, but statistically significant, contribution from PDE3 as well. Our laboratory is currently working with collaborators to identify the specific PDE isoforms present in this complex.

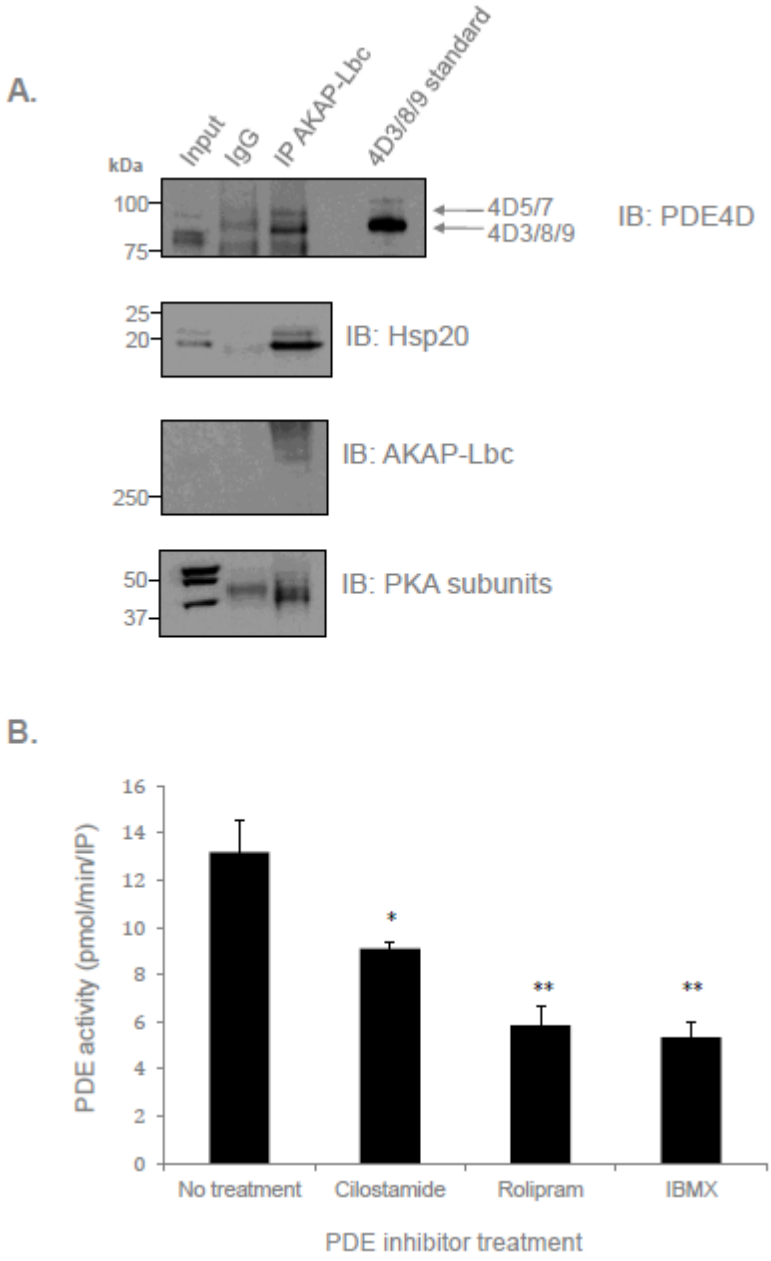

Figure 5-13 PDE4 activity is associated with AKAP-Lbc-Hsp20 complexes in NRVM. AKAP-Lbc was immunoprecipitated from NRVM using an anti-AKAP-Lbc antibody. A. Immune complexes were screened for the presence of PDE4D isoforms (upper panel), Hsp20 (second panel) and PKA subunits (lower panel) by immunoblotting with the appropriate anti-sera. AKAP-Lbc immunoblotting was also performed to test the efficacy of the IP (third panel). B. AKAP-Lbc IPs were treated with inhibitors of PDE3 (cilostamide; 10µM), PDE4 (rolipram; 10µM) or non-specific PDE inhibitor (IBMX; 100µM) and subjected to PDE activity assay (described in Section 3.7.1). All of the inhibitors tested caused a statistically significant reduction in PDE activity in the IP, in the following order of magnitude: non-specific PDE inhibition>PDE4 inhibition>PDE3 inhibition. Data represents the mean ± SEM for an n of 3 experiments. * P<0.05; ** P<0.01.

Based on the experiments in this chapter, and data from (Sin et al 2011), a model of the macromolecular complex co-ordinated by AKAP-Lbc and Hsp20 in the heart can be proposed, whereby in resting cells, anchored PDE4 hydrolyses local cAMP, inactivating the pool of PKA anchored to AKAP-Lbc, and maintaining Hsp20 in a hypophosphorylated, less cardioprotective state. Following β-adrenergic stimulus, cAMP is generated and this saturates the tethered PDE4, leading to PKA activation and phosphorylation of Hsp20. Hsp20-Ser16 phosphorylation enhances its cardioprotective abilities.

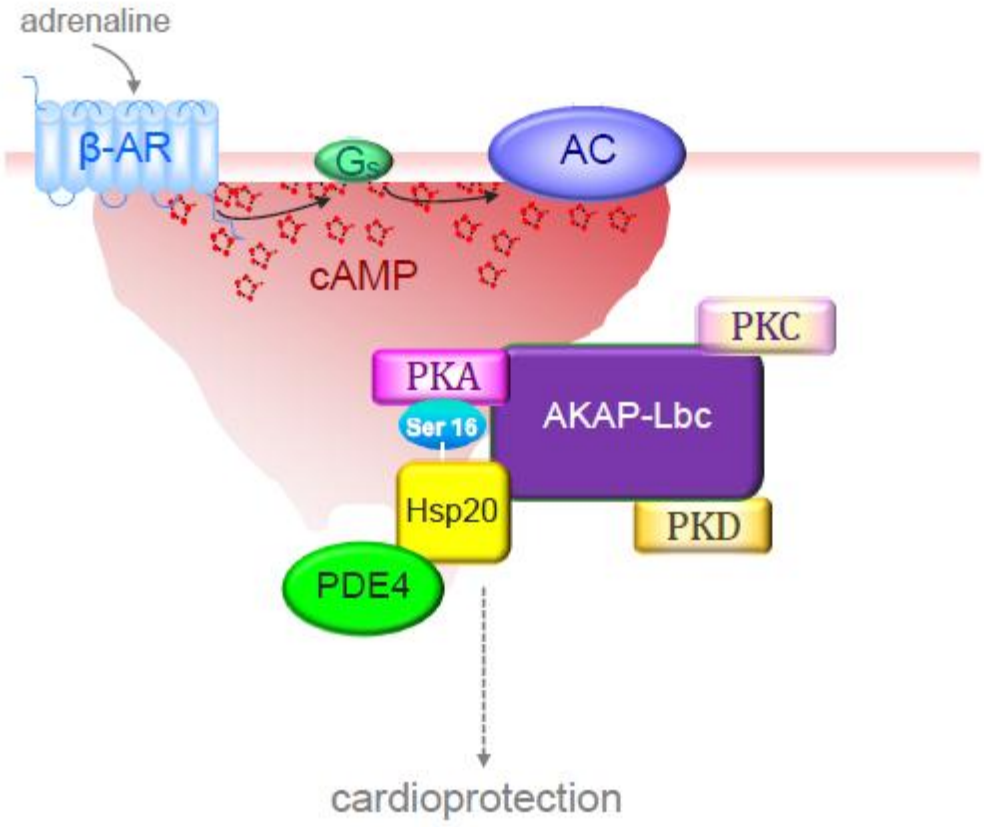

Figure 5-14 Schematic representation of the macromolecular complex co-ordinated by AKAP-Lbc and containing Hsp20 in the heart.
AKAP-Lbc scaffolds the signaling enzymes PKA, PKCη and PKD (Carnegie et al 2008). This experiments presented in this chapter demonstrate a novel association between Hsp20 and AKAP-Lbc, which facilitates cardioprotective PKA phosphorylation of the heat shock protein on Ser16. Recent work from our laboratory has identified an interaction between Hsp20 and the catalytic unit of PDE4 (Sin et al 2011), and PDE4D isoforms were shown to be present in cardiac AKAP-Lbc immune complexes.

5.3 Discussion

PKA phosphorylation events are integral to cardiac processes such as excitation-contraction coupling and cardioprotection, and therefore the precise regulation of PKA activity is vital to cardiac function (Bers & Despa 2006, Fan et al 2005a). cAMP-dependent PKA activation is regulated by the creation of localised cAMP gradients secondary to the actions of tethered phosphodiesterase enzymes (Houslay 2010), and by the physical compartmentation of discrete pools of PKA by AKAPs (Scott & Santana 2010). It is now appreciated that the functions of AKAPs are infinitely more complicated than simply scaffolding PKA; indeed, they have been shown to simultaneously associate with multiple binding partners to facilitate the integration of a number of diverse signaling networks (Smith et al 2010, Welch et al 2010). A major focus of current cyclic nucleotide research is on the characterisation of these macromolecular signaling complexes, or signalosomes. AKAP-nucleated complexes may contain various combinations of cAMP effectors (PKA, Epac and ion channels), signal terminating enzymes (protein phosphatases and PDEs) and other scaffold proteins, which can link cAMP signal transduction to Ca^{2+} and growth factor signals (Dodge-Kafka & Kapiloff 2006, Terrenoire et al 2009). Physical compartmentalisation of signaling enzymes within these macromolecular complexes confers spatial regulation of cAMP signal transduction, whilst bringing multiple cAMP effectors into close proximity allows for rapid and efficient signal transmission, facilitating temporal regulation of cAMP signaling (Scott & Santana 2010).

One of the major mediators of cardioprotection is the small heat shock protein Hsp20. Hsp20 is phosphorylated by PKA at Ser16 on its N terminus, and this modification is vital for its cardioprotective actions (Section 1.7.3.2.). As with the myofilament protein TnI, levels of phosphorylated Hsp20 have been shown to be reduced in failing human hearts, underlining the importance of this protein in normal cardiac functioning (Qian et al 2009). Phosphorylated Hsp20 has been demonstrated to protect against ischaemia-reperfusion injury (Fan et al 2005b), apoptosis and necrosis (Qian et al 2009), and cardiac hypertrophy (Fan et al 2006). Selective targeting of signaling elements that can enhance this modification therefore represents a new therapeutic avenue for the prevention and treatment of pathological cardiac remodelling and ischaemic injury. Previously, no AKAP

had been identified for the pool of PKA that phosphorylates Hsp20. The data presented in this chapter identifies the cytosolic AKAP, AKAP-Lbc, as this scaffold protein in cardiac myocytes. Co-immunoprecipitation and colocalisation studies demonstrated a specific association between AKAP-Lbc and Hsp20 (Figure 5-3 and 5-4). Hsp20 Ser16 phosphorylation was attenuated in cells where AKAP-Lbc was either specifically knocked down by siRNA-mediated gene silencing (Figure 5-5), or competed out by a PKA anchoring-defective AKAP-Lbc mutant (Figure 5-6).

AKAP-Lbc is expressed at high levels in the heart, and has been implicated in the development of cardiac hypertrophy (Carnegie et al 2008), therefore its association with Hsp20, a cardioprotective protein with known anti-hypertrophic effects, is immediately intriguing. AKAP-Lbc is a large, multi-domain protein which contains tandem Dbl homology (DH) and pleckstrin homology (PH) domains. The DH domain is associated with guanine nucleotide exchange activity for small GTPases such as Rho, and so AKAP-Lbc functions as a guanine nucleotide exchange factor (GEF) for the small GTPase Rho (Appert-Collin et al 2007). RhoA is a well known mediator of cardiac hypertrophy, though the downstream signaling pathways involved are incompletely understood (Brown et al 2006). The Rho-GEF activity of AKAP-Lbc is stimulated by Gα12, but is inhibited by PKA phosphorylation of AKAP-Lbc on Ser1565 (Diviani et al 2004). Anchored PKA was shown to phosphorylate AKAP-Lbc on Ser1565 in response to forskolin stimulus, and it can be postulated that factors promoting PKA phosphorylation of AKAP-Lbc might also promote phosphorylation of Hsp20 and lead to the induction of its anti-hypertrophic effects.

AKAP-Lbc contains binding sites for PKA (Diviani et al 2001), PKC and PKD isoforms (Carnegie et al 2004), and has recently been shown to scaffold B-Raf and the signaling scaffold protein KSR-1 to organise a growth factor- and cAMP-dependent signaling network critical to cell growth and proliferation (Smith et al 2010). The ability of AKAP-Lbc to scaffold both PKA and PKD isoforms is intriguing, as unpublished data from our laboratory has recently indicated that Hsp20 can be phosphorylated by PKD, and that this phosphorylation may be linked to the development of cardiac hypertrophy. Thus, the interaction of Hsp20 with AKAP-Lbc could facilitate its phosphorylation by both of these kinases to modulate hypertrophic signaling. AKAP-Lbc has been shown to assemble an

activation complex for PKD by synchronising PKCη phosphorylation and activation of the catalytic domain of PKD with PKA phosphorylation of the C terminus of PKD, which facilitates its release from the AKAP (Carnegie et al 2004). PKD has been proposed to act downstream of RhoA to mediate hypertrophic signals. Carnegie and co-workers found that activated PKD translocates to the nucleus, where it phosphorylates class II histone deacetylases (HDACs). This promoted nuclear export of HDACs, and resulted in derepression of the transcription factor myocyte enhancer factor 2 (MEF2), and the transcription of hypertrophic genes (Carnegie et al 2008) (Section 1.6.6.1.). Expression of AKAP-Lbc is known to be upregulated in hypertrophic NRVM, and this has been proposed to augment activation of PKD and promote development of a hypertrophic phenotype (Carnegie et al 2008). Hsp20 phosphorylation by PKA in response to β-adrenergic stimulus is known to have anti-hypertrophic effects (Sin et al 2011). Thus, the induction of cardiac hypertrophy may involve a complex signaling network centring on AKAP-Lbc, where activation of RhoA and PKD favours a hypertrophic phenotype, and PKA activation, with subsequent phosphorylation of Hsp20 and AKAP-Lbc, opposes these effects. Future studies must determine the relative contributions of PKA and PKD phosphorylation of AKAP-Lbc-anchored Hsp20 to the hypertrophic response.

As well as enhancing its anti-hypertrophic actions, PKA phosphorylation of Hsp20 has been shown to protect against β-agonist-induced apoptosis in the heart. Adult cardiac myocytes infected with adenoviral Hsp20 constructs where Ser16 is mutated to Asp to mimic constitutive phosphorylation (S16D mutants) display a significant reduction in cellular markers of apoptosis, including caspase-3 activity (Fan et al 2004a). The anti-apoptotic effects of Hsp20 are thought to be mediated by its association with the pro-apoptotic protein Bax, which physically prevents translocation of Bax to the mitochondria, where it could damage mitochondrial integrity by releasing cytochrome c, with subsequent activation of caspase-3 (Fan et al 2005b). Transfection of NRVM with a PKA anchoring mutant of AKAP-Lbc to attenuate Hsp20 Ser16 phosphorylation was associated with increased caspase-3 activity. This phenotype could be partially rescued by co-transfection of an Hsp20-S16D mutant, but was not rescued by co-transfection of a phospho-null mutant of Hsp20 (Figure 5-7). This effect should be confirmed by monitoring other markers of apoptosis, such as pyknotic nuclei or DNA laddering, or by TUNEL

(terminal deoxynucleotidyltransferase-mediated dUTP nick-end labeling) assay, which detects DNA fragmentation. The importance of AKAP-Lbc-mediated phosphorylation of Hsp20 should also be determined for Hsp20's other cardioprotective effects, such as ischaemia-reperfusion injury.

Though AKAP-Lbc itself has not been directly implicated as a mediator of apoptosis, PKC signaling and RhoA activation have both been linked with phorbol ester-mediated apoptosis (Chang & Lee 2006). Thus, it appears that signal transduction pathways co-ordinated by this AKAP are involved in the induction of apoptosis. AKAP-Lbc scaffolding of PKA and Hsp20 may counter these pro-apoptotic effects. It would be interesting to determine whether Bax can also interact directly with AKAP-Lbc, as another pro-apoptotic protein, BAD, has previously been shown to reside in a complex together with the AKAP WAVE-1, PKA and PP1, to regulate glycolysis and apoptosis in the liver (Danial et al 2003).

The effects observed on apoptosis in cells expressing the AKAP-Lbc anchoring mutant may not have been specific to Hsp20. The pool of PKA scaffolded by AKAP-Lbc is likely to have more far-reaching effects than just directing the phosphorylation of a single heat shock protein. In order to selectively inhibit AKAP-Lbc-mediated PKA phosphorylation of Hsp20, the disrupter peptide strategy employed in Chapter 4 could be used to displace Hsp20 from its binding site on the AKAP. Mapping studies described above have narrowed this site to the central portion of AKAP-Lbc, between residues 1388 and 1922 (Figure 5-8 and 5-9). This spans a 60kDa region, so further studies will be required to determine the exact binding site of Hsp20. Truncation analysis and mutagenesis studies could be employed but are often very time consuming. The peptide array approach adopted in Chapter 4 can provide a rapid way of identifying interaction sites between two proteins. An Hsp20 peptide array could be overlayed with the GST-AKAP-Lbc fragment containing the Hsp20 binding site, and this information used to design a specific cell permeable peptide disruptor of the Hsp20-AKAP-Lbc interaction. This would then provide an ideal strategy to specifically monitor the effect of AKAP-Lbc-mediated PKA phosphorylation on the cardioprotective effects of Hsp20.

Macromolecular complexes regulating β-adrenergic signaling pathways in the heart often contain signal terminating enzymes, such as protein phosphatases and phosphodiesterases, as a way of regulating their activities. For example, in the macromolecular complex co-ordinated by mAKAP and the ryanodine receptor, PKA and PDE4D3 constitute a negative feedback loop, whereby activation of PKA in response to increased local cAMP levels also leads to the phosphorylation and activation of PDE4D3. which then hydrolyses local cAMP (Dodge et al 2001). It has also been shown that PP2A scaffolded by mAKAP contributes to this regulation by promoting the dephosphorylation and deactivation of PDE4D3 (Dodge-Kafka et al 2010). Hsp20 has recently been found to associate with the protein phosphatase PP1 in the heart, to modulate Ca^{2+} handling at the SR (Qian et al 2011). PP1 has been identified in complexes nucleated by Yotiao (Westphal et al 1999), WAVE-1 (as described above) (Danial et al 2003) and AKAP220 (Schillace & Scott 1999), and it would be interesting to determine whether it is present in the Hsp20-AKAP-Lbc complex, in association with either Hsp20 or the AKAP, as inhibition or displacement of this enzyme could provide a means of modulating Ser16 phosphorylation of Hsp20 to enhance cardioprotection. Though many AKAP complexes include a protein phosphatase, none have yet been specifically linked with complexes nucleated by AKAP-Lbc, so such a finding might have implications for other pathways co-ordinated by this multi-purpose AKAP.

Prior to the work detailed in this chapter, no specific PDE activity had been associated with AKAP-Lbc. PDE4 activity was found to co-purify with AKAP-Lbc in heart cell lysates, together with a smaller amount of PDE3 activity (Figure 5-13B) and PDE4D isoforms were demonstrated in an AKAP-Lbc immune complex together with Hsp20 and PKA (Figure 5-13A). Recent work from our laboratory, some of which is detailed above (Figure 5-12), has demonstrated a specific interaction between Hsp20 and PDE4 isoforms, which is mediated by a binding domain within the conserved catalytic unit of the PDE (Sin et al 2011). Biochemical studies are currently underway to determine whether PDE3 and PDE4 isoforms also associate directly with AKAP-Lbc, or whether, in the case of PDE4, this interaction is mediated indirectly via Hsp20.

In summary, the data presented in this chapter identify a new macromolecular complex in the heart which is nucleated by AKAP-Lbc, and includes the cardioprotective heat shock protein Hsp20 along with PKA and signal terminating phosphodiesterase 4D isoforms. Selective modulation of the signaling elements within this complex affects the cardioprotective functions of Hsp20. It has previously been shown that disruption of the Hsp20-PDE4D interaction enhances phosphorylation at Ser16 to protect against cardiac hypertrophy (Sin et al 2011), and I now show that disruption of the AKAP-Lbc-Hsp20 interaction promotes cardiac myocyte apoptosis. Elucidating the structural components of the macromolecular complex formed by AKAP-Lbc, Hsp20 and other signaling enzymes in the heart will enable the development of novel peptides or small molecule inhibitors that can selectively enhance phosphorylation of Hsp20 at Ser16 to promote cardioprotection.

6.

Final Discussion

The discovery of the second messenger 3'5'-cyclic adenosine monophosphate in 1958 revolutionised our understanding of cellular signal transduction pathways (Sutherland & Rall 1958). The realisation that cAMP helped mediate the actions of the hormone adrenaline on glycogenolysis in liver cells was followed by the identification of the cAMP-dependent protein kinase (PKA) as a major effector of cAMP signals (Walsh et al 1968). Since then, hundreds of PKA substrates have been identified, and modification of protein function by PKA phosphorylation has been shown to produce cellular outcomes as diverse as cardiac myocyte contraction (Solaro et al 1976) and gene transcription (Delghandi et al 2005).

cAMP is a freely diffusible molecule, and could potentially flood the interior of the cell, leading to the indiscriminate activation of multiple downstream effectors (Houslay et al 2007). It is now accepted that this situation is avoided by the compartmentalisation of cAMP signals. Discrete microdomains of cAMP, created by the actions of phosphodiesterase enzymes, have been directly visualised in live cells using genetically encoded cAMP sensors (Zaccolo & Pozzan 2002). PKA is anchored to specific subcellular targets by its interaction with AKAPs, therefore only particular pools of PKA are exposed to activating concentrations of cAMP at any one time (Baillie 2009). Thus, signals from one second messenger can result in the activation of distinct signal transduction pathways, and diverse physiological responses (Buxton & Brunton 1983).

More than 50 years on from the discovery of cAMP, the field of cyclic nucleotide research is still expanding, and some of the accepted paradigms of compartmentalised cAMP signaling are being challenged. For example, it has recently been shown that under certain circumstances cAMP signaling may persist once initiating GPCRs have been

internalised (Calebiro et al 2010a, Calebiro et al 2010b). Emerging evidence also indicates that Epac can also be compartmentalised within cells, and compartmentalised Epac signaling has been linked with the cAMP-dependent regulation of vascular endothelial cell permeability (Rampersad et al 2010) and cellular proliferation (Hochbaum et al 2010).

Much of current cyclic nucleotide research is focused on the characterisation of macromolecular signaling complexes, or signalosomes. These complexes are nucleated by AKAPs, and consist of various combinations of cAMP effectors (PKA, Epac and ion channels), signal terminating enzymes (protein phosphatases and PDEs) and other scaffold proteins which link cAMP signal transduction to Ca^{2+} and growth factor signaling pathways (Welch et al 2010). A number of important signalosomes have been identified in the heart, which are critical to the regulation of excitation-contraction coupling. cAMP-dependent PKA phosphorylation of proteins involved in ECC plays an integral part of the body's fight or flight response, and has been shown to directly influence Ca^{2+} transport (Marx et al 2000), myofilament Ca^{2+} sensitivity (Stelzer et al 2007), and cardiac contractility (Takimoto et al 2004) in order to increase cardiac output (Mudd & Kass 2008). New associations and participants are continually being identified within these macromolecular complexes, for example, PDE4B has recently been shown to associate with the LTCC to influence Ca^{2+} transients (Leroy et al 2011).

cAMP dynamics are particularly important at the cardiac myofilament. During times of physiological stress, cardiac output increases in response to β-adrenergic stimulation, which leads to PKA phosphorylation of the myofilament proteins troponin I and myosin-binding protein-C. These phosphorylation events contribute to enhanced force development during systole and an accelerated rate of relaxation during diastole (Stelzer et al 2007). PKA phosphorylation of myofilament proteins is known to be reduced in cardiac failure (Zakhary et al 1999); however, the precise signaling elements regulating PKA activation at the myofilament, and the subsequent phosphorylation of myofilament proteins, are poorly understood. In the first part of this thesis, I investigated the signaling elements modulating cAMP-dependent phosphorylation of TnI at the myofilament. cAMP levels in the vicinity of TnI were shown to be regulated by members of the phosphodiesterase 4 family using a genetically encoded FRET-based cAMP sensor

targeted to TnI. A specific interaction was then demonstrated between TnI and the PDE4 isoform PDE4D9. This study represents the first demonstration of an interaction between a myofilament protein and a phosphodiesterase enzyme, and could provide the basis for a novel therapeutic strategy for heart failure, as modulation of this interaction could promote TnI phosphorylation and an increase in cardiac output.

In the second part of the thesis, I focused on identifying factors which regulate PKA phosphorylation of the small heat shock protein Hsp20. Hsp20 is known to protect against ischaemic injury and hypertrophy in the heart, and these cardioprotective actions are enhanced by its PKA phosphorylation on Ser16. A combination of biochemical techniques and FRET-based studies identified a novel macromolecular complex comprising PKA, Hsp20 and the scaffolding protein AKAP-Lbc, which facilitated Ser16 phosphorylation of Hsp20. AKAP-Lbc scaffolding of PKA was demonstrated to be vital for the anti-apoptotic actions of Hsp20 in the heart. This novel complex also includes members of the phosphodiesterase 4D subfamily. The AKAP-Lbc/PKA/Hsp20/PDE4D complex appears to play a key role in cardioprotection via the modulation of Hsp20 Ser16 phosphorylation, and selective targeting of these signaling elements in order to enhance this modification and promote cardioprotection could be of benefit in the treatment of pathological cardiac remodelling and ischaemic injury.

In this thesis, members of the PDE4 family were found to regulate the PKA phosphorylation of both Hsp20 and TnI. The development of PDE4 inhibitors would therefore seem to be an attractive option in the treatment of diseases where these phosphorylation events are known to be downregulated, such as heart failure. The PDE4 family has generated significant interest from pharmaceutical companies due to its involvement in a number of chronic disease states, particularly inflammatory diseases such as asthma and chronic obstructive pulmonary disease (COPD) (Houslay et al 2007). PDE4 provides the primary cAMP hydrolytic activity in inflammatory cells such as macrophages, eosinophils and neutrophils (Bielekova et al 2000, Spina 2008), and PDE4B has been shown to regulate the release of inflammatory cytokines from immune cells (Jin et al 2005). Increased intracellular cAMP levels suppress the production of pro-inflammatory cytokines, and induce anti-inflammatory cytokines in macrophages (Wall et

al 2009). Thus, there is considerable interest in inhibition of PDE4 as an anti-inflammatory strategy. PDE4B and PDE4D have also been linked with depression (Millar et al 2007, Zhang et al 2002), therefore PDE4 inhibitors would appear to have huge therapeutic potential. However, the development of these inhibitors has been plagued with difficulties, and there are few real success stories. The non-selective PDE inhibitor theophylline has been used for many years as a second line treatment for asthma, but has relatively low efficacy and causes a number of side-effects, including nausea, vomiting, diarrhoea and headaches. Theophylline has also been linked with the development of cardiac arrhythmias, and so patients also require careful plasma monitoring of drug levels, which is both expensive and time consuming (Spina 2008). PDE4 inhibitors such as rolipram have also undergone clinical trials for depression, but their licensing was prevented by the presence of similar side-effects, particularly emesis (Hebenstreit et al 1989). Second generation PDE4 inhibitors have now been developed which exhibit lesser side-effects, and one such inhibitor, Roflumilast (DAXAS®) was recently licensed in the UK for the treatment of severe exacerbations of COPD (Rabe 2010). It is clear that inhibition of PDE4 as a therapeutic strategy is problematic due to the number of cellular processes which involve this large enzyme family, and therefore a more specific strategy must be considered.

In Chapter 4, I made use of a peptide disruptor of the TnI-PDE4D9 complex to increase PKA phosphorylation of TnI in cells. Cell permeable peptides have previously been shown by us to disrupt the interaction between Hsp20 and PDE4 and protect against cardiac hypertrophy in cultured cardiac myocytes (Sin et al 2011). These peptides therefore have great therapeutic potential. Unlike other methods of inhibiting PDE4 in cells, such as gene silencing, which knocks down expression of a whole isoform, peptide disruptors displace one specific pool of a single PDE isoform within the cell, and allow more precise identification of protein function. From a pharmacological point of view, this targeted approach should also result in significantly fewer side-effects. It will be interesting to determine the effects of the TnI-PDE4D9 disruptor peptide in physiological assays of myocyte shortening, as it would be predicted to enhance cardiac contraction. It should also be noted that the studies detailed in this thesis were largely performed in rat tissue. The PDE4 complement does not differ significantly between rodent and humans, showing

similar expression levels and functions; however, human hearts exhibit higher non-PDE4 activity (Richter et al 2010), and therefore the effects of these peptides, and indeed the significance of the TnI-PDE4D9 interaction, may differ across species.

A major finding of the work detailed in this thesis is the association between Hsp20 and AKAP-Lbc. AKAP-Lbc is an intriguing protein which scaffolds PKA, PKC and PKD isoforms, and possesses intrinsic Rho-GEF activity. AKAP-Lbc is upregulated in hypertrophic cardiac myocytes, and it is thought that this enhances its activation of anchored PKD, and that augmented PKD signaling contributes to a fetal gene response and a hypertrophic cellular phenotype (Carnegie et al 2008). The Rho-GEF activity of AKAP-Lbc may also contribue to hypertrophy, as activated RhoA is a well known mediator of hypertrophic signaling(Diviani et al 2004). The finding that Hsp20, a cardioprotective protein with known anti-hypertrophic effects, directly interacts with AKAP-Lbc, could be highly significant. PKA phosphorylation of Hsp20 on Ser16 enhances its cardioprotective actions, and would protect against hypertrophy. It has previously been shown that the Rho-GEF activity of AKAP-Lbc is inhibited by phosphorylation of AKAP-Lbc by the same pool of PKA. Thus, factors which promote Hsp20 phosphorylation would also promote phosphorylation of AKAP-Lbc, resulting in dual actions against hypertrophy.

6.1 Final conclusion

The work presented in this thesis advances our understanding of how cAMP/PKA signals are regulated in the heart, both at the myofilament and in the cytosol. Novel interacting partners have been identified for the key cardiac proteins TnI and Hsp20. These interacting partners function to regulate PKA phosphorylation of TnI and Hsp20, and therefore have the potential to modulate cardiac contraction and cardioprotection. Selective disruption of interactions within macromolecular signaling complexes in the heart (and other organs) using cell permeable peptides or small molecule disruptors could provide a novel, targeted therapeutic strategy for the treatment of many diseases where cAMP signaling is dysregulated. Future studies should concentrate on defining the roles of such peptides within physiological systems, and identifying other interacting partners within these complexes, such as protein phosphatases.

7.

References

Adler J, Parmryd I. 2010. Quantifying Colocalization by Correlation:The Pearson Correlation Coefficient is Superior to the Mander's Overlap Coefficient. *Cytometry* 77A: 733-42

Ai X, Curran JW, Shannon TR, Bers DM, Pogwizd SM. 2005. Ca2+/calmodulin-dependent protein kinase modulates cardiac ryanodine receptor phosphorylation and sarcoplasmic reticulum Ca2+ leak in heart failure. *Circ Res* 97: 1314-22

Appert-Collin A, Cotecchia S, Nenninger-Tosato M, Pedrazzini T, Diviani D. 2007. The A-kinase anchoring protein (AKAP)-Lbc-signaling complex mediates alpha-1 adrenergic receptor-induced cardiomyocyte hypertrophy. *Proceedings of the National Academy of Sciences of the United States of America* 104: 10140-5

Aravind L, Ponting CP. 1997. The GAF domain: an evolutionary link between diverse phototransducing proteins. *Trends in Biochemical Sciences* 22: 458-9

Ariga M, Neitzert B, Nakae S, Mottin G, Bertrand C, et al. 2004. Nonredundant function of phosphodiesterases 4D and 4B in neutrophil recruitment to the site of inflammation. *Journal of Immunology* 173: 7531-8

Arshavsky VY, Lamb TD, Pugh EN. 2002. G proteins and phototransduction. *Annual Review of Physiology* 64: 153-87

Azzi A, Boscoboinik D, Hensey C. 1992. The protein kinase C family. *European Journal of Biochemistry* 208: 547-57

Baillie GS. 2009. Compartmentalized signalling: spatial regulation of cAMP by the action of compartmentalized phosphodiesterases. *Febs Journal* 276: 1790-9

Baillie GS, Houslay MD. 2005. Arrestin times for compartmentalised cAMP signalling and phosphodiesterase-4 enzymes. *Current Opinion in Cell Biology* 17: 129-34

Baillie GS, MacKenzie SJ, McPhee I, Houslay MD. 2000. Sub-family selective actions in the ability of Erk2 MAP kinase to phosphorylate and regulate the activity of PDE4 cyclic AMP-specific phosphodiesterases. *Br J Pharmacol* 131: 811-9

Baruscotti M, Barbuti A, Bucchi A. 2010. The cardiac pacemaker current. *Journal of Molecular and Cellular Cardiology* 48: 55-64

Beall A, Bagwell D, Woodrum D, Stoming TA, Kato K, et al. 1999. The small heat shock-related protein, HSP20, is phosphorylated on serine 16 during cyclic nucleotide-dependent relaxation. *Journal of Biological Chemistry* 274: 11344-51

Beavo JA. 1995. Cyclic nucleotide phosphodiesterases - Functional implications of multiple isoforms. *Physiological Reviews* 75: 725-48

Beavo JA, Brunton LL. 2002. Cyclic nucleotide research -- still expanding after half a century. *Nat Rev Mol Cell Biol* 3: 710-8

Bender AT, Beavo JA. 2006. Cyclic nucleotide phosphodiesterases: Molecular regulation to clinical use. *Pharmacological Reviews* 58: 488-520

Berridge MJ. 1984. Inositol trisphosphate and diacylglycerol as second messengers. *Biochem J* 220: 345-60

Bers DM. 2002. Cardiac excitation-contraction coupling. *Nature* 415: 198-205

Bers DM. 2004. Macromolecular complexes regulating cardiac ryanodine receptor function. *Journal of Molecular and Cellular Cardiology* 37: 417-29

Bers DM. 2012. Ryanodine receptor s2808 phosphorylation in heart failure: smoking gun or red herring. *Circ Res* 110: 796-9

Bers DM, Despa S. 2006. Cardiac myocytes Ca2+ and Na+ regulation in normal and failing hearts. *Journal of Pharmacological Sciences* 100: 315-22

Bielekova B, Lincoln A, McFarland H, Martin R. 2000. Therapeutic potential of phosphodiesterase-4 and -3 inhibitors in Th1-mediated autoimmune diseases. *J Immunol* 164: 1117-24

Biesiadecki BJ, Tachampa K, Yuan C, Jin J-P, de Tombe PP, Solaro RJ. 2010. Removal of the Cardiac Troponin I N-terminal Extension Improves Cardiac Function in Aged Mice. *Journal of Biological Chemistry* 285: 19688-98

Blackwood DHR, Fordyce A, Walker MT, St Clair DM, Porteous DJ, Muir WJ. 2001. Schizophrenia and affective disorders - Cosegregation with a translocation at chromosome 1q42 that directly disrupts brain-expressed genes: Clinical and P300 findings in a family. *American Journal of Human Genetics* 69: 428-33

Boerner S, Schwede F, Schlipp A, Berisha F, Calebiro D, et al. 2011. FRET measurements of intracellular cAMP concentrations and cAMP analog permeability in intact cells. *Nature Protocols* 6: 427-38

Boess FG, Hendrix M, van der Staay FJ, Erb C, Schreiber R, et al. 2004. Inhibition of phosphodiesterase 2 increases neuronal cGMP, synaptic plasticity and memory performance. *Neuropharmacology* 47: 1081-92

Bolger GB, Baillie GS, Li X, Lynch MJ, Herzyk P, et al. 2006. Scanning peptide array analyses identify overlapping binding sites for the signalling scaffold proteins, beta-arrestin and RACK1, in cAMP-specific phosphodiesterase PDE4D5. *Biochemical Journal* 398: 23-36

Bolger GB, McCahill A, Huston E, Cheung YF, McSorley T, et al. 2003. The unique amino-terminal region of the PDE4D5 cAMP phosphodiesterase isoform confers preferential interaction with beta-arrestins. *Journal of Biological Chemistry* 278: 49230-8

Boolell M, Allen MJ, Ballard SA, Gepi-Attee S, Muirhead GJ, et al. 1996. Sildenafil: an orally active type 5 cyclic GMP-specific phosphodiesterase inhibitor for the treatment of penile erectile dysfunction. *International journal of impotence research* 8: 47-52

Bos JL. 2003. Epac: a new cAMP target and new avenues in cAMP research. *Nature Reviews Molecular Cell Biology* 4: 733-8

Bradford MM. 1976. Rapid and sensitive method for quantitation of microgram quantities of protein utlizing principle of protein-dye binding *Analytical Biochemistry* 72: 248-54

Bristow MR, Ginsburg R, Minobe W, Cubicciotti RS, Sageman WS, et al. 1982. Decreased catecholamine sensitivity and beta-adrenergic-receptor density in failing human hearts. *N Engl J Med* 307: 205-11

Brophy CM, Dickinson M, Woodrum D. 1999a. Phosphorylation of the small heat shock-related protein, HSP20, in vascular smooth muscles is associated with changes in the macromolecular associations of HSP20. *Journal of Biological Chemistry* 274: 6324-9

Brophy CM, Lamb S, Graham A. 1999b. The small heat shock-related protein-20 is an actin-associated protein. *Journal of Vascular Surgery* 29: 326-33

Brophy CM, Woodrum DA, Pollock J, Dickinson M, Komalavilas P, et al. 2002. cGMP-dependent protein kinase expression restores contractile function in cultured vascular smooth muscle cells. *J Vasc Res* 39: 95-103

Brown JH, Del Re DP, Sussman MA. 2006. The Rac and Rho hall of fame: a decade of hypertrophic signaling hits. *Circ Res* 98: 730-42

Brunton LL, Hayes JS, Mayer SE. 1981. Functional compartmentation of cyclic-AMP and protein-kinase in heart *Advances in Cyclic Nucleotide Research* 14: 391-7

Buja LM. 2005. Myocardial ischemia and reperfusion injury. *Cardiovascular Pathology* 14: 170-5

Burgin AB, Magnusson OT, Singh J, Witte P, Staker BL, et al. 2010. Design of phosphodiesterase 4D (PDE4D) allosteric modulators for enhancing cognition with improved safety. *Nature Biotechnology* 28: 63-U93

Burkart EM, Sumandea MP, Kobayashi T, Nili M, Martin AF, et al. 2003. Phosphorylation or glutamic acid substitution at protein kinase C sites on cardiac troponin I differentially depress myofilament tension and shortening velocity. *J Biol Chem* 278: 11265-72

Buxton ILO, Brunton LL. 1983. Compartments of cyclic-AMP and protein-kinase in mammalian cardiomyocytes. *Journal of Biological Chemistry* 258: 233-9

Calebiro D, Nikolaev VO, Lohse MJ. 2010a. Imaging of persistent cAMP signaling by internalized G protein-coupled receptors. *J Mol Endocrinol* 45: 1-8

Calebiro D, Nikolaev VO, Persani L, Lohse MJ. 2010b. Signaling by internalized G-protein-coupled receptors. *Trends Pharmacol Sci* 31: 221-8

Calverley PMA, Rabe KF, Goehring U-M, Kristiansen S, Fabbri LM, Martinez FJ. 2009. Roflumilast in symptomatic chronic obstructive pulmonary disease: two randomised clinical trials. *Lancet* 374: 685-94

Carnegie GK, Smith FD, McConnachie G, Langeberg L, Scott JD. 2004. AKAP-Lbc Nucleates a Protein Kinase D Activation Scaffold. *Molecular Cell* 15: 889-99

Carnegie GK, Soughayer J, Smith FD, Pedroja BS, Zhang F, et al. 2008. AKAP-Lbc mobilizes a cardiac hypertrophy signaling pathway. *Molecular Cell* 32: 169-79

Carr DW, Hausken ZE, Fraser IDC, Stofkohahn RE, Scott JD. 1992. Association of the type-II cAMP-dependent protein-kinase with a human thyroid RII-anchoring protein - cloning and characterization of the RII binding domain. *Journal of Biological Chemistry* 267: 13376-82

Carr DW, Scott JD. 1992. Blotting and band-shifting: techniques for studying protein-protein interactions. *Trends Biochem Sci* 17: 246-9

Carr DW, Stofkohahn RE, Fraser IDC, Bishop SM, Acott TS, et al. 1991. Interaction of the regulatory subunit (RII) of cAMP-dependent protein-kinase with RII-anchoring proteins occurs through an amphipathic helix binding motif. *Journal of Biological Chemistry* 266: 14188-92

Cerione RA, Zheng Y. 1996. The Dbl family of oncogenes. *Current Opinion in Cell Biology* 8: 216-22

Chandrasekaran A, Toh KY, Low SH, Tay SKH, Brenner S, Goh DLM. 2008. Identification and characterization of novel mouse PDE4D isoforms: Molecular cloning, subcellular distribution and detection of isoform-specific intracellular localization signals. *Cellular Signalling* 20: 139-53

Chang ZF, Lee HH. 2006. RhoA signaling in phorbol ester-induced apoptosis. *J Biomed Sci* 13: 173-80

Chen L, Kass RS. 2011. A-Kinase Anchoring Protein 9 and I(Ks) Channel Regulation. *Journal of Cardiovascular Pharmacology* 58: 459-61

Chen L, Marquardt ML, Tester DJ, Sampson KJ, Ackerman MJ, Kass RS. 2007. Mutation of an A-kinase-anchoring protein causes long-QT syndrome. *Proceedings of the National Academy of Sciences of the United States of America* 104: 20990-5

Choi SY, Mintz GS. 2010. What have we learned about plaque rupture in acute coronary syndromes? *Current Cardiology Reports* 12: 338-43

Conti M, Beavo J. 2007. Biochemistry and physiology of cyclic nucleotide Phosphocliesterases: Essential components in cyclic nucleotide signaling. *Annual Review of Biochemistry* 76: 481-511

Cooper DMF, Crossthwaite AJ. 2006. Higher-order organization and regulation of adenylyl cyclases. *Trends in Pharmacological Sciences* 27: 426-31

Corbin JD, Sugden PH, Lincoln TM, Keely SL. 1977. Compartmentalization of adenosine 3'5'-monophosphate-dependent protein kinase in heart tissue. *Journal of Biological Chemistry* 252: 3854-61

Cote RH. 2004. Characteristics of Photoreceptor PDE (PDE6): similarities and differences to PDE5. *International journal of impotence research* 16: S28-S33

Danial NN, Gramm CF, Scorrano L, Zhang CY, Krauss S, et al. 2003. BAD and glucokinase reside in a mitochondrial complex that integrates glycolysis and apoptosis. *Nature* 424: 952-6

Davi G, Patrono C. 2007. Platelet activation and atherothrombosis. *New England Journal of Medicine* 357: 2482-94

De Arcangelis V, Liu R, Soto D, Xiang Y. 2009. Differential Association of Phosphodiesterase 4D Isoforms with beta(2)-Adrenoceptor in Cardiac Myocytes. *Journal of Biological Chemistry* 284: 33824-32

de Rooij J, Rehmann H, van Triest M, Cool RH, Wittinghofer A, Bos JL. 2000. Mechanism of regulation of the Epac family of cAMP-dependent RapGEFs. *Journal of Biological Chemistry* 275: 20829-36

de Rooij J, Zwartkruis FJT, Verheijen MHG, Cool RH, Nijman SMB, et al. 1998. Epac is a Rap1 guanine-nucleotide-exchange factor directly activated by cyclic AMP. *Nature* 396: 474-7

Delghandi MP, Johannessen M, Moens U. 2005. The cAMP signalling pathway activates CREB through PKA, p38 and MSK1 in NIH 3T3 cells. *Cellular Signalling* 17: 1343-51

Dessauer CW. 2009. Adenylyl Cyclase-A-kinase Anchoring Protein Complexes: The Next Dimension in cAMP Signaling. *Molecular Pharmacology* 76: 935-41

Di Benedetto G, Zoccarato A, Lissandron V, Terrin A, Li X, et al. 2008. Protein kinase a type I and type II define distinct intracellular signaling compartments. *Circulation Research* 103: 836-44

Diviani D, Abuin L, Cotecchia S, Pansier L. 2004. Anchoring of both PKA and 14-3-3 inhibits the Rho-GEF activity of the AKAP-Lbc signaling complex. *EMBO J* 23: 2811-20

Diviani D, Soderling J, Scott JD. 2001. AKAP-Lbc anchors protein kinase A and nucleates G alpha(12)-selective Rho-mediated stress fiber formation. *Journal of Biological Chemistry* 276: 44247-57

Dodge-Kafka KL, Bauman A, Mayer N, Henson E, Heredia L, et al. 2010. cAMP-stimulated Protein Phosphatase 2A Activity Associated with Muscle A Kinase-anchoring Protein (mAKAP) Signaling Complexes Inhibits the Phosphorylation and Activity of the cAMP-specific Phosphodiesterase PDE4D3. *Journal of Biological Chemistry* 285: 11078-86

Dodge-Kafka KL, Kapiloff MS. 2006. The mAKAP signaling complex: Integration of cAMP, calcium, and MAP kinase signaling pathways. *European Journal of Cell Biology* 85: 593-602

Dodge-Kafka KL, Soughayer J, Pare GC, Michel JJC, Langeberg LK, et al. 2005. The protein kinase A anchoring protein mAKAP coordinates two integrated cAMP effector pathways. *Nature* 437: 574-8

Dodge K, Scott JD. 2000. AKAP79 and the evolution of the AKAP model. *Febs Letters* 476: 58-61

Dodge KL, Khouangsathiene S, Kapiloff MS, Mouton R, Hill EV, et al. 2001. mAKAP assembles a protein kinase A/PDE4 phosphodiesterase cAMP signaling module. *Embo Journal* 20: 1921-30

Dreiza CM, Brophy CM, Komalavilas P, Furnish EJ, Joshi L, et al. 2005. Transducible heat shock protein 20(HSP20) phosphopeptide alters cytoskeletal dynamics. *Faseb Journal* 19: 261-3

Dreiza CM, Komalavilas P, Furnish EJ, Flynn CR, Sheller MR, et al. 2010. The small heat shock protein, HSPB6, in muscle function and disease. *Cell Stress & Chaperones* 15: 1-11

Engel AC, Franzini-Armstrong C, Craig RW, Padron R. 2004. Molecular Structure of the Sarcomere. *Myology* 3rd edition: 129-66

Enserink JM, Christensen AE, de Rooij J, van Triest M, Schwede F, et al. 2002. A novel Epac-specific cAMP analogue demonstrates independent regulation of Rap1 and ERK. *Nature Cell Biology* 4: 901-6

Erneux C, Couchie D, Dumont JE, Baraniak J, Stec WJ, et al. 1981. Specificity of cyclic-GMP activation of a multi-substrate cyclic-nucleotide phosphodiesterase from rat liver. *European Journal of Biochemistry* 115: 503-10

F'Entzke RC, Buck SH, Patel JR, Lin H, Wolska BM, et al. 1999. Impaired cardiomyocyte relaxation and diastolic function in transgenic mice expressing slow skeletal troponin I in the heart. *Journal of Physiology-London* 517: 143-57

Fabbri LM, Calverley PMA, Luis Izquierdo-Alonso J, Bundschuh DS, Brose M, et al. 2009. Roflumilast in moderate-to-severe chronic obstructive pulmonary disease treated with longacting bronchodilators: two randomised clinical trials. *Lancet* 374: 695-703

Fan GC, Chu GX, Kranias EG. 2005a. Hsp20 and its cardioprotection. *Trends in Cardiovascular Medicine* 15: 138-41

Fan GC, Chu GX, Mitton B, Song QJ, Yuan QY, Kranias EG. 2004a. Small heat-shock protein Hsp20 phosphorylation inhibits beta-agonist-induced cardiac apoptosis. *Circulation Research* 94: 1474-82

Fan GC, Chu GX, Song QJ, Kranias EG. 2003. Phosphorylation of cardiac HSP20 increases contractility and protects myocytes from beta-agonist-induced apoptosis. *Circulation* 108: 541

Fan GC, Kranias EG. 2010. Small heat shock protein 20 (HspB6) in cardiac hypertrophy and failure. *Journal of Molecular and Cellular Cardiology* Article in press, corrected proof

Fan GC, Ren XP, Qian J, Yuan QY, Nicolaou P, et al. 2005b. Novel cardioprotective role of a small heat-shock protein, Hsp20, against ischemia/reperfusion injury. *Circulation* 111: 1792-9

Fan GC, Ren XP, Qian J, Yuan QY, Wang Y, et al. 2004b. Cardiac-specific overexpression of small heat-shock protein Hsp20 alleviates ischemia/reperfusion injury and myocardial dysfunction. *Circulation* 110: 1439

Fan GC, Yuan QY, Song GJ, Wang YG, Chen GL, et al. 2006. Small heat-shock protein Hsp20 attenuates beta-agonist-mediated cardiac remodeling through apoptosis signal-regulating kinase 1. *Circulation Research* 99: 1233-42

Fawcett L, Baxendale R, Stacey P, McGrouther C, Harrow I, et al. 2000. Molecular cloning and characterization of a distinct human phosphodiesterase gene family: PDE11A. *Proceedings of the National Academy of Sciences of the United States of America* 97: 3702-7

Fink MA, Zakhary DR, Mackey JA, Desnoyer RW, Apperson-Hansen C, et al. 2001. AKAP-mediated targeting of protein kinase a regulates contractility in cardiac myocytes. *Circ Res* 88: 291-7

Fischmeister R, Castro LRV, Abi-Gerges A, Rochais F, Jurevicius J, et al. 2006. Compartmentation of cyclic nucleotide signaling in the heart - The role of cyclic nucleotide phosphodiesterases. *Circulation Research* 99: 816-28

Fisher DA, Smith JF, Pillar JS, St Denis SH, Cheng JB. 1998. Isolation and characterization of PDE8A, a novel human cAMP-specific phosphodiesterase. *Biochemical and Biophysical Research Communications* 246: 570-7

Flynn CR, Komalavilas P, Tessier D, Thresher J, Niederkofler EE, et al. 2003. Transduction of biologically active motifs of the small heat shock-related protein, HSP20, leads to relaxation of vascular smooth muscle. *Faseb Journal* 17: 1358-60

Förster T. 1948. Intermolecular energy migration and fluorescence. *Annals of Physics* 2: 55-7

Francis SH. 2005. Phosphodiesterase 11 (PDE11): is it a player in human testicular function? *International journal of impotence research* 17: 467-8

Francis SH, Turko IV, Corbin JD. 2001. Cyclic nucleotide phosphodiesterases: Relating structure and function. *Progress in Nucleic Acid Research and Molecular Biology, Vol 65* 65: 1-52

Frank R. 2002. The SPOT-synthesis technique: Synthetic peptide arrays on membrane supports- principles and applications. *Journal of Immunological Methods* 267: 13-26

Fraser ID, Scott JD. 1999. Modulation of ion channels: a "current" view of AKAPs. *Neuron* 23: 423-6

Fujishige K, Kotera J, Michibata H, Yuasa K, Takebayashi S, et al. 1999. Cloning and characterization of a novel human phosphodiesterase that hydrolyzes both cAMP and cGMP (PDE10A). *Journal of Biological Chemistry* 274: 18438-45

Fukao M, Mason HS, Britton FC, Kenyon JL, Horowitz B, Keef KD. 1999. Cyclic GMP-dependent protein kinase activates cloned BKCa channels expressed in mammalian cells by direct phosphorylation at serine 1072. *Journal of Biological Chemistry* 274: 10927-35

Futaki S, Ohashi W, Suzuki T, Niwa M, Tanaka S, et al. 2001. Stearylated arginine-rich peptides: a new class of transfection systems. *Bioconjug Chem* 12: 1005-11

Galinska-Rakoczy A, Engel P, Xu C, Jung H, Craig R, et al. 2008. Structural basis for the regulation of muscle contraction by troponin and tropomyosin. *Journal of Molecular Biology* 379: 929-35

Galinska A, Hatch V, Craig R, Murphy AM, Van Eyk JE, et al. 2010. The C Terminus of Cardiac Troponin I Stabilizes the Ca(2+)-Activated State of Tropomyosin on Actin Filaments. *Circulation Research* 106: 705-U148

Gao TY, Yatani A, DellAcqua ML, Sako H, Green SA, et al. 1997. CAMP-dependent regulation of cardiac L-type Ca2+ channels requires membrane targeting of PKA and phosphorylation of channel subunits. *Neuron* 19: 185-96

Geiss-Friedlander R, Melchior F. 2007. Concepts in sumoylation: a decade on. *Nature Reviews Molecular Cell Biology* 8: 947-56

Geoffroy V, Fouque F, Lugnier C, Desbuquois B, Benelli C. 2001. Characterization of an in vivo hormonally regulated phosphodiesterase 3 (PDE3) associated with a liver Golgi-endosomal fraction. *Archives of Biochemistry and Biophysics* 387: 154-62

Gillespie PG, Beavo JA. 1988. Characterization of a bovine cone photoreceptor phosphodiesterase purified by cyclic GMP-sepharose chromatography. *Journal of Biological Chemistry* 263: 8133-41

Giordano D, De Stefano ME, Citro G, Modica A, Giorgi M. 2001. Expression of cGMP-binding cGMP-specific phosphodiesterase (PDE5) in mouse tissues and cell lines using an antibody against the enzyme amino-terminal domain. *Biochimica Et Biophysica Acta-Molecular Cell Research* 1539: 16-27

Golenhofen N, Perng MD, Quinlan RA, Drenckhahn D. 2004. Comparison of the small heat shock proteins alpha B-crystallin, MKBP, HSP25, HSP20, and cvHSP in heart and skeletal muscle. *Histochemistry and Cell Biology* 122: 415-25

Gretarsdottir S, Thorleifsson G, Reynisdottir ST, Manolescu A, Jonsdottir S, et al. 2003. The gene encoding phosphodiesterase 4D confers risk of ischemic stroke. *Nature Genetics* 35: 131-8

Guipponi M, Scott HS, Kudoh J, Kawasaki K, Shibuya K, et al. 1998. Identification and characterization of a novel cyclic nucleotide phosphodiesterase gene (PDE9A) that maps to 21q22.3: alternative splicing of mRNA transcripts, genomic structure and sequence. *Human Genetics* 103: 386-92

Gustaffson AB, Gottlieb R. 2009. Autophagy in ischemic heart disease. *Circulation Research* 104: 150-8

Hage T, Langen B, Hoefgen N, Stange H, Egerland U, et al. 2009. PDE10A inhibitors show anti-psychotic, pro-cognitive and negative symptom activities suggesting a broad-spectrum utility for the treatment of schizophrenia. *Society for Neuroscience Abstract Viewer and Itinerary Planner* 39

Hagiwara M, Endo T, Hidaka H. 1984. Effects of vinpocetine on cyclic-nucleotide metabolism in vascular smooth muscle. *Biochemical Pharmacology* 33: 453-7

Hanoune J, Defer N. 2001. Regulation and role of adenylyl cyclase isoforms. *Annual Review of Pharmacology and Toxicology* 41: 145-74

Hayashi M, Matsushima K, Ohashi H, Tsunoda H, Murase S, et al. 1998. Molecular cloning and characterization of human PDE8B, a novel thyroid-specific isozyme of 3 ',5 '-cyclic nucleotide phosphodiesterase. *Biochemical and Biophysical Research Communications* 250: 751-6

Hebenstreit GF, Fellerer K, Fichte K, Fischer G, Geyer N, et al. 1989. Rolipram in major depressive disorder: results of a double-blind comparative study with imipramine. *Pharmacopsychiatry* 22: 156-60

Heineke J, Molkentin JD. 2006. Regulation of cardiac hypertrophy by intracellular signalling pathways. *Nature Reviews Molecular Cell Biology* 7: 589-600

Herberg FW, Maleszka A, Eide T, Vossebein L, Tasken K. 2000. Analysis of A-kinase anchoring protein (AKAP) interaction with protein kinase A (PKA) regulatory subunits: PKA isoform specificity in AKAP binding. *Journal of Molecular Biology* 298: 329-39

Herget S, Lohse MJ, Nikolaev VO. 2008. Real-time monitoring of phosphodiesterase inhibition in intact cells. *Cellular Signalling* 20: 1423-31

Hernandez OM, Housmans PR, Potter JD. 2001. Invited Review: pathophysiology of cardiac muscle contraction and relaxation as a result of alterations in thin filament regulation. *J Appl Physiol* 90: 1125-36

Hetman JM, Soderling SH, Glavas NA, Beavo JA. 2000. Cloning and characterization of PDE7B, a cAMP-specific phosphodiesterase. *Proceedings of the National Academy of Sciences of the United States of America* 97: 472-6

Heusch G, Boengler K, Schulz R. 2008. Cardioprotection: nitric oxide, protein kinases, and mitochondria. *Circulation* 118: 1915-9

Ho YSJ, Burden LM, Hurley JH. 2000. Structure of the GAF domain, a ubiquitous signaling motif and a new class of cyclic GMP receptor. *Embo Journal* 19: 5288-99

Hochbaum D, Barila G, Ribeiro-Neto F, Altschuler DL. 2010. Radixin assembles cAMP effectors Epac and PKA into a functional cAMP compartment: role in cAMP-dependent cell proliferation. *J Biol Chem* 286: 859-66

Hoffmann R, Baillie GS, MacKenzie SJ, Yarwood SJ, Houslay MD. 1999. The MAP kinase ERK2 inhibits the cyclic AMP-specific phosphodiesterase HSPDE4D3 by phosphorylating it at Ser579. *Embo Journal* 18: 893-903

Hollmann MW, Strumper D, Herroeder S, Durieux ME. 2005. Receptors, G proteins, and their interactions. *Anesthesiology* 103: 1066-78

Houslay MD. 2010. Underpinning compartmentalised cAMP signalling through targeted cAMP breakdown. *Trends in Biochemical Sciences* 35: 91-100

Houslay MD, Adams DR. 2003. PDE4 cAMP phosphodiesterases: modular enzymes that orchestrate signalling cross-talk, desensitization and compartmentalization. *Biochemical Journal* 370: 1-18

Houslay MD, Adams DR. 2010. Putting the lid on phosphodiesterase 4. *Nature Biotechnology* 28: 38-40

Houslay MD, Baillie GS. 2006. Phosphodiesterase-4 gates the ability of protein kinase A to phosphorylate G-protein receptor kinase-2 and influence its translocation. *Biochem Soc Trans* 34: 474-5

Houslay MD, Baillie GS, Maurice DH. 2007. cAMP-specific phosphodiesterase-4 enzymes in the cardiovascular system - A molecular toolbox for generating compartmentalized cAMP signaling. *Circulation Research* 100: 950-66

Howarth JW, Meller J, Solaro RJ, Trewhella J, Rosevear PR. 2007. Phosphorylation-dependent conformational transition of the cardiac specific N-extension of troponin I in cardiac troponin. *Journal of Molecular Biology* 373: 706-22

Huai Q, Liu YD, Francis SH, Corbin JD, Ke HM. 2004. Crystal structures of phosphodiesterases 4 and 5 in complex with inhibitor 3-isobutyl-1-methylxanthine suggest a conformation determinant of inhibitor selectivity. *Journal of Biological Chemistry* 279: 13095-101

Hubbard MJ, Cohen P. 1993. On target with a new mechanism for the regulation of protein phosphorylation. *Trends in Biochemical Sciences* 18: 172-7

Huke S, Bers DM. 2008. Ryanodine receptor phosphorylation at Serine 2030, 2808 and 2814 in rat cardiomyocytes. *Biochemical and Biophysical Research Communications* 376: 80-5

Ji TH, Grossmann M, Ji I. 1998. G protein-coupled receptors. I. Diversity of receptor-ligand interactions. *J Biol Chem* 273: 17299-302

Jin SLC, Lan L, Zoudilova M, Conti M. 2005. Specific role of phosphodiesterase 4B in lipopolysaccharide-induced signaling in mouse macrophages. *Journal of Immunology* 175: 1523-31

Kadoshima-Yamaoka K, Murakawa M, Goto M, Tanaka Y, Inoue H, et al. 2009. Effect of phosphodiesterase 7 inhibitor ASB16165 on development and function of cytotoxic T lymphocyte. *International Immunopharmacology* 9: 97-102

Kapiloff MS, Chandrasekhar KD. 2011. A-kinase Anchoring Proteins:Temporal and Spatial Regulation of Intracellular Signal Transduction in the Cardiovascular System. *Journal of Cardiovascular Pharmacology* 58: 337-8

Kapiloff MS, Piggott LA, Sadana R, Li JL, Heredia LA, et al. 2009. An Adenylyl Cyclase-mAKAP beta Signaling Complex Regulates cAMP Levels in Cardiac Myocytes. *Journal of Biological Chemistry* 284: 23540-6

Kapiloff MS, Schillace RV, Westphal AM, Scott JD. 1999. mAKAP: an A-kinase anchoring protein targeted to the nuclear membrane of differentiated myocytes. *Journal of Cell Science* 112: 2725-36

Kappe G, Franck E, Verschuure P, Boelens WC, Leunissen JAM, De Jong WW. 2003. The human genome encodes 10 α-crystallin–related small heat shock proteins: HspB1–10. *Cell Stress & Chaperones* 8: 53-61

Kaupp UB, Seifert R. 2002. Cyclic Nucleotide-Gated Ion Channels. *Physiological Reviews* 82: 769-824

Kawasaki H, Springett GM, Mochizuki N, Toki S, Nakaya M, et al. 1998. A family of cAMP-binding proteins that directly activate Rap1. *Science* 282: 2275-9

Kemp BE, Graves DJ, Benjamini E, Krebs EG. 1977. Role of multiple basic residues in determining substrate specificity of cyclic AMP-dependent protein kinase. *Journal of Biological Chemistry* 252: 4888-94

Kho C, Lee A, Jeong D, Oh JG, Chaanine AH, et al. 2011. SUMO1-dependent modulation of SERCA2a in heart failure. *Nature* 477: 601-5

Kilpinen S, Autio R, Ojala K, Iljin K, Bucher E, et al. 2008. Systematic bioinformatic analysis of expression levels of 17,330 human genes across 9,783 samples from 175 types of healthy and pathological tissues. *Genome Biology* 9

Kirchhoff SR, Gupta S, Knowlton AA. 2002. Cytosolic heat shock protein 60, apoptosis, and myocardial injury. *Circulation* 105: 2899-904

Kohout TA, Lefkowitz RJ. 2003. Regulation of g protein-coupled receptor kinases and arrestins during receptor desensitization. *Molecular Pharmacology* 63: 9-18

Kolch W. 2005. Coordinating ERK/MAPK signalling through scaffolds and inhibitors. *Nature Reviews Molecular Cell Biology* 6: 827-37

Kotera J, Fujishige K, Imai Y, Kawai E, Michibata H, et al. 1999. Genomic origin and transcriptional regulation of two variants of cGMP-binding cGMP-specific phosphodiesterases. *European Journal of Biochemistry* 262: 866-72

Kotera J, Sasaki T, Kobayashi T, Fujishige K, Yamashita Y, Omori K. 2004. Subcellular localization of cyclic nucleotide phosphodiesterase type 10A variants, and alteration of the localization by cAMP-dependent protein kinase-dependent phosphorylation. *Journal of Biological Chemistry* 279: 4366-75

Kozawa O, Matsuno H, Niwa M, Hatakeyama D, Oiso Y, et al. 2002. HSP20, low-molecular-weight heat shock-related protein, acts extracellularly as a regulator of platelet functions: a novel defense mechanism. *Life Sciences* 72: 113-24

Laddha SS, Bhatnagar SP. 2009. A new therapeutic approach in Parkinson's disease: Some novel quinazoline derivatives as dual selective phosphodiesterase 1 inhibitors and anti-inflammatory agents. *Bioorganic & Medicinal Chemistry* 17: 6796-802

Layland J, Solaro RJ, Shah AM. 2005. Regulation of cardiac contractile function by troponin I phosphorylation. *Cardiovascular Research* 66: 12-21

Lehnart SE, Wehrens XHT, Reiken S, Warrier S, Belevych AE, et al. 2005. Phosphodiesterase 4D deficiency in the ryanodine-receptor complex promotes heart failure and arrhythmias. *Cell* 123: 25-35

Leroy J, Richter W, Mika D, Castro LRV, Abi-Gerges A, et al. 2011. Phosphodiesterase 4B in the cardiac L-type Ca(2+) channel complex regulates Ca(2+) current and protects against ventricular arrhythmias in mice. *Journal of Clinical Investigation* 121: 2651-61

Lissandron V, Rossetto MG, Erbquth K, Fiala A, Daga A, Zaccolo M. 2007. Transgenic fruit flies expressing a FRET-based sensor for in vivo imging of cAMP dynamics. *Cellular Signalling* 19: 2296-303

Lissandron V, Zaccolo M. 2006. Compartmentalized cAMP/PKA signalling regulates cardiac excitation-contraction coupling. *Journal of Muscle Research and Cell Motility* 27: 399-403

Lohmann SM, Decamilli P, Einig I, Walter U. 1984. High-affinity binding of the regulatory subunit (RII) of cAMP-dependent protein kinase to microtubule-associated and other cellular proteins. *Proceedings of the National Academy of Sciences of the United States of America-Biological Sciences* 81: 6723-7

Luu JK, Chappelow AV, McCulley TJ, Marmor MF. 2001. Acute effects of sildenafil on the electroretinogram and multifocal electroretinogram. *American Journal of Ophthalmology* 132: 388-94

Lygren B, Carlson CR, Santamaria K, Lissandron V, McSorley T, et al. 2007. AKAP complex regulates Ca2+ re-uptake into heart sarcoplasmic reticulum. *Embo Reports* 8: 1061-7

Lynch MJ, Baillie GS, Houslay MD. 2007. cAMP-specific phosphodiesterase-4D5 (PDE4D5) provides a paradigm for understanding the unique non-redundant roles that PDE4 isoforms play in shaping compartmentalized cAMP cell signalling. *Biochemical Society Transactions* 35: 938-41

Lynch MJ, Hill EV, Houslay MD. 2006. Intracellular targeting of phosphodiesterase-4 underpins compartmentalized cAMP signaling. *Current Topics in Developmental Biology, Vol 75* 75: 225-59

Lynex CN, Li Z, Chen ML, Toh KY, Low RWC, et al. 2008. Identification and molecular characterization of a novel PDE4D11 cAMP-specific phosphodiesterase isoform. *Cellular Signalling* 20: 2247-55

Maass AH, Buvoli M. 2007. Cardiomyocyte Preparation, Culture and Gene Transfer. *Methods in Molecular Biology* 366: 321-30

MacKenzie SJ, Baillie GS, McPhee I, Bolger GB, Houslay MD. 2000. ERK2 mitogen-activated protein kinase binding, phosphorylation, and regulation of the PDE4D cAMP-specific phosphodiesterases - The involvement of COOH-terminal docking sites and NH2-terminal UCR regions. *Journal of Biological Chemistry* 275: 16609-17

MacKenzie SJ, Baillie GS, McPhee I, MacKenzie C, Seamons R, et al. 2002. Long PDE4 cAMP specific phosphodiesterases are activated by protein kinase A-mediated

phosphorylation of a single serine residue in Upstream Conserved Region 1 (UCR1). *British Journal of Pharmacology* 136: 421-33

MacLennan DH, Kranias EG. 2003. Phospholamban: A crucial regulator of cardiac contractility. *Nature Reviews Molecular Cell Biology* 4: 566-77

Malamas M, Ni Y, Erdei J, Fan K, Hoefgen N, et al. 2011a. Benzo[e]imidazo[5,1-c][1,2,4]triazines as selective PDE10A inhibitors for the treatment of schizophrenia. *Abstracts of Papers of the American Chemical Society* 241

Malamas M, Ni Y, Erdei J, Fan K, Hoefgen N, et al. 2011b. Imidazo[1,5-a]quinoxalines as selective PDE10A inhibitors for the treatment of schizophrenia. *Abstracts of Papers of the American Chemical Society* 241

Manganiello VC, Degerman E. 1999. Cyclic nucleotide phosphodiesterases: Diverse regulators of cyclic nucleotide signals and inviting molecular targets for novel therapeutic agents. *Thrombosis and Haemostasis* 82: 407-11

Manganiello VC, Taira M, Degerman E, Belfrage P. 1995. Type III cGMP-inhibited cyclic nucleotide phosphodiesterases (PDE3 gene family). *Cellular Signalling* 7: 445-55

Mao YW, Liu JP, Xiang H, Li DWC. 2004. Human aA- and aB-crystallins bind to Bax and Bcl-XS to sequester their translocation during staurosporine induced apoptosis

Y-W Mao1,4, J-P Liu2, H Xiang1,5 and D W-C Li*,. *Cell death and differentiation* 11: 512-26

Marchmont RJ, Houslay MD. 1980. A peripheral and an intrinsic enzyme constitute the cyclic AMP phosphodiesterase activity of rat liver plasma membranes. *Biochem J* 187: 381-92

Martinez SE, Wu AY, Glavas NA, Tang XB, Turley S, et al. 2002. The two GAF domains in phosphodiesterase 2A have distinct roles in dimerization and in cGMP binding. *Proceedings of the National Academy of Sciences of the United States of America* 99: 13260-5

Marx SO, Kurokawa J, Reiken S, Motoike H, D'Armiento J, et al. 2002. Requirement of a macromolecular signaling complex for beta adrenergic receptor modulation of the KCNQ1-KCNE1 potassium channel. *Science* 295: 496-9

Marx SO, Reiken S, Hisamatsu Y, Jayaraman T, Burkhoff D, et al. 2000. PKA phosphorylation dissociates FKBP12.6 from the calcium release channel (ryanodine receptor): Defective regulation in failing hearts. *Cell* 101: 365-76

Matsuno H, Ishisaki A, Nakajima K, Kato K, Kozawa O. 2003. A peptide isolated from alpha B-crystallin is a novel and potent inhibitor of platelet aggregation via dual prevention of PAR-1 and GPIb/V/IX. *Journal of Thrombosis and Haemostasis* 1: 2636-42

Mayers CM, Wadell J, McLean K, Venere M, Malik M, et al. 2010. Rho Guanine Nucleotide Exchange Factor AKAP13 (BRX) Is Essential for Cardiac Development in Mice. *Journal of Biological Chemistry* 285: 12344-54

McAllister-Lucas LM, Haik TL, Colbran JL, Sonnenburg WK, Seger D, et al. 1995. An essential aspartic acid at each of two allosteric cGMP-binding sites of a cGMP-specific phosphodiesterase. *Journal of Biological Chemistry* 270: 30671-9

McLemore E, Tessier D, Flynn CR, Furnish E, Komalavilas P, et al. 2004. Transducible recombinant small heat shock-related protein, HSP20, inhibits vasospasm and platelet aggregation

Surgery 136: 573-8

McLemore EC, Tessier DJ, Thresher J, Komalavilas P, Brophy CM. 2005. Role of the small heat shock proteins in regulating vascular smooth muscle tone. *Journal of the American College of Surgeons* 201: 30-6

Means CK, Lygren B, Langeberg LK, Jain A, Dixon RE, et al. 2011. An entirely specific type I A-kinase anchoring protein that can sequester two molecules of protein kinase A at the mitochondria. *Proceedings of the National Academy of Sciences of the United States of America* doi: 10.1073/pnas.1107182108

Meng D, Lynch MJ, Huston E, Beyermann M, Eichhorst J, et al. 2009. MEK1 binds directly to betaarrestin1, influencing both its phosphorylation by ERK and the timing of its isoprenaline-stimulated internalization. *J Biol Chem* 284: 11425-35

Michie AM, Lobban M, Muller T, Harnett MM, Houslay MD. 1996. Rapid regulation of PDE-2 and PDE-4 cyclic AMP phosphodiesterase activity following ligation of the T cell antigen receptor on thymocytes: Analysis using the selective inhibitors erythro-9-(2-hydroxy-3-nonyl)-adenine (EHNA) and rolipram. *Cellular Signalling* 8: 97-110

Millar JK, Mackie S, Clapcote SJ, Murdoch H, Pickard BS, et al. 2007. Disrupted in schizophrenia 1 and phosphodiesterase 413: towards an understanding of psychiatric illness. *Journal of Physiology-London* 584: 401-5

Millar JK, Pickard BS, Mackie S, James R, Christie S, et al. 2005. DISC1 and PDE4B are interacting genetic factors in schizophrenia that regulate cAMP signaling. *Science* 310: 1187-91

Mongillo M, McSorley T, Evellin S, Sood A, Lissandron V, et al. 2004. Fluorescence resonance energy transfer-based analysis of cAMP dynamics in live neonatal rat cardiac myocytes reveals distinct functions of compartmentalized phosphodiesterases. *Circulation Research* 95: 67-75

Morimoto RI. 1993. Cells in Stress: Transcriptional Activation of Heat Shock Genes. *Science* 259: 1409-10

Mou HM, Cote RH. 2001. The catalytic and GAF domains of the rod cGMP phosphodiesterase (PDE6) heterodimer are regulated by distinct regions of its inhibitory gamma subunit. *Journal of Biological Chemistry* 276: 27527-34

Mou HM, Grazio HJ, Cook TA, Beavo JA, Cote RH. 1999. cGMP binding to noncatalytic sites on mammalian rod photoreceptor phosphodiesterase is regulated by binding of its gamma and delta subunits. *Journal of Biological Chemistry* 274: 18813-20

Mudd JO, Kass DA. 2008. Tackling heart failure in the twenty-first century. *Nature* 451: 919-28

Murphy E, Steenburgen C. 2008. Mechanisms Underlying Acute Protection From Cardiac Ischemia-Reperfusion Injury. *Physiological Reviews* 88: 581-609

Murray AJ. 2008. Pharmacological PKA Inhibition: All May Not Be What It Seems. *Science Signaling* 1: 1-6

Newlon MG, Roy M, Morikis D, Hausken ZE, Coghlan V, et al. 1999. The molecular basis for protein kinase A anchoring revealed by solution NMR. *Nature Structural Biology* 6: 222-7

Nicolaou P, Knoll R, Haghighi K, Fan GC, Dorn GW, et al. 2008. Human Mutation in the Anti-apoptotic Heat Shock Protein 20 Abrogates Its Cardioprotective Effects. *Journal of Biological Chemistry* 283: 33465-71

Nikolaev VO, Bunemann M, Hein L, Hannawacker A, Lohse MJ. 2004. Novel single chain cAMP sensors for receptor-induced signal propagation. *Journal of Biological Chemistry* 279: 37215-8

Nikolaev VO, Lohse MJ. 2006. Monitoring of cAMP synthesis and degradation in living cells. *Physiology* 21: 86-92

Niwa M, Kozawa O, Matsuno H, Kato K, Uematsu T. 2000. Small molecular weight heat shock-related protein, HSP20, exhibits an anti-platelet activity by inhibiting receptor-mediated calcium influx. *Life Sciences* 66: PL7-PL12

Noland TA, Jr., Guo X, Raynor RL, Jideama NM, Averyhart-Fullard V, et al. 1995. Cardiac troponin I mutants. Phosphorylation by protein kinases C and A and regulation of Ca(2+)-stimulated MgATPase of reconstituted actomyosin S-1. *J Biol Chem* 270: 25445-54

Nomura-Furuwatari C, Wakitani S, Hashimoto Y, Imai Y, Ohta Y, et al. 2008. Expression profiles of phosphodiesterase 4D splicing variants in osteoblastic cells. *J Bone Miner Metab* 26: 152-8

O'Donnell JM, Zhang HT. 2004. Antidepressant effects of inhibitors of cAMP phosphodiesterase (PDE4). *Trends Pharmacol Sci* 25: 158-63

Ouyang M, Zhang L, Zhu JJ, Schwede F, Thomas SA. 2008. Epac signaling is required for hippocampus-dependent memory retrieval. *Proceedings of the National Academy of Sciences of the United States of America* 105: 11993-7

Padma-Nathan H, McMurray JG, Pullman WE, Whitaker JS, Saoud JB, et al. 2001. On-demand IC351 (Cialis (TM)) enhances erectile function in patients with erectile dysfunction. *International journal of impotence research* 13: 2-9

Pages L, Gavalda A, Lehner MD. 2009. PDE4 inhibitors: a review of current developments (2005-2009). *Expert Opinion on Therapeutic Patents* 19: 1501-19

Pare GC, Bauman AL, McHenry M, Carlisle Michel JJ, Dodge-Kafka KL, Kapiloff MS. 2005. The mAKAP complex participates in the induction of cardiac myocyte hypertrophy by adrenergic receptor signaling. *Journal of Cell Science* 118: 5637-46

Patrizio M, Vago V, Musumeci M, Fecchi K, Sposi NM, et al. 2008. cAMP-mediated beta-adrenergic signaling negatively regulates Gq-coupled receptor-mediated fetal gene response in cardiomyocytes. *Journal of Molecular and Cellular Cardiology* 45: 761-9

Patrucco E, Albergine MS, Santana LF, Beavo JA. 2010. Phosphodiesterase 8A (PDE8A) regulates excitation-contraction coupling in ventricular myocytes. *Journal of Molecular and Cellular Cardiology* 49: 330-3

Pearl LH, Prodromou C. 2006. Structure and mechanism of the Hsp90 molecular chaperone machinery. In *Annual Review of Biochemistry*, pp. 271-94

Perez-Torres S, Cortes R, Tolnay M, Probst A, Palacios JM, Mengod G. 2003. Alterations on phosphodiesterase type 7 and 8 isozyme mRNA expression in Alzheimer's disease brains examined by in situ hybridization. *Experimental Neurology* 182: 322-34

Perry SJ, Baillie GS, Kohout TA, McPhee I, Magiera MM, et al. 2002. Targeting of cyclic AMP degradation to beta(2)-adrenergic receptors by beta-arrestins. *Science* 298: 834-6

Perry SJ, Lefkowitz RJ. 2002. Arresting developments in heptahelical receptor signaling and regulation. *Trends in Cell Biology* 12: 130-8

Pi YQ, Kemnitz KR, Zhang DH, Kranias EG, Walker JW. 2002. Phosphorylation of troponin I controls cardiac twitch dynamics - Evidence from phosphorylation site mutants expressed on a troponin I-null background in mice. *Circulation Research* 90: 649-56

Pi YQ, Zhang DH, Kemnitz KR, Wang H, Walker JW. 2003. Protein kinase C and A sites on troponin I regulate myofilament Ca2+ sensitivity and ATPase activity in the mouse myocardium. *Journal of Physiology-London* 552: 845-57

Podzuweit T, Nennstiel P, Muller A. 1995. Isozyme-selective inhibition of cGMP-stimulated cyclic nucleotide phosphodiesterases by erythro-9-(2-hydroxyl-3-nonyl) adenine. *Cellular Signalling* 7: 733-8

Qian J, Ren XP, Wang XH, Zhang PY, Jones WK, et al. 2009. Blockade of Hsp20 Phosphorylation Exacerbates Cardiac Ischemia/Reperfusion Injury by Suppressed Autophagy and Increased Cell Death. *Circulation Research* 105: 1223-31

Qian J, Vafiadaki E, Florea SM, Singh VP, Song W, et al. 2011. Small heat shock protein 20 interacts with protein phosphatase-1 and enhances sarcoplasmic reticulum calcium cycling. *Circ Res* 108: 1429-38

Rabe KF. 2010. Roflumilast for the treatment of chronic obstructive pulmonary disease. *Expert Rev Respir Med* 4: 543-55

Rampersad SN, Ovens JD, Huston E, Umana MB, Wilson LS, et al. 2010. Cyclic AMP phosphodiesterase 4D (PDE4D) Tethers EPAC1 in a vascular endothelial cadherin (VE-Cad)-based signaling complex and controls cAMP-mediated vascular permeability. *J Biol Chem* 285: 33614-22

Reinhardt RR, Chin E, Zhou J, Taira M, Murata T, et al. 1995. Distinctive anatomical patterns of gene expression for cGMP-inhibited cyclic nucleotide phosphodiesterases. *Journal of Clinical Investigation* 95: 1528-38

Rembold CM. 2007. Force suppression and the crossbridge cycle in swine carotid artery. *American Journal of Physiology-Cell Physiology* 293: C1003-C9

Rembold CM, Foster DB, D. SJ, Wingard CJ, Van Eyk JE. 2000. cGMP-mediated phosphorylation of heat shock protein 20 may cause smooth muscle relaxation without myosin light chain dephosphorylation in swine carotid artery. *Journal of Physiology* 524: 865-78

Ren XP, Wu JH, Wang XH, Sartor MA, Qian J, et al. 2009. MicroRNA-320 Is Involved in the Regulation of Cardiac Ischemia/Reperfusion Injury by Targeting Heat-Shock Protein 20. *Circulation* 119: 2357-U128

Reyes-Irisarri E, Ittersum MM-V, Mengod G, de Vente J. 2007. Expression of the cGMP-specific phosphodiesterases 2 and 9 in normal and Alzheimer's disease human brains. *European Journal of Neuroscience* 25: 3332-8

Reynolds JG, McCalmon SA, Tomczyk T, Naya FJ. 2007. Identification and mapping of protein kinase A binding sites in the costameric protein myospryn. *Biochimica et Biophysica Acta (BBA) - Molecular Cell Research* 1773: 891-902

Richter W, Day P, Agrawal R, Bruss MD, Granier S, et al. 2008. Signaling from beta(1)- and beta(2)-adrenergic receptors is defined by differential interactions with PDE4. *Embo Journal* 27: 384-93

Richter W, Jin SLC, Conti M. 2005. Splice variants of the cyclic nucleotide phosphodiesterase PDE4D are, differentially expressed and regulated in rat tissue. *Biochemical Journal* 388: 803-11

Richter W, Xie M, Scheitrum C, Krall J, Movsesian MA, Conti M. 2010. Conserved expression and functions of PDE4 in rodent and human heart. *Basic Res Cardiol* 106: 249-62

Roman BB, Goldspink PH, Spaite E, Urboniene D, McKinney R, et al. 2004. Inhibition of PKC phosphorylation of cTnI improves cardiac performance in vivo. *Am J Physiol Heart Circ Physiol* 286: H2089-95

Rosman GJ, Martins TJ, Sonnenburg WK, Beavo JA, Ferguson K, Loughney K. 1997. Isolation and characterization of human cDNAs encoding a cGMP-stimulated 3',5'-cyclic nucleotide phosphodiesterase. *Gene* 191: 89-95

Ruehr ML, Russell MA, Ferguson DG, Bhat M, Ma JJ, et al. 2003. Targeting of protein kinase A by muscle a kinase-anchoring protein (mAKAP) regulates phosphorylation and function of the skeletal muscle ryanodine receptor. *Journal of Biological Chemistry* 278: 24831-6

Russell MA, Lund LM, Haber R, McKeegan K, Cianciola N, Bond M. 2006. The intermediate filament protein, synemin, is an AKAP in the heart. *Arch Biochem Biophys* 456: 204-15

Rybalkin SD, Bornfeldt KE, Sonnenburg WK, Rybalkina IG, Kwak KS, et al. 1997. Calmodulin-stimulated cyclic nucleotide phosphodiesterase (PDE1C) is induced in human arterial smooth muscle cells of the synthetic, proliferative phenotype. *Journal of Clinical Investigation* 100: 2611-21

Rybalkin SD, Yan C, Bornfeldt KE, Beavo JA. 2003. Cyclic GMP phosphodiesterases and regulation of smooth muscle function. *Circulation Research* 93: 280-91

Sah VP, Hoshijima M, Chien KR, Brown JH. 1996. Rho is required for G alpha(q) and alpha(1)-adrenergic receptor signaling in cardiomyocytes - Dissociation of Ras and Rho pathways. *Journal of Biological Chemistry* 271: 31185-90

Sakhuja R, Yeh RW, Bhatt DL. 2010. Antiplatelet agents in acute coronary syndromes. *Curr Probl Cardiol* 35: 123-70

Sarparanta J. 2008. Biology of myospryn: what's known? *J Muscle Res Cell Motil* 29: 177-80

Schillace RV, Scott JD. 1999. Association of the type 1 protein phosphatase PP1 with the A-kinase anchoring protein AKAP220. *Curr Biol* 9: 321-4

Schlossmann J, Feil R, Hofmann F. 2003. Signaling through NO and cGMP-dependent protein kinases. *Annals of Medicine* 35: 21-7

Sciandra JJ, Subjeck JR. 1983. The effects of glucose on protein synthesis and thermostability in Chinese hamster ovary cells. *Journal of Biological Chemistry* 258: 12091-3

Scott JD, Santana LF. 2010. A-Kinase Anchoring Proteins Getting to the Heart of the Matter. *Circulation* 121: 1264-71

Scott JD, Stofko RE, McDonald JR, Comer JD, Vitalis EA, Mangili JA. 1990. Type II regulatory subunit dimerization determines the subcellular localization of the cAMP-dependent protein kinase. *Journal of Biological Chemistry* 265: 21561-6

Sette C, Conti M. 1996. Phosphorylation and activation of a cAMP-specific phosphodiesterase by the cAMP-dependent protein kinase - Involvement of serine 54 in the enzyme activation. *Journal of Biological Chemistry* 271: 16526-34

Shibasaki T, Takahashi H, Miki T, Sunaga Y, Matsumura K, et al. 2007. Essential role of Epac2/Rap1 signaling in regulation of insulin granule dynamics by CAMP. *Proceedings of the National Academy of Sciences of the United States of America* 104: 19333-8

Sin YY, Edwards HV, Li X, Day JP, Christian F, et al. 2011. Disruption of the cyclic AMP phosphodiesterase-4 (PDE4)–HSP20 complex attenuates the β-agonist induced hypertrophic response in cardiac myocytes. *Journal of Molecular and Cellular Cardiology* 50: 872-83

Singh TP. 2010. Clinical use of sildenafil in pulmonary artery hypertension. *Expert review of respiratory medicine* 4: 13-9

Siuciak JA, McCarthy SA, Chapin DS, Fujiwara RA, James LC, et al. 2006. Genetic deletion of the striatum-enriched phosphodiesterase PDE10A: Evidence for altered striatal function. *Neuropharmacology* 51: 374-85

Siuciak JA, McCarthy SA, Chapin DS, Martin AN, Harms JF, Schmidth CJ. 2008. Behavioral characterization of mice deficient in the phosphodiesterase-10A (PDE10A) enzyme on a C57/B16N congenic background. *Neuropharmacology* 54: 417-27

Smith FD, Langeberg LK, Cellurale C, Pawson T, Morrison DK, et al. 2010. AKAP-Lbc enhances cyclic AMP control of the ERK1/2 cascade. *Nature Cell Biology* 12: 1242-U287

Smith FD, Langeberg LK, Scott JD. 2011. Plugging PKA into ERK scaffolds. *Cell Cycle* 10: 731-2

Smith FD, Scott JD. 2006. Anchored cAMP signaling: Onward and upward - A short history of compartmentalized cAMP signal transduction. *European Journal of Cell Biology* 85: 585-92

Smith JK, Reed RB, Francis SH, Grimes K, Corbin JD. 2000. Distinguishing the roles of the two different cGMP-binding sites for modulating phosphorylation of exogenous substrate (heterophosphorylation) and autophosphorylation of cGMP-dependent protein kinase. *Journal of Biological Chemistry* 275: 154-8

Smith SJ, Brookes-Fazakerley S, Donnelly LE, Barnes PJ, Barnette MS, Giembycz MA. 2003. Ubiquitous expression of phosphodiesterase 7A in human proinflammatory and immune cells. *American Journal of Physiology-Lung Cellular and Molecular Physiology* 284: L279-L89

Soderling SH, Bayuga SJ, Beavo JA. 1998. Identification and characterization of a novel family of cyclic nucleotide phosphodiesterases. *Journal of Biological Chemistry* 273: 15553-8

Soderling SH, Bayuga SJ, Beavo JA. 1999. Isolation and characterization of a dual-substrate phosphodiesterase gene family: PDE10A. *Proceedings of the National Academy of Sciences of the United States of America* 96: 7071-6

Solaro RJ. 2008. Multiplex kinase signaling modifies cardiac function at the level of sarcomeric proteins. *Journal of Biological Chemistry* 283: 26829-33

Solaro RJ. 2010. Sarcomere Control Mechanisms and the Dynamics of the Cardiac Cycle. *Journal of Biomedicine and Biotechnology* 2010: 105648

Solaro RJ, Moir AJG, Perry SV. 1976. Phosphorylation of troponin I and the inotropic effect of adrenalin in the perfused rabbit heart. *Nature* 262: 615-7

Solaro RJ, Rosevear P, Kobayashi T. 2008. The unique functions of cardiac troponin I in the control of cardiac muscle contraction and relaxation. *Biochemical and Biophysical Research Communications* 369: 82-7

Solaro RJ, van der Velden J. 2010. Why does troponin I have so many phosphorylation sites? Fact and fancy. *Journal of Molecular and Cellular Cardiology* 48: 810-6

Spina D. 2008. PDE4 inhibitors: current status. *British Journal of Pharmacology* 155: 308-15

Stangherlin A, Gesellchen F, Zoccarato A, Terrin A, Fields LA, et al. 2011. cGMP Signals Modulate cAMP Levels in a Compartment-Specific Manner to Regulate Catecholamine-Dependent Signaling in Cardiac Myocytes. *Circulation Research* 108: 929-U110

Stelzer JE, Patel JR, Walker JW, Moss RL. 2007. Differential roles of cardiac myosin-binding protein C and cardiac troponin I in the myofibrillar force responses to protein kinase a phosphorylation. *Circulation Research* 101: 503-11

Sterpetti P, Hack AA, Bashar MP, Park B, Cheng SD, et al. 1999. Activation of the Lbc Rho exchange factor proto-oncogene by truncation of an extended C terminus that regulates transformation and targeting. *Molecular and Cellular Biology* 19: 1334-45

Strandness DE, Jr., Dalman RL, Panian S, Rendell MS, Comp PC, et al. 2002. Effect of cilostazol in patients with intermittent claudication: a randomized, double-blind, placebo-controlled study. *Vascular and endovascular surgery* 36: 83-91

Sumandea CA, Garcia-Cazarin ML, Bozio CH, Sievert GA, Balke CW, Sumandea MP. 2010. Cardiac troponin T, a sarcomeric AKAP, tethers protein kinase A at the myofilaments. *J Biol Chem* 286: 530-41

Surks HK, Mochizuki N, Kasai Y, Georgescu SP, Tang KM, et al. 1999. Regulation of myosin phosphatase by a specific interaction with cGMP-dependent protein kinase I alpha. *Science* 286: 1583-7

Sutherland EW. 1972. Studies on the mechanism of hormone action. *Science* 177: 401-8

Sutherland EW, Rall TW. 1958. Fractionation and characterization of a cyclic adenine ribonucleotide formed by tissue particles. *J Biol Chem* 232: 1077-91

Suvarna NU, O'Donnell JM. 2002. Hydrolysis of N-methyl-D-aspartate receptor-stimulated cAMP and cGMP by PDE4 and PDE2 phosphodiesterases in primary neuronal cultures of rat cerebral cortex and hippocampus. *Journal of Pharmacology and Experimental Therapeutics* 302: 249-56

Szentesi P, Pignier C, Egger M, Kranias EG, Niggli E. 2004. Sarcoplasmic reticulum Ca2+ refilling controls recovery from Ca2+-induced Ca2+ release refractoriness in heart muscle. *Circulation Research* 95: 807-13

Takeda S, Yamashita A, Maeda K, Maeda Y. 2003. Structure of the core domain of human cardiac troponin in the Ca2+-saturated form. *Nature* 424: 35-41

Takimoto E, Soergel DG, Janssen PML, Stull LB, Kass DA, Murphy AM. 2004. Frequency- and afterload-dependent cardiac modulation in vivo by troponin I with constitutively active protein kinase a phosphorylation sites. *Circulation Research* 94: 496-504

Tasken K, Aandahl EM. 2004. Localized effects of cAMP mediated by distinct routes of protein kinase A. *Physiological Reviews* 84: 137-67

Taylor SS, Buechler JA, Yonemoto W. 1990. cAMP-dependent protein kinase - framework for a diverse family of regulatory enzymes. *Annual Review of Biochemistry* 59: 971-1005

Taylor SS, Kim C, Vigil D, Haste NM, Yang J, et al. 2005. Dynamics of signaling by PKA. *Biochimica Et Biophysica Acta-Proteins and Proteomics* 1754: 25-37

Tei H, Okamura H, Shigeyoshi Y, Fukuhara C, Ozawa R, et al. 1997. Circadian oscillation of a mammalian homologue of the Drosophila period gene. *Nature* 389: 512-6

Terrenoire C, Houslay MD, Baillie GS, Kass RS. 2009. The Cardiac I(Ks) Potassium Channel Macromolecular Complex Includes the Phosphodiesterase PDE4D3. *Journal of Biological Chemistry* 284: 9140-6

Tesmer JJ, Sunahara RK, Gilman AG, Sprang SR. 1997. Crystal structure of the catalytic domains of adenylyl cyclase in a complex with Gsalpha.GTPgammaS. *Science* 278: 1907-16

Tessier DJ, Komalavilas P, McLemore E, Thresher J, Brophy CM. 2004. Sildenafil-induced vasorelaxation is associated with increases in the phosphorylation of the heat shock-related protein 20 (HSP20). *Journal of Surgical Research* 118: 21-5

Tessier DJ, Komalavilas P, Panitch A, Joshi L, Brophy CM. 2003. The small heat shock protein (HSP) 20 is dynamically associated with the actin cross-linking protein actinin. *J Surg Res* 111: 152-7

Theurkauf WE, Vallee RB. 1982. Molecular characterization of the cAMP-dependent protein kinase bound to microtubule-associated protein-2. *Journal of Biological Chemistry* 257: 3284-90

Tissieres A, Mitchell HK, Tracy UM. 1974. Protein synthesis in salivary glands of Drosophila melanogaster: Relation to chromosome puffs. *Journal of Molecular Biology* 85: 389-98

Toksoz D, Williams DA. 1994. Novel human oncogene Lbc detected by transfection with distinct homology regions to signal transduction products. *Oncogene* 9: 621-8

Triposkiadis F, Karayannis G, Giamouzis G, Skoularigis J, Louridas G, Butler J. 2009. The Sympathetic Nervous System in Heart Failure: Physiology, Pathophysiology, and Clinical Implications. *Journal of the American College of Cardiology* 54: 1747-62

van der Staay FJ, Rutten K, Baerfacker L, DeVry J, Erb C, et al. 2008. The novel selective PDE9 inhibitor BAY 73-6691 improves learning and memory in rodents. *Neuropharmacology* 55: 908-18

Van der Velden J, Papp Z, Zaremba R, Boontje NM, De Jong WW, et al. 2002. Increased Ca2+ sensitivity of the contractile apparatus in end-stage human heart failure results from altered phosphorylation of contractile proteins. *Cardiovascular Research* 57: 37-47

Van Eyk JE, Powers F, Law W, Larue C, Hodges RS, Solaro RJ. 1998. Breakdown and release of myofilament proteins during ischemia and ischemia/reperfusion in rat hearts: identification of degradation products and effects on the pCa-force relation. *Circ Res* 82: 261-71

Vandeput F, Wolda SL, Krall J, Hambleton R, Uher L, et al. 2007. Cyclic nucleotide phosphodiesterase PDE1C1 in human cardiac myocytes. *Journal of Biological Chemistry* 282: 32749-57

Verschuure P, Croes Y, van den Ijssel P, Quinlan RA, de Jong WW, Boelens WC. 2002. Translocation of small heat shock proteins to the actin cytoskeleton upon proteasomal inhibition. *Journal of Molecular and Cellular Cardiology* 34: 117-28

Virshup DM, Shenolikar S. 2009. From Promiscuity to Precision: Protein Phosphatases Get a Makeover. *Molecular Cell* 33: 537-45

Wall EA, Zavzavadjian JR, Chang MS, Randhawa B, Zhu X, et al. 2009. Suppression of LPS-induced TNF-alpha production in macrophages by cAMP is mediated by PKA-AKAP95-p105. *Sci Signal* 2: ra28

Walsh DA, Perkins JP, Krebs EG. 1968. An adenosine 3',5'-monophosphate-dependent protein kinase from rabbit skeletal muscle. *Journal of Biological Chemistry* 243: 3763-&

Wang DG, Deng CJ, Bugaj-Gaweda B, Kwan M, Gunwaldsen C, et al. 2003. Cloning and characterization of novel PDE4D isoforms PDE4D6 and PDE4D7. *Cellular Signalling* 15: 883-91

Wang H-Y, Tao J, Shumay E, Malbon CC. 2006. G-protein-coupled receptor-associated A-kinase anchoring proteins: AKAP79 and AKAP250 (gravin). *European Journal of Cell Biology* 85: 643-50

Wang H, Yan Z, Yang S, Cai J, Robinson H, Ke H. 2008. Kinetic and Structural Studies of Phosphodiesterase-8A and Implication on the Inhibitor Selectivity. *Biochemistry* 47: 12760-8

Wang HC, Liu YD, Chen YX, Robinson H, Ke HM. 2005. Multiple elements jointly determine inhibitor selectivity of cyclic nucleotide phosphodiesterases 4 and 7. *Journal of Biological Chemistry* 280: 30949-55

Wayman C, Phillips S, Lunny C, Webb T, Fawcett L, et al. 2005. Phosphodiesterase 11 (PDE11) regulation of spermatozoa physiology. *International journal of impotence research* 17: 216-23

Welch EJ, Jones BW, Scott JD. 2010. Networking with AKAPs: Context-dependent Regulation of Anchored Enzymes. *Molecular Interventions* 10: 86-97

Westfall MV, Lee AM, Robinson DA. 2005. Differential contribution of troponin I phosphorylation sites to the endothelin-modulated contractile response. *J Biol Chem* 280: 41324-31

Westphal RS, Tavalin SJ, Lin JW, Alto NM, Fraser ID, et al. 1999. Regulation of NMDA receptors by an associated phosphatase-kinase signaling complex. *Science* 285: 93-6

Willis MS, Patterson C. 2010. Hold Me Tight: Role of the Heat Shock Protein Family of Chaperones in Cardiac Disease. *Circulation* 122: 1740-51

Willoughby D, Cooper DMF. 2007. Organization and Ca2+ regulation of adenylyl cyclases in cAMP microdomains. *Physiological Reviews* 87: 965-1010

Xiang Y, Kobilka B. 2003. Myocyte Adrenoceptor Signaling Pathways. *Science* 300: 1530-2

Xiao B, Jiang MT, Zhao M, Yang D, Sutherland C, et al. 2005. Characterization of a novel PKA phosphorylation site, serine-2030, reveals no PKA hyperphosphorylation of the cardiac ryanodine receptor in canine heart failure. *Circ Res* 96: 847-55

Xiao RP. 2000. Cell logic for dual coupling of a single class of receptors to G(s) and G(i) proteins. *Circ Res* 87: 635-7

Xiao RP, Zhu WZ, Zheng M, Chakir K, Bond R, et al. 2004. Subtype-specific beta-adrenoceptor signaling pathways in the heart and their potential clinical implications. *Trends in Pharmacological Sciences* 25: 358-65

Xu RX, Hassell AM, Vanderwall D, Lambert MH, Holmes WD, et al. 2000. Atomic structure of PDE4: Insights into phosphodiesterase mechanism and specificity. *Science* 288: 1822-5

Yan C, Zhao AZ, Bentley JK, Beavo JA. 1996. The calmodulin-dependent phosphodiesterase gene PDE1C encodes several functionally different splice variants in a tissue-specific manner. *Journal of Biological Chemistry* 271: 25699-706

Yan L, Vatner DE, O'Connor JP, Ivessa A, Ge H, et al. 2007. Type 5 adenylyl cyclase disruption increases longevity and protects against stress. *Cell* 130: 247-58

Yanaka N, Kurosawa Y, Minami K, Kawai E, Omori K. 2003. cGMP-phosphodiesterase activity is up-regulated in response to pressure overload of rat ventricles. *Bioscience Biotechnology and Biochemistry* 67: 973-9

Yang Q, Paskind M, Bolger G, Thompson WJ, Repaske DR, et al. 1994. A Novel Cyclic GMP Stimulated Phosphodiesterase from Rat Brain. *Biochemical and Biophysical Research Communications* 205: 1850-8

Young JC. 2010. Mechanisms of the Hsp70 chaperone system. *Biochemistry and Cell Biology-Biochimie Et Biologie Cellulaire* 88: 291-300

Young JC, Agashe VR, Siegers K, Hartl FU. 2004. Pathways of chaperone-mediated protein folding in the cytosol. *Nature Reviews Molecular Cell Biology* 5: 781-91

Yu FH, Yarov-Yarovoy V, Gutman GA, Catterall WA. 2005. Overview of molecular relationships in the voltage-gated ion channel superfamily. *Pharmacological Reviews* 57: 387-95

Zaccolo M, Cesetti T, Di Benedetto G, Mongillo M, Lissandron V, et al. 2005. Imaging the cAMP-dependent signal transduction pathway. *Biochemical Society Transactions* 33: 1323-6

Zaccolo M, Pozzan T. 2002. Discrete microdomains with high concentration of cAMP in stimulated rat neonatal cardiac myocytes. *Science* 295: 1711-5

Zakhary DR, Moravec CS, Stewart RW, Bond M. 1999. Protein kinase A (PKA)-dependent troponin-I phosphorylation and PKA regulatory subunits are decreased in human dilated cardiomyopathy. *Circulation* 99: 505-10

Zhang H, Makarewich CA, Kubo H, Wang W, Duran JM, et al. 2012. Hyperphosphorylation of the cardiac ryanodine receptor at serine 2808 is not involved in cardiac dysfunction after myocardial infarction. *Circ Res* 110: 831-40

Zhang HT, Huang Y, Jin SLC, Frith SA, Suvarna N, et al. 2002. Antidepressant-like profile and reduced sensitivity to rolipram in mice deficient in the PDE4D phosphodiesterase enzyme. *Neuropsychopharmacology* 27: 587-95

Zhang KYJ, Card GL, Suzuki Y, Artis DR, Fong D, et al. 2004. A glutamine switch mechanism for nucleotide selectivity by phosphodiesterases. *Molecular Cell* 15: 279-86

Zhao AZ, Huan JN, Gupta S, Pal R, Sahu A. 2002. A phosphatidylinositol 3kinase-phosphodiesterase 3B-cyclic AMP pathway in hypothalamic action of leptin on feeding. *Nature Neuroscience* 5: 727-8

Zhao AZ, Yan C, Sonnenburg WK, Beavo JA. 1997. Recent advances in the study of Ca-2+/CaM-activated phosphodiesterases: Expression and physiological functions. In *Advances in Second Messenger and Phosphoprotein Research; Signal transduction in health and disease*, pp. 237-51

Zhao RM, Davey M, Hsu YC, Kaplanek P, Tong A, et al. 2005. Navigating the chaperone network: An integrative map of physical and genetic interactions mediated by the Hsp90 chaperone. *Cell* 120: 715-27

Zhu WZ, Wang SQ, Chakir K, Yang D, Zhang T, et al. 2003. Linkage of beta1-adrenergic stimulation to apoptotic heart cell death through protein kinase A-independent activation of Ca2+/calmodulin kinase II. *J Clin Invest* 111: 617-25

Zhu WZ, Zheng M, Koch WJ, Lefkowitz RJ, Kobilka BK, Xiao RP. 2001. Dual modulation of cell survival and cell death by beta(2)-adrenergic signaling in adult mouse cardiac myocytes. *Proc Natl Acad Sci U S A* 98: 1607-12